A FULL-SCALE LABORATORY INVESTIGATION INTO RAILWAY TRACK SUBSTRUCTURE PERFORMANCE AND BALLAST REINFORCEMENT

By

Justin Kennedy

Submitted for the degree of Doctor of Philosophy

Heriot-Watt University
School of the Built Environment
January 2011

Abstract

To reduce railway track maintenance costs and meet the growing demand for rail travel the railway industry needs to significantly increase the performance of old existing tracks and design any new tracks accordingly. In this thesis, a new full-scale laboratory Geopavement & Railway Accelerated Fatigue Testing (GRAFT) facility at Heriot-Watt University is developed to study the performance of both unreinforced and reinforced railway track substructure systems. The new GRAFT facility enables accelerated testing of full-scale railway tracks and innovative railway products under realistic railway loading conditions. The unreinforced track systems represent typical railway tracks in the UK while the reinforced track systems represent sections of track implemented with various geosynthetic products. GRAFT consists of a track constructed within a steel tank. The track comprises a 750mm clay subgrade layer overlain by a clay formation layer overlain by a 300mm ballast layer. The track includes three hardwood sleeper sections overlain by an I-section steel beam which has similar stiffness properties to a BS 113 A rail section. Cyclic loading is applied to the track from a hydraulic testing machine with the centre sleeper directly under the loading actuator. The loading mechanism replicates a repeated quasi static single wheel load on the central sleeper of one half of a 3m long section of railway track.

Based on the results found from the testing programme in GRAFT empirical relationships are developed between the unreinforced track performance in terms of track settlement and stiffness and the subgrade modulus, applied load and number of applied cycles. These relationships fit the GRAFT data presented in this thesis well and it is thought that they could be used (tentatively) to estimate track settlement on track after tamping/ballast renewal/new track. These relationships are shown to be consistent with other well known track settlement models and they indicate that subgrade stiffness and applied vertical load are two of the most significant parameters that influence track substructure deterioration.

The results found from the reinforced track tests quantify the improvement in track performance available with each product under various track conditions. Two ballast

reinforcement products have been tested; XiTRACK reinforcement and geocell reinforcement, along with a reinforced geocomposite used primarily for separation at the ballast/subgrade interface. In addition, a geocomposite product designed to replace a traditional sand blanket, used on the tracks where severe subgrade erosion conditions prevail, has been tested in GRAFT under flooding conditions. The most significant results show that XiTRACK reinforcement can considerably improve the performance of railway tracks while the performance of the track implemented with the sand blanket replacement product indicates that currently a traditional sand blanket with a geotextile separator is the recommended option for tracks with subgrade wet spots. From all the data recorded empirical settlement models are proposed for each of the geosynthetics compared for reinforcement purposes. These models form the basis for reinforced track design graphs that could potentially be used to form part of an initial cost-benefit analysis of different track reinforcement techniques considered for improving track performance and reducing maintenance.

In order to use the track settlement design graphs developed within this thesis (in the field) a reliable measure of subgrade stiffness needs to be made on track. A reliable in-situ measuring device could enhance railway site investigations. Several in-situ measuring devices that could potentially be used to measures subgrade stiffness and strength in the field have been tested within GRAFT. The devices studied include the Dynamic Cone Penetrometer (DCP), Light Falling Weight Deflectometer (LFWD), Pocket Penetrometer and Proving Ring Penetrometer. The accuracy of these devices is compared to Plate Load Tests (PLT) and unconfined compression strength tests and suggestions towards the use of such devices on track made. The results indicate that the DCP has the potential to be a quick and accurate in-situ measuring device for railway track site investigations.

The GRAFT facility and the results found in GRAFT have been validated using a basic static 3D FE computer model termed SART3D (Static Analysis of Railway Track 3D). The program has been calibrated to GRAFT by modifying the FE mesh for the dimensions of GRAFT and inputting the GRAFT track properties. The validated results from this thesis have direct practical implications to the railway industry in terms of

design recommendations on how best to investigate and improve key geotechnical parameters that influence railway track performance and hence reduce maintenance costs and extend asset life. A review of current design procedures used in the railway industry is given and a new design procedure is suggested to reduce track maintenance and offer an optimised design and maintenance strategy.

Acknowledgements

I would like to give my sincere thanks to my PhD supervisor, Dr. Peter Woodward, for his continuous advice, guidance and encouragement throughout this research project; his constant enthusiasm and support has helped overcome all the research challenges encountered.

I would also like to thank Dr. Gabriela Medero, my second supervisor, for her advice and support with aspects of the experimental testing. The help from the laboratory technicians with the experimental programme was also much appreciated.

Special thanks are due to my friend and colleague Meysam Banimahd who read and gave expert comments on this thesis. In addition, thanks are due to all my colleagues at Heriot-Watt University for their help and support, especially Nawras Hamdan.

My greatest gratitude goes to my family and my beloved fiancée Gabriella for their continuous love, belief, encouragement and support throughout this period of my life. Without them this research would not have been possible.

This research was funded by EPSRC and funding was provided by the School of the Built Environment at Heriot-Watt University for developing the research facilities.

ACADEMIC REGISTRY
Research Thesis Submission

Name*:*	Justin Kennedy		
School/PGI:	School of the Built Environment		
Version: *(i.e. First, Resubmission, Final)*	Final	Degree Sought (Award **and** Subject area)	PhD Civil Engineering

Declaration

In accordance with the appropriate regulations I hereby submit my thesis and I declare that:

1) the thesis embodies the results of my own work and has been composed by myself
2) where appropriate, I have made acknowledgement of the work of others and have made reference to work carried out in collaboration with other persons
3) the thesis is the correct version of the thesis for submission and is the same version as any electronic versions submitted*.
4) my thesis for the award referred to, deposited in the Heriot-Watt University Library, should be made available for loan or photocopying and be available via the Institutional Repository, subject to such conditions as the Librarian may require
5) I understand that as a student of the University I am required to abide by the Regulations of the University and to conform to its discipline.

* *Please note that it is the responsibility of the candidate to ensure that the correct version of the thesis is submitted.*

Signature of Candidate*:*		Date:	

Submission

Submitted By *(name in capitals):*	
Signature of Individual Submitting:	
Date Submitted:	

For Completion in Academic Registry

Received in the Academic Registry by *(name in capitals):*			
Method of Submission *(Handed in to Academic Registry; posted through internal/external mail):*			
*E-thesis Submitted (**mandatory for final theses from January 2009)***			
Signature:		Date:	

Table of Contents

List of Publications

Kennedy, J. H., Woodward, P. K., Banimahd, M. and Medero, G. M. (In Press). Railway track performance study using a new testing facility. Accepted in September 2010 for publication in Proceedings of the Institute of Civil Engineers, Geotechnical Engineering.

Kennedy, J. H., Woodward, P., Medero, G. and McKinney, J. (2009). Full-scale cyclic Geopavement & Railway Accelerated Fatigue Testing. 10th International Railway Engineering Conference, University of Westminster, London.

Kennedy, J. H., Woodward, P. and Medero, G. (2009). Validation of the new full scale geopavement & railway testing facility at Heriot-Watt University, UK. Proceedings of GIGSA GeoAfrica Conference, Cape Town, South Africa.

Kennedy, J. H., Woodward, P. K., Banimahd, M. and Medero, G. M. (2008). Application of geocell reinforcement in stabilising railway track substructures, Proceedings of 4th European Geosynthetics Conference, Edinburgh, UK.

Woodward, P. K., Kennedy, J. H. and Medero, G. M. (2010). Improving the safety of railway track infrastructure using insitu polyurethane geocomposites. Proceedings of the American Railway Engineering and Maintenance of Way Association (AREMA), Chicago, USA.

Woodward, P. K., Kennedy, J. H. and Medero, G. M. (2009). XiTRACK reinforcement of high speed railway track over peat formations. 10th International Railway Engineering Conference, University of Westminster, London.

Woodward, P. K., Kennedy, J. H. and Medero, G. M. (2009). Reinforcing railway tracks using insitu polymer geocomposites. Proceedings of GIGSA GeoAfrica Conference, Cape Town, South Africa.

Woodward, P. K., Kennedy, J. H. and Medero, G. M. (2009). Three dimensional track reinforcement using polymer geocomposites. Proceedings of the American Railway Engineering and Maintenance of Way Association (AREMA), Chicago, USA.

Banimahd, M., Woodward, P.K., Kennedy, J.H. and Medero, G.M. (In Press). Behaviour of railway train-track interaction in stiffness transitions. Accepted in August 2010 for publication in the Proceedings of the Institution of Civil Engineers, Transport.

Banimahd, M., Woodward, P.K., Kennedy, J.H. and Medero, G.M. (In Press). Geotechnical performance of high-speed ballasted railway tracks. Accepted in December 2010 for publication in the Proceedings of the Institution of Civil Engineers, Transport.

Chapter 1 - Introduction

1.1 General Considerations

The world wide increasing demand for rail travel has led to an increase in traffic volume, higher line speeds on passenger routes and heavier axle loads for freight vehicles. However, the railway infrastructure in many countries has evolved over the last 120 years and large sections would not have been originally designed to accommodate these increased axle loads and line speeds (Woodward *et al*., 2009c). It is therefore likely that this increasing demand will result in increased track maintenance. The performance of the railway track, and hence required track maintenance, under these conditions depends upon the interaction between the track support, the superstructure and the train vehicles (Priest and Powrie, 2009). Track support characteristics have a direct influence on railway track deterioration, which has considerable cost and time implications to the rail industry through maintenance operations, track renewals and line speed restrictions. This was confirmed by Brough *et al*. (2003) who reported on research stating that a track section with track modulus (supporting force per unit length of rail per unit deflection) of 14 MPa required 183% more maintenance input than one with a track modulus of 27 MPa. A sensitivity analysis using different track degradation models undertaken by Sadeghi and Askarinejad (2007) found that the allowable annual tonnage for a track with a good quality foundation (subgrade) is 4 times more than that of one with a poor quality subgrade. Optimum subgrade stiffness beneath railway tracks should therefore significantly reduce maintenance frequency and increase total asset life (Brough *et al*., 2003).

Brough *et al*. (2006) reported on research that suggests that the subgrade is the most significant factor governing global track stiffness and hence the deterioration of vertical track geometry. A low track stiffness value can result in a flexible track with poor energy dissipation and a high track stiffness value can cause greater dynamic overloads on the rail with increased train-track interaction forces (Pita *et al*., 2004). Berggren

(2009) however commented that the current understandings about track stiffness and its effect on track performance are insufficient, which is observed by the fact that currently there is no European standard for vertical track stiffness available. This is a result of most research historically having been concentrated on understanding the performance of the train and the superstructure (Priest and Powrie, 2009).

The main consequence of track deterioration from the sub track aspect is settlement of the substructure. Differential track settlement can result in faults in the vertical track geometry, which can lead to derailment if not treated. Selig and Waters (1994) stated that for most tracks the granular upper part of the substructure (ballast layer) is the main source of both average and differential settlement between surfacing operations and is known as short term settlement, compared to long term settlement which is subgrade related.

To counteract substructure deterioration several well established geosynthetic products are available that can be used to undertake various functions within the substructure of rail tracks, to ultimately increase track resistance to deformation. These functions include separating the ballast layer from the subgrade to prevent ballast penetration, reinforcing the ballast layer to reduce ballast settlement and attrition, filtration to prevent subgrade pumping and drainage to prevent excessive wetting of the subgrade. These techniques can reduce the depth of the required granular layer and also reduce the frequency of the required maintenance. However, the use of these techniques is somewhat sporadic and there is limited guidance on the quantifiable benefits of using such techniques.

1.2 Research Objectives

To meet the growing demand for rail travel the railway industry needs to significantly increase the performance of existing tracks and design new tracks accordingly, without increasing maintenance costs or downtime. The primary purpose of the thesis is therefore to investigate new methods that are available to provide increased track

substructure performance under load using laboratory experiments backed up by computer modelling. To meet this purpose the following research objectives were set:

- Design and commission a new full-scale laboratory Geopavement & Railway Accelerated Fatigue Testing (GRAFT) facility at Heriot-Watt University which enables accelerated testing of full-scale railway tracks and new innovative railway products under realistic railway loading conditions.

- Undertake a series of unreinforced control tests within GRAFT to investigate the factors that influence the unreinforced substructure performance and develop empirical relationships between track performance and track substructure parameters and applied load.

- Undertake GRAFT tests on track implemented with different geosynthetics to quantify the improvement in track performance available with each product under various track conditions. Develop design charts for each product that could be used in a cost-benefit analysis of different track reinforcement techniques considered for improving track performance and reducing maintenance.

- Validate the GRAFT facility and the results found in GRAFT using a basic static 3D FE computer model termed SART3D (Static Analysis of Railway Track 3D).

In addition to these research objectives the accuracy of some typical in-situ testing devices, in measuring subgrade stiffness and strength, has also been investigated within GRAFT and presented within this thesis. The aim was to study different devices that could potentially be used to enhance railway site investigations; in order to allow regular monitoring to take place in an accurate, consistent and safe manner within the physical and time restrictions of working on the railway track.

Through the above research objectives this thesis presents validated results that have direct practical implications to the railway industry in terms of design recommendations

on how best to investigate and improve key geotechnical parameters that influence railway track performance and hence reduce maintenance costs and extend asset life.

1.3 Thesis Outline

Within this thesis the relevant literature review is presented within each associated chapter, although Chapter 2 serves to give a brief overview of the research area. The thesis is divided into the following eight chapters:

Chapter 1 gives a general introduction to the research area and sets out the research objectives and thesis outline.

Chapter 2 presents a brief overview of railway track behaviour. The track structure and components are initially described followed by an explanation of the imposed vertical load applied to the track from the train traffic. The train loading dynamic amplification factor is discussed in terms of different track conditions and train speeds. Track deterioration and track failure mechanisms under repeated traffic loading are then studied, followed by the routine track maintenance undertaken on the railways. This chapter is concluded by exploring different methods that can be used to prevent and reduce the required maintenance.

Chapter 3 describes the design, construction, calibration and preliminary testing of the experimental arrangements, instrumentation and the materials used to conduct this research investigation. Initially, the development of the new full-scale laboratory Geopavement & Railway Accelerated Fatigue Testing (GRAFT) facility at Heriot-Watt University is given. This is followed by specific geomechanical test details and results, before the initial GRAFT track results are presented and the full testing programme undertaken within this thesis set out.

Chapter 4 presents the findings from a series of unreinforced GRAFT control tests that investigate railway track performance in terms of track substructure deterioration. The influence of clayey subgrade Young's modulus and applied vertical load on track

settlement is initially studied before the influence on track stiffness is considered. Other factors that can influence substructure deterioration have also been discussed. Two empirical track settlement prediction models are developed and presented from the GRAFT findings. These models can be used to estimate track settlement for a typical track section based on combinations of the subgrade modulus, applied load and track stiffness. These models are compared to previously published models from empirical results and are found to compare favourably.

In Chapter 5 the influence of four different geosynthetic products on the performance of the track is studied. The results from two ballast reinforcement products are presented; XiTRACK reinforcement and geocell reinforcement, before the results from a multi-functional reinforced geocomposite and a geocomposite product, designed to replace a traditional sand blanket, are discussed. From the results further empirical settlement models have been developed for each of the three geosynthetics compared for reinforcement purposes. Design charts that incorporate these models are presented and suggested for use to predict the track settlement of a typical UK track in which track reinforcement is implemented within a track renewal.

Chapter 6 investigates the accuracy of some typical in-situ testing devices, in measuring subgrade stiffness and strength, in order to try and enhance railway site investigation techniques. The devices studied include Dynamic Cone Penetrometer (DCP), Light Falling Weight Deflectometer (LFWD), Pocket Penetrometer and Proving Ring Penetrometer. The accuracy of these devices is compared to Plate Load Tests (PLT) and unconfined compression strength tests taken throughout the GRAFT testing programme.

In Chapter 7 a three dimensional finite element (FE) computer program termed SART3D (Static Analysis of Railway Track 3D) has been used to validate the results found in GRAFT. The program is first calibrated to GRAFT by modifying the FE mesh for the dimensions of GRAFT and incorporating the GRAFT track properties. The program is then run to validate that the applied load in GRAFT produces the same level of stresses within the track substructure for a 25 tonne axle train load that the testing program is trying to represent. A short parametric study is then presented to look at the

influence of changing some of the track properties that could not practically be studied within the GRAFT experimental program. The chapter concludes by incorporating the findings of this thesis into a new railway track design method to reduce the required track maintenance. The new procedure includes the empirical track design results from the experimental program for unreinforced (Chapter 4) and reinforced track (Chapter 5), and the SART3D model.

Chapter 8 presents a brief overview of the research presented in this thesis and summaries the conclusions drawn from each chapter. Recommendations on future research to develop the testing facilities and to continue the unreinforced and reinforced railway track research are also presented within this chapter,

Chapter 2 - Railway Track Behaviour

2.1 Introduction

Railway track structures undertake a fundamental role within the transportation infrastructure of a country and contribute significantly in sustaining a healthy economy. With the current increase in demand for passenger train travel along with higher required axle loads for freight vehicles it is essential that a better understanding of how the trackbed behaviour influences track performance is sought. This will help to reduce future track maintenance costs. This chapter presents a basic overview of railway track behaviour. The sections within this chapter focus on:

- The track structure and components
- The vertical traffic loads imposed on the track structure (static and dynamic)
- The deterioration and failure of the track structure under repeated traffic loading
- The routine track maintenance required to maintain the track structure geometry
- Methods that can be used to prevent track failure and reduce the required maintenance

2.2 Track structure

The purpose of a railway structure is to provide safe and economical train transportation. This requires the track to serve as a stable guide way with appropriate vertical and horizontal alignment. To achieve this role each component of the system must perform specific functions satisfactorily in response to traffic loads and environmental factors imposed on the system (Selig and Waters, 1994).

Traditionally rail tracks are laid on a bed of ballast material and the track components of ballasted track can be grouped into two main components; the superstructure and substructure. The superstructure consists of rails, fastening system and sleepers while

the substructure consists of ballast, subballast and subgrade. Figure 2.1 and Figure 2.2 show the components of a typical ballasted track from the longitudinal and transverse directions respectively. Within this thesis only ballasted track is considered. Moreover, although each of the superstructure components are important to the stability of the overall track structure, within this thesis the substructure components have been concentrated on as they typically contribute the most to track deterioration (Selig and Waters, 1994).

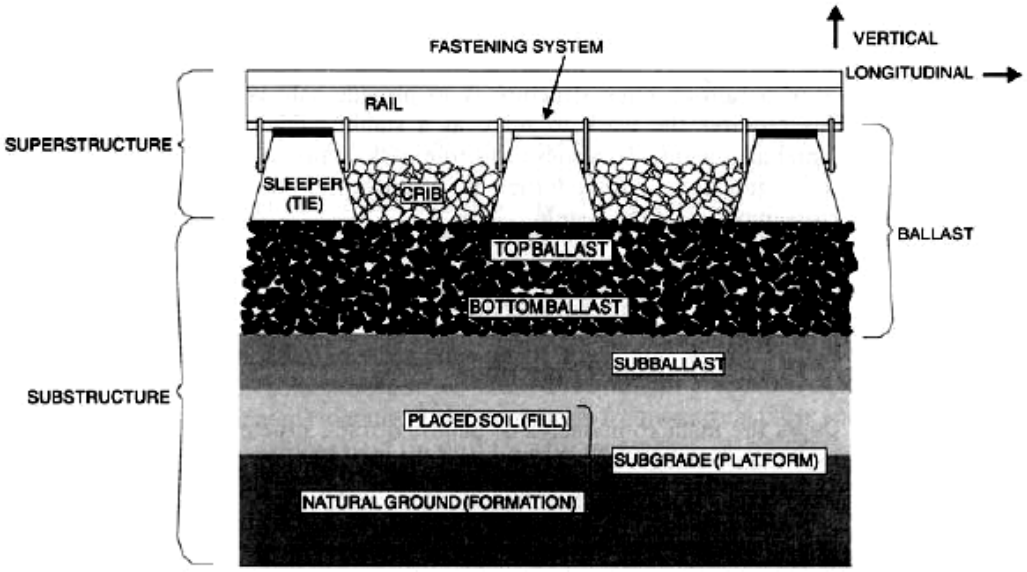

Figure 2.1. Longitudinal cross section of ballasted track structure (Selig and Waters, 1994)

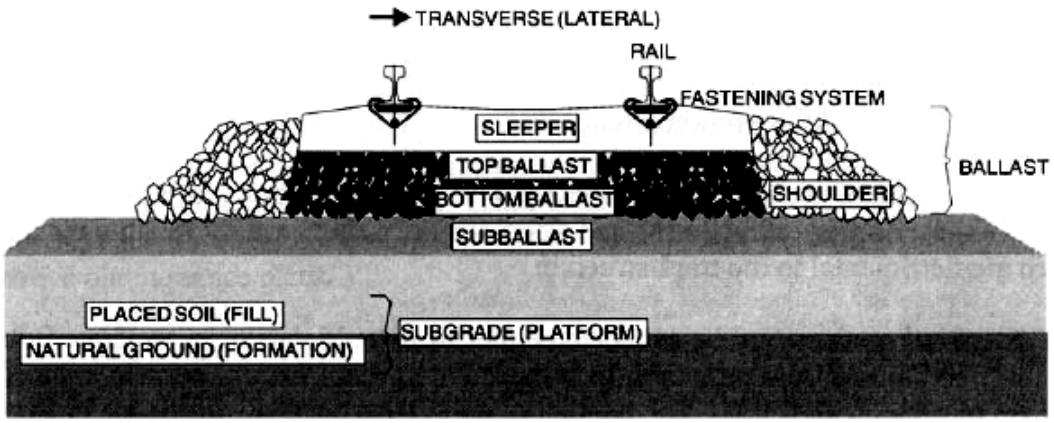

Figure 2.2. Transverse cross section of ballasted track structure (Selig and Waters, 1994)

Rails guide the train wheels and transfer the vertical and horizontal components of the wheel loads to the underlying spaced sleeper sections. Rail pads are used as a fastening system between the sleeper and rail to retain the rails against the sleepers and maintain the correct track gauge. In addition, the rail pads resist the vertical, lateral, longitudinal, and overturning movements of the rail by anchoring in the superstructure to the ballast (Selig and Waters, 1994). The sleepers act to distribute the applied load over the ballast and are generally either wooden (timber) or prestressed/reinforced concrete. Sleeper dimensions vary although the normal European concrete sizes are 250-300mm wide and 2300-2600mm long, with wooden sleepers being slightly narrower but longer. Sleepers are usually spaced at between 600 to 700mm on the UK mainline (Fair, 2003).

Ballast is a crushed granular material placed as the top layer of the substructure in which the sleepers are embedded. Crib ballast is placed between the sleepers and in the shoulders beyond the sleeper ends. A wide range of ballast materials can be found on the tracks, such as granite, basalt, limestone, slag and gravel. The typical ballast material is gravel-size with most particles between 6 and 64mm diameter. The primary purpose of the ballast layer is to distribute the applied loads from the sleepers down to the underlying soil layers and protect the subgrade from high stresses. The voids in the ballast layer provide essential drainage of water falling onto the track and also allow the maintenance requirement of rearranging ballast particles to adjust track geometry (Selig and Waters, 1994). Subballast is the granular layer of material separating the ballast and the subgrade and generally, subballast materials consist of broadly graded sand-gravel mixtures or broadly graded crushed natural aggregates or slags. The subballast layer further reduces the stress at the bottom of the ballast layer to a tolerable level for the top of the subgrade, offering a cheaper option to the otherwise thicker ballast layer. Another important function of the subballast layer, is to act as a separator and prevent interpenetration between the subgrade and the ballast. By acting as a separator the subballast layer prevents the upward migration of fine material emanating from the subgrade, the attrition of subgrade by ballast and can provide drainage of water either flowing to the subgrade form the ballast or vice versa.

The subgrade is the foundation for the track structure and it can either consist of the existing natural soil, which is most likely to be a fine grained soil with silt and clay components, or placed fill. The main function of the subgrade is to provide a stable foundation for the track structure and therefore the subgrade has a significant influence on track performance and maintenance. The strength and stiffness of the subgrade ultimately dictates the amount of load that can be applied to the track and consequently controls the required depth of overlying granular material.

2.3 Track Loading

The loads imposed on the track structure can be classified as either mechanical or thermal and they are applied to the track structure in the form of repeated vertical, lateral and longitudinal forces resulting from traffic and changing temperatures. Lateral and longitudinal forces are more complex and harder to predict than vertical forces, which act perpendicular to the plane of the rails (Selig and Waters, 1994). Within this thesis only vertical forces resulting from traffic wheel loadings are considered.

Vertical loads applied to the track from moving trains are a combination of a static load and a dynamic component. The static wheel load is the dead weight of the train divided by the number of wheels while the dynamic component is caused by interactions between the wheels and the rails and is a function of the track, vehicle, and train characteristics, such as track irregularities and train speed. The maximum static axle load permitted in the UK is 25 tonnes. With continuously welded rail and good maintenance, the dynamic wheel load will probably not exceed the static wheel load by more than 10 to 20%. However, wheel and rail defects and track irregularities can cause very high loads as much as 3 times the nominal static wheel load (Selig and Waters, 1994). Furthermore, dynamic impact forces caused from these high dynamic wheel loads can produce high frequency vibrations (Selig and Waters, 1994).

The dynamic component can be considered by increasing the static load by a factor termed the Dynamic Amplification Factor (DAF). The DAF can be calculated by

employing simple empirical equations. Eisenman's equation was cited by Esveld (2001):

$$\text{DAF} = 1 + t\varphi \qquad \text{if } V < 60km/h$$

$$\text{DAF} = 1 + t\varphi\left(1 + \frac{V - 60}{140}\right) \qquad \text{if } 60 \le V \le 200km/h \tag{2.1}$$

where t is a multiplication factor depending on the confidence interval, φ is an empirical factor depending on the track quality, and V is the train speed in km/h. The values used for these factors are presented in Table 2.1 and it can be seen that the DAF increases with an increase in train speed and with a decrease in track quality.

Probability (%)	t	Application	Track condition	φ
68.3	1	Contact stress, subgrade	Very good	0.1
95.4	2	Lateral load, ballast bed	Good	0.2
99.7	3	Rail stresses, fastenings, supports	Bad	0.3

Table 2.1. Parameters used for the determination of the Dynamic Amplification Factor (Esveld, 2001)

A summary of other equations suggested for calculating the DAF is given in Table 2.2, where V is the train speed (km/h), D_w is the wheel diameter (mm), and k is the track modulus (MPa). Stewart and O'rourke (1988) suggested that typical k values of 7, 14 and 21 MN/m/m could be used for poor, average and good quality tracks respectively.

Researcher	Suggested DAF equation
Talbot (1918)	$\text{DAF} = 1 + 0.0062(V - 8)$
Clarke (1957)	$\text{DAF} = 1 + \frac{19.65}{D_w\sqrt{k}}$
Sirinivasan (1969)	$\text{DAF} = 1 + \frac{0.017V}{\sqrt{k}}$
AREA (1984)	$\text{DAF} = 1 + \frac{5.2V}{D_w}$

Table 2.2. Summary of equations suggested for calculating the Dynamic Amplification Factor

2.4 Track performance

Track performance can be measured in terms of the response of the track to traffic loading. The magnitude of individual loads and the repetition of loading are the two main factors that influence the loading of the track, and with routine traffic it is typically the repetition of loading that is the main problem for the track substructure (Fair, 2003). The track components combine to control how the traffic loads are transmitted through the track structure and ultimately determine the degradation of the track. The main factors that affect track degradation are the deterioration of the superstructure components (rails, sleepers, rail pads), densification and breakage of the ballast, and subgrade deterioration.

Different failure mechanisms can form in the subgrade layers to cause deterioration, including (after Selig and Waters, 1994, and Brough *et al*., 2003):

- Massive subgrade shear failure
- Progressive subgrade shear failure
- Subgrade surface attrition
- Excessive subgrade plastic deformation

The factors that contribute to these failure mechanisms are repeated dynamic loading, excessive moisture, and fine grained or poor quality soil (Radampolo, 2006). The forces that can cause massive shear failure in the subgrade are from the weights of the train and the track superstructure. The resisting force is from the substructure shearing resistance and as most of the failure zone is in the subgrade, the subgrade strength properties have a significant effect on the factor of safety against massive shear failure. Massive shear failure of the subgrade under repeated loading generally occurs at stress levels above that which cause progressive shear failure. Therefore, massive shear failure is likely only to be a problem when the subgrade strength diminishes due to increasing water content, and hence progressive shear failure should govern performance (Selig and Waters, 1994).

Progressive shear failure (Figure 2.3) may occur if the stresses imposed on the subgrade by the axle loads are large enough. This failure mechanism is most likely to develop in the top part of the subgrade where the traffic induced stresses are the highest. Overstressed soil will be squeezed sideways from beneath the track and upwards to give a bearing capacity failure (cess heave). The probability of cess heave can be minimised by ensuring an adequate depth of ballast/subballast to reduce the induced stress level on the subgrade surface and by ensuring a low water table level (Selig and Waters, 1994).

Subgrade attrition by the overlying ballast in the presence of water can result in the formation of slurry at the ballast/subgrade interface. Under certain conditions cyclic loading can cause the slurry to be pumped up to the surface of the ballast. Such failures are associated with hard, fine grained materials, such as clay, and soft rocks, such as chalk (Selig and Waters, 1994). Pumping failures can be prevented by placing a layer of blanketing material between the ballast and the subgrade to prevent subgrade attrition and penetration from the overlying granular material.

Excessive plastic deformation of the subgrade from repeated loading (Figure 2.4) can result from cumulative compaction, consolidation and shear strain in the subgrade. Subgrade plastic deformation can result in ballast pockets forming under the railheads and the resulting track settlement is non-uniform along the track.

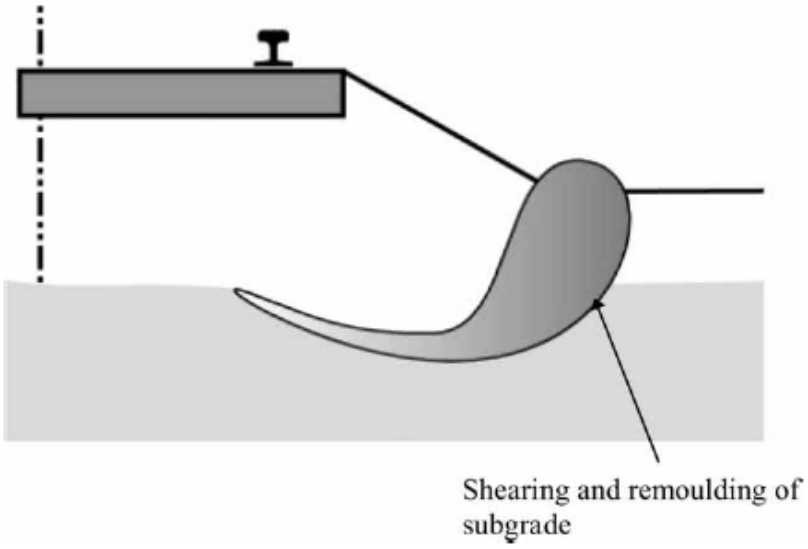

Figure 2.3. Progressive subgrade shear failure (Selig and Waters, 1994).

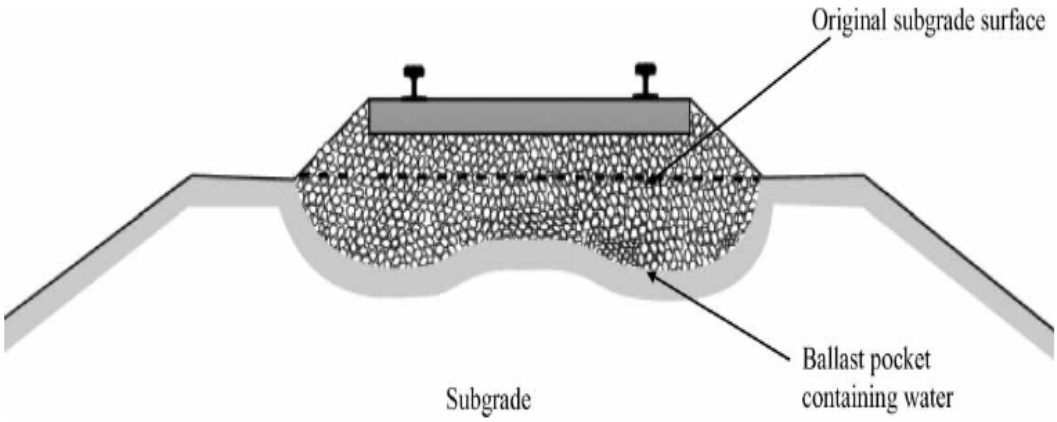

Figure 2.4. Excessive subgrade plastic deformation (Li and Selig, 1998a)

Ballast settlement is caused by densification due to particle rearrangement under repeated train loading, penetration of ballast into the underlying layer, and particle breakage and/or abrasive wear. It is thought by many track engineers that in most existing tracks ballast is the main source of both average and differential settlement between surfacing operations. Ballast settlement is known as short term settlement whereas subgrade settlement is known as long term settlement as it accumulates very

slowly for most tracks (Selig and Waters, 1994). Therefore, in order to maintain the track geometry, regular ballast maintenance operations are required. Track geometry deterioration reduces ride quality and increases the dynamic loads, causing increased geometry degradation, and can eventually result in derailment if not treated. Figure 2.5 illustrates the substructure contributions to settlement for track that has been in service for a long time and has a stable subgrade.

There are generally two forms of track geometry maintenance to correct from the effects of repeated traffic loading; tamping and stoneblowing. Ballast tamping is the process of lifting and laterally adjusting track to the desired geometry while rearranging the upper portion of the ballast layer to fill the resulting voids under the sleepers (Selig and Waters, 1994). Tamping is effective at correcting track geometry faults, however it results in ballast breakage and ballast loosening. Ballast loosening results in further settlement with additional traffic, the degree of settlement increasing as the ballast deteriorates. Tamping is eventually needed again. Fair (2003) noted that when the track is maintained by tamping the rate of decay of track geometry increases with each maintenance cycle. Over a period of time fine particles derived from many sources accumulate in the ballast, a process known as fouling. This reduces the track drainage and the ability of the track to maintain geometry after tamping. Eventually the ballast will need to be replaced or cleaned and returned to track (Selig and Waters, 1994).

According to the current normal practise in the UK, stoneblowing is used on sections of track with high tamping frequency as it causes less damage to the ballast (Aursudkij, 2007). Stoneblowing is the process of blowing a layer of smaller, single sized (20mm) stone under a raised sleeper, leaving the sleeper at the desired level and the compact ballast virtually undisturbed. Stoneblower maintenance thus creates a two-layer granular foundation on which the sleeper sits (Fair, 2003).

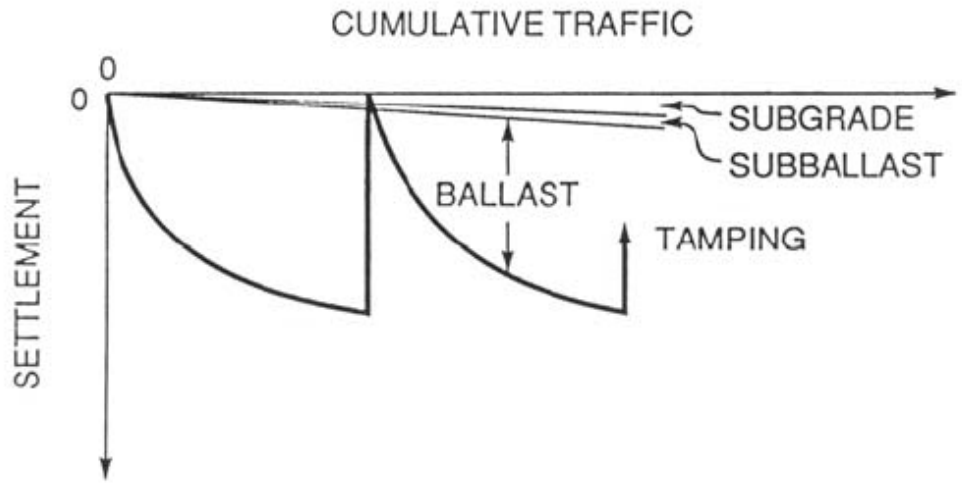

Figure 2.5. Typical substructure contributions to settlement for existing track with a stable subgrade (Selig and Waters, 1994)

Geometry deterioration is detected through continuous monitoring of the railways and there are several intrusive and non-intrusive sampling and testing methods used regularly to detect such defects and discover the source of the deterioration (ballast fouling, soft subgrade etc.). Once poor quality track geometry has been detected and the source of the fault investigated then a remediation strategy can be identified. The minimum geometric quality to which the track has to be maintained is a function of the speed and type of traffic that is being carried. Clearly, tracks carrying high speed and/or passenger traffic will need to be maintained to a higher geometric quality than will tracks dedicated to low speed and/or freight traffic. The level of geometric quality that can be achieved above the minimum required is indicative of the time that will elapse before the track will require resurfacing (Selig and Waters, 1994).

2.5 Track performance improvement

The strength and stiffness of the subgrade generally dictates the behaviour of the track substructure under repeated loading and defines the settlement contributions from each layer. For a weak subgrade layer the subgrade will be the main source of settlement and

the general solution to stabilise the track is to increase the depth of the overlying granular layers to reduce the subgrade stresses and reach acceptable track geometry. However, if the subgrade is too weak or has too low a stiffness that the track with any depth of granular material will not meet the minimum required track geometry under a particular load, then improvement of the subgrade is required. In addition, subgrade improvement may also be required when the train speed on a particular line approaches a threshold value for the track, namely the track 'critical velocity' (Banimahd, 2008). This phenomenon is associated with low velocity surface wave propagation. Subgrade improvement methods include modifying the subgrade properties in-situ (grouting, lime slurry stabilisation, electrical treatment), modifying the subgrade properties by reconstruction and replacement (compaction, admixture stabilisation), strengthening with asphalt concrete, and slip stabilisation (drainage, retaining structure). For a relatively firm subgrade the ballast layer will be the main source of the settlement, although the depth of ballast is still dictated by the strength and stiffness of the subgrade.

As described above the conventional solution to ballast settlement is regular maintenance tamping, although this process has many unfavourable effects and can ultimately result in the total replacement of ballast. In order to reduce the required ballast maintenance there are several well established granular stabilisation techniques that can be used to improve the mechanical properties of the granular ballast and subballast layers to increase their resistance to deformation. These techniques can reduce the frequency of the required maintenance resulting in significant cost savings. One of the most recent stabilisation techniques is the use of geosynthetics within the granular layers of the track. In this thesis the subgrade quality in which subgrade improvement is required is not considered and ballast improvement is concentrated on using geosynthetics.

Geosynthetics can be defined as any product manufactured from a polymeric base and used in conjunction with soils and aggregates in construction projects. Consequently, there are various different types of geosynthetic products available which can fulfil a variety of functions within the construction industry. Table 2.3 lists the main types of

geosynthetics and their functions. In the rail industry several geosynthetic products are used for separation, filtration, drainage and reinforcement because they can provide an economical solution to common track problems. For example, geotextiles are commonly used to fulfil some of the functions of subballast and can either be used in place of, or to assist, subballast. In terms of stabilisation of the substructure through reinforcement, three main geosynthetics are used; geogrids, geocells and XiTRACK.

Type of geosynthetic	Function
Geotextile	Separation, Filtration, Reinforcement, Protection
Geomembrane	Separation, Barrier
Geogrid	Reinforcement
Geocell	3D Reinforcement
Geonet	Drainage
Geomat	Drainage, Protection
Geostrip	Reinforcement
Geospacer	Drainage
Geocomposite	Combinations
XiTRACK	3D Reinforcement

Table 2.3. Various types of geosynthetics and their functions

Geogrids are 2D planar structures that have a regular open network of interconnected tensile elements (Figure 2.6). These elements may be linked by extrusion, bonding, knitting or lacing and the apertures are normally larger than the elements forming the mesh. The grids interlock with the soil to create tensile reinforcement when the soil strains are extensional in the plane of the grid (Selig and Waters, 1994).

Geocells are a 3D cellular confinement system that consists of interlocking cells integrated in a honeycomb structure into which granular materials are placed and compacted. Once filled, each cell acts in conjunction with adjacent cells to form a

stabilised composite mattress that disperses load and resists lateral movement and shear failure. Figure 2.7 illustrates a typical geocell system.

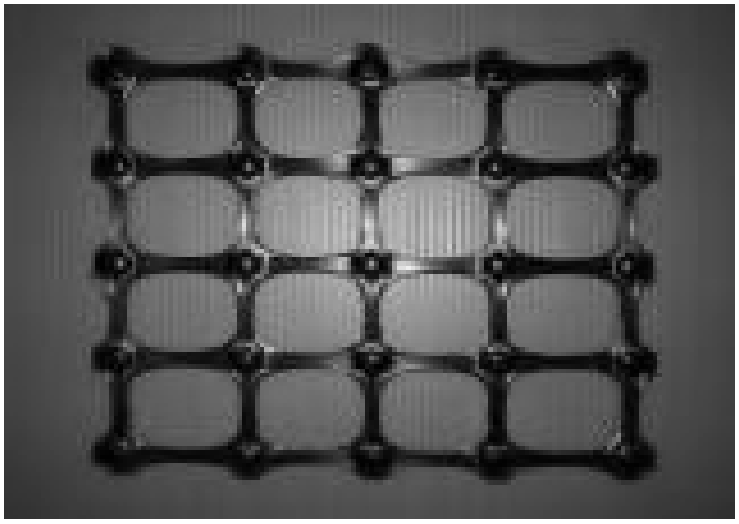

Figure 2.6. Typical Geogrid mesh

Figure 2.7. Typical geocell system

XiTRACK is a 3D polymer track reinforcement technique that improves the load distributing properties of ballast by forming a flexible but very resilient geocomposite across the formation, significantly reducing long-term settlements at high loading locations (Woodward *et al.*, 2007). Figure 2.8 illustrates a typical XiTRACK application on track.

Figure 2.8. Typical XiTRACK application on site (XiTRACK Ltd, 2010)

2.6 Conclusion

This chapter has presented different aspects of railway track behaviour. The track structure and components were described and the static and dynamic vertical loads acting on these components from repeated train loading discussed. Different relationships to account for the dynamic component were explored. Track performance in terms of substructure deterioration was explained as well as the track maintenance techniques used to maintain the required track geometry. Methods to improve the track performance by reducing the required track substructure maintenance were discussed and the functions of different types of geosynthetics that can be used on track presented.

The consequences of track deterioration are that ride quality decreases and dynamic loads increase, causing increased geometry degradation. It was shown that the main cause of track deterioration is settlement of the substructure which eventually results in the track geometry needing to be improved before differential track settlements give rise to faults in the vertical track geometry. These faults can cause serious problems to rail traffic and ultimately could result in derailment. Therefore, track settlement is a serious problem in modern day railway engineering and has considerable cost and time implications to the rail industry through maintenance operations, track reconstructions and line speed restrictions, which all cause disruption to the network. Total track

settlement is a combination of ballast, subballast and subgrade settlement and the strength of the subgrade generally dictates the settlement contributions from each layer. When the subballast/ballast is the main source of settlement geogrid, geocell and XiTRACK reinforcement can be used to try and reduce the degree of ballast deformation.

Chapter 3 - Testing Methodology: Development of a Railway Track Testing Facility

3.1 Introduction

This chapter describes the design, construction, calibration and preliminary testing of the experimental arrangements, instrumentation and the materials used to conduct this research investigation. Initially a detailed description of the new full-scale laboratory Geopavement & Railway Accelerated Fatigue Testing (GRAFT) facility at Heriot-Watt University and the individual instruments used is given. This is followed by specific geomechanical test details and results, before the initial GRAFT track construction is described and the full testing programme undertaken within this thesis set out. This chapter shows how the testing programme and track construction procedures were developed throughout the research to allow realistic substructure track data to be collected from consistent procedures for a range of different track conditions.

The primary purpose for constructing GRAFT was to construct a realistic rail testing facility that would enable accelerated testing of ballast reinforcement products under realistic loading conditions. The implications of placing these products within the harsh substructure environment of railway tracks could be found and the benefits of the products could be quantified and compared, including any reduction in track settlement and any increase in track stiffness. Therefore, any benefits to the rail industry could be measured with confidence, encouraging the industry to take these products forward into site trials and ultimately, implement them within the rail network. This fits into the general objective of most practical railway track research, which is to assist with the development of the design and construction of track that provides enhanced performance.

As well as investigating products that can be used to improve track performance some of the fundamental track substructure properties and loading conditions that influence

track performance were also researched (subgrade stiffness, ballast depth, applied load, number of applied cycles, rate of loading). Furthermore, GRAFT has also been used to assess different subgrade modulus in-situ testing technology, including the standard Plate Load Test (PLT), Light Falling Weight Deflecotometer (LFWD) and Dynamic Cone Penetrometer (DCP). Factors that have not been studied within this thesis, and are considered to remain constant throughout the testing programme, include subgrade type and depth, ballast properties, rail type, sleeper type, sleeper spacing, sleeper dimensions, track irregularities, and other track construction components such as rail pads etc. The overall aim of the research undertaken in GRAFT was to work towards track design recommendations on how best to investigate and improve key geotechnical parameters that influence railway track performance and hence reduce maintenance costs and extend asset life.

Recent laboratory railway substructure research has involved the use of full-scale laboratory railway testing facilities, mainly as a result of the need to test innovative railway products within a controlled environment prior to site trials or full implementation. In the UK new facilities at both GEOfabrics Ltd. (Sharpe and Caddick, 2006) and Nottingham University (Brown *et al*., 2007a) have been used to study the functioning of various geosynthetics within the substructure. Brown *et al*. (2007a) found that placing a geogrid of 65mm aperture size within the ballast layer reduced sleeper settlement from 10mm to around 8mm after one million load cycles at a load of 100kN. However, the geogrid was found to have no effect on subgrade stress level or on the resilient sleeper deflection and hence stiffness. Sharpe and Caddick (2006) undertook a series of tests on geotextiles placed between the ballast and clay subgrade layer to assess their efficiency in preventing subgrade erosion and it was found that after one million load cycles at 100kN that none of the products tested matched that of a traditionally used sand blanket. In general it was shown that without a 50mm sand blanket that the settlements doubled for each of the geotextiles tested and it was recommended that at present a sand/separator combination remains the best solution. Indraratna *et al*. (2004) used a large prismoidal triaxial rig at the University of Wollongong Australia and found that a geocomposite made from a 27 x 40mm aperture geogrid and a non-woven geotextile reduced the track settlement of wet recycled ballast from 22mm to 13mm

after 100,000 cycles of a 25 tonne axle load. Diversely the geogrid alone only reduced the settlement to 20mm after 100,000 cycles. Within the literature little work has been done to investigate the influence of subgrade properties on track performance and this is an area that has been researched thoroughly within this thesis.

3.2 GRAFT facility

3.2.1 Design and construction

The design of the test track facility at Heriot-Watt University has been limited to the available resources within the University to both manoeuvre and apply a cyclic load to such a facility. After considering many loading options, including purposely building a new facility and also adapting an existing slab testing facility at Heriot-Watt University, the recently (2007) upgraded Losenhausen UPS200 (LOS) testing machine was considered the most feasible option.

The LOS testing machine can support the required loading of the test track through a strong 2.1m x 1.9m x 0.5m thick base and cross head reaction frame. However, due to this reaction frame, the size of specimen that can be tested within the LOS machine is limited to a maximum width of 1.072m and a height of 2.45m. Further design limitations to the test track were dictated through the lifting facilities in the heavy structures lab as only two 5 Tonne capacity cranes are available for lifting the test track into position on the LOS machine base; when both cranes are in operation together their capacity is reduced to 7.5 Tonnes.

Figure 3.1 illustrates the LOS testing machine in its original upgraded condition as of January 2008. The cross head and grips of the LOS can be moved to allow different types of specimens to be tested within the machine. Figure 3.1 shows the bottom and top grips of the LOS, which can be used to grip specimens and apply either tensile or compressive loading. For the purposes of the GRAFT facility the bottom grip was removed and the top grip was used solely as an actuator to apply cyclic compressive

loading. The top grip cannot be removed, but it can retract inside the cross head up to a limit of 400mm from the bottom of the cross head. This was an important consideration in the preliminary design of the height of the test track facility.

Figure 3.1. LOS hydraulic cyclic testing machine in the heavy structures lab

The new GRAFT facility consists of a track constructed within a steel tank 1.072m wide x 3.0m long x 1.15m high constructed from five 6mm mild steel plates cut to size and double welded. The steel tank was designed to fit the dimensions of the LOS base and crosshead columns while also being capable of being lifted by the cranes in the laboratory. This led to a tank that weighs approximately 7.5 tonnes when a fully constructed track is within it. The tank is supported laterally from four 50 x 50mm steel angles around the top of the tank and two 127 x 64 x 14.9mm channel sections welded continuously around the tank at 200 and 500mm from the base of the tank. In addition, five 20mm steel tie rods are bolted laterally through the tank with three at 200mm from the base and two at 500mm from the base. In order to prevent the tank from buckling vertically while being lifted by the cranes a support lattice of two longitudinal 203 x 102

x 25.3mm joists and nine transverse joists were constructed and bolted to the bottom of the tank. Figure 3.2 shows the lifting frame and Figure 3.3 shows the tank being lifted into position under the loading actuator of the LOS machine via two lifting beams attached to the overhead cranes at either end of the lifting frame.

Figure 3.2. GRAFT tank lifting frame

Figure 3.3. Steel tank to hold track being lifted into position under loading actuator

The track constructed within the tank for the full-scale testing programme includes three 250mm x 125mm x 600mm length hardwood sleeper sections (five used in initial test trial) positioned at 650mm centres overlain by a 3m long I-section steel beam which has similar stiffness properties to a BS 113 A rail section, as shown in Table 3.1. The I-section beam (rail) was bolted to each sleeper section to prevent voids developing between the sleepers and rail and stop the rail from deviating from position.

Rail section	E (Young's Modulus N/m^2)	I (second moment of area m^4)	EI (bending stiffness Nm^2)
BS 113 A	2.10×10^{11}	2.349×10^{-5}	4.933×10^{6}
GRAFT I-Section	2.05×10^{11}	2.210×10^{-5}	4.531×10^{6}

Table 3.1. Comparison between typical rail section and I-section beam used in GRAFT

Once the tank is in place cyclic loading is applied to the centre sleeper directly under the LOS loading actuator. The LOS machine operates as a closed loop control hydraulic machine from 2 pumps and it has a 200 Tonne maximum capacity, of which 150 Tonnes can be applied cyclically. The LOS loading actuator can therefore easily apply realistic loads of both typical passenger and freight traffic, generating realistic stress levels in the ballast and subgrade layers. The response of the hydraulic actuator is controlled through a servo valve which reacts to an electrical signal command to deliver oil pressure and flow specifically to match that of the signal. The load and displacement transducers provide feedback to the controller for comparison with the command signal and a process of error reduction between the command and feedback signal is undertaken which maintains the required load or displacement applied by the actuator. The same servo-hydraulic feedback system is used by Brown *et al*. (2007a) to control their test facility at Nottingham University. It should be noted here that as the LOS machine only has one actuator to apply vertical compressive loads, the load contributions from either side of the centrally loaded sleeper from a rolling wheel are not taken into consideration.

At least three loaded sleepers are required to realistically monitor the response of the central sleeper to a rolling wheel load. This means that within GRAFT the loading mechanism replicates a repeated quasi static single wheel load on the central sleeper of one half of a 3m long section of railway track and the effects of principal stress rotation are not considered. The performance of the track is therefore based on the middle sleeper only.

The command signals for the actuator of the LOS machine are provided through a MOOG FCS controller, which is attached to a host computer where the control functions are replicated through MOOG FCS BaseTEST software (Kennedy *et al*., 2009b). Figure 3.4 shows the controller and host computer. The control modes available are either position (displacement) or force control and several safeguarding limits can be set up within these control modes. The controller is also used to tune the system through altering the settings of the control loop gains to find the optimum values for the particular specimen. To ensure correct performance of the actuator it is necessary to tune the system for each test specimen that has unique material characteristics such as stiffness, mass and damping. If the required bandwidth and sufficient stability cannot be achieved by tuning the feedback loop, the FCS controller system can incorporate amplitude and phase matching to achieve the required performance.

Figure 3.4. LOS machine controller and host computer

The frequency of the applied loads in the GRAFT facility was selected to be 3Hz as this frequency was found to operate best with the required load amplitude range. This frequency fits well with the predominant frequency of train induced loading, which is considered to be approximately 1 to 3Hz (Ghataora *et al*., 2004). This frequency is dependent on the speed of the train and the axle, bogie and coach spacing's. Priest *et al*. (2010) found that on a section of track with an average line speed of 50km/h, pairs of bogies at the ends of adjacent wagons had a loading frequency of 1Hz, although individual bogies and axles had loading frequencies of 2Hz and 6Hz respectively. This complex loading mechanism cannot be simulated in GRAFT. To the Authors knowledge no other railway track testing facility applies the loading frequencies required to model the track exactly. Therefore, the loading frequency in GRAFT does not directly relate to a particular train speed, although it is within the loading frequency experienced on track from a typical low to medium speed train (represents repeated quasi static single wheel loading). To simulate the dynamic effects from higher train speeds the load can be increased in GRAFT according to the DAF empirical equations presented in Chapter 2. The effects of high speed train traffic on soft subgrade soils have not been studied within this thesis and the train speed is not considered to be approaching the track critical velocity, where subgrade improvement may be required due to wave propagation effects.

Using GRAFT initially it was thought that a loading amplitude range from 0 up to 12.5 tonnes was required to simulate an axle load of 25 tonnes (maximum axle load permitted on UK line) being repeatedly applied to the track. However, the LOS machine cannot fully decrease the load applied to zero during cyclic loading as tensile drift of the system can occur when no load is applied; this results in the actuator lifting off the track. Therefore, a sinusoidal loading range from 5 to 130kN was adopted for the initial tests, which represents a 5kN seating load. On subsequently undertaking Finite Element (FE) analysis of GRAFT using the basic static code SART3D (explained within Chapter 7) it was found that induced track stresses for the GRAFT model with a 90kN actuator load, and not a 130kN load as initially thought, match favourably with induced stresses found from a free field track model with a 25 tonne axle load and a 1.2 DAF (25 x 1.2 = 30 tonnes). 40,000 cycles in GRAFT at 90kN is therefore the equivalent of one million

gross tonnes (MGT) of applied traffic in the field. This is due to a combination of only having three successive sleepers to distribute load and having short 600mm length wooden sleeper sections. Although the sleeper section lengths are designed to replicate one half of a twin block sleeper used in the rail industry (680mm length manufactured by Stanton Bonna, 2009), these twin block sleepers are concrete and 80mm longer and hence distribute the applied load better. The GRAFT sleepers were designed with consideration of the restricted width of GRAFT as they allow 230mm on either side of the sleepers between the end of the loaded sleepers and the tank walls. Using an approach adopted by Li *et al*. (2007), on research undertaken using a small test facility at Nottingham University, the 90kN GRAFT actuator load was confirmed. Li *et al*. (2007) used the following relationship:

Applied load in test = Axle load x Sleeper load factor x Load area stress factor x Dynamic load factor (3.1)

The sleeper load factor in GRAFT was taken as 85% due to reduced load distribution along successive sleepers as three sleeper sections were used instead of five (100% load distributed over five sleepers as found from FE analysis undertaken by Watanabe (cited from Profillidis, 2006)). Figure 3.5 shows the assumed load distribution along successive sleepers used in GRAFT. Analysis of the load distribution in GRAFT was undertaken to check this assumption and will be presented at the end of this chapter. The load stress factor was calculated from the deflection profile along a sleeper on the ballast surface after Selig and Waters (1994) and was approximated as 35% (50% load distributed under approx. 750mm of wooden sleeper length directly under the rail head). Figure 3.6 shows the vertical stress distribution in the ballast at the sleeper base contact according to Shenton (1974). It can be seen that the majority of the stress is distributed under around 70% of the sleeper. The dynamic load factor was taken as 120% and hence:

Applied load in GRAFT = 250kN x 85% x 35% x 120% = 89kN

As a result of this analysis the loading range applied for the majority of tests undertaken in GRAFT was from 5 to 90kN with a range of 5 to 130kN applied only in the initial tests and/or tests looking at higher axle loads/increased DAF (130kN actuator load = 37 tonne axle load with a 1.2 DAF or 25 tonne axle load with 1.75 DAF). It should be noted here that axle load calculations should only be used as a guide because the exact value depends on many factors, including type of sleeper, spacing and dimensions, rail used, subgrade quality etc.

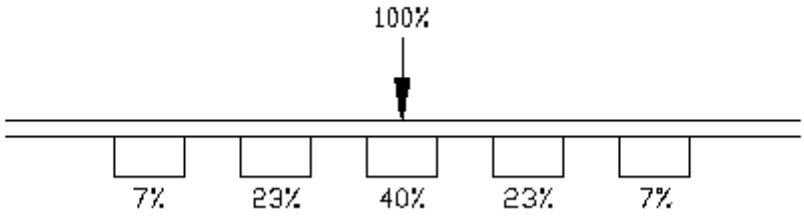

Figure 3.5. Axle load distribution along successive sleepers assumed in GRAFT (after Profillidis, 2006)

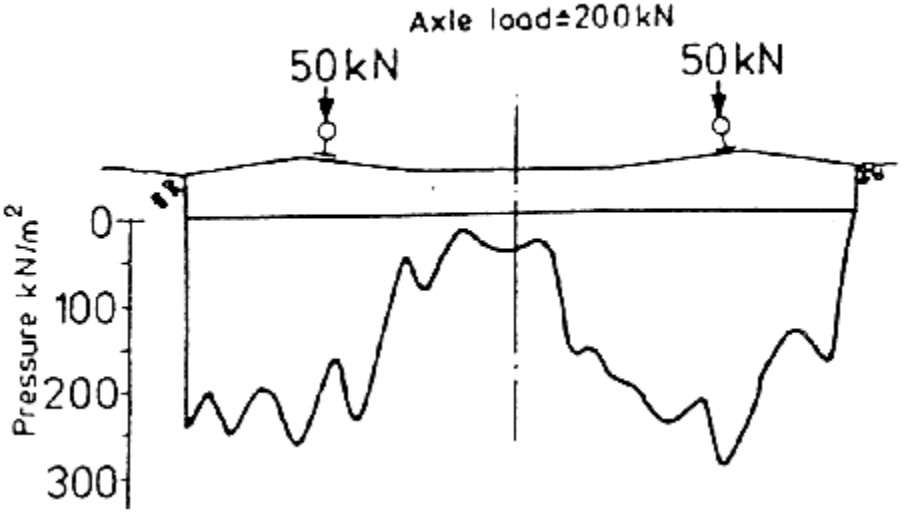

Figure 3.6. Sleeper base contact pressure distribution (Shenton, 1974)

To limit the lateral support provided to the substructure, from the rigid walls of the steel tank and to provide lateral support similar to the horizontal residual support experienced in the field, the tank was lined with 12mm thick neoprene rubber. Neoprene was chosen

for its low stiffness and high resistance to abrasion. FE modelling using SART3D was used to simulate the tank lined with neoprene and compare the induced track stresses with and without neoprene compared with a free field track. This analysis is presented in Chapter 7. The GRAFT facility can also incorporate a removable pipe running the length of the tank at a height of 850mm from the base (which acts as a drain) to enable flooding and drainage to be simulated during specific tests (Kennedy *et al*., 2009a).

During a test, the load and displacement transducer feedback signals from the actuator can be recorded on a separate 16Bit 200KHz PCI OMEGA data acquisition board (DAQBOARD 505) and host computer through BCN connections on the back of the MOOG FCS controller. The data acquisition board and computer are independent from the LOS controller and host computer. The data board can accommodate up to 16 single ended input channels which are controlled through DaqView software. DaqView is a 32-bit Windows-based data acquisition program that can be used to set up system parameters to acquire data from various transducer types. Once acquired, the data can be transferred to spreadsheets and databases for manipulation. During the GRAFT tests six input channels were used, two for the LOS actuator load and displacement feedbacks, two for 50mm Positek Ltd. P103 Linear Variable Displacement Transducers (LVDT's) set up 100mm from either end of the middle sleeper, one for a HLP190 50mm capacity floating LVDT, and one for an Applied Measurements Ltd. CCDG 100 tonne load cell placed between the actuator and the rail. The 100 tonne load cell and LVDT's provide an independent check on the load and displacement readings of the actuator (Kennedy *et al*., 2009a). For in-situ testing of track parameters before and after full GRAFT tests an additional input channel was used for an Applied Measurements Ltd. DSCC 100 Tonne capacity load cell.

The outputs from the instrumentation were connected to separate signal conditioning equipment prior to being connected to the data board. The signal conditioning equipment was used to excite and amplify the instrumentation, which connected via a terminal board and expansion cable to the data system. The signal conditioning equipment provides analogue outputs of + 10 and -10 Volts. These outputs connect to the specific analogue input channel and the analogue ground on the terminal board

respectively, as they are floating source signals. The signal conditioning equipment used included a Unimeter XQL universal instrument that was used to excite the DSCC 100 Tonne capacity load cell and an RDP DATASPAN module which was used to excite the CCDG 100 Tonne capacity load cell. The Unimeter instrument includes preset programmes for load cells that only need to be selected while the RDP instrument has several panel controls to provide adjustment of fine gain, balance, calibration, and amplification. The LVDT's were excited from an external Thurlby Thandar instrument PL310 power source, which was set to supply 5 Volts. Figure 3.7 shows the data acquisition system including the signal conditioning equipment and terminal board.

Figure 3.7. GRAFT data acquisition system, signal condition equipment and terminal board

3.2.2 Instrumentation calibration

All the load cells connected to the DAQBOARD data acquisition system were calibrated from the calibrated 50 Tonne capacity Denison monotonic testing machine. For this purpose the Denison and load cell voltage outputs were connected to a remote computer through a USB connected input board. The load cells output a voltage of 1V for an applied load of 100kN. The load cells were each loaded up to 500kN (capacity of Denison) and using the DaqView software the voltage outputs from both the calibrated Denison and load cell instrumentation were recorded simultaneously. Hence, the

specific load cell output voltage which relates to the applied load (kN) could be found. Figure 3.8 illustrates this relationship and the equations of the best-fit straight lines for the two 100 Tonne capacity load cells are shown. The fact that the 100 Tonne capacity load cells could not be calibrated beyond 500kN does not pose a problem as the maximum applied load in GRAFT is 130kN. The equations of the calibration lines shown in Figure 3.8 highlight that the average error is 0.44% for load cell DSCC and 0.36% for load cell CCDG, which is considered acceptable for these experiments.

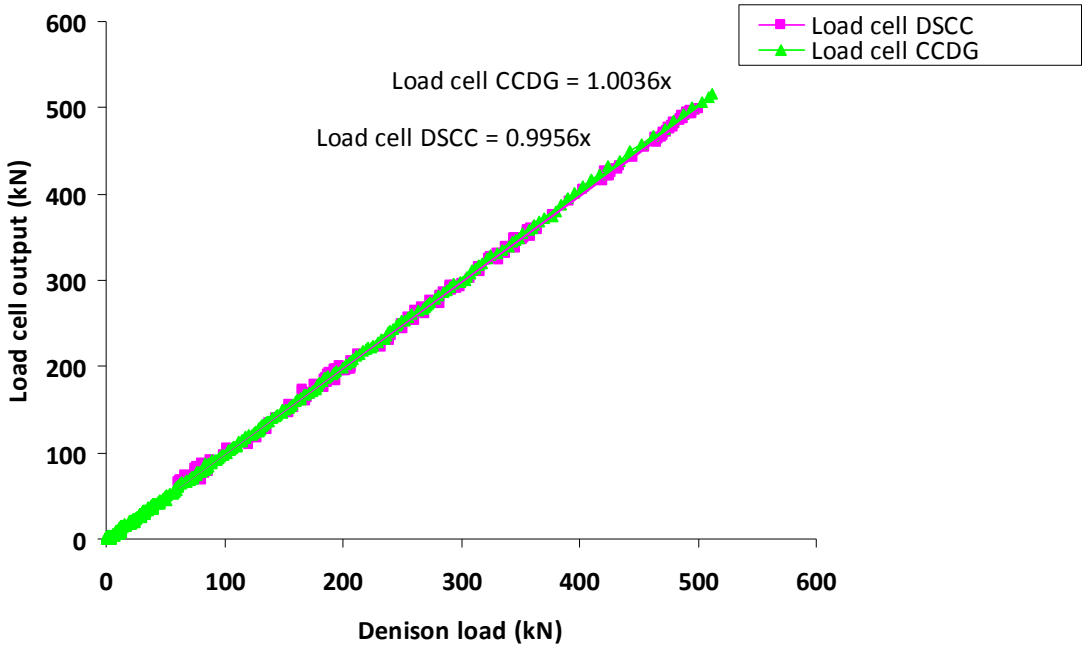

Figure 3.8. Plot of calibrated Denison load against output load from load cells

The two Positek Ltd. LVDT's (numbers 15327 and 15328) were supplied calibrated for a 50mm travel length and as such only a check of this calibration was required. A micrometer was used for this purpose and the supplied calibration for the two LVDT's was found to be accurate. The additional HLP190 LVDT was also calibrated using the micrometer and the calibration lines for the three LVDT's are shown in Figure 3.9. The average error was found to be 0.19% for the three transducers.

Although the LOS machine was calibrated by Systems Services Ltd. prior to being used an independent check was undertaken on the LOS applied load by loading the two calibrated load cells up to 750kN. Figure 3.10 shows the calibration results where the average difference between the LOS and the two load cells was found to 0.92%. Thus, the LOS and all the monitoring instrumentation were calibrated and the system was ready to be calibrated against a full-scale track test. However, prior to full-scale GRAFT calibration the initial track had to be designed and constructed. The next section describes the geomechanical tests that had to be undertaken to find the properties of the clay subgrade and ballast particles prior to initial track construction.

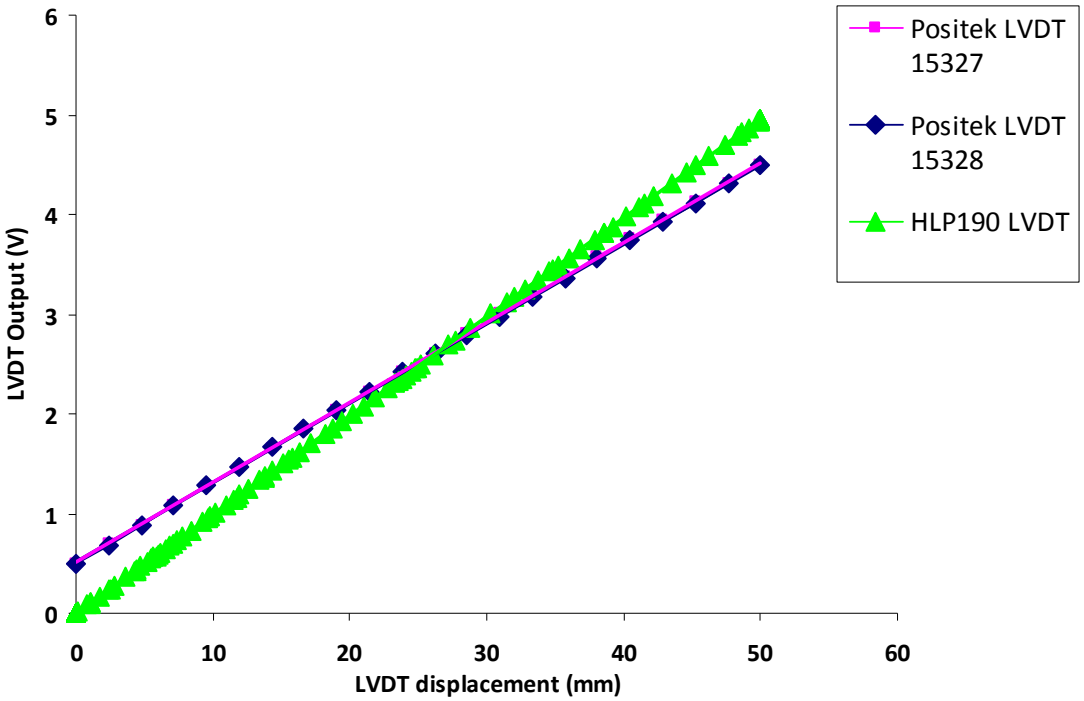

Figure 3.9. Calibration lines for LVDT's

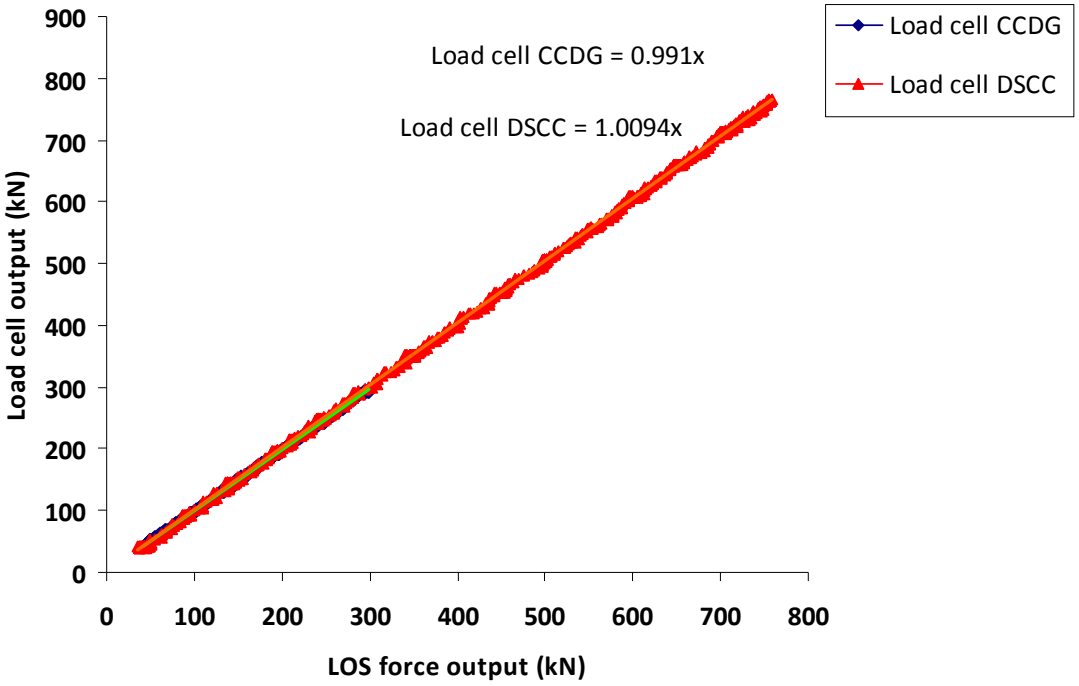

Figure 3.10. Plot of applied LOS load against output load from load cells

3.3 Geomechanical testing

Several geomechanical tests have been undertaken on the clay subgrade and railway ballast materials to be used in the full-scale testing programme. The properties determined dictate the sample preparation procedures and can be used as input parameters for the SART3D FE model of GRAFT, which will be discussed in detail within Chapter 7.

3.3.1 Kaolin clay tests

The clay material used for the track subgrade in the experimental testing programme is Kaolin clay. Tests undertaken on the Kaolin clay to determine how the clay should be prepared during track construction include Atterberg limits, Specific Gravity and compaction.

3.3.1.1 Atterberg limits

The Atterberg limits were an important consideration when deciding the moisture content of the clay subgrade to be used; to provide a workable yet stiff soil that could be easily compacted. BS1377: Part 2:1990 was followed for the determination of the Atterberg limits. The liquid limit (LL) of the Kaolin clay was determined using the cone penetrometer test based on the measurement of penetration into the soil of a standardised cone of specific mass. The cone penetrometer apparatus and Kaolin clay sample is shown in Figure 3.11. Five tests were undertaken in total and preparation for each test was undertaken from the bag, and the samples were not matured. The results of the LL test can be seen in Figure 3.12 where the average cone penetration of each test has been plotted against the moisture content of the sample and a best fit straight line has been drawn. The results show that at 20mm penetration the LL equals 55%. This value is consistent with past research on Kaolin clay by Lin and Penumadu (2005), Thu *et al*. (2006) and Sachan and Penumadu (2007) who found 53%, 51% and 62% respectively.

The plastic limit (PL) was found by hand rolling 3mm diameter threads of Kaolin clay until one crumbled. Two tests were undertaken and it was found that the average moisture content from the two tests at the plastic limit was 32%. This value is consistent with past research on Kaolin clay by Lin and Penumadu (2005) and Sachan and Penumadu (2007) who found 31% and 32% respectively. From these results the plasticity index (PI) can be determined as 23% (LL-PL).

Figure 3.11. Cone penetrometer test undertaken on Kaolin clay

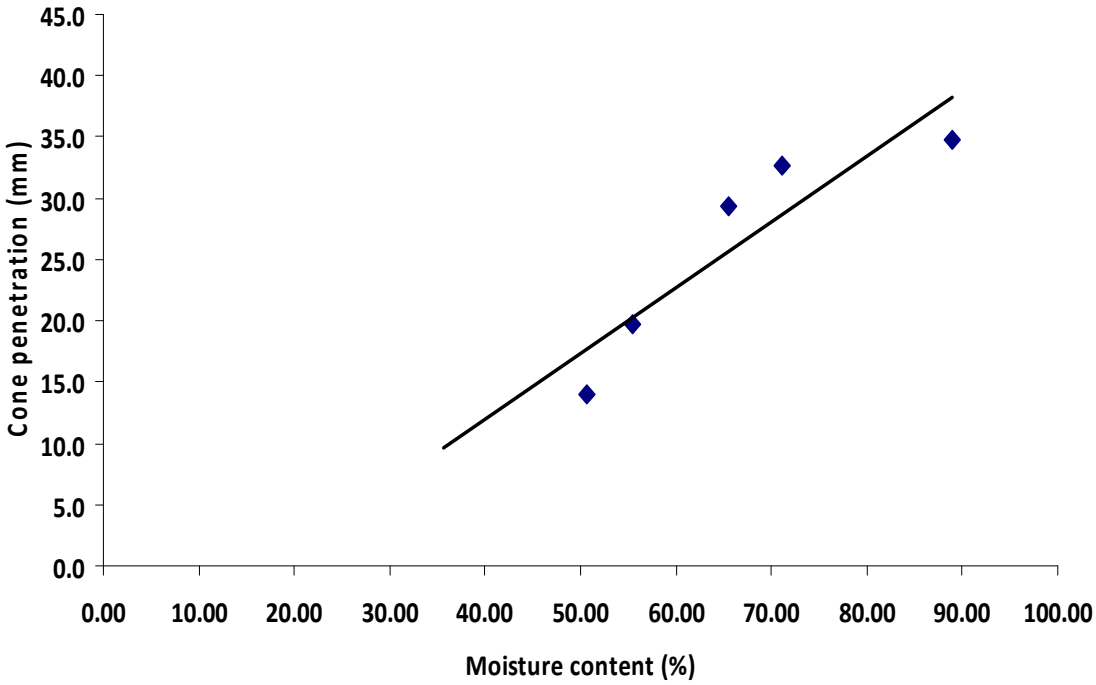

Figure 3.12. Cone penetrometer test results

3.3.1.2 Specific gravity

The Kaolin clay Specific Gravity (Gs) was determined by dividing the mass of dry clay particles in a slender glass cylinder by the mass of de-aired water displaced by the dry clay particles. The test was repeated eight times for accuracy and the results are shown in Table 3.2. The average clay Gs found from the tests was 2.50. Comparing this to published Kaolin clay Gs values from Lin and Penumadu (2005) and Sachan and Penumadu (2007) who both found 2.63, shows that the Gs value found from these tests is slightly lower. Nonetheless, a value of 2.50 was adopted as the Specific Gravity of the Kaolin clay used in these experiments.

Mass of soil (g)	Mass of water displaced by soil particles (g)	Gs
10.4	4.2	2.48
9.60	3.6	2.67
13.2	5.5	2.40
17.1	6.8	2.51
10.3	4.1	2.51
11.9	5.1	2.33
7.70	3.0	2.57
7.60	3.0	2.53

Table 3.2. Kaolin clay Specific Gravity test results

3.3.1.3 Compaction test

In order to determine the amount of water to add to the Kaolin clay to achieve the maximum dry density two compaction tests were undertaken. The tests were undertaken following British Standard BS1377: Part 4 (1990) using an ELE International automatic compactor with a 2.5kg rammer falling from a height of 300mm to compact the soil in three layers into a CBR compaction mould. Sixty two blows were administered to each

layer from the compactor. The automatic compactor and CBR mould are shown in Figure 3.13.

The first test undertaken ranged from 11.8% initial moisture added to 24.4% moisture in 6 increments while the second test ranged from 17.3 to 24.9% in 10 increments. The increased increments in the second test were intended to accurately find the optimum moisture content and maximum dry density. The results from the second test are shown in Figure 3.14 and the maximum dry density was taken as 1.54Mg/m³ at an optimum moisture content of 23.7%. The maximum void ratio was found to be 0.628 occurring at 94.3% saturation and the corresponding bulk unit weight was found to be 18.6kN/m³.

Figure 3.13. Automatic compactor and CBR mould

Comparing the results to published Kaolin clay compaction results of Thu *et al*. (2006), who found a maximum dry density of 1.35 (Mg/m³) and optimum water content of 22%, and Rammah *et al*. (2004) who gave the value of 1.54 (Mg /m³) as the maximum dry density and 23% as optimum water content, shows that the measured results are

consistent. The results were therefore considered to give an accurate representation of the dry density/moisture content relationship and 23.7% was adopted as the optimum moisture content to which the Kaolin clay was compacted to form the track subgrade in GRAFT.

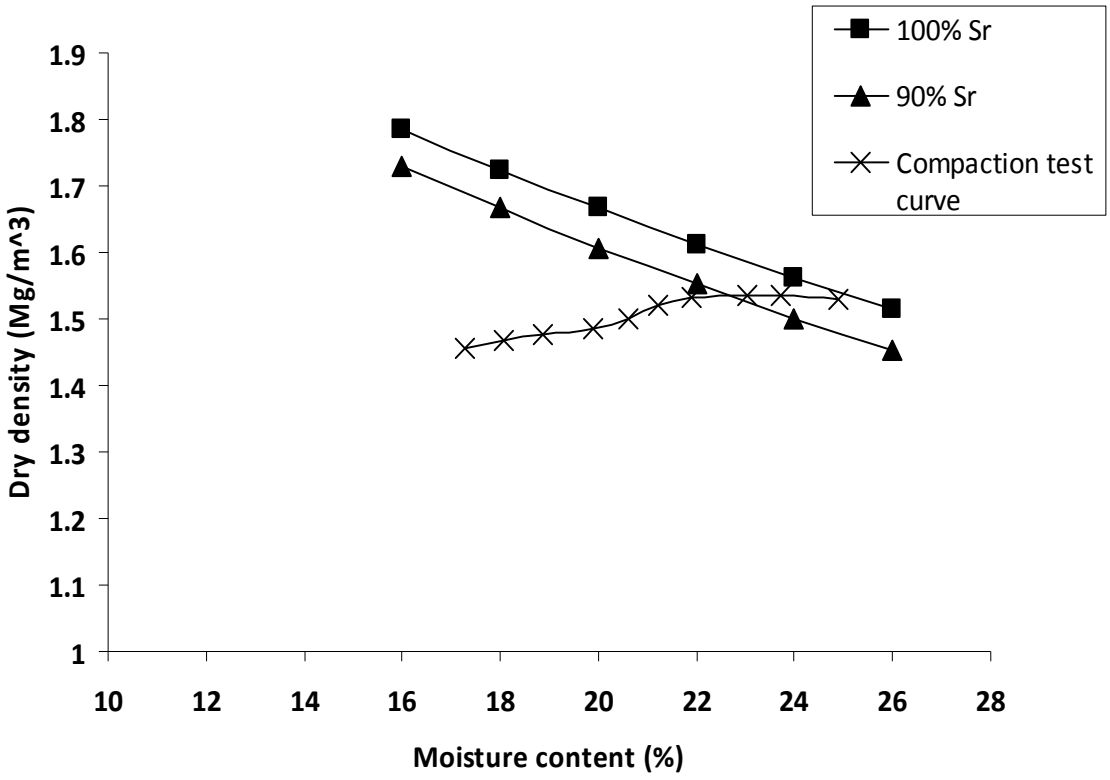

Figure 3.14. Kaolin clay compaction test curve

3.3.2 Ballast tests

The ballast material used in the experimental programme was from Cloburn quarry located outside Edinburgh where they operate a railhead transfer site for long term use by Network Rail (Cloburn Quarry Company Ltd., 2009). In order to determine the ballast properties several tests were undertaken including Specific Gravity, large shear box and particle distribution tests.

3.3.2.1 Specific Gravity

The Specific Gravity of the ballast was determined in the same way as the Kaolin clay, by dividing the mass of dry ballast particles in a large steel container by the mass of de-aired water displaced by the dry ballast particles. The test was repeated eight times for repeatability and to enable a representative sample of the large ballast particles to be tested. The results are shown in Table 3.3.

The average ballast Gs found from the tests was 2.65. This value matches well with Ionescu (2004) who quoted a value of 2.67 for fresh ballast in his study of the engineering behaviour of ballast. The ballast Gs value of 2.65 was adopted and used in these experiments.

Mass of ballast (kg)	Mass of water displaced by ballast particles (kg)	Gs
4.17	1.56	2.67
4.89	1.89	2.63
3.82	1.45	2.64
4.72	1.83	2.58
3.08	1.13	2.73
5.10	1.93	2.65
4.19	1.59	2.64
5.21	1.97	2.65

Table 3.3. Ballast specific gravity test results

3.3.2.2 Large shear box

To find the strength of the ballast the large shear box testing equipment in the geotechnics laboratory was used. The large shear box has a sample area of 300x300mm and can be seen below in Figure 3.15. The test was undertaken following BS1377: Part

7:1990 and the ballast was compacted in three layers to achieve a bulk density of 13.6kN/m³. Vertical loads of 20, 30 and 40kN were applied to the ballast with a horizontal force applied at a constant rate of 2.5mm/min until the sample failed in shear.

Figure 3.15. Large shear box equipment

Figure 3.16 shows the Mohr-Coulomb failure envelope found from the shear box test at increasing vertical stresses with corresponding increasing failure stresses. The equation of the best fit line of the failure envelope can be used to find the peak angle of shearing resistance, which was found to be 57.1° (assuming cohesion = 0). However, past studies on the shear behaviour of granular materials have shown that the Mohr-Coulomb failure envelope is curved (Ionescu, 2004). This curvature has been associated with the crushing process of grains (Ionescu, 2004). The likely Mohr-Coulomb curved failure envelope has also been plotted in Figure 3.16. For new ballast the peak angle of internal friction typically ranges from 48° (Suiker *et al*., 2005) to 55° (Indraratna *et al*., 2006) and decreases to around 44° after continual train loading on track due to the effects of particle breakage (Indraratna *et al*., 2006). It should be noted here though that undertaking a triaxial test is the typical method for determining the ballast friction angle as the large shear box apparatus should only be used for particles up to 37.5mm (Head, 1988). Furthermore, failure may not occur along the weakest plane in the shear box test due to the predetermined horizontal failure plane. Thus, the ballast strength found here is only an indicative value (an extremely large diameter triaxial cell was not available).

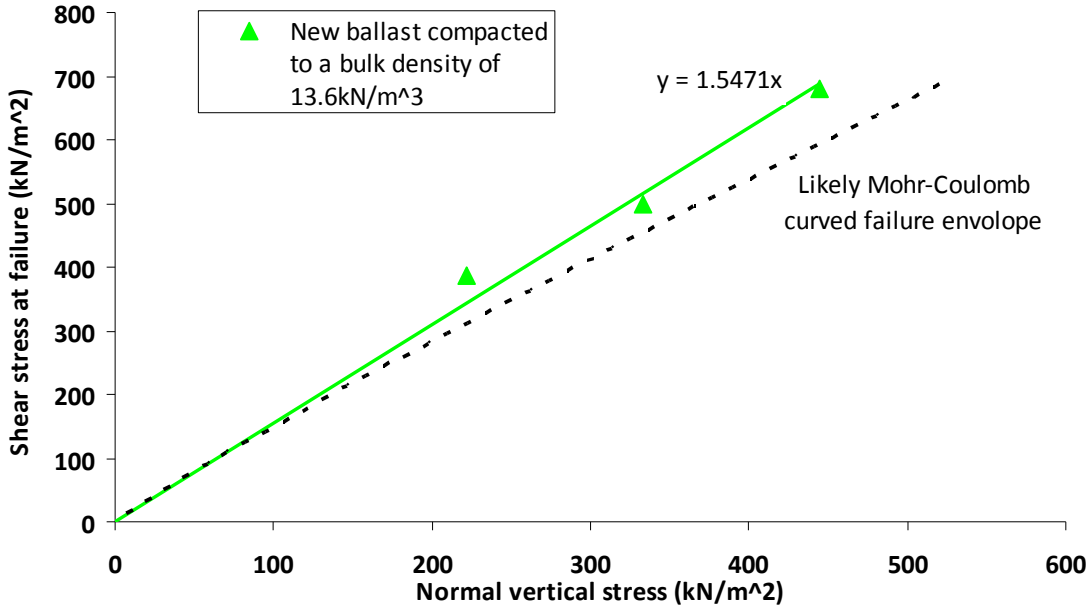

Figure 3.16. Mohr-Coulomb failure envelope for new ballast

3.3.2.3 Particle distribution

A particle size distribution (PSD) test was undertaken to determine the relative proportions of the different grain sizes that make up the mass of railway track ballast. The test was carried out to British Standard BS812 Section 103.1 (1989) as specified in the Network Rail line specification for track ballast RT/CE/S/006 (2000).

As ballast particles are predominantly large particles consisting of a mixture of sizes between 32 and 50mm a large quantity of ballast was required for the PSD tests to produce representative results. From BS812 (1989), 35kg was the minimum mass of ballast required to be taken for sieving and as a result seven tests of 5kg each were required. Each 5kg sample was passed through the nested set of sieves with diminishing apertures and mechanically sieved for 10 minutes using the vibrating shaker in the laboratory.

The particle size distribution of the ballast is plotted in Figure 3.17 along with Network rail maximum and minimum specifications for rail track ballast (RT/CE/S/006). It can be seen that the ballast has a mixture of sizes mainly between 37 and 55mm. The ballast

used in these tests is at the larger end of the permitted sizes in the UK, which is consistent with the upper range value found for the friction angle. It is evident however that the particle distribution curve can only be an approximation due to the physical limitations on obtaining a statistically representative sample, the practical limitations of using square sieve mesh openings for irregularly shaped soil particles and the limit on the number of sieves that can be used in a stack for the analysis (Bowles, 1992). The quantification of the range of particle sizes and the relative uniformity found in the ballast is shown in Table 3.4. It can be seen that the ballast has a Coefficient of Uniformity (Cu) value less than 2 indicating that the D10 and the D60 values do not differ appreciably and consequently the ballast is uniformly graded. Furthermore, a Coefficient of Curvature (Cc) value close to 1 signifies that the majority of particle sizes fall between the D60 and D10 sizes and the gradation will be a straight line between the D10 and D60 particle sizes, as can be seen in the particle distribution curve.

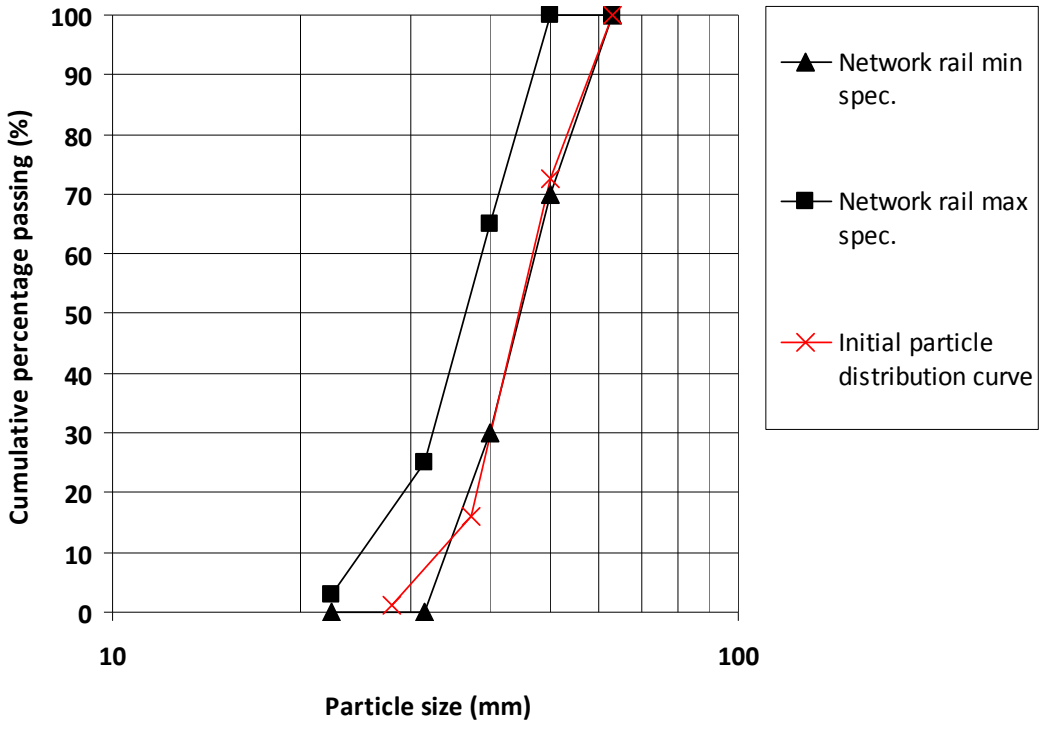

Figure 3.17. Ballast particle distribution curve

Ballast property	Value
D50 (mm)	45.0
Cu	1.42
Cc	1.06

Table 3.4. Ballast properties obtained from particle size distribution test

Once these geomechanical tests were complete an initial track was constructed in GRAFT with the geomechanical properties of both the Kaolin clay and railway ballast found from these tests used to determine the sample preparation procedures. The next section describes the construction of the initial track in GRAFT and presents the results of the initial GRAFT validation test.

3.4 Initial track construction and GRAFT validation

A summary of the Kaolin clay properties found from the laboratory geomechanical tests is shown in Table 3.5. To construct the initial subgrade in GRAFT the clay was mixed, from dry, with water in a large mechanical mixer at a moisture content of 27% in order to achieve a maximum dry density after compaction, allowing for some drying out between mixing and compaction. The clay subgrade was initially compacted in five layers using a Kango hammer up to a depth of 644mm. The subgrade was then compacted in four sections with the LOS to a final depth of 585mm. The average moisture content found for the subgrade layers after compaction was 23.8% giving a relative density of 90.2%, initial void ratio of 0.81 and degree of saturation of 73.8%.

Unconfined compression tests were undertaken on samples from the clay subgrade surface after compaction following a procedure described by Head (1982) based on ASTM Designation D2166. To extract the samples a 76 x 38mm mould was used and the cylindrical samples were extruded from the mould and compressed to failure in a 5kN capacity loading machine at a rate of 1mm/min. Figure 3.18 illustrates a typical sample under test. The load and displacement outputs from the machine were recorded

on a separate computer and the result found from the initial subgrade test is shown in Figure 3.19, which shows an unconfined compression strength (q) of 284kPa. This graph assumes that the subgrade is unsaturated and hence no correction is made to take into account the effect of barrelling of the samples during compression. It should be noted here that the sample taken may have been disturbed during coring and extrusion from the mould, and hence the compression strength value can only be regarded as indicative. In subsequent tests three samples were taken from across each layer and an average value was found to determine the unconfined compression strength of each clay layer. The full GRAFT track preparation procedures adopted for the full testing programme are described at the end of this section. These procedures were determined after the initial validation test.

In addition to the unconfined compression strength, pocket penetrometer and proving ring penetrometer readings were also taken to measure the clay strength. Twenty one pocket penetrometer readings and five proving ring penetrometer readings were taken across the full subgrade layer. Based on experience of using the three methods to estimate the strength of Kaolin clay throughout this research, it was thought that the unconfined compression strength values were the most accurate. Throughout this thesis the unconfined compression strength values have been used as an indicative value of the clay strength. Full details of the in-situ geotechnical testing devices used in GRAFT are given in Chapter 6.

Characteristic	Value
Specific Gravity	2.50
Maximum dry density (Mg/m³)	1.54
Optimum moisture content (%)	23.7
Liquid limit (%)	55.0
Plastic limit (%)	32.0
Plasticity index (%)	23.0

Table 3.5. Kaolin clay characteristics (Kennedy *et al*., 2009a)

Figure 3.18. Typical unconfined compression test on clay sample

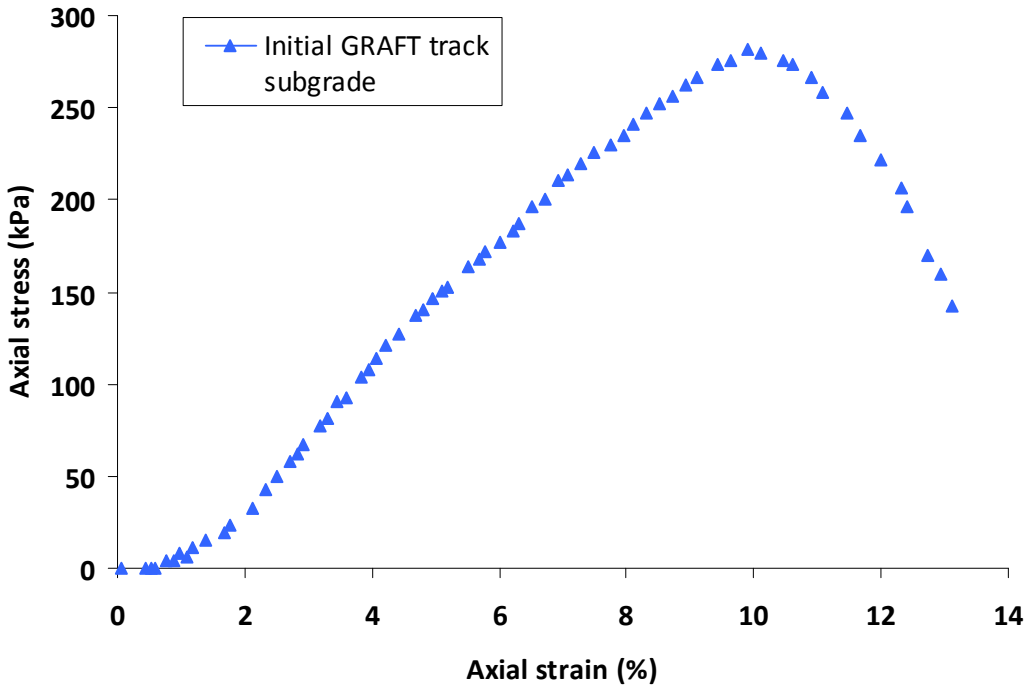

Figure 3.19. Initial track subgrade unconfined compression test result

In order to measure the subgrade stiffness a plate load test (PLT) on the subgrade surface was undertaken following BS EN1997-2: 2007. The PLT consisted of applying load from the LOS actuator onto a series of stacked circular plates (440mm diameter steel plate on subgrade surface overlain by a 400mm diameter load cell and three 300mm diameter steel plates) in the middle of the tank and measuring the corresponding deflection of the bottom plate. Two LVDT's were placed on the bottom plate to measure deflection. A typical PLT undertaken in GRAFT is shown in Figure 3.20. The influence depth of the PLT is considered to be about two times the diameter of the plate (Ping *et al*., 2002). This includes the full depth of the subgrade in GRAFT.

To produce an accurate load-deflection curve an initial 5 monotonic load cycles were applied at a rate of 1kN/s and then 50 cycles were applied at a rate of 0.1Hz. All data was recorded at 30Hz. The load applied was 15kN, which was calculated to prevent any significant plastic settlement of the clay surface and to provide a stress level beneath the bottom plate of around 100kPa. This is within range of the stress level experienced by a track subgrade under loading at 300mm below the underside of a sleeper (Okada and Ghataora, 2002, Brough *et al*., 2003).

Figure 3.20. Typical plate load test undertaken in GRAFT

An effective Young's modulus of the subgrade can be found using the following equation based on German standards for the design of pavement structures (Alshibli *et al*., 2005):

$$E_{PLT} = \frac{2P(1-\nu^2)}{\pi r \delta} \tag{3.2}$$

where E_{PLT} = Young's elastic modulus; P = applied load; r = radius of plate; ν = Poisson's ratio; δ = deflection of plate. Poisson's ratio was taken as 0.49 for the clay subgrade within GRAFT, to be conservative, even though the subgrade was considered unsaturated. Alshibli *et al*. (2005) undertook similar laboratory plate load tests and used the above equation to define both an initial elastic modulus from the tangent of the initial portion of the curve and a reloading tangent modulus from the reloading curve of the 2nd cycle. A similar methodology has been used here with the tangent modulus ($E_{PLT(t)}$) taken from the tangent drawn from the initial portion of the second cycle curve to determine the load and corresponding deflection to be used in the above equation. The second cycle was used for $E_{PLT(t)}$ to avoid any initial set-up effects on the results (plate-surface contact etc.). The reloading modulus ($E_{PLT(r)}$) was defined as the mean modulus value calculated over the 50 cycles applied at 0.1Hz. The load-deflection data for each of the cycles used in the equation to find the mean modulus was taken from the difference between the maximum and minimum applied load and resulting deflection for each cycle.

Typical load-deflection curves found from a plate load test in GRAFT are shown in Figure 3.21 where it can be seen that the reloading modulus after 50 cycles is slightly greater than after the first cycle. The load-deflection graph found from the PLT undertaken on the initial subgrade surface is not shown as data recording errors occurred during the initial PLT. Nonetheless, the subgrade tangent modulus could still be estimated from the manual recorded load and displacement readings and a value of 25MPa was calculated. This is typical of a soft subgrade where track deterioration problems can occur. In some subsequent tests further measurements of subgrade

Young's modulus were estimated using a Dynamic Cone Penetrometer (DCP) and a Light Falling Weight Deflectometer (LFWD). However, as these measurements were only undertaken during a few tests while the PLT was undertaken on every test the PLT values of modulus have been taken throughout this thesis as the standard. The results from the other measuring devices will be discussed in Chapter 6.

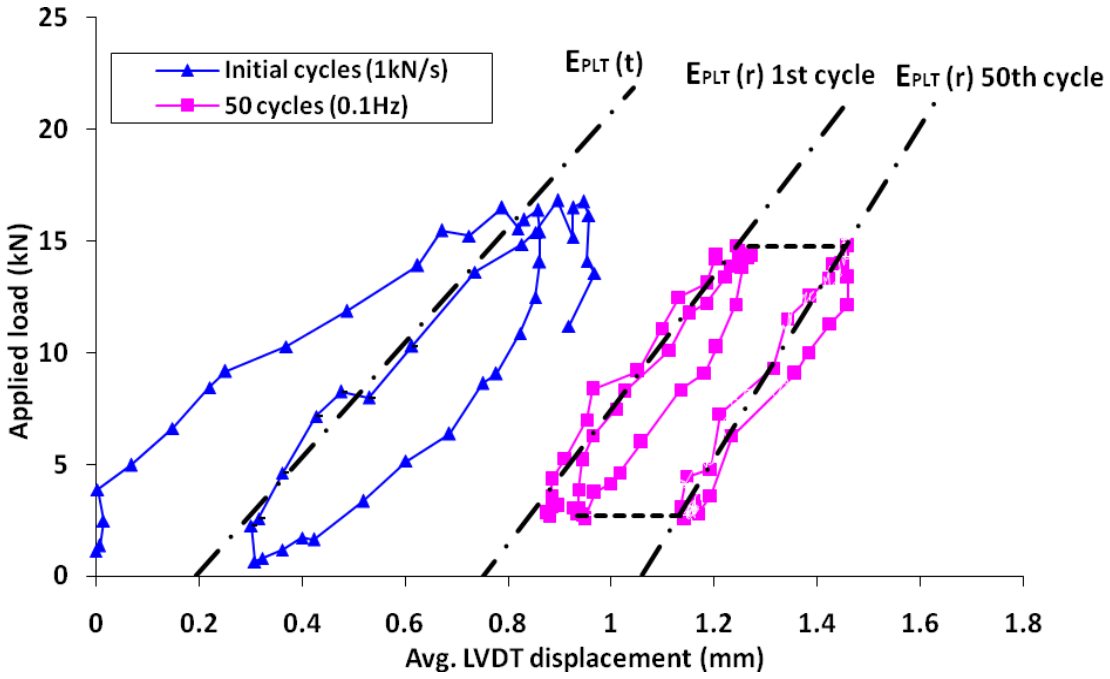

Figure 3.21. Typical plate load test result from GRAFT

Overlying the subgrade layer a 265mm deep Kaolin clay formation layer was placed and compacted in GRAFT. This initial formation layer was mixed at 30% moisture content and compacted in three layers to achieve an in-situ moisture content of 27.1% and an unconfined compression strength of 216kPa. Figure 3.22 shows the compacted formation layer for the initial track. The full formation layer was planned to be removed after each test and remoulded to the same initial conditions prior to placement for the next test. This was to prevent any significant change in strength and stiffness of the formation and subgrade layers between tests and allow a direct comparison of track performance between different tests to be measured. Furthermore, the formation layer could be changed to suit particular test conditions without overly influencing the properties of the subgrade.

Figure 3.22. Initial track compacted Kaolin clay formation

Overlying the clay formation layer 300mm of ballast was placed from the discharge spout of one tonne bags as shown in Figure 3.23. Once placed in tank the ballast was compacted in three 100mm layers using the same Kango hammer as for the clay. To achieve three equal 100mm layers the ballast bags were weighed using a load cell to achieve around 500kg per bag prior to placement (assuming a bulk density after compaction of around 1.60Mg/m^3). The 300mm ballast depth is the typical ballast depth on a UK railway line and hence this GRAFT test represents a typical UK railway track with a poor quality subgrade. A summary of the ballast properties is shown in Table 3.6. Subballast has not been used so as to ensure that only ballast and subgrade behaviour are investigated. After compacting the top layer of ballast, five (later reduced to three) hardwood sleeper sections were positioned at 650mm centres on the ballast bed. Further ballast was then placed between and around the sleeper sections to provide lateral stability and help prevent sleeper rotation during loading.

Figure 3.23. Ballast placement from one tonne bag

Characteristic	Value
Specific Gravity	2.65
Bulk density after compaction (Mg/m³)	1.64
Void ratio after compaction	0.64
D50 (mm)	45.0
Coefficient of uniformity	1.42
Internal friction angle (°)	57.1

Table 3.6. Ballast properties for initial GRAFT track (Kennedy *et al*., 2009a)

Once the sleepers were in place the I-section beam was located centrally across all five sleepers and the ballast was packed under all sleepers using the Kango hammer until the section was level. The top of the tank was used as a reference for the sleepers to level from and a system using string and weights was used to give a 'track geometry' reference. The full track was then lifted onto the base of the LOS machine with the centre sleeper directly under the loading actuator. Prior to loading, a 50mm thick steel

plate and a 200 tonne hemispherical bearing were fitted to the underside of the actuator to ensure that load is applied centrally during testing. Figure 3.24 shows the GRAFT facility with the fully constructed initial track ready to be loaded.

Figure 3.24. GRAFT facility ready for loading prior to initial validation tests (5 sleepers)

The first test provided validation of the GRAFT facility and the influence on the track behaviour of a range of actions was investigated including; the effect of tamping maintenance and the effect of pumping water through the tank under load. Furthermore, dial gauges were placed around the tank walls at mid height to check that no lateral displacement of the tank occurred under loading. Initially, a range of monotonic and cyclic tests of increasing amplitude and frequency were applied to the track to gauge the performance of the system. After tuning the system it was found that in order to achieve the required load amplitude range the maximum loading frequency possible was 3Hz. Thus, the testing routine decided upon for the first track tests was a cyclic sinusoidal loading range from 5 to 130kN applied at a frequency of 3Hz directly to the centre sleeper via the I-section beam.

During loading of the first track an initial 70,000 cycles were applied and Figure 3.25 illustrates the transient settlement development of the track taken at the minimum of the loading amplitude range at 5kN, as found from the actuator head readings. The actuator head measurements were used as the stands, set up to hold the LVDT's, were found to be unstable during loading (a new system for locating the LVDT's was later adopted). Comparing the results to other laboratory railway research (Indraratna *et al*. 2004, Ionescu, 2004, Ghataora *et al*., 2004, Aursudkij, 2007) the track behaviour exhibited here is similar with most of the settlement occurring early in the test before starting to stabilise. This is a result of initial ballast densification followed by a second stage settlement that develops as per a linear relationship with time/number of applied cycles (Dahlberg, 2001). A review of track settlement will be presented in Chapter 4.

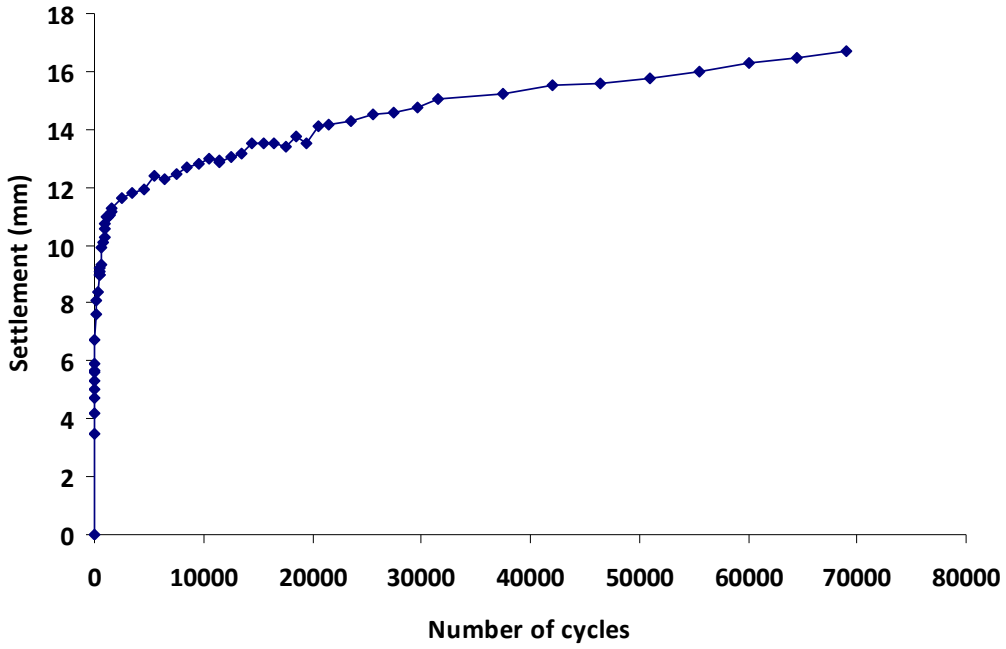

Figure 3.25. Development of middle sleeper settlement during initial test

After the initial 70,000 cycles the ballast layer was tamped beneath the sleepers using the Kango hammer to bring the track back up to level (i.e. correct track geometry) and a further 20,000 cycles were then applied. This process was repeated to see the effect of regular tamping maintenance on track settlement. The results from these cycles can be

seen in Figure 3.26 along with the settlement development of the track during flooding, which was undertaken after the tamping cycles. The settlement values shown are from the average of the two centre sleeper LVDT's relative to the LOS crosshead. For the flooding test water was pumped across the full length of the ballast layer from a container and the track drained water back into the container once the water head on top of the formation layer had reached a certain level. It took around 5000 cycles before any water started to drain from the tank and thus, around 50mm standing water was on top of the formation from 5000 cycles onwards. Pumping water through the tank was undertaken to replicate a fully saturated clay formation where settlement and clay pumping problems occur in the field.

Figure 3.26 shows that after the first tamping cycle the rate of settlement increases slightly, which is supported by Aursudkij (2007) and Selig and Waters (1994) who also found that tamping causes a faster rate of settlement. Figure 3.26 also shows that the rate of settlement during the flooding test is significantly higher and it illustrates that as the top surface of the formation layer becomes more saturated, the induced weakening causes the rate of settlement to increase. This condition causes a rapid deterioration of the track geometry and can create slurry that is pumped upward through the ballast under the action of loading (Selig and Waters, 1994). On removal of the ballast layer, after the flooding test, visual inspection found considerable penetration of the formation layer with ballast particles (Figure 3.27) and it was concluded that after 45,000 cycles the beginning of a slurry was forming. This is an important consideration for future tests as many geocomposite materials are now being developed to specifically prevent the pumping of slurry. One such geocomposite was tested in GRAFT (sand blanket replacement geocomposite) and the results are presented in Chapter 5.

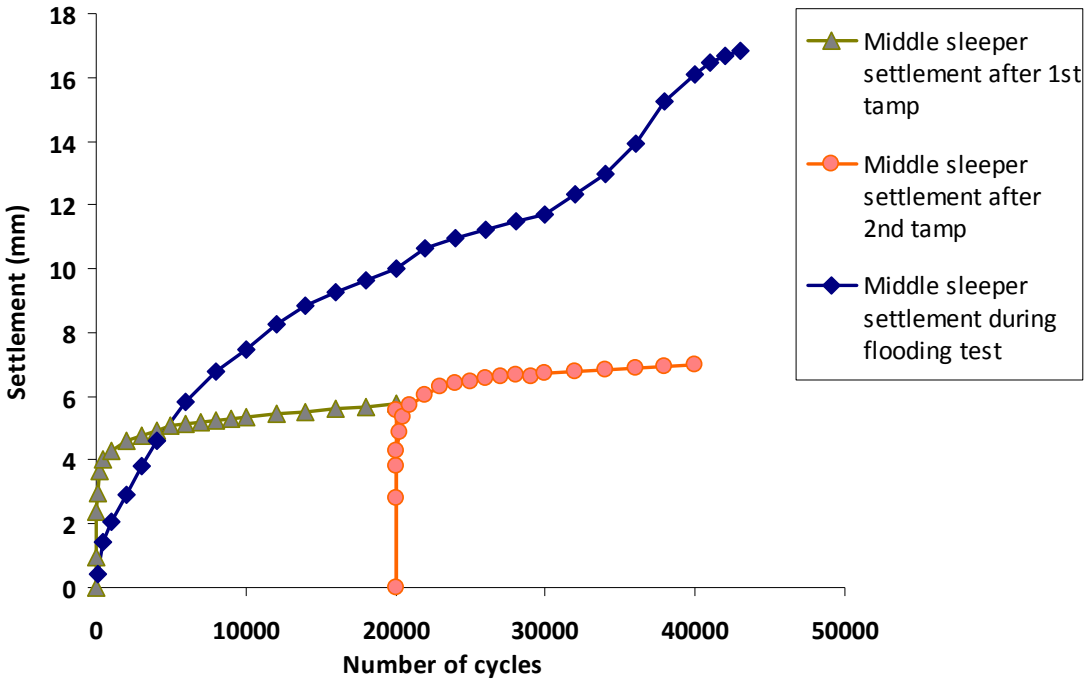

Figure 3.26. Development of middle sleeper settlement after tamping and flooding

Figure 3.27. Penetration of formation layer with ballast particles after flooding test

After completion of this initial validation test it was concluded that the GRAFT facility operated successfully and the orders of magnitude of initial track settlement data produced were appropriate for a typical railway track. Hence, these initial tests indicate that GRAFT can simulate realistic railway test conditions and can be used to simulate a range of track problems, including ballast/formation intermixing and poor track drainage that can result in subgrade erosion. Prior to the initiation of the full-scale testing programme however, several amendments were made to improve the track construction and testing procedures. These included changing the formation depth from 265mm to 70mm to save time on removing and replacing the formation layer for each test as replacing a full 265mm clay layer for each test was found not to be practical. This left the subsequent track with a 585mm layer at the bottom of tank (initial subgrade, q = 284kPa) overlain by a weaker layer from 585 to 750mm (new subgrade, q = 215kPa) overlain by an even weaker layer from 750 to 820mm (new formation, q = 162kPa).

Further changes included switching from 5 to 3 sleepers to prevent additional support from end sleepers being developed as the test proceeds and settlement occurs underneath the middle sleeper. This was found during the initial validation test after around 70,000 cycles where a void was visible between the underside of the I-section and the middle sleeper when the load was at a minimum of each cycle. To stop this occurring in future tests the three sleeper sections were bolted to the I-section to form a three sleeper track panel and hence, any void that was to develop would be underneath the centre sleeper, as occurs in the field. Figure 3.28, Figure 3.29 and Figure 3.30 illustrate how the track was constructed and loaded after the validation tests with three sleepers bolted to an I-section (rail). Furthermore, an electric plate vibrator was purchased to replace the Kango hammer and enable more uniform compaction of the formation and ballast layers. An electric plate was purchased as no fumes are permitted within the laboratory. However, as it can only provide around 40kPa of compaction force it was decided to compact the formation further with the use of the LOS machine. For each test the formation was compacted in four sections under a 100kPa cyclic load for 1000 cycles. Finally, a new system was adopted for securing the LVDT's.

Figure 3.28. Fully constructed track prior to loading - after validation tests (3 sleepers)

Figure 3.29. Track under loading - after validation tests (3 sleepers bolted to rail)

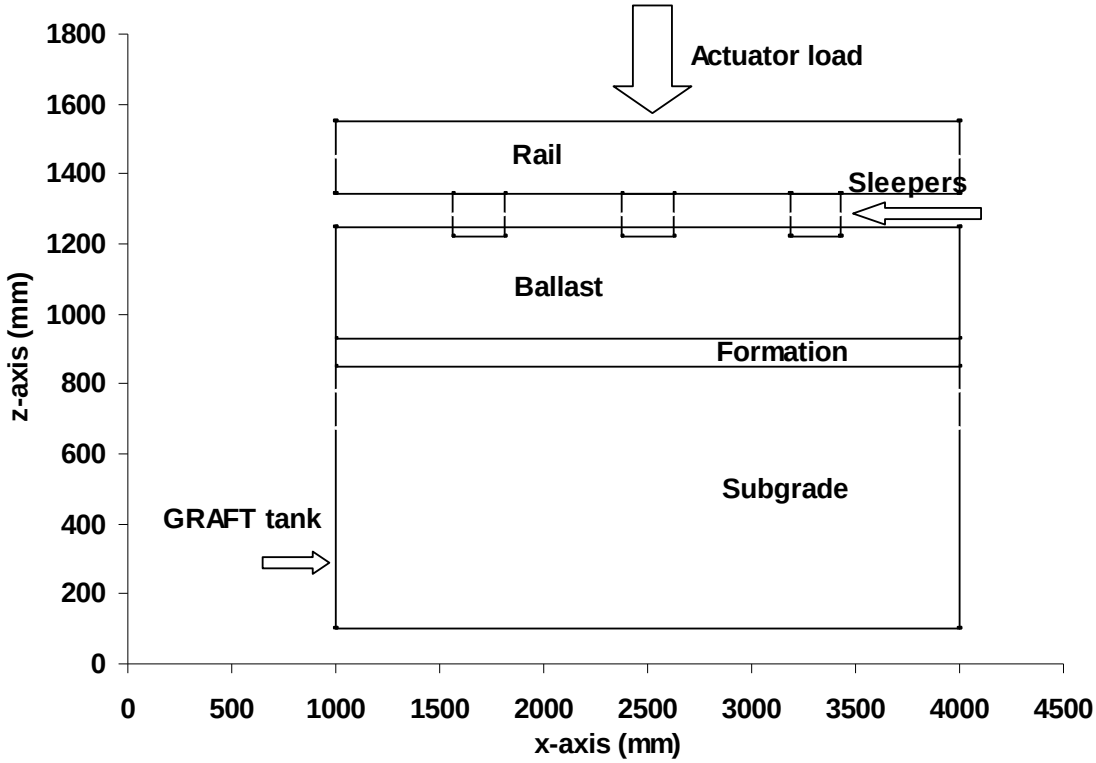

Figure 3.30. Cross section of GRAFT - after validation tests

On completion of the initial GRAFT validation test, a formal set of track construction procedures were developed that were followed for each track construction to help ensure consistency throughout the testing programme. The GRAFT track construction and test procedures were as follows:

1. Undertake PLT on subgrade (apply 100kPa load). Take moisture content samples and three unconfined compression test samples of subgrade surface.
2. Place 35mm clay layer (180kg) and compact in 0.75m length sections for five minutes per section using plate compactor. Check strength with proving ring penetrometer and pocket penetrometer, take height measurements and moisture content samples.
3. Place another 35mm clay layer and compact as in No. 2 above.

4. Move tank into LOS and compact in four sections to 100kPa (1000 cycles per section). Take proving ring and pocket penetrometer readings, height measurements, moisture content samples. Take three unconfined compression samples of formation.
5. Remove tank from LOS and place and compact the ballast in three 100mm layers (500kg/bag). Compact in 0.75m sections for five minutes per section with plate compactor. Calculate ballast density of each layer by measuring height after compacted.
6. Place track panel with three sleepers on ballast. Place crib ballast and Kango pack to achieve vertical geometry. Geometry taken from the top of the tank using string and weights.
7. Move tank back into LOS and put on monotonic load to bed track in (repeat 5 cycles). Repeat every day at the start of the test. Ignore first cycle settlement when plotting results as the track is bedding in (some variation in results due to nature of granular material regardless of preparation).
8. Test specific track sample for 0.5 million cycles at 3Hz (100,000 cycles per day). Stop cycles after 250, 500, 1000, 2000, 4000, 8000, 16000, 32000, 64000, 100,000, 150,000, 200,000, 250,000, 300,000, 350,000, 400,000, 450,000, 500,000 cycles to record permanent settlement.
9. At the end of the test remove ballast and test particle size distribution and shear strength under centre sleeper using a large shear box apparatus. Take 0.3m deep x 0.25m x 0.3m section from directly under centre sleeper for worst case.
10. Take three unconfined compression samples of formation. Measure formation height and take pocket and proving ring penetrometer readings.
11. Remove full 70mm formation layer and take moisture content samples. Measure subgrade height and take pocket and proving ring penetrometer samples.
12. Repeat procedure from step 1 if other tests planned or repeat step 1 if at the end of testing phase.

These track preparation procedures were followed to undertake a series of tests in GRAFT ranging from control tests to tests on various geosynthetic products. The next section describes the full testing programme undertaken.

3.5 Testing programme

The full scale test programme undertaken in this study is shown Table 3.7, in order of tests undertaken. For all tests the clay subgrade depth was 750mm with a formation depth of 70mm and ballast depth of 300mm. All the track properties shown in Table 3.7 were found from plate load tests and unconfined compression tests as discussed previously and these track properties represent typical clay subgrade and formation track properties found in the UK. The applied loading cycles is also typical of UK traffic tonnages, ranging from approx. 18.5MGT for the XiTRACK test (moderate to high tonnage (GC/RT5023)) to 0.25MGT for the geocell test onwards (low tonnage (GC/RT5023)). Additional in-situ test results found using different measurement devices are presented in Chapter 6, however these were not used to characterise the subgrade or formation layers.

In addition to the full scale individual tests undertaken in GRAFT an additional study was also undertaken to consider the influence on both the ballasted track and clay subgrade performance with variations in loading frequency and magnitude, for both single impulse and cyclic loading. The influence of ballast depth was also considered. Table 3.8 presents the specific details of the tests undertaken within the additional study, which was undertaken directly after 500,000 applied cycles in CT4. The results of this additional study are presented throughout Chapter 4.

The original purpose of the testing programme shown in Table 3.7 was to compare the performance (in terms of track settlement and stiffness) of different ballast reinforcement products (XiTRACK, geocell, reinforced geocomposite) and different products used to prevent clay slurry pumping into the ballast (sand blanket replacement geocomposite) to that of unreinforced track (control tests) with the same initial track properties. These tests concentrate on two separate railway track geosynthetic functions: ballast-clay interface separation and filtration to prevent subgrade attrition and slurry formation, and reinforcement of ballast to prevent ballast deterioration. However, as the tests were undertaken the programme evolved to take into account the unexpected changing subgrade properties.

Test	Subgrade tangent modulus (MPa)	Subgrade reloading modulus (MPa)	Subgrade unconfined compression strength (kPa)	Subgrade moisture content (%)	Formation unconfined compression strength (kPa)	Formation moisture content (%)	Actuator load applied (kN)	No. of load cycles applied
XiTRACK test	24.7	33.2	215	25.9	162	25.5	130	500,000
Control test 1 (CT1)	35.5	47.9	285	25.8	186	24.2	130	100,000
Geocomposite test (Part 1)	35.5	47.9	285	25.8	186	24.2	90	400,000
Geocomposite test (Part 2)	-	-	-	-	112	31.4	90	401,458
Control test 2 (CT2)	32.7	45.6	272	27.5	246*	27.5	90	500,000
Control test 3 (CT3)	51.4	66.7	302	25.4	199	24.8	90	500,000
Control test 4 (CT4)	61.1	91.1	344	24.0	173	24.1	90	500,000
Additional study using same track as CT4	See Table 3.8 for details							
Geocell test	65.3	87.9	239*	24.1	132*	23.7	90	10,000
Reinforced geocomposite test	-	-	-	-	-	23.3	90	10,000
Control test 5 (CT5)	-	-	-	-	-	22.5	90	10,000
After CT5	65.2	101.9	369	22.5	-	21.9	-	-

Table 3.7. Full testing programme with initial track properties for each test (*values are not considered accurate due to sampling errors)

Study	Rate of loading applied (Hz)	Load applied (kN)	Ballast depth (mm)	No. of load cycles applied
Rate and magnitude of single impulse load on ballasted track	0.02 to 6	50,70,90,110,130	300	-
Rate and magnitude of single impulse load on clay subgrade	0.25 to 20	5, 7.5, 10	-	-
Cyclic load magnitude on ballasted track	3	40,90,110,130	300	10,000
Change of ballast depth	3	40	250	10,000

Table 3.8. Test details for additional study after CT4

The order of the tests shown in Table 3.7 was determined from a combination of when specific equipment was available (XiTRACK test), external deadlines (geocomposite tests) and results found (from CT3 and CT4). The geocomposite tests after CT1 were undertaken to test a geocomposite designed to replace a traditional sand blanket used on the track. This test involved flooding the tank to produce a slurried formation (Part 1) prior to placing the geocomposite on the slurried formation to test its performance under loading (Part 2). Part 1 of this test was undertaken on the same track as CT1 after 100,000 cycles applied, hence the initial subgrade and formation layer properties are assumed to be same for both tests, as shown in Table 3.7. It should be noted here that the formation unconfined compression strength value given for Part 2 of the sand blanket geocomposite test is assuming that the formation is fully saturated. Full details of these sand blanket replacement geocomposite tests are presented in Chapter 5, along with the results from all other geosynthetic tests.

The reason that four control tests were undertaken was due to the increase in subgrade modulus throughout the testing programme until CT4. This was meant to be prevented by the formation layer; it can be concluded that replacing the 70mm thick formation layer was therefore insufficient. Nonetheless, the variation in subgrade modulus throughout the testing programme enabled the influence of subgrade modulus on track settlement and stiffness to be studied directly, which is presented in Chapter 4. After CT4 it was assumed that the subgrade had reached a resilient state and was no longer increasing significantly with applied load during tests. This was proven at the end of the testing programme with the subgrade modulus values after CT5 showing little change from before CT4 and before the geocell test. Therefore, in order to speed the testing programme up it was decided to use the same subgrade and formation layers after the geocell test for the reminder of the testing programme. The only difference between tests may be a slight increase in formation stiffness, but this was considered negligible and the whole clay layer was assumed to be in resilient state. As it was found in the early tests that track performance at the start of the tests was critical to performance over a larger number of cycles, only 10,000 cycles were undertaken on the last three tests.

The reason that the subgrade modulus and strength properties increase throughout the testing programme until the subgrade reaches a resilient state is thought to be due to cumulative subgrade compaction and consolidation with an increasing number of cycles applied and also due to small changes in the subgrade moisture content. Thomson and Robnett (1979) found a similar relationship revealing an increase in resilient modulus with an increase in unconfined compressive strength. The exception to this is the subgrade unconfined compression strength value found for the geocell test, which was thought to be due to a sampling error and can be ignored. The formation strength values shown in Table 3.7 are fairly consistent with the exception of CT2 (too high) and geocell test (too low). Again, it was thought that these values were a result of sampling errors. As a result the unconfined compression strength values found in GRAFT can only be regarded as indicative and the subgrade modulus values found from plate load tests have been used instead to describe the subgrade performance under load, as these values were considered accurate.

The indicative remoulded formation layer strength values were assumed to be constant within the range of 170 to 200kPa (+ or – 20%) throughout the testing programme. The low unconfined compression strength value given for the geocomposite Part 2 test was a result of flooding the tank in Part 1 of the test (formation assumed to be fully saturated). After Part 2 of the geocomposite test the subgrade had to be left to dry out considerably before a new remoulded formation could be constructed. However, the subgrade and new formation layer moisture content for CT2 (after geocomposite test Part 2) was still higher than any other tests, which influenced the measured subgrade modulus and strength values. Li and Selig (1994) stated that three major factors influence the magnitude of subgrade resilient modulus; the loading condition or stress state and the number of repetitive loadings; the soil type and structure; the soil physical state. The soil physical state was defined by the moisture content and dry density of the soil by Li and Selig (1994). A detailed study of experimental results by Li and Selig (1994) found that an increase in moisture content leads to a significant decrease in soil stiffness. The following correlations were proposed relating subgrade resilient modulus to soil physical state for specific stress conditions and soil type:

for the case of constant dry density;

$$\frac{M_r}{M_{r(opt)}} = 0.98 - 0.28(w - w_{opt}) + 0.029(w - w_{opt})^2 \tag{3.3}$$

where M_r = resilient modulus at moisture content w(%) and the same dry density as $M_{r(opt)}$; $M_{r(opt)}$ = resilient modulus at maximum dry density and optimum moisture content $w_{(opt)}$(%) for any compactive effort.

For the case of constant compaction;

$$\frac{M_r}{M_{r(opt)}} = 0.96 - 0.18(w - w_{opt}) + 0.0067(w - w_{opt})^2 \tag{3.4}$$

where M_r = resilient modulus at moisture content $w(\%)$ and the same compactive effort as $M_{r(opt)}$.

Using these correlations and the following relationship used by Li and Selig (1994) the resilient modulus can be estimated for each test at the breakpoint stress:

$$M_{r(opt)} = 30{,}800 + 677(\%clay) + 821(PI) \tag{3.5}$$

where $M_{r(opt)}$ = resilient modulus (kPa) at optimum moisture content and maximum dry density; % clay = % particles finer than 2 microns; PI = plasticity index, and the breakpoint stress = deviator stress at which the gradient of resilient modulus versus deviator stress changes. $M_{r(opt)}$ for the subgrade clay in GRAFT was estimated to be 117MPa at the breakpoint stress. The estimated resilient modulus values at the breakpoint stress for each test are plotted in Figure 3.31. These values were taken from the mean of the values found at both constant dry density and constant compactive effort and it can be seen that they generally follow the same trend as the measured PLT modulus values. It is thought that repeated loading of the track subgrade in GRAFT increased the subgrade stiffness due to a combination of a reduction in moisture content and an increase in dry density, while the influences of the change in stress state and soil structure cannot be calculated using equations 3.3 to 3.5.

The ratio of subgrade modulus (E) to unconfined compression strength (q) throughout the testing programme is shown in Figure 3.32. The values for the geocell test have not been included due to the error in the unconfined compression strength value for this test. Figure 3.32 is very similar to Figure 3.31 and hence, changes in subgrade moisture content and dry density due to repeated loading are thought to influence subgrade modulus to a greater extent than subgrade strength. As a result the E/q relationship is not constant as stated by Network Rail in NR/SP/TRK/9039 who use E/Cu = 250. If the subgrade was assumed to be saturated throughout the testing programme in GRAFT and barrelling was taken account of from the unconfined tests results, then the E/Cu relationship would range from around 400 at the start of the programme to 600 at the

end using the tangent modulus. However, as previously stated the unconfined strength measurements can only be regarded as indicative.

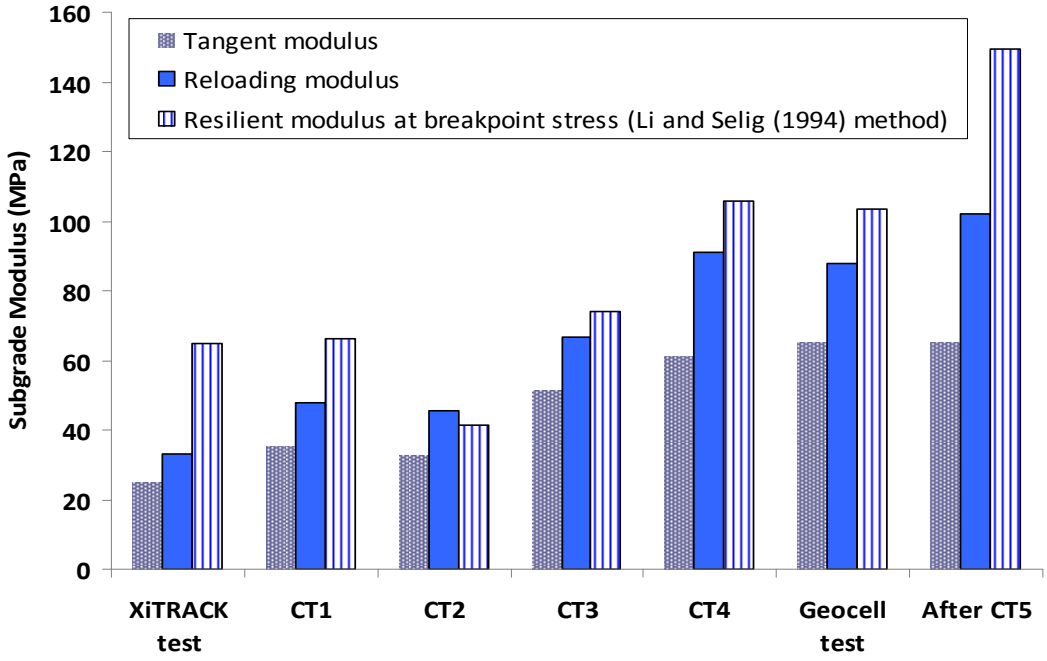

Figure 3.31. Variation of subgrade modulus throughout testing programme

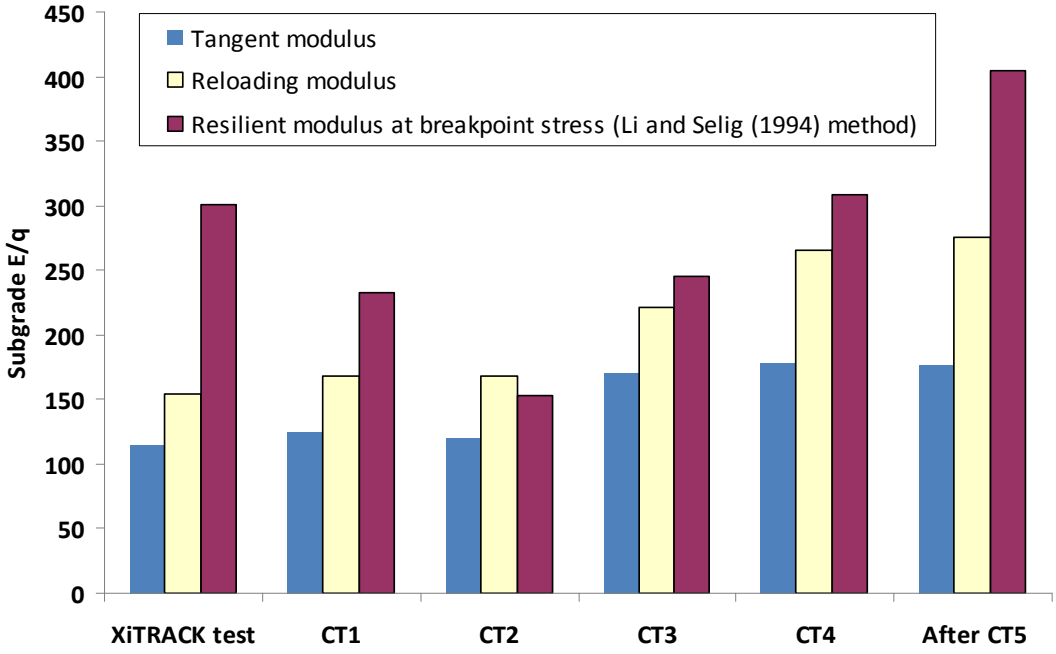

Figure 3.32. Variation of subgrade modulus to unconfined compression strength ratio throughout testing programme

The ballast D50 particle size and internal friction angle found after each test from the ballast sampling taken from directly underneath the centrally loaded sleeper is shown in Table 3.9. These tests were undertaken to monitor the condition of the ballast and it can be seen that there is very little variation in the ballast properties of the samples tested with exception of the ballast tested after the geocomposite tests (i.e. the flooding tests). This was a result of the abrasive slurry forming in these tests; after these tests the ballast had to be power washed and sieved to remove the slurry prior to being placed for the next test. Ballast breakage was also analysed after each test from the particle size distribution results. The results did not show any significant changes throughout the testing programme and hence it was assumed that the ballast properties remained the same throughout the programme. It was therefore assumed that the different applied loads, number of cycles applied and the different subgrade modulus values shown in Table 3.7 are the only significant differences between tests. It should be noted here though that this assumption was based on limited representative samples of ballast as it was not practical to test the whole ballast layer.

Ballast sample	D50 (mm)	Friction angle (°)
Original ballast	45	57.1
Ballast after validation tests	42	57.6
Ballast after geocomposite tests	39	54.1
Ballast after CT2	43	58.3
Ballast after CT3	44	61.3
Ballast after CT4	46	60.2

Table 3.9. Variation of ballast properties throughout testing programme

At the end of some tests the LVDT's were rearranged to enable the displacement of each sleeper to be monitored during cyclic loading. As the applied load is proportional to the deflection (Hunt, 2005) the load distribution over the three sleepers could be estimated. Figure 3.33 illustrates the deflection of the three sleepers under load for

different tests and for a different number of cycles. The different magnitude of deflections shown is due to different subgrade stiffness's and different applied loads for these tests, which will be explained in detail within Chapter 4. From Figure 3.33 the load distribution can be estimated in GRAFT for each test. Table 3.10 shows the average load distribution for different tests in GRAFT. Table 3.10 assumes that the load which is not carried by the middle sleeper is distributed evenly between the two adjacent sleepers. The results show that on average the central sleeper beneath the applied load carries 40% of the load while the adjacent sleepers carry 30% each. This matches well with several other researchers and it is generally accepted that the sleeper under load takes 40-50% of the load. Thus, the load distribution in GRAFT is considered accurate and the load applied to the middle sleeper in GRAFT can be estimated with confidence.

Hunt (2005) stated that typically the load is shared mostly between three sleepers with 40-50% beneath the loaded sleeper, however, as shown in Figure 3.5, FE analysis undertaken by Watanabe (cited from Profillidis, 2006) showed that the load is distributed over 5 sleepers, with 40% beneath the loaded sleeper. Using the SART3D FE code the load distribution in GRAFT was checked using both three and five sleepers and it was found that reducing from five to three sleepers increases the induced stress on the formation layer by around 15%. Hence, the end sleepers in a five sleeper GRAFT track account for around 7% load distribution each. This analysis is explained further in Chapter 7. A comparison of different load distribution results along successive sleepers, found from various researchers, is shown in Table 3.11. It is assumed that the load is distributed over either three or five sleepers and the distribution is symmetrical. From the GRAFT results it was thought that the Watanabe distribution was the most likely with 40% distributed to the middle sleeper, 23% distributed onto adjacent sleepers and 7% distributed to outer sleepers. As such this middle sleeper distribution was assumed throughout this thesis. It should be noted here though that the distribution depends on many factors, including type of sleeper, sleeper spacing and dimensions, rail type and size used, subgrade quality etc., and hence will vary slightly from track to track.

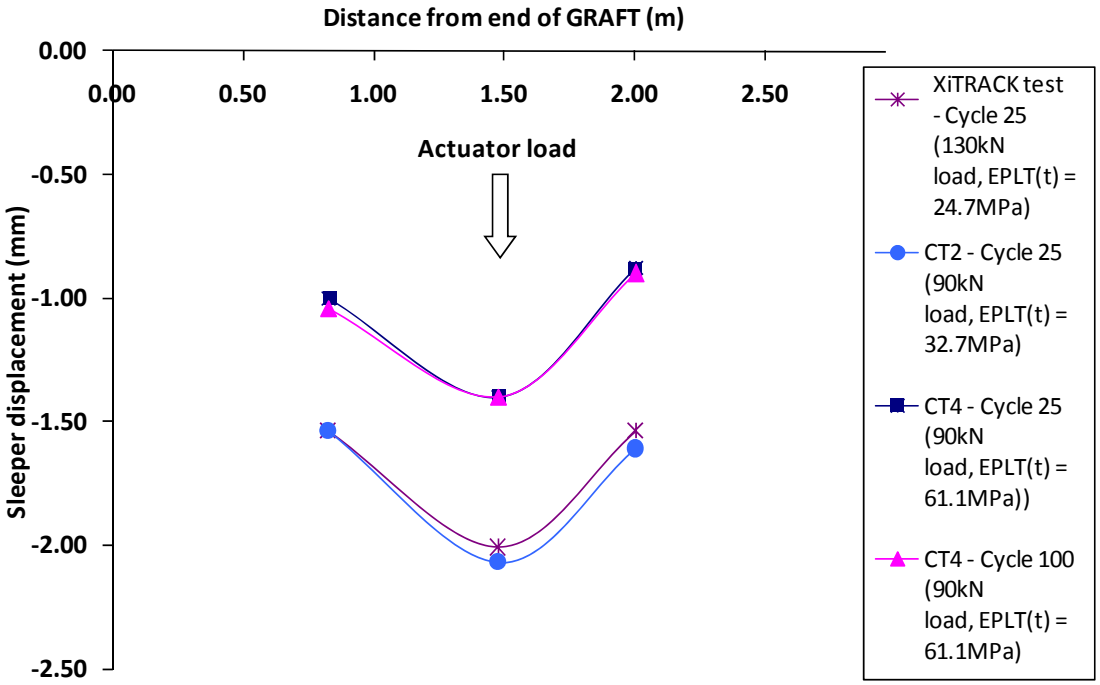

Figure 3.33. Load distribution over three sleepers in GRAFT (note: the applied load is higher in the XiTRACK test)

Test	Average centre sleeper load distribution (%)	Average adjacent sleeper load distribution (%)
XiTRACK test	37.0	31.5
CT1	37.0	31.5
Geocomposite test (Part 1)	42.0	29.0
Geocomposite test (Part 2)	38.0	31.0
CT2	43.0	28.5
CT3	40.0	30.0
CT4	40.0	30.0
Average	**40.0**	**30.0**

Table 3.10. Sleeper load distribution within GRAFT tests (from sleeper deflections)

Analysis	End sleeper load distribution (%)	Adjacent sleeper load distribution (%)	Centre sleeper load distribution (%)
Watanabe FE analysis (cited from Profillidis, 2006)	7	23	40
Awoleye (cited from Aursudkij, 2007)	0	25	50
Kwan 'beam on elastic foundation analysis' (cited from Li *et al*., 2007)	10	18	34
GRAFT experimental program (3 sleepers)	-	30	40
GRAFT FE analysis using SART3D	7.5	-	-

Table 3.11. Comparison of various sleeper load distribution analyses

3.6 Conclusion

This chapter has described the design, construction, and calibration of GRAFT and has set out the testing programme followed within this thesis. The testing procedures used to keep consistency throughout the testing programme have also been presented and an explanation of how the procedures evolved given. The initial limitations of testing in GRAFT have been overcome by lining the tank with neoprene rubber to reduce confinement effects from walls of the tank; by incorporating 600mm length sleeper sections (similar to twin block sections) to allow 230mm between the end of the sleeper sections and the tank walls (to reduce confinement affects and allow some tensile force development for reinforced geosynthetics in the transverse direction); and by focussing on the performance of the middle sleeper only and ignoring rolling wheel affects and the complex loading frequencies on track (1 GRAFT cycle = 1 wheel load).

This chapter has also shown how GRAFT can realistically represent different railway track conditions and is ideal for studying the performance of various innovative railway products used to solve various track problems. Within this research these have included a geocomposite separator to act as sand blanket to aid track filtration & drainage and to prevent the pumping of slurry; and reinforcement products to try and increase the strength and stiffness of the ballast layer and hence help prevent ballast deterioration. To this end, GRAFT can be used as part of a formal assessment procedure for track products prior to field trials.

As well as investigating products that can be used to improve track performance some of the fundamental track substructure properties and loading conditions that influence track performance can also been researched in GRAFT. Within this research the following parameters have been studied; subgrade stiffness, ballast depth, applied load, number of applied cycles, and rate of loading. Furthermore, GRAFT has also been used to assess different subgrade modulus in-situ testing technology including the standard Plate Load Test (PLT), Light Falling Weight Deflectometer (LFWD) and Dynamic Cone Penetrometer (DCP). Factors that have not been studied within this thesis and are considered to remain constant throughout testing programme include subgrade type and depth, ballast properties, rail type, sleeper type, sleeper spacing, sleeper dimensions, track irregularities, and other track construction components such as rail pads etc. The overall objective of the testing programme was to collect reliable and realistic data that could be used to work towards track design recommendations on how best to investigate and improve key geotechnical parameters that influence railway track performance and hence reduce maintenance costs and extend asset life. The next few chapters present the results from the testing program with the aim of investigating this objective.

Chapter 4 - Track Performance: Influence of Subgrade Modulus and Axle Load

4.1 Introduction

The performance of the railway track depends upon the interaction between the track support, the superstructure and the train vehicles. Many factors influence each of these interaction mechanisms and track performance can be separated into substructure deterioration (differential ballast and subgrade settlements) and superstructure deterioration (rail wear and fatigue, sleeper wear etc.). Within this chapter the influence of the subgrade Young's modulus and applied vertical load on track substructure deterioration of typical track sections is investigated. The track support characteristics and the applied load have a direct influence on substructure track deterioration. For example, Dahlberg (2001) found that track settlement is proportional to the fifth power of applied pressure and Brough *et al*. (2003) reported that a track section with track modulus of 14MPa required 183% more maintenance input than one with a track modulus of 27MPa. Furthermore, a sensitivity analysis using different track degradation models undertaken by Sadeghi and Askarinejad (2007) found that the allowable annual tonnage for a track with a good quality subgrade is 4 times more than that of one with a poor quality subgrade. Hence, optimum subgrade stiffness beneath railway tracks should significantly reduce maintenance frequency and increase total asset life depending on the applied load. Several other factors that influence substructure deterioration have also been considered and discussed within this chapter although are not fully investigated.

Substructure deterioration is a result of settlement of the substructure and while rail traffic can tolerate a certain degree of unevenness in the track, a point is eventually reached at which the track geometry has to be improved before differential track settlements give rise to faults in the vertical track geometry (Selig and Waters, 1994). Selig and Waters (1994) stated that for most tracks ballast is the main source of both

average and differential settlement between surfacing operations and is known as short term settlement, compared to long term settlement which is subgrade related. One reason is that, except for new track locations, the subgrade has been subjected to traffic for decades and hence subgrade settlement from repeated loading accumulates very slowly. Another reason is that, where subgrade settlements are large, the ballast depth is increased to compensate, eventually leading to a reduced rate of settlement. For ballast to be the main source of settlement the following three conditions are necessary (after Selig and Waters, 1994):

1. Existence of separation layer between coarse ballast and fine subgrade
2. Sufficiently strong subgrade
3. Good drainage of water entering from the surface

Otherwise track settlement and hence maintenance could be dictated by subgrade problems. Within this chapter the theory of both ballast settlement and subgrade settlement will be examined and how they relate to overall track settlement reported.

Settlement of the substructure is heavily influenced by vertical track stiffness as changes in track stiffness along the track can cause vehicle-track interaction dynamic forces and lead to differential settlement and potentially vibration problems. Vertical track stiffness is a combination of the stiffness of all the substructure layers and superstructure components, and the way the local stiffness of each layer/component combine determines the displacements of each layer (Berggren, 2009). For low stiffness, high ballast strains can occur and hence ballast settlement. Track stiffness is a complex and broad area and it is highly variable from site to site and even from sleeper to sleeper or from rail to rail. Berggren (2009) commented that the current understandings about track stiffness and its effect on track performance are insufficient, which is observed by the fact that currently there is no European standard for vertical track stiffness available.

It is known that track stiffness varies with frequency, dynamic amplitude and applied load (Hosseingholian *et al*., 2009) although recent research suggests that the subgrade is the most significant factor governing track stiffness and hence the deterioration of

vertical track geometry (Brough *et al*., 2006). This was also found in a review of track performance by Hunt (2005) who stated that the subgrade properties are the primary determinant of the overall track stiffness. The influences of the subgrade Young's modulus, applied load and rate of loading on track stiffness have been investigated within GRAFT and will be presented in this chapter.

From the findings in this chapter two track settlement prediction models are presented that fit the GRAFT data. These models can be used to estimate track settlement for a typical track section based on combinations of the subgrade modulus, applied load and track stiffness. These models are compared to previously published models from empirical results and are found to compare favourably. The GRAFT results from CT1 to CT4 have been used in this chapter along with the results from the additional study after CT4.

4.2 Track settlement

Railway track will settle with repeated traffic loading due to permanent deformation in the ballast and underlying soil and hence the level of settlement depends directly on the quality and behaviour of the ballast and subgrade as well as the loading level. Mechanisms of plastic deformation in the subgrade from repeated loading include plastic shear strain, cumulative consolidation, cumulative compaction and ballast void infiltration by subgrade particles. Cumulative consolidation and compaction are thought to have influenced the increase in subgrade modulus in GRAFT as discussed in the previous chapter while shear failure and ballast infiltration were not studied in the tests considered within this chapter. Various models have been developed for predicting cumulative plastic strain in fine-grain subgrade soil under repeated loading. A review of which can be found in Banimahd (2008), where it is stated that the most commonly used model is the following power model:

$$\varepsilon_p = AN^b \tag{4.1}$$

where ε_p and N are the cumulative plastic strain and number of load cycles respectively; A and b are model parameters depending on soil properties and stress state. Studying the available experimental data in the literature, Li and Selig (1996) stated that the exponent b is independent of deviator stress and soil physical state. Using cyclic penetration tests to build a subgrade plastic settlement prediction model Okada and Ghataora (2002) also found that the parameter b does not depend on deviator stress (plunger pressure) or physical state (CBR value). Li and Selig (1996) concluded that this parameter is only related to soil type whereas coefficient A strongly depends on soil stress and physical state. Li and Selig (1996) proposed the following relationship for A where a soil strength parameter under static loading has been used to indirectly represent the influence of the soil physical state:

$$A = a(\frac{q}{q_s})^m \tag{4.2}$$

where a and m are material parameters, q is the deviator stress and q_s is the soil static strength (compressive strength under monotonic loading). Okada and Ghataora (2002) found a similar relationship for the parameter A in their subgrade settlement prediction model using plunger pressure and CBR values to represent the stress state and soil properties respectively.

At low deviator stress levels, permanent deformation has been shown to increase with the logarithm of the number of cycles, the rate of accumulation of permanent strain increasing as the stress increases (Seed *et al*., 1955, Monismith *et al*., 1975 & Brown *et al*., 1975). This eventually leads to a deviator stress level denoted as the *threshold* stress, under which the rate of accumulation of deformation increases exponentially (Frost *et al*., 2004). This phenomenon has been observed by several researchers. Brown (2004) defined threshold stress as the magnitude of repeated deviator stress below which the accumulation of plastic shear strain is negligible and reported that it increases with overconsolidation ratio. Li and Selig (1996) stated that threshold stress can be related to the history and water content of the soil, and thus shear strength and stiffness. Within GRAFT the subgrade modulus values have been used as an indicator of the soil

physical state as it is considered they are more accurate than the strength values found from unconfined compression tests. Li and Selig (1996) noted that the use of soil static strength may also represent the influence of other factors such as soil structure, since changes in soil structure and properties will lead to a change of soil static strength. The same may be true in GRAFT and soil structure may indirectly be accounted for within the subgrade modulus values.

The effect of clay subgrade soil structure factors such as fabric anisotropy, interparticle bonding and degradation of bonds on the behaviour of the track subgrade are not directly considered within this thesis. The importance of these factors on the mechanical behaviour of soft clays can be found in Karstunen *et al*. (2005) and Karstunen and Koskinen (2008). Karstunen *et al*. (2005) investigated the influence of these factors on the behaviour of a test embankment on soft clay in Finland. It was found that in order to accurately predict deformations, anisotropy should be taken account of within the constitutive modelling of such soft clays, and to explain the measured decrease in shear strength during consolidation, destructuration should be incorporated. Therefore, it is recommended that for new track in the field overlying a very soft natural subgrade soil (normally consolidated) at depth these factors should be considered to prevent the under prediction of subgrade deterioration at the design stage.

The cumulative permanent plastic deformation characteristics of the ballast are a function of both the confining pressure and the cyclic deviator stress (Selig and Waters, 1994). Selig and Waters (1994) reported on studies that were undertaken in the laboratory and in the field by the ORE (Office for Research and Experiments of the International Union of Railways) to determine the behaviour of the ballast layer under repetitive loading. The following relationship was found:

$$\varepsilon_n = 0.082(100n - 38.2)(q)^2\left[1 + 0.2\log(N)\right] \tag{4.3}$$

where ε_n is the permanent strain after N cycles, n is the initial porosity of ballast and q is the deviator stress. Hence, the permanent deformation is very dependent on initial ballast compaction and applied deviator stress. The presence of a threshold stress for

granular soils, similar to fine-grain subgrade soils, has been discussed by several researchers and reviews can be found in Ionescu (2004) & Banimahd (2008), however this will not be discussed further here.

From the equations set out above the permanent settlement of the railway track is assumed to be a function of initial ballast porosity, soil type, soil physical state and structure, the number of applied load cycles and applied deviator stress. As the soil type in GRAFT remains constant this variable can be removed. Furthermore, if the initial porosity of the ballast in GRAFT is assumed constant throughout the tests, as the same compactive effort was applied to the ballast in each test, then track settlement in these GRAFT tests would appear to be a function of only the soil physical state and structure (indirectly the subgrade modulus), the number of applied cycles and the applied cyclic vertical load (with confining pressure in GRAFT assumed constant for each test).

4.2.1 Influence of applied load

Dahlberg (2001) conducted a critical review of various mathematical models of railway track settlement and stated that settlement of ballasted railway track occurs in two distinct phases:

1. Initial ballast densification after tamping/new ballast placed (settlement is relatively rapid)
2. Second stage settlement is slower and develops as a linear relationship with time and load (number of load cycles applied as in case for GRAFT).

The settlement development of the central sleeper with number of cycles for the four GRAFT tests examined within this chapter is shown in Figure 4.1. The two phases of settlement development are clear; however it can be seen that the applied load level and subgrade stiffness play a significant role in determining the initial track settlement. This may be due to the increased ballast shear strains caused by a reduction in subgrade modulus, as found by Hunt (2005). Banimahd (2008) also stated that the softer the

underlying soil is, the higher the level of induced plasticity in the ballast layer due to increasing cyclic ballast shear strains.

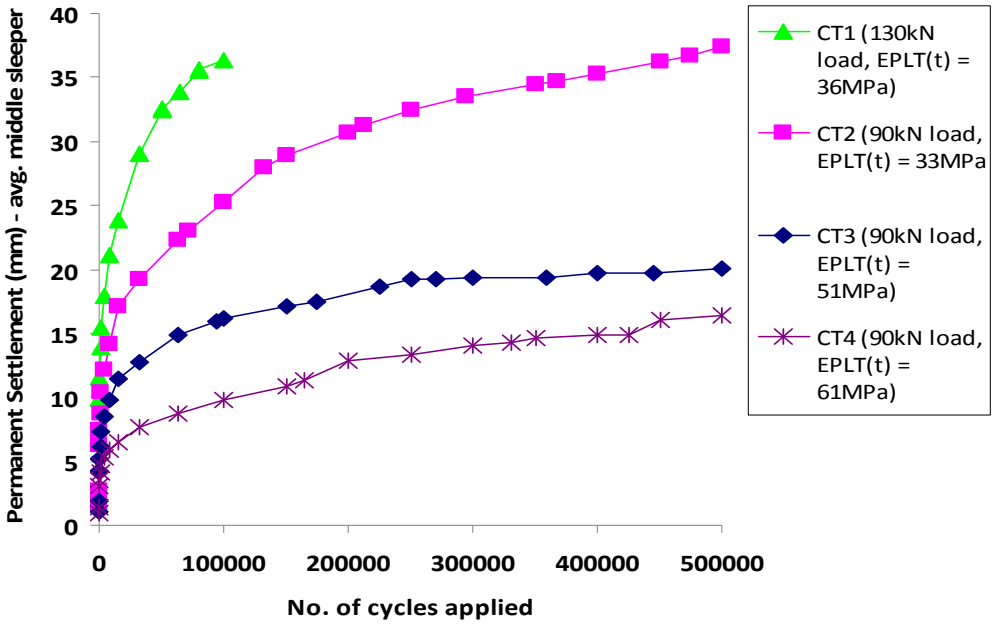

Figure 4.1. Permanent settlement of middle sleeper throughout various GRAFT control tests

Based on experimental observations, Sato (1995) proposed the following expression to estimate track settlement directly where the first part of the equation represents short term settlement and the second part long term:

$$y = \gamma(1 - e^{-\alpha x}) + \beta x \tag{4.4}$$

where y is the track settlement; x is the number of loading cycles or tonnage applied to the track; γ is a constant that determines the magnitude of short term settlement; α is a constant indicating the speed of attenuation of the short term settlement; and β is a constant that dictates the magnitude of the long term settlement. Sato (1995) suggested that several factors influence β, including the velocity of repeated loading, ballast fouling, sleeper pressure and vertical ballast acceleration, which can be influenced by the speed of the train and by the irregularities on the rail head and on the wheel face. With the exception of sleeper pressure, these factors have not been considered within

this thesis as the study would have been too large. These factors are assumed constant for each test.

While reviewing empirical track settlement models Dahlberg (2001) found that the key parameter influencing settlement is sleeper–ballast contact pressure. Dahlberg (2001) re-plotted the measured data from a settlement model and concluded that a threshold value of sleeper-ballast contact force exists, below which track settlement will be negligible. Loading close to or below this threshold value the track settlement is purely elastic. This threshold theory matches directly with the threshold stress findings of both the ballast and fine-grained subgrade materials discussed above. Loading around the threshold for moderate values of sleeper-ballast contact force results in a linear relationship between loading level and track settlement per loading cycle. For larger contact force values a non-linear region exists where settlement depends heavily on sleeper-ballast force and may be proportional to the fifth power or more of the pressure. An additional study undertaken in GRAFT after CT4 found similar results by investigating in further detail the effect of increasing the applied load on track settlement. This involved applying loads of 40, 90, 110 and 130kN for 10,000 cycles each and measuring central sleeper track settlement after the 10,000 applied cycles. This study was undertaken on the same track as CT4 after the application of 500,000 cycles and all test details were the same as for the full control tests.

Figure 4.2 compares the results from this additional study to the findings of Dahlberg (2001). The Dahlberg (2001) correlation has been fitted to the applied load data from GRAFT to predict track settlement and to compare settlement values measured in GRAFT. A best fit line has been plotted through the GRAFT results and it can be seen that this line matches the shape of correlation curve presented by Dahlberg (2001). However, the two curves are not directly comparable as the relationship given by Dahlberg (2001) is based on sleeper-ballast contact force while the correlation in Figure 4.2 has been fitted to the load applied to the track in GRAFT spread over three sleepers. Nonetheless, it is clear that as the applied load/sleeper-ballast contact force increases a non-linear relationship with settlement develops. The GRAFT data predicts a similar relationship between settlement and pressure as Dahlberg (2001) where settlement is proportional to between the fifth and sixth power of applied pressure. Using a

spreadsheet based track settlement predictive technique Thom (2007) suggested that a much higher exponent between 8 and 10 is more appropriate, although this has not been found to be supported elsewhere in the literature.

From these results it is likely that a track threshold value does exist and that loading up to 90kN in GRAFT for CT4 is within the range of moderate sleeper-ballast contact force where a linear relationship exists between load level and track settlement per cycle. As shown in Figure 4.1 initial non-linear settlement is heavily influenced by both applied load and the subgrade modulus and it is thought that the subgrade modulus plays a major role in dictating the track threshold value. Hence, the GRAFT curve in Figure 4.2 may be different for each track with varying subgrade modulus. Therefore, within GRAFT the threshold value of the track has been illustrated by the Author as the ratio of subgrade modulus (soil physical state) to applied cyclic load, assuming that the ballast properties are constant throughout the testing programme. This ratio is defined within this thesis as the track parameter (t):

$$t = \frac{E_{PLT}}{p} = \frac{stiffness}{pressure} \tag{4.5}$$

where p is the sleeper-ballast contact pressure on the middle sleeper in GRAFT. The applied load in GRAFT is converted into a sleeper–ballast contact pressure for the middle sleeper by assuming 40% of the load is transferred to the middle sleeper in GRAFT (shown in Chapter 3). It is thought that the track parameter (t) heavily influences initial non-linear settlement with a low value resulting in an extended and severe initial non-linear stage while a high value may reduce the length and magnitude of this stage. From Figure 4.2 however it is unclear whether the non-linearity in settlement over 10,000 cycles can be separated into the two stages of settlement previously discussed or whether different mechanisms are involved at different loading ranges. Dahlberg (2001) suggested that the different behaviour at different loading ranges is due to different degradation or failure mechanisms where ballast abrasion and compaction may occur at lower loading ranges and/or fracture of ballast particles may occur in higher loading ranges.

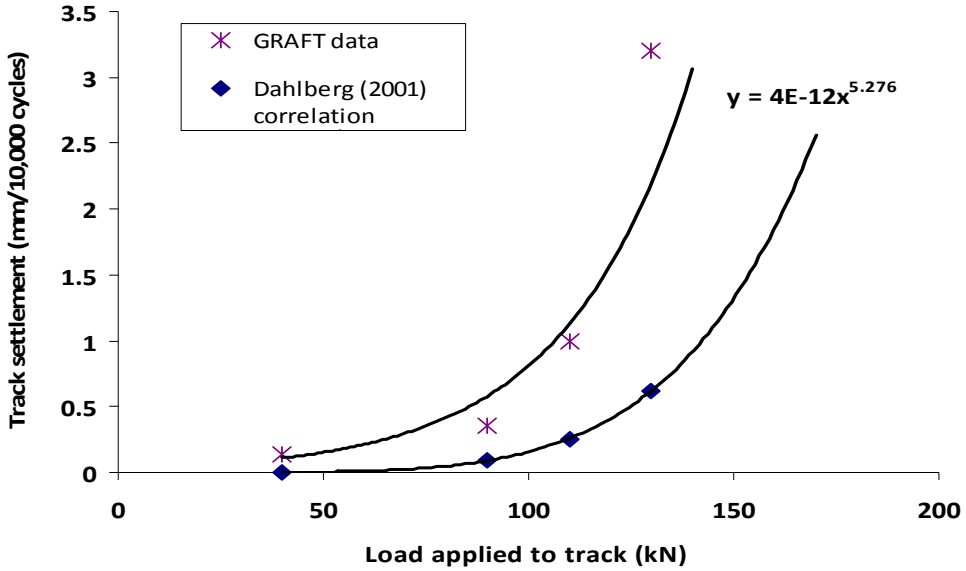

Figure 4.2. GRAFT settlement against applied load data with Dahlberg (2001) correlation superimposed (note GRAFT results based on loading over 3 sleepers by the rail)

4.2.2 Influence of subgrade modulus and number of cycles

Adding power trend lines to the GRAFT test settlement curves in Figure 4.1 a power settlement law can be represented by the following equation which was developed within this thesis:

$$y = K_1 N^{0.23} \tag{4.6}$$

where y = settlement after N number of cycles in mm and K_1 is a constant depending on applied load and subgrade modulus and has units of mm. To account for the non-linear variation in settlement with applied load and subgrade modulus, the track parameter (t) was plotted against the K_1 constant and is shown in Figure 4.3. The resilient modulus correlation has been omitted from Figure 4.3 as the R^2 value of 0.64 is less than the other two correlations shown due to a variation in the trend for the resilient modulus/settlement from CT1 at higher load.

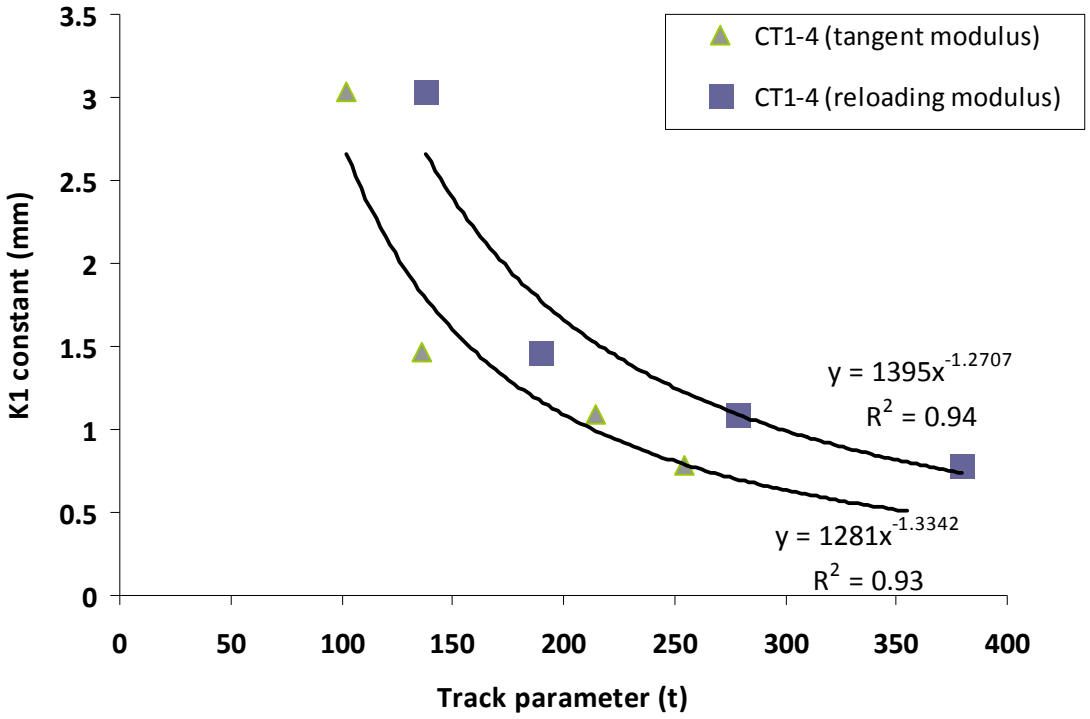

Figure 4.3. Variation of GRAFT constant K_1 with GRAFT track parameter (t)

The trend lines through the tangent subgrade modulus and reloading subgrade modulus data points produced the following regression correlations:

$K_1 = 1281t^{-1.3342}$ ($R^2 = 0.93$) for tangent subgrade modulus values (4.7)

$K_1 = 1395t^{-1.2707}$ ($R^2 = 0.94$) for reloading subgrade modulus values (4.8)

Hence, two models developed within this thesis for settlement prediction are as follows:

$y = 1281t^{-1.3342}N^{0.23}$ for tangent modulus values (4.9)

$y = 1395t^{-1.2707}N^{0.23}$ for reloading modulus values (4.10)

These particular subgrade modulus models can estimate settlement in GRAFT after N number of cycles based on the subgrade modulus and applied cyclic load, assuming that

all other factors remain the same. If the subgrade modulus is increased the estimated settlement is reduced and if the applied load is increased the estimated settlement increases significantly. Changing this model into a more generalised form, it can be seen that it is very similar to the fine-grained subgrade model presented by Li and Selig (1996) in equations 4.1 and 4.2:

$$y = a(\frac{E_{PLT}}{p})^m N^b \tag{4.11}$$

where $a(\frac{E_{PLT}}{p})^m$ is equivalent to the coefficient A in the Li and Selig (1996) equation where A depends on stress state (p) and physical state (E_{PLT}). The relationship between coefficient A and these states may vary for different soil types, as characterised by a and m. As the soil type was the same in these GRAFT tests and the ballast properties are assumed the same the factors a and m are constant, depending on how E_{PLT} is measured. The variation of a and m with tangent and reloading modulus values is a result of using subgrade modulus to indirectly model subgrade physical state. The b factor in the above equation relates to the b factor in the Li and Selig (1996) equation, which is dictated by the soil type and within GRAFT, is constant at 0.23, again assuming that ballast properties are the same with each test.

Furthermore, this settlement model found in GRAFT is similar to the findings of Shenton (1985) based on laboratory and field experiments. Shenton (1985) proposed:

$$y = K_1 N^{0.2} + K_2 N \tag{4.12}$$

where K_1 and K_2 are material constants based on a number of factors and are selected so that the linear term only becomes significant for values of N above 10^6. It may be the case that for a greater number of applied cycles in GRAFT that the additional linear term may be appropriate; however the tests were stopped after 500,000 applied cycles. This linear term will be investigated in more detail later in this chapter.

Regarding equation 4.12 above Sadeghi and Askarinejad (2007) stated that:

$$K_1 = K_s \frac{A_e}{20}(0.64 + 0.028L) \text{ and } K_2 = 2.7 \times 10^{-6} \quad (4.13)$$

where K_s is a function of sleeper spacing, type and size, track stiffness and rail section; A_e is the equivalent axle load and L is the lift given by the tamping machine. Referenced model parameters taken from Sadeghi and Askarinejad (2007) give K_s = 1, A_e = 20ton, L = 20mm. Using these parameters and matching the equation to the data from GRAFT with 90kN being the equivalent of a 25 tonne axle load (GRAFT A_e value) and 130kN being the equivalent to a 37 tonne axle load, a direct comparison can be made.

In addition, the GRAFT subgrade modulus model (equation 4.6) compares favourably with settlement trends found by Selig and Waters (1994) based on field measurements as well as box tests. Within the field study Selig and Waters (1994) distinguished between the contributions of the ballast and subgrade settlement after N cycles and found that:

$$y = K_1 N^b + K_2 N^c \quad (4.14)$$

where the first part of the equation accounts for ballast settlement and the second part subgrade settlement; y is the track settlement in inches; K_1 is the ballast settlement from the first cycle; b is a ballast exponent; K_2 is the subgrade settlement after the first cycle and c is a subgrade exponent. It should be noted here that this equation is based on results from new track and Selig and Waters (1994) found that the second part of the equation becomes linear after a certain amount of cycles, similar to the linear term in the Shenton (1985) equation (equation 4.12). Thus, the contribution of the subgrade to track settlement is less after the track has been in service for a while.

From the field study Selig and Waters (1994) found the following parameters; K_1: range 0.027 to 0.042, b: range 0.21 to 0.22, K_2: range 0.0014 to 0.00052 and c: range 0.37 to 0.52. Using these parameters equation 4.14 can be fitted to the GRAFT data. Figure 4.4 compares the relationship found by Selig and Waters (1994) to the GRAFT data for CT4 and the GRAFT subgrade modulus model presented within this chapter. The equation proposed by Shenton (1985) is also shown in Figure 4.4. Subgrade tangent modulus data has been used in Figure 4.4 to calculate the track parameter values (equation 4.9). The parameters used in each equation are shown in Table 4.1. A K_s value of 0.72 was used in the Shenton (1985) equation to represent the tangent subgrade modulus value in CT4, assuming all other variables, that K_s is a function of, are constant.

As shown the GRAFT subgrade modulus model predicts settlements almost identical to both the Selig and Waters (1994) and Shenton (1985) equation. Similar matches have been found for all GRAFT controls tests with the parameters adjusted accordingly to fit the data. This particular GRAFT subgrade modulus model does not distinguish between ballast and subgrade and hence the Shenton (1985) model is more appropriate for direct comparison as it also does not distinguish between these components. Table 4.2 shows the values of the Shenton (1985) parameters found to best match the data for changes in applied load and subgrade modulus and Figure 4.5 compares the Shenton equation with these parameters to all the control tests in GRAFT and the GRAFT subgrade modulus model predictions. From this data an equation for K_s can be estimated based solely on the subgrade modulus assuming all other parameters that influence K_s are constant. The best fit trend lines through the data give:

$$K_s = 7.619 - 1.678\ln(E_{PLT(t)}) \quad (R^2 = 0.99) \text{ for tangent subgrade modulus values} \qquad (4.15)$$

$$K_s = 258(E_{PLT(r)})^{-1.3095} \quad (R^2 = 0.99) \text{ for reloading subgrade modulus values} \qquad (4.16)$$

Therefore, a particular subgrade modulus settlement model has been produced here to fit the experimental data from GRAFT and its parameters have been compared to other

similar models (Shenton (1985), Selig and Waters (1994)). A track example will now be shown to illustrate the use of the developed model.

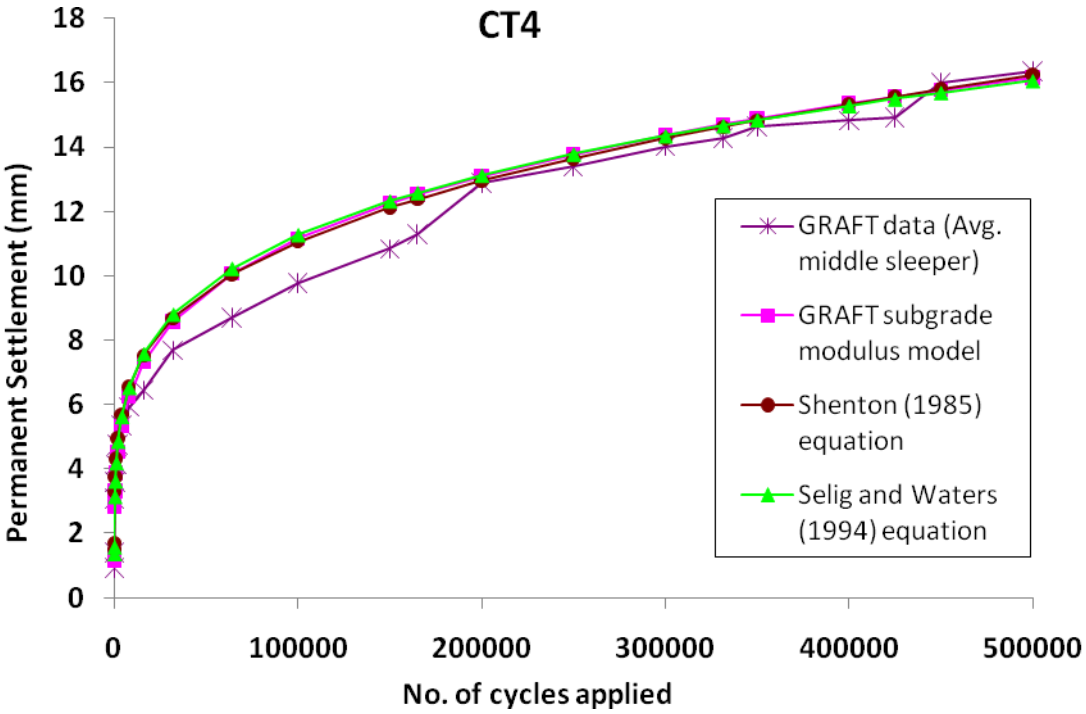

Figure 4.4. Comparison of settlement models with GRAFT data from CT4

Settlement model	K_1	b	K_2	c	K_s	L (mm)	A_e (tonnes)
Selig and Waters (1994)	0.038 (inches)	0.21	0.0014 (inches)	0.42	-	-	-
Shenton (1985)	-	-	2.7×10^{-6}	-	0.72	20	25
GRAFT model	$1281t^{-1.3342} = 0.79$ (mm)	0.23	-	-	-	-	-

Table 4.1. CT4 model parameters used to estimate settlements after N number of cycles

GRAFT test	Applied load (kN)	Subgrade tangent modulus (MPa)	K_s (to account for subgrade modulus)	A_e (tonnes)
CT1	130	35.5	1.65	37
CT2	90	32.7	1.75	25
CT3	90	51.4	1.00	25
CT4	90	61.1	0.72	25

Table 4.2. Shenton (1985) equation parameters that were found to match well with GRAFT data

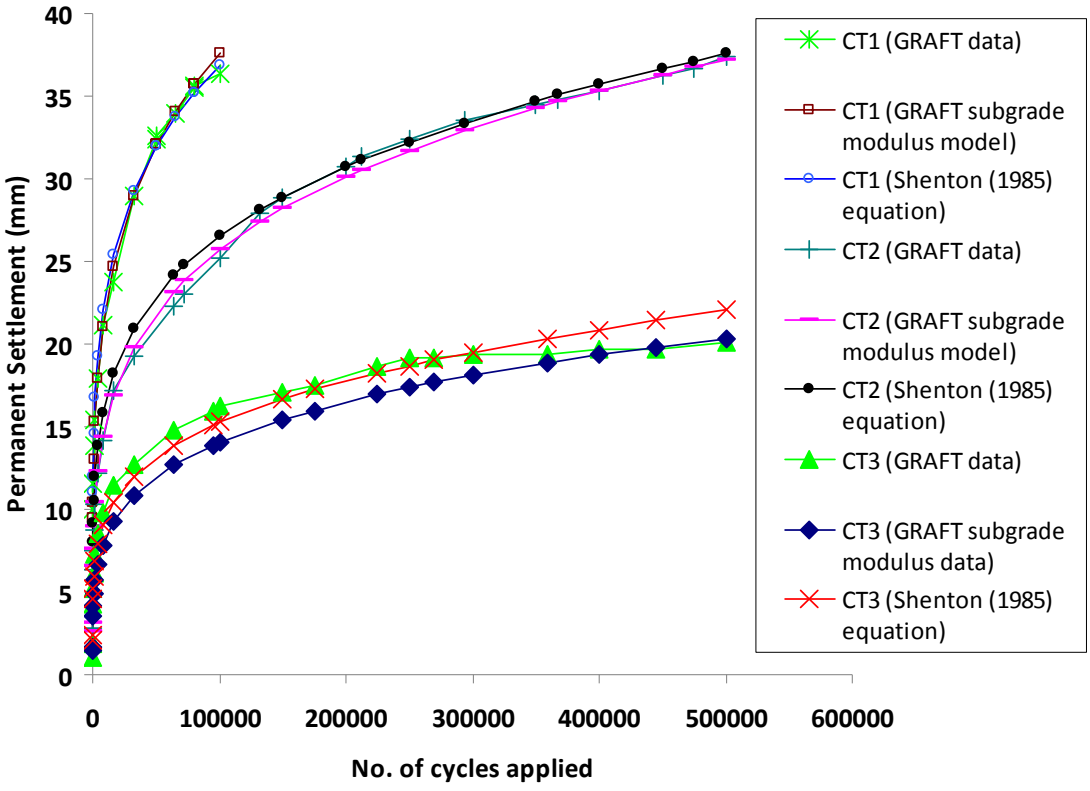

Figure 4.5. Comparison of settlement models with all control test GRAFT data

4.2.3 Example of track settlement calculation

Assume a new track has a clay subgrade, a BS 113A rail with 250mm x 125mm full length wooden sleepers spaced at 650mm. A ballast depth of 300mm and the same ballast properties as those used in GRAFT (Table 3.6), and assuming that ballast stiffness is the same as that in GRAFT. If it is also assumed that the initial tangent subgrade modulus is 25MPa and the axle load applied to the track is consistently 25 tonnes (with a 1.2 DAF for 10 Million Gross Tonnes (MGT)). The track settlement can then be estimated from the GRAFT subgrade modulus model. The traffic is converted into an equivalent number of cycles N in GRAFT by assuming that each cycle in GRAFT is the equivalent of 1 axle load, giving 40,000 cycles in GRAFT = 1MGT. The axle load is converted into an equivalent GRAFT load by multiplying by 85% to account for reduced load distribution along successive sleepers as three sleeper sections were used in these GRAFT tests instead of five, then multiplying by 35% to account for the reduced length sleeper sections and finally multiply by 120% for the DAF. Thus, the calculation is as follows (from Equation 4.9):

Equivalent number of GRAFT cycles N :- $N = \dfrac{10MGT}{25tonnes} = 400{,}000$

Equivalent GRAFT load P :- $P = 250kN \times 85\% \times 35\% \times 120\% = 89kN$

Track parameter t (Equation 4.5):- $t = \dfrac{E_{PLT(t)}}{p} = \dfrac{25{,}000kPa}{\left[\dfrac{89kN \times 0.4}{0.25m \times 0.6m}\right]} = 105$

Constant K_1 (Equation 4.7):- $K_1 = 1281(105)^{-1.3342} = 2.57mm$

$\therefore$ Track settlement y (Equation 4.6):- $y = 2.57 \times 400{,}000^{0.23} = 50mm$

This estimated settlement is high, and if the subgrade tangent modulus was improved to 60MPa then the estimated settlement reduces to 15.5mm. Alternatively, if the track was designed for a maximum settlement of 5mm after 10 MGT of applied traffic, the allowable axle load on the track = 10.5 tonnes with a 1.2 DAF (38kN in GRAFT). Using the Shenton (1985) equation, with the K_s term estimated based solely on the

subgrade modulus correlation found in this paper (equation 4.15), then an estimated settlement of 45mm for the initial case, 16mm for the improved subgrade case and 7.3mm for the final reduced load case is obtained. These values are similar to the values estimated using the GRAFT subgrade modulus model, however various assumptions have been made in this comparison regarding the Shenton (1985) equation.

This example has shown how the GRAFT subgrade modulus settlement prediction equation can be used indicatively for real track and using the same assumptions made in this example, a design graph has been produced to limit the initial track settlement after a track renewal/tamping to a preset level. Figure 4.6 shows the design graph for two different traffic levels. The design graph can be used by initially selecting the allowable track settlement for the specific MGT applied to track. The track parameter (t) can then be scaled off the graph, and for a specific subgrade modulus, the allowable axle load can be specified or, for a specific axle load, the required subgrade modulus can be specified (for 300mm ballast depth and all assumptions made above). For example, assume that the allowable track settlement for the above example is 10mm for 12.5MGT of applied traffic; using Figure 4.6 the track parameter (t) can be scaled off as 365 and assuming the initial subgrade tangent modulus is 60MPa then the permissible axle load to achieve 10mm settlement after 12.5MGT can be calculated as 17 tonnes using equation 4.5.

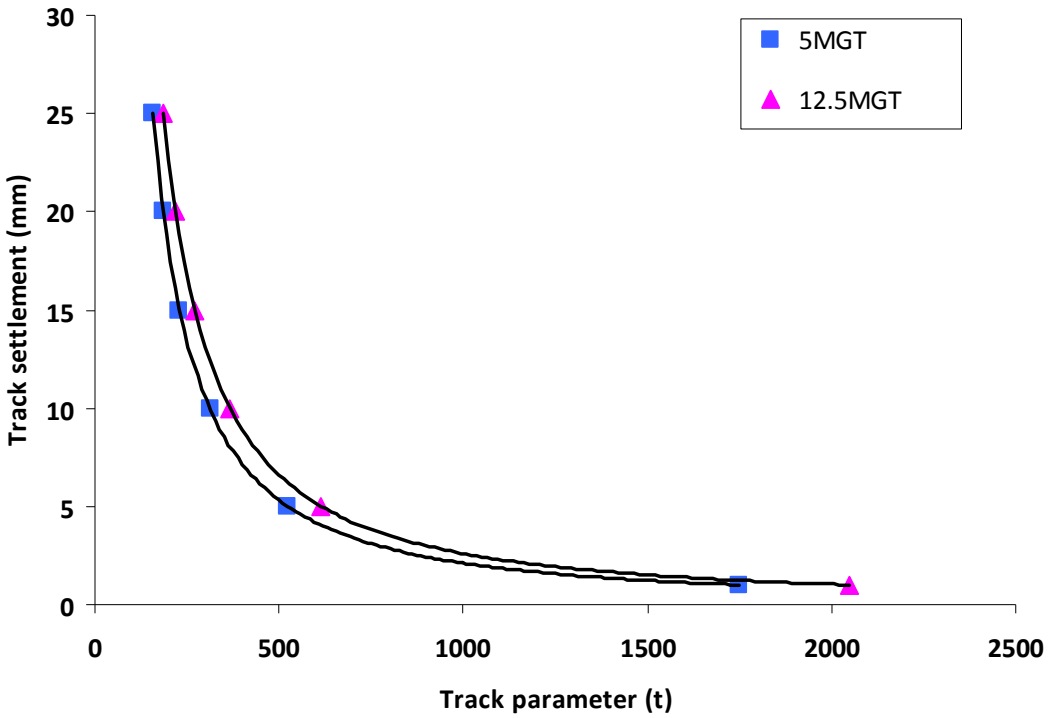

Figure 4.6. Allowable GRAFT initial track settlement design chart

This design procedure is obviously limited due to the reduced depth of GRAFT and as it does not consider the influence of different ballast depths and properties, different track constructions and track components, mixed loads, different train speeds and high cumulative tonnages (greater than around 15MGT). A discussion of the influence of high cumulative tonnages (long term linear settlement), mixed loads and different ballast depths are discussed next whereas the influence of speed, ballast properties and track constructions and track components are out with the scope of this thesis. A full review of design models used around the world, that include variations of these factors, will be discussed in Chapter 7. The work presented in this thesis therefore can be used as an excellent starting point to determine an overarching track settlement calculation methodology that is fully supported by full-scale laboratory testing. This aspect forms the basis of the recommended future work.

4.2.4 Long term linear settlement and mixed loads

The linear term shown in the settlement equations 4.4 and 4.12, as presented by Sato (1995) and Shenton (1985) respectively, indicates that after a certain number of applied cycles the settlement varies linearly with further cycles. Selig and Waters (1994) also suggested that a linear term exists after a certain number of cycles and Jeffs and Marich (1987) reported that independent of different test variables, a linear variation of settlement with the number of cycles was observed beyond 200,000 cycles. Shenton (1985) stated that the linear term only becomes significant after 1 million cycles and it may be the case that if the tests in GRAFT were undertaken beyond 500,000 cycles a linear term would be shown in equation 4.6. From the trends found of settlement against cycles in Figure 4.1, it is clear that settlement does vary linearly with cycles after a certain point (second stage settlement). This linear trend is shown in Figure 4.7 where trend lines from cycle 250,000 onwards have been plotted for CT2 to CT4. The smoothed out settlement curves from the tangent modulus GRAFT settlement model (equation 4.9) have been used in Figure 4.7 to remove scatter in the actual data. It can be seen that after 250,000 cycles a linear trend can accurately be used to represent the relationship between settlement and number of cycles at the same applied load with subgrade modulus only apparently having a slight influence on the gradient of the linear trend. However, it is unknown if this linear trend would continue beyond 500,000 cycles or whether the rate of settlement would continue to decrease with cycles as the track reaches a complete resilient track, where essentially no permanent settlement occurs (at the same applied load). Therefore, no conclusions can be drawn from the GRAFT results regarding the inclusion of a linear term to describe the long term track settlement. It can however be stated that equations 4.9 and 4.10 presented from the GRAFT data can only be accurately used for short term settlement (approx. up to 15MGT) after a track renewal/tamping.

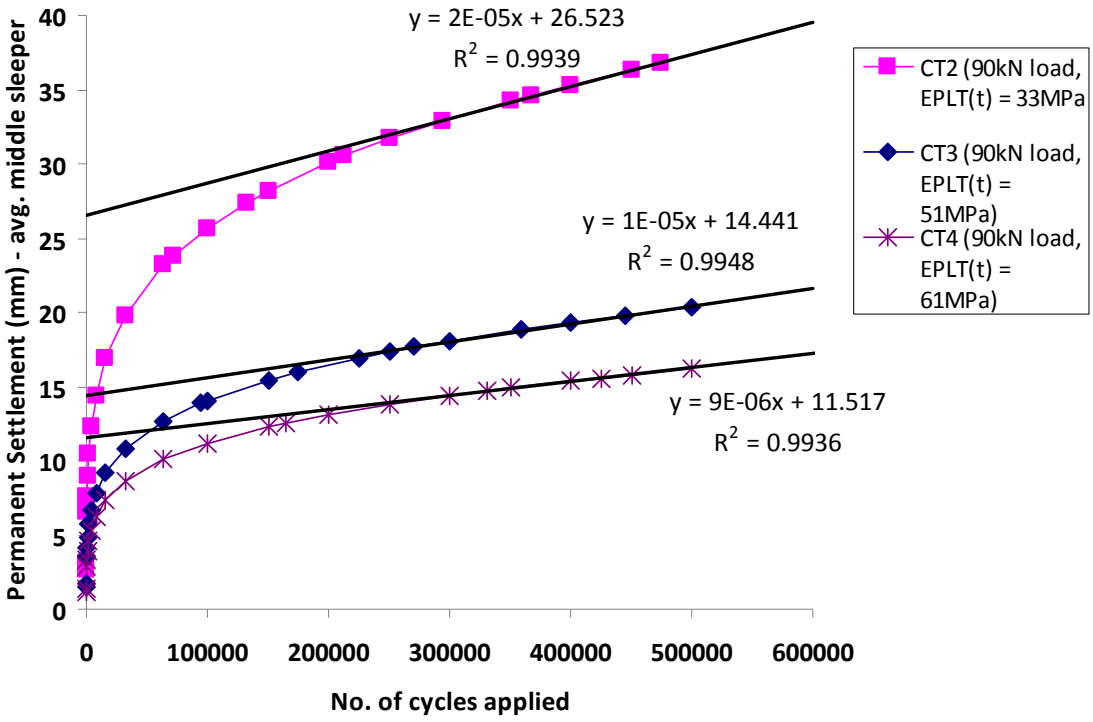

Figure 4.7. Linear trend of settlement with cycles after 250,000 cycles

It is likely that for long term track settlement (well beyond 500,000 applied cycles) that the equations 4.4 and 4.12 presented by Sato (1995) and Shenton (1985) respectively, which incorporate a linear term, are accurate. The non-linear first part of the Shenton (1985) equation, which is similar to the GRAFT equations, was found to agree well with site measurements up to 1 million cycles. This is the same as found in GRAFT for up to 500,000 cycles. The linear second part of the Shenton (1985) equation was added to obtain an acceptable fit to the site measurements for cycles above 1 million. Therefore, from these findings it is thought that short term settlement after a track renewal/tamping is non-linear with applied cycles and dependant on subgrade modulus and applied load whereas long term settlement is linear with applied cycles and is less dependent on subgrade modulus.

One problem with the subgrade modulus models presented so far are that they do not account for a change in axle load on the track, which is essential when considering the range of vehicles and train speeds used on most mainline train tracks. Selig and Waters (1994) reported on repeated-load triaxial tests on ballast, where the applied deviator

stress was changed after every 1000 applied cycles and some important trends were identified. Firstly, when the deviator stress was increased to a value greater than the past maximum, the permanent strains continued to increase. When the deviator stress was reduced to a value less than any past maximum, negligible changes in permanent strain resulted with additional cycling. Finally, it was found that for any given effective confining pressure, the sequence of applied stresses did not affect the final values of permanent strain, when the total number of cycles at each stress level was about the same. These results imply that the maximum wheel loads will have a dominating influence on the amount of plastic strain accumulation.

To account for multi-stress levels and multi-soil physical states Li and Selig (1996) proposed the procedure illustrated in Figure 4.8 to calculate the total cumulative permanent strain in fine-grained subgrade soils. In the PhD thesis by Fröhling (1997) a similar procedure for superimposing permanent strains in the ballast to account for a mix of wheel loads at a particular sleeper was presented. The procedure illustrated in Figure 4.8 is for a two load level case and it is assumed that the β_i term for the two load cases represents the track parameter (t) (equation 4.5) presented for the GRAFT tests. If the subgrade modulus is constant then the track parameter (t) is solely a function of applied load and in Figure 4.8 the higher load case (β_2) shows higher plastic strain for the same number of applied cycles as the lower load case (β_1). From Figure 4.8 the parameters N_1, N_2 and n are self explanatory, with n representing an equivalent number of cycles on the higher load curve that would cause the same strain as developed by the lower load. In GRAFT if N_1 number of cycles were applied at the lower load case before $N_2 - n$ additional cycles were applied at the higher load case then the total settlement after N_2 number of cycles can be calculated as follows:

1. Calculate settlement at N_1 number of cycles at lower load case using either equation 4.9 or 4.10.
2. Calculate the equivalent number of cycles (n) on the higher load curve that would cause the same strain as developed by the lower load by back calculating using equations 4.9 or 4.10. Assuming the subgrade modulus is constant.

3. Add the additional cycles applied at the higher load to n to get to N_2 number of cycles.

4. Use equation 4.9 or 4.10 for the higher load case with the number of applied cycles N equal to $N_2 - n$.

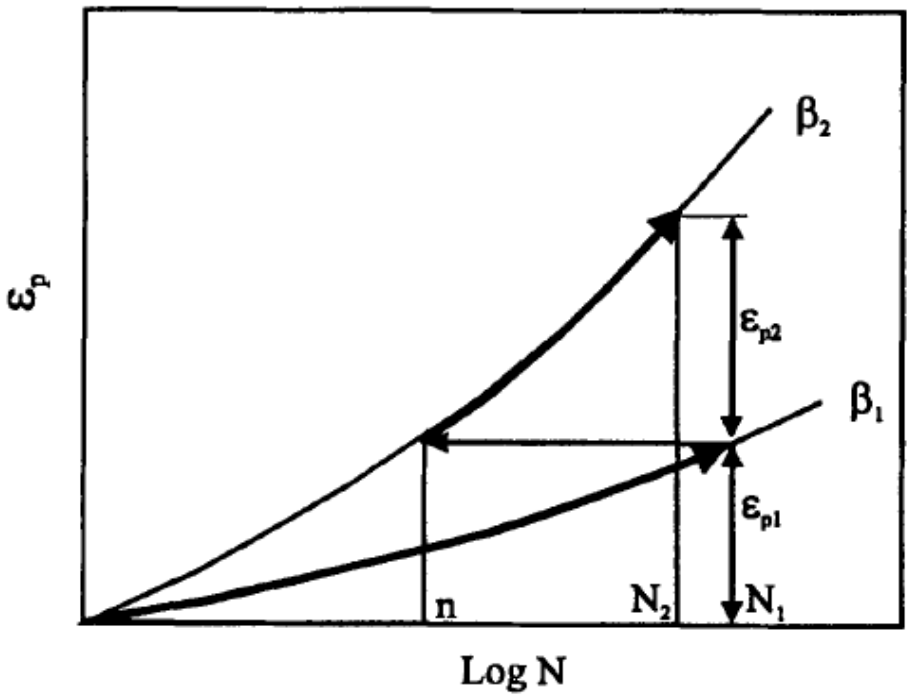

Figure 4.8. Model for total cumulative plastic strain (Li and Selig, 1996)

Within GRAFT after CT2 an additional 100,000 cycles were applied at the higher load level of 110kN. The settlement curve for CT2 is shown in Figure 4.9 and the GRAFT subgrade modulus settlement prediction model has been plotted against the data with the above procedure used to calculate the additional settlement after the load level was increased from 90 to 110kN. It can be seen that at the initial increase in load level after 500,000 cycles the rate of settlement increases considerably, similar to what was found in the triaxial results reported by Selig and Waters (1994). This particular GRAFT subgrade modulus model for the increased load section slightly underestimates the observed settlement over the additional 100,000 applied cycles and it seems as if this underestimation is increasing with cycles. Further research is required here before multi load level settlements can be accurately predicted within GRAFT. This is important for

the application of such a settlement prediction model on track as it has been shown that total cumulative settlement is the same regardless of sequence of load, but is dominated by the maximum load exerted on track. This has direct implications for existing track where an increase in axle load is considered.

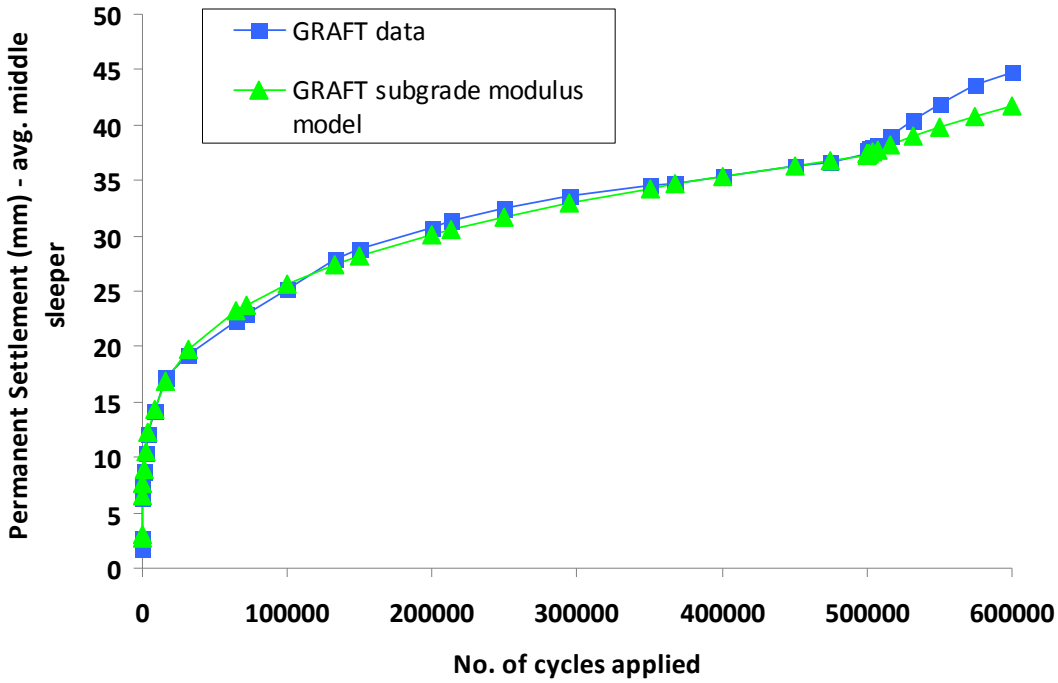

Figure 4.9. Comparison of GRAFT data to GRAFT subgrade modulus model for CT2 with increase in applied load

4.2.5 Influence of ballast depth

As part of the additional study after CT4 the ballast depth was reduced from 300mm to 250mm and 10,000 cycles were applied. The load applied was 40kN and all other test details were the same as for the full control tests previously described. Table 4.3 shows the settlement found after 10,000 cycles for all the tests undertaken as part of the additional study after CT4. Table 4.3 shows that by reducing the ballast depth by 50mm the settlement has increased by 350% over 10,000 cycles for the same applied load level. Alos, it can be extrapolated that applying a load of 40kN with a 250mm ballast depth in GRAFT is approximately the equivalent to applying 100kN at a 300mm ballast

depth over 10,000 cycles. This is significant and is thought to be due to an increase in the induced formation deviatoric shear stress. Using the finite element programme SART3D and undertaking a static analysis Woodward *et al*. (2009b) showed that the induced formation deviatoric shear stress ratio increased from the range of 0.35 to 0.4 for a 500mm ballast depth to the range of 0.45 to 0.5 for a 300mm ballast depth. Furthermore, Li and Selig (1998a) stated that to control cumulative plastic strain at the subgrade surface either the subgrade strength can be improved or deviator stress transmitted to the subgrade can be reduced. Alternative techniques to reduce the deviator stress in the subgrade, such as the use of geosynthetics will be discussed in the next chapter. Therefore, although it has been shown here that ballast depth can have a crucial role in track settlement, considerable more testing is required in GRAFT at a range of ballast depths before the ballast depth could be incorporated into the GRAFT subgrade modulus track settlement model.

No. Of Cycles	Settlement (mm)				
	40kN load (300mm ballast depth)	90kN load (300mm ballast depth)	110kN load (300mm ballast depth)	130kN load (300mm ballast depth)	40kN load (250mm ballast depth)
10,000	0.14	0.35	0.99	3.2	0.63

Table 4.3 Permanent settlement of middle sleeper during additional study after CT4 for different ballast depths

4.2.6 Track settlement summary

The track settlement results presented have shown the importance of the subgrade modulus and applied vertical load on track settlement for a typical track and a particular track settlement model has been produced to fit the data. Both the subgrade modulus and applied load show non-linear trends when plotted against settlement and a threshold value seems to exist on both factors beyond which track settlement increases significantly. Similar threshold values have been found for increases in deviator stress for both fine-grained materials (Frost *et al*., 2004) and granular materials (discussed in

Banimahd (2008)). Furthermore, threshold values were also found for track behaviour (Dahlberg, 2001). Therefore, within GRAFT it was decided to define a track parameter based on the subgrade modulus and applied cyclic load, where the applied cyclic load is the dominating factor. It is thought that the length and magnitude of the initial non-linear stage of track settlement shown in Figure 4.1 is dictated by the track parameter value (t) in GRAFT for each test. The non-linear influence of both the applied cyclic load and subgrade modulus may heavily influence the non-linear stage of track settlement after a track renewal or tamping.

This particular GRAFT subgrade modulus track settlement model presented in this chapter can predict initial track settlement in GRAFT after a number of cycles (up to 500,000) for any applied load and clay subgrade modulus. For the ballast properties considered the model fits the measured data in GRAFT well and is similar to field measurements found by other researchers. The model is similar to the fine-grained subgrade model proposed by Li and Selig (1996) in that settlement is dependent on stress state and soil physical state and structure. The influence of soil type was not investigated within this study. Other limitations of the model include not accounting for different ballast depths and properties, mixed loads, different track constructions and track components, train speeds, and high tonnages (long term linear track settlement). Several of these limitations were discussed with suggestions on how they could be included within the subgrade modulus GRAFT settlement model, however, further research is required. Some of these parameters have been included in other track settlement prediction models, which have not been included here as their parameters cannot be correlated to GRAFT. A full review of these models can be found in Dahlberg (2001) and Thom (2007) and other research considering the influence of track irregularities can be found in Iwnicki *et al*. (1999) and Lundqvist and Dahlberg (2005) who considered dipped joints and sleeper voiding, respectively. Dahlberg (2001) however stated that there does not seem to be any widely accepted settlement equation describing the behaviour of the track. Regardless, when comparing the parameters of the GRAFT subgrade modulus settlement model to the well know Shenton (1985) model a good match with the GRAFT results was found. Furthermore, when comparing these two models to predict settlement for a track example similar results were found.

In addition, the GRAFT subgrade modulus model presented is similar to the model proposed by Shenton (1985) in that the settlement after a number of cycles is a function of the track stiffness (measured in the GRAFT model as function of subgrade modulus) and the applied axle load. However, the influence of the ballast physical state, structure and confining pressure, which also influences track stiffness, was not considered. Banimahd (2008) states that in order to decrease the level of ballast maintenance the stress level in the ballast has to be limited to a threshold to avoid the generation of excessive plasticity. As the strength of unreinforced ballast depends on the mean (confining) pressure, Banimahd (2008) recommends that the threshold is based on a plasticity ratio defined as the ratio of induced stress (ratio of deviatoric stress to mean stress) to stress ratio at plastic yielding (peak Mohr-Coulomb failure criterion value). Therefore, track stiffness maybe a more appropriate measure of track physical state than purely the subgrade modulus. Track stiffness will now be discussed in detail and the influence of subgrade modulus and applied load on track stiffness investigated.

4.3 Track stiffness

Vertical track stiffness is the relationship between vertical applied force and displacement response of the rails. Thus track stiffness is a function of the structural properties of the rails, rail pads, sleepers, ballast, subballast and subgrade soil. For example, the vertical track stiffness is 7% greater for UIC60 rail than for BS113A (Hunt, 2005). Furthermore, sleeper spacing influences track stiffness with reduced spacing resulting in an increase in track stiffness. Hunt (2005) notes that the subgrade is typically the primary determinant of overall track stiffness. Fundamental analysis and mathematical models of track stiffness are often based on the idealised Beam On Elastic Foundation (BOEF) approach that considers the track as an infinite bending beam resting on a continuous linear elastic foundation (Priest and Powrie, 2009). This approach is illustrated in Figure 4.10 and this analysis introduces the concept of the track modulus, which is the stiffness of the spring (k) per unit length of track. Using the software GEOTRACK Selig and Waters (1994) found that the track modulus can increase by around 10 to 20% for a decrease in sleeper spacing, as well as increases in

ballast Young's modulus, ballast depth and rail moment of inertia. In general, relatively high track stiffness is beneficial as it provides sufficient track resistance to applied loads and results in decreased track deflection, which reduces track deterioration. Low track stiffness results in a flexible track with poor energy dissipation and ballast abrasion due to ballast flexural deformations. On the other hand, very high track stiffness leads to increased dynamic forces in the wheel-rail interface as well as on the sleepers and ballast, which can cause wear and fatigue of track components (Berggren, 2009). An optimum track stiffness value is likely to be present at some intermediate value. Track stiffness is also reported as sleeper end stiffness (i.e. track stiffness which does not include the rail pad stiffness).

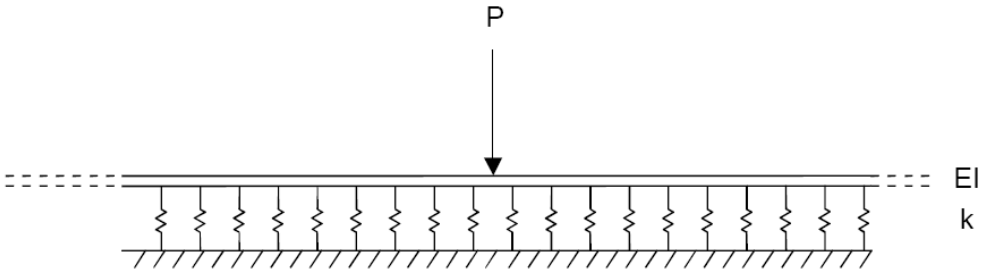

Figure 4.10. Track as a Beam On Elastic Foundation (BOEF) (Hunt, 2005)

Based on reviews of track stiffness by Hunt (2005) and Berggren (2009) vertical track stiffness (k) can be defined as the ratio between track load (F) and track deflection (z) as a function of time (t), where the force can either be axle load or wheel load:

$$k(t) = \frac{F(t)}{z(t)} \tag{4.17}$$

The stiffness of different components of the track structure is mostly non-linear, such as the rail pads and subgrade, and can vary with temperature and moisture content for example. Furthermore, the sleepers may have voids beneath them, leading to large deflections at low load levels, as shown in Figure 4.11. The secant stiffness is often used to eliminate the effect due to poor contact between ballast and sleeper and can be defined as:

$$k_{xy} = \frac{\Delta F}{\Delta z} = \frac{F_b - F_a}{z_b - z_a} \tag{4.18}$$

where ΔF and Δz are the difference between the values obtained at two predefined points with point a being taken at the seating load. The points a and b may be selected based on various definitions to give both secant and tangent stiffness values (Hosseingholian *et al.*, 2009). Hunt (2005) noted that for a realistic representation of non-linear behaviour a tangent stiffness to the design axle loading is a reasonably relevant parameter.

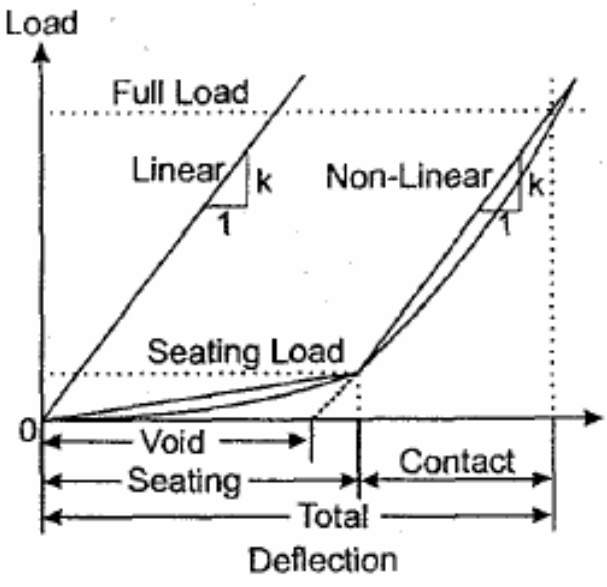

Figure 4.11. Load-deflection diagram illustrating voids (Berggren, 2009)

The track modulus (u) is defined as the supporting force per unit length of rail per unit deflection (δ) and is sometimes used instead of track stiffness:

$$u = \frac{q}{\delta} \tag{4.19}$$

where q is the vertical foundation supporting force per unit length (kN/m). Using the BOEF theory, a relationship between track modulus and track stiffness can be obtained:

$$u = \frac{k^{4/3}}{(64EI)^{1/3}} \tag{4.20}$$

where EI is the rail bending stiffness. Hence, track stiffness includes the influence of the rail while track modulus does not.

From extensive field observations Narayanan *et al*. (2004) suggested that track modulus values less than 13.7MPa indicate poor track performance, while values between 13.7MPa and 27.5MPa indicate average performance. A track modulus value of 28MPa may therefore be considered a minimum for good track performance under traffic loading (Selig and Waters, 1994). Based on rail type UIC 60 this equates to a stiffness of 55kN/mm/wheel (Berggren, 2009). Very high track modulus values above 137MPa can cause component failure including ballast degradation and sleeper cracking due to increased dynamic loads (Narayanan *et al*., 2004). Therefore, the existence of an optimum track stiffness for the cases of track geometry maintenance, rail fatigue life and track component degradation have been considered in the literature. It was found that current tracks exhibit stiffness values over a wide range of values, of which the extremes are likely to be unacceptable. Based on studies of a Spanish high speed railway line Pita *et al*. (2004) proposed that an optimal stiffness value for high speed tracks is about 70 to 80kN/mm/wheel, based on an energy costs and energy consumption basis. The optimisation of the vertical stiffness of the track has a favourable effect not only on the reduction in the vertical stresses exerted on the track by the vehicles, but also on the reduction in the level of vibrations generated in the ballast layer. However, Hunt (2005) identified that further research is required to reach a consensus on the optimum track stiffness range for all tracks. It should be noted here that track stiffness and modulus values change when multiple axle loads are in close proximity to each other.

Hunt (2005) noted that as railway vehicle loading is never static, it is typical to distinguish between quasi-static loading with each axle pass and the dynamic loading due to wheel/rail or other irregularities. For most cases the quasi-static load and unsprung mass of the vehicle are the most important issues (Hunt, 2005). Track

irregularities are out with the scope of this thesis and will not be discussed in any detail. Dynamic track stiffness can be analysed for railway tracks using Fourier transforms and associated transfer functions if the stiffness is assumed to be linear about a certain reference preload. This assumption is approximately valid for a limited portion of the force-deflection diagram. The transfer function between force and displacement is called receptance (α) or dynamic flexibility:

$$\alpha(f) = \frac{z(f)}{F(f)} \tag{4.21}$$

Receptance is the inverse of dynamic stiffness and is often used in preference. An example of receptance magnitude is shown in Figure 4.12 based on measurements on track with a clay subgrade made with a track loading test vehicle in Sweden. It can be seen that resonance occurs at a loading frequency of around 5 to 8 Hz due to the soft clay subsoil. It can also be seen that the track is stiffer (lower receptance) for higher frequencies up to at least 50 Hz. Ground borne vibration problems (typically in range between 4 and 30Hz) are associated with subgrade soils of low stiffness and/or a clear resonance as these tend to propagate vibrations more effectively. Where the trackbed stiffness is low, the train speed may approach the speed at which the deflection wave of the rails underneath the wheel propagates (Hunt, 2005). This is referred to as the critical speed phenomenon and it is normal to apply a speed limit of typically 70% of the critical speed (Hunt, 2005 & Banimahd, 2008). The critical speed phenomenon has not been considered within GRAFT and the GRAFT tests are not concerned with high speed train effects on soft soils.

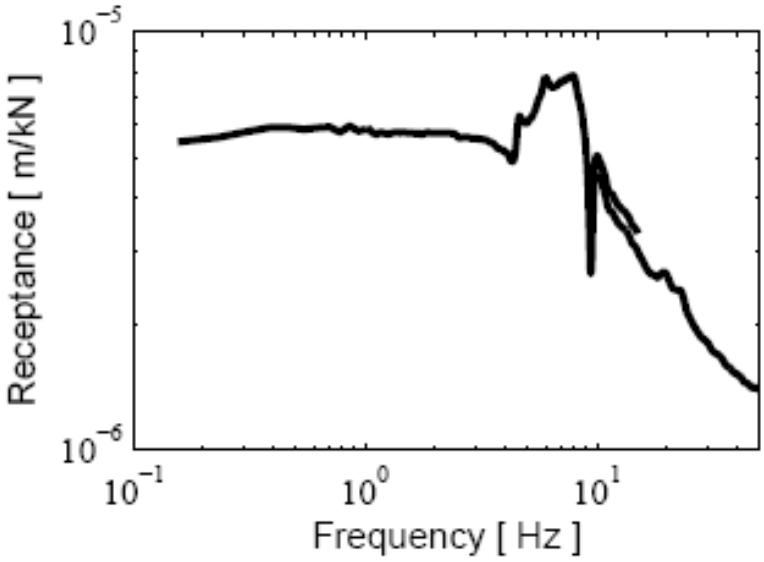

Figure 4.12. Measurement of track receptance of track with clay subgrade (Berggren, 2009)

Track stiffness in the field can be measured both at standstill at discrete intervals and continuously while rolling along the track. As track stiffness is a function of frequency it is necessary to select an appropriate measuring device depending on the frequency of interest (Berggren, 2009). Static and low frequency measurements of track stiffness (<50Hz) are related to the geotechnical track issues while high frequencies (>50Hz) relate to problems associated with noise and train-track interaction forces. The most important factors that decide the vertical frequency content in the train-track interaction are the train (speed, axle distance etc.), the track receptance and the track irregularities. High frequency issues will not be considered within this thesis as they do not directly influence the track substructure. Some typical standstill measurement devices used for low frequency geotechnical related monitoring include simple instrumentation, Falling Weight Deflectometer (FWD) and track loading vehicles (TLV).

Simple instrumentation such as displacement transducers or accelerometers can be used on any number of sleepers, and/or rails to measure the response during the passage of a train. The associated stiffness can then be calculated for that track section if the axle load is known; typical load-deflection diagrams are produced where the vertical track

stiffness and modulus are calculated from the above definitions. For multiple axle loads the rail deflection may be obtained by superposing the effects of the various wheel loads (Kerr, 2000). Bowness *et al*. (2007) reported on a remote video monitoring technique using a webcam and a small telescope to measure peak-to-peak displacements on track to within 0.04mm for frequencies less than 4Hz. Priest and Powrie (2009) described a method to record the dynamic track stiffness where geophones were placed on the track to measure the dynamic displacement during passage of a train.

The FWD is a device that is used in the UK to measure the stiffness of the track structure excluding the rails. The standard FWD consists of a mass that is dropped from a known height onto a set of rubber buffers mounted on a circular footplate (Figure 4.13). The resulting impact force is measured by a load cell on the centre of the plate, and geophones are used to measure surface velocity at various distances from the footplate (Burrow *et al*., 2007b). These velocities are integrated to give vertical displacements. For railway tracks in the UK, the device is designed to apply an equivalent 125kN load to a sleeper disconnected from the rails, via a 1.1m loading beam. The loading system is considered to produce a load pulse similar to that applied by a single 25 tonne axle load of a train travelling at high speed (Burrow *et al*., 2007b). The magnitude of the applied load is measured in the centre of the loading beam and the geophones are positioned on the loaded sleeper and on the ballast at various distances from the centre of the beam to produce a deflection basin. The track stiffness is calculated from the load and deflections measured at some of the geophones, depending on the application. However, the FWD shows a large degree of scatter in the results (Burrow *et al*., 2007b) and as such a high degree of interpretation is required. Network Rail standard NR/SP/TRK/9039 (2005) defines the FWD stiffness measurement as a dynamic sleeper support stiffness and 60kN/mm/sleeper end is a minimum requirement for a new track construction. Further interpretation is required here though as the influences of the rail and sleeper spacing are not included. Hence, it has been recommended by Woodward *et al*. (2009b) that further research be undertaken to compare the dynamic FWD sleeper support stiffness to both quasi-static and dynamic stiffness measurements from standstill TLV and rolling wheel devices.

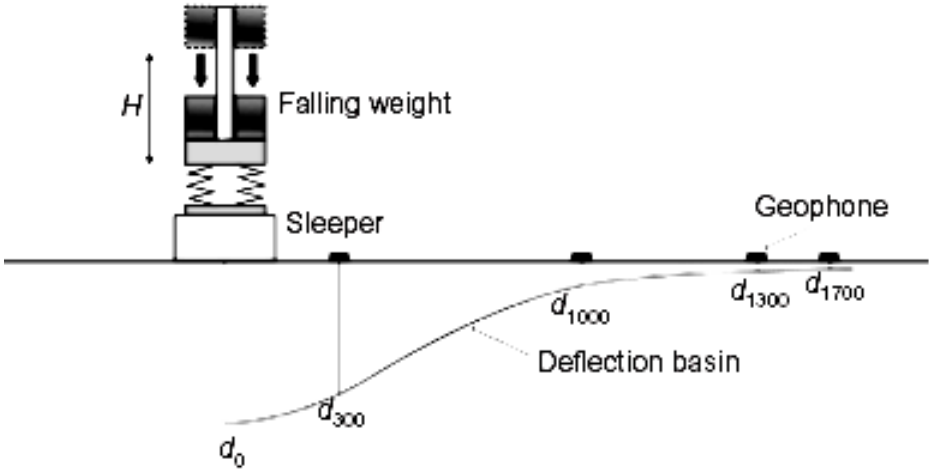

Figure 4.13. FWD measuring principles (Burrow *et al*., 2007b)

TLV use their own weight to load the track via hydraulic jacks and depending on the equipment used different loads can be applied. The loads are usually applied to the rail heads, although sleepers can also be loaded with the rails decoupled (Berggren, 2009). Examples of TLV used worldwide have been detailed by Berggren (2009) and include those developed in the USA by the Transportation Technology Centre (TTCI); The South African BSSM, and a modified tamper. The Swedish TLV described by Berggren (2009) has a weight of 49 tons and can load each rail statically up to 150kN and excite dynamically by up to 200Hz. The main advantage of a standstill TLV compared to rolling measurements is that the preload, dynamic load and frequency can be varied to a greater degree (Berggren, 2009). However, the process is much more time consuming and requires the track to be closed. Rolling measurements on the other hand have the potential to be used on a more regular basis for maintenance purposes if the vehicle travelling speed is relatively high.

Most rolling measurement devices currently available measure the displacement under one or two axles and with knowledge of the static axle loads, the vertical track stiffness can be calculated. For systems with two axle loads, the axle loads are different and the lightest axle load is used to remove the effect of track irregularities (sleeper voiding

etc.) on the stiffness measurement. A number of organisations around the world have developed rolling devices to measure track stiffness and these have been summarised by Berggren (2009). Figure 4.14 shows the measuring principle behind the Swedish rolling measuring device developed by Banverket called RSMV (Rolling Stiffness Measurement Vehicle). Berggren (2009) noted that the vertical track stiffness measured by each device is unlikely to be identical due to different static preloads, different excitation frequencies due to different vehicle running speeds, different spatial resolutions, different rail bending models used to determine the rail deflection under the wheel set, and track irregularities such as wheel flats and wheel out-of-roundness. A comparison between the different methods, both standstill and rolling wheel, is difficult to perform without measuring the same track. On that point, Berggren (2009) states that not all of the current methods have shown confident results. Therefore, further research and analysis is required in the area of track stiffness measurement devices until a unified standard is obtained. Berggren (2009) noted that a system that could continuously measure stiffness directly under the wheel at speed with the ability to measure both different frequencies and preloads is favourable.

Within GRAFT vertical track stiffness measurements have been measured continuously throughout each test stated in Table 3.7. The GRAFT track stiffness measurements represent a quasi-static stiffness measurement under wheel loading, ignoring track irregularities (dynamic factor) and assuming that the static stiffness does not vary across GRAFT. As no rail pads were used in GRAFT their influence is unknown. It was observed by Hunt (2005) however that even soft rail pads are generally much stiffer than the trackbed and as such their effects often neglected. Nonetheless, an estimate of their influence has been made and is presented within the next section. The additional study undertaken after CT4 investigated the influence on track stiffness of the applied load and rate of loading and is also presented within this chapter. Within this study GRAFT was acting effectively as a TLV. In addition, as the subgrade modulus varies throughout the testing programme the influence of the subgrade modulus on track stiffness has been studied and will be presented along with the relationship found between track stiffness and settlement. Hence, the importance of track stiffness in terms

of track geometry deterioration will be discussed and some of the most significant factors that influence track stiffness considered.

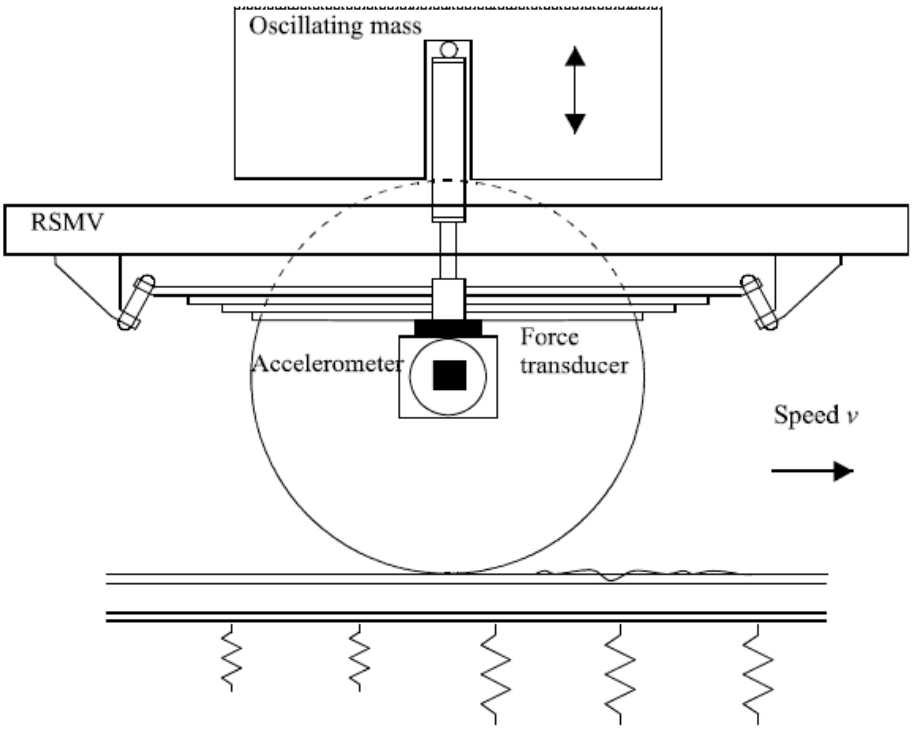

Figure 4.14. Swedish rolling wheel measuring device principle (Berggren, 2009)

4.3.1 Measurement of track stiffness in GRAFT

The central sleeper transient deflection plotted against the number of applied cycles for the four control tests is shown in Figure 4.15. The deflection was measured from the average deflection of the two LVDT's placed at either end of the central sleeper and it can be seen from Figure 4.15 that the applied load and the subgrade modulus directly influence the sleeper deflection. The general trend shown for all tests is that the sleeper deflection decreases as the number of cycles increases. This is due to initial ballast densification during the accumulation of loading cycles and this trend will continue until the ballast reaches a resilient state. Nottingham University found a similar trend using their laboratory railway testing facility (Brown *et al*., 2007a).

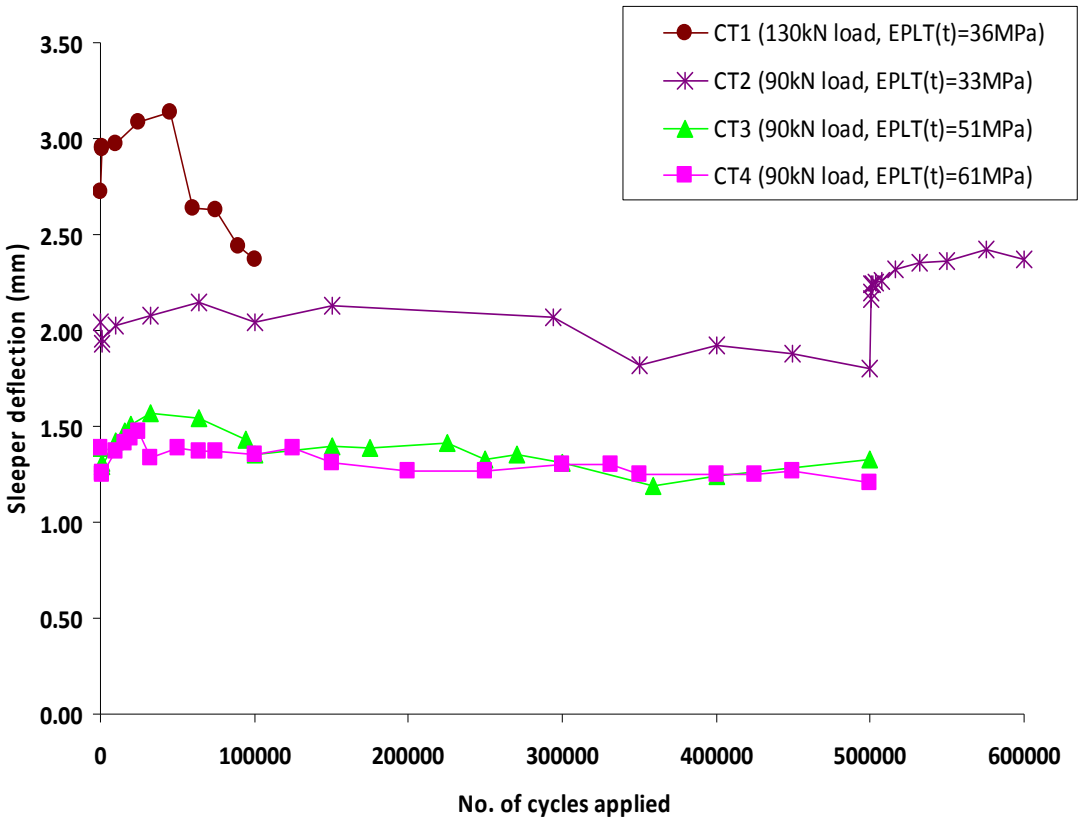

Figure 4.15. Centre sleeper deflection throughout control tests.

Ballast densification at the start of CT1 is greater than other control tests due to the increased applied load, resulting in an increased rate of reduction of transient sleeper deflection with number of cycles. The same increased rate of reduction of transient deflection is not seen when the load is increased from 90kN to 110kN after 500,000 applied cycles in CT2. On the application of the higher load the transient sleeper deflection increases by around 25% and does not change much over the course of an additional 100,000 cycles at the higher load. These transient sleeper deflection values, however, do not translate directly into track stiffness values due to the loading mechanism assumed in GRAFT (Figure 3.5). The track stiffness in GRAFT has been measured by recording the deflection of the rail for the known applied vertical load using an LVDT placed on the centre of the rail. From the rail deflection data the vertical track stiffness can be calculated for each cycle. However, only CT3 and CT4 had an LVDT placed on the rail to give an accurate measure of track stiffness. The track stiffness has been estimated for the other control tests based on the actuator head displacement. In addition to the track stiffness and track modulus values found in

GRAFT the trackbed stiffness excluding the rail can also be estimated. The trackbed stiffness estimations assume a 40% load distribution on the middle sleeper (shown in Chapter 3) and use the deflection from the middle sleeper LVDT's.

The load-deflection curves at different cycles in CT3 are illustrated in Figure 4.16 & Figure 4.17. The curves are non-linear and show hysteresis, which is typical of most railway track behaviour. This non-linearity is due to the particle re-arrangement during densification. Hence, the stiffness of the track depends heavily on the applied load and when determining the track stiffness it is appropriate to apply a load similar to the maximum axle load for that section of track. Using the secant track stiffness definition in equation 4.18, with point a being taken as the minimum applied load and resulting deflection and point b the maximum, the track stiffness and trackbed stiffness for individual cycles throughout the testing programme can be found. It should be noted here though that, as only 10 data points are recorded per cycle (cycling at 3 Hz and data recorded at 30 Hz), the absolute maximum and minimum values may not be recorded as can be seen in Figure 4.16 and Figure 4.17. The calculated secant stiffness values are therefore an approximation and when plotted against the cycles the data is more scattered than in Figure 4.17. As such, the track stiffness and trackbed stiffness values do not show a clear increase in stiffness with cycles as suggested from the deflections shown in Figure 4.15. As a result a mean track stiffness and trackbed stiffness value for each test in GRAFT has been taken from all the applied cycles. These values ignore the slight increase in track stiffness with cycles and assume that track stiffness is constant throughout each test. The Mean track stiffness, track modulus and trackbed stiffness values found for the control tests in GRAFT are shown in Table 4.4. It should be noted here though that these values are specific to GRAFT and not equivalent to the field as the load applied in GRAFT is to simulate a particular axle load applied in the field (equation 3.1). In addition, due to the reduced depth of GRAFT the track deflection values in GRAFT underestimate the field. This will be discussed in Chapter 7.

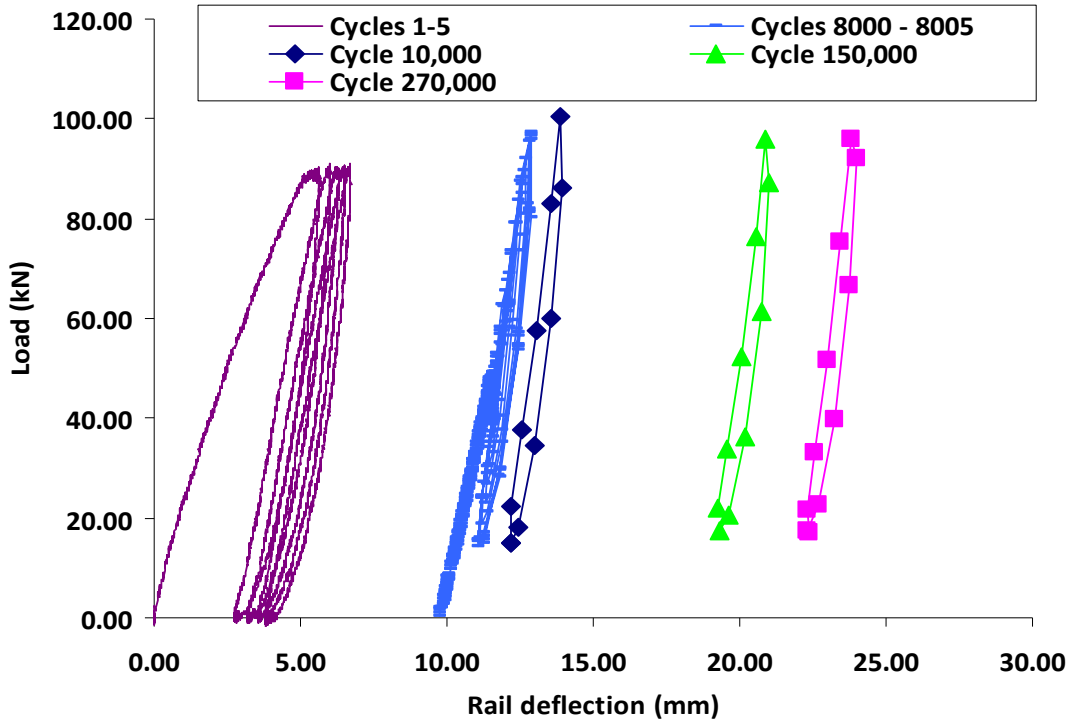

Figure 4.16. CT3 vertical load-deflection curves measured on rail (deflection data is cumulative with cycles)

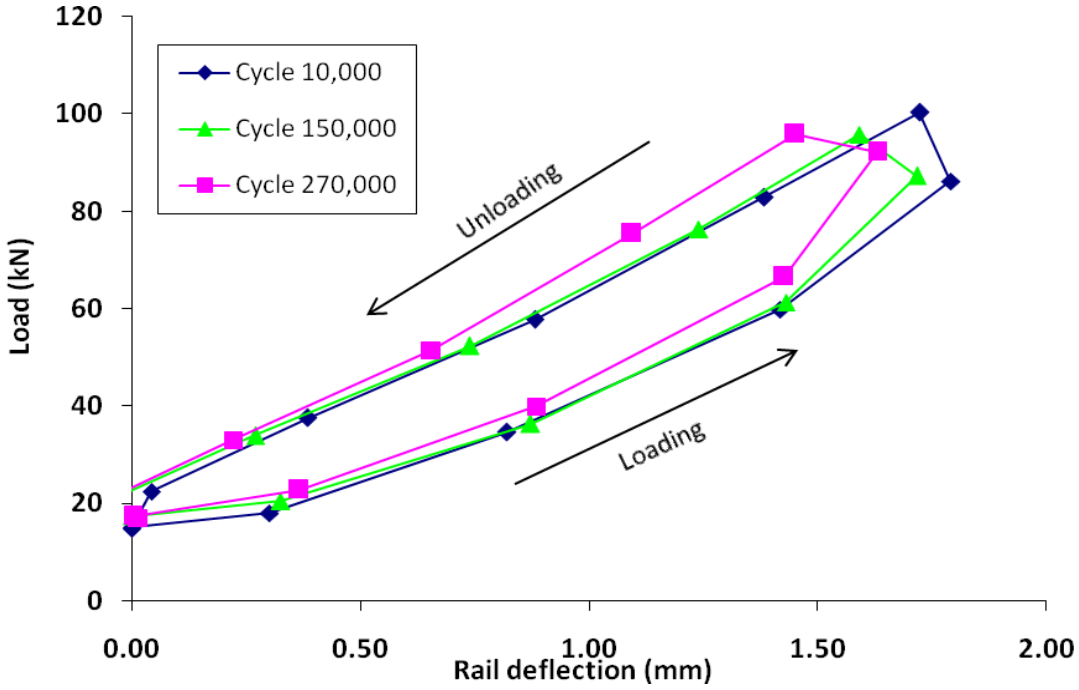

Figure 4.17. CT3 vertical load-deflection curves measured on rail (deflection data is taken from zero for each cycle)

GRAFT test	Mean Trackbed stiffness (kN/mm/sleeper end)	Mean Track stiffness (kN/mm/wheel)	Mean track modulus (MPa)
CT1	17.7	36.9	19.2
CT2	18.4	38.2	19.5
CT3	23.9	47.0	25.6
CT4	24.8	50.0	27.8

Table 4.4. Mean trackbed stiffness, track stiffness and track modulus values found in GRAFT tests

From Table 4.4 it can be seen that the track stiffness values are around 104% greater on average than the estimated trackbed stiffness values. This is similar to the ratio shown in an example by Hunt (2005) for a typical track section. This ratio depends on the rail bending stiffness and sleeper spacing. The advantage of estimating the trackbed stiffness in GRAFT is that the effect on track stiffness of different rail pads can be estimated by determining the series stiffness of the two components as follows (after Hunt, 2005):

$$\frac{1}{K_{series}} = \frac{1}{K_{railpads}} + \frac{1}{K_{trackbed}} \tag{4.22}$$

If rail pads with a stiffness of 150MN/m (typical rail pads) were used in GRAFT then the trackbed stiffness for CT1 (in GRAFT) would be reduced from 17.7kN/mm/sleeper end to 15.8kN/mm/sleeper end. Table 4.5 shows the effects that using different types of rail pads would have on the trackbed stiffness measured within GRAFT for each test. The values highlight that the stiffer the rail pad used the greater the vertical track stiffness, as would be expected. Pita *et al*. (2004) found similar results when investigating the influence of rail pad stiffness on vertical track stiffness on both conventional and high speed lines in France and Germany. Therefore, it can be seen how the rail pads can play an important role when considering the optimum track stiffness for a specific track; Pita *et al*. (2004) stated that if an optimum vertical track stiffness of 75kN/mm is desired with a trackbed stiffness for high speed lines taken as

98kN/mm then the rail pad should have a stiffness of approximately 30-50kN/mm (soft).

Type of rail pad	Rail pad stiffness (MN/m)	CT1 trackbed stiffness (kN/mm/sleeper end)	CT2 trackbed stiffness (kN/mm/sleeper end)	CT3 trackbed stiffness (kN/mm/sleeper end)	CT4 trackbed stiffness (kN/mm/sleeper end)
Soft	75	14.3	14.8	18.1	18.6
Typical	150	15.8	16.4	20.6	21.3
Stiff	500	17.1	17.8	22.8	23.6

Table 4.5. The influence different rail pads would have on the trackbed stiffness values found in GRAFT

4.3.2 Influence of rate and magnitude of applied loading

To study the influence of load level and rate of loading on track stiffness the additional study after CT4 was used. The specific details relating to the track stiffness investigations are shown in Table 3.8. As well as cyclic loading the effect on track stiffness of the rate of applied loading of a single cycle impulse load was also investigated at different load levels, both on the ballasted track and on the subgrade surface. The response of the subgrade surface was monitored exactly the same way as the routine plate load tests undertaken in GRAFT prior to each test and the load was applied in the same way via a series of stacked plates. The subgrade loading was undertaken after the removal of the ballast and formation layers at the end of the additional study after CT4.

The influence on track stiffness of the impulse loading rate for different applied loads is shown in Figure 4.18 for loading rates up to 6Hz. The rail displacement has been used here again as an indicator of track stiffness and it can be seen that for all load cases there is a slight decreases in rail deflection with an increase in loading rate. However, as these applied loads are single impulse loads the rate of loading and resulting

displacements cannot be related to the frequency of loading that is required to develop resonant conditions as in Figure 4.12; cyclic loading is required (the LOS is incapable of applying such high frequency loading of greater than 5Hz at these loading ranges). The GRAFT results, from varying the applied rate of loading on the clay subgrade surface, did not produce any significant trends and hence have been omitted from the presented results.

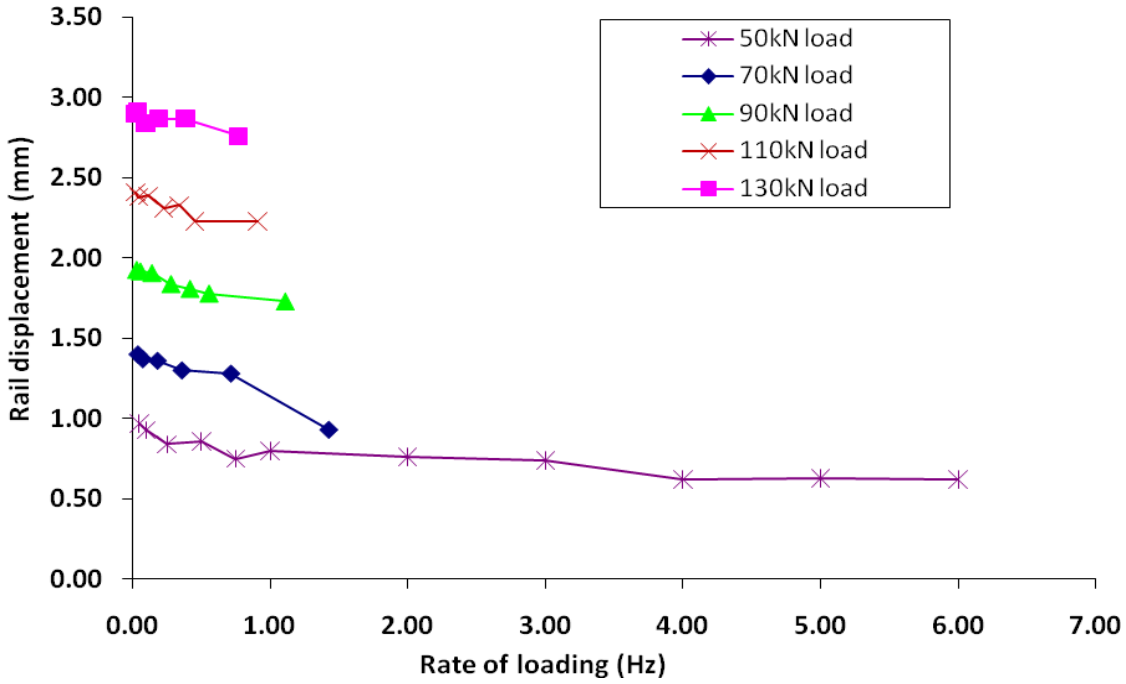

Figure 4.18. Influence on track stiffness of impulse loading rate for different applied loads

The influence of the applied load on track stiffness found from this additional study is illustrated in Figure 4.19. Both the mean track stiffness calculated from cyclic loading (3Hz) over 10,000 applied cycles at different load levels and the mean track stiffness calculated at different loading rates from the single impulse loads at different load levels are shown. The trend of these two lines both show that track stiffness in GRAFT increases with an increase in load to a certain point and then levels off before starting to decrease once the applied vertical load passes around 110kN. The difference in track stiffness magnitude between the impulse load values and the cyclic load values is thought to be due to a combination of the change in loading rate of the applied loading

and also due to an increase in stiffness during cyclic loading; ballast particles continually compressed into the voids and re-arranged. Undertaking both static and cyclic triaxial tests on ballast Suiker *et al*. (2005) found that cyclic loading can increase the ballast stiffness by a factor of 3.5 (after 1 million load cycles) compared with static loading. The mean track stiffness values found at different load levels in CT2 and CT1 are also shown in Figure 4.19. If it is assumed that the subgrade modulus in CT1 (36MPa) is the same as CT2 (33MPa) then CT1 and CT2 can be combined to show the same trend as the additional study results found after CT4. This trend ignores the different number of cycles involved regarding each data point and assumes that the influence here is negligible. The difference in track stiffness magnitude between the CT1-CT2 line and the stiffness measurements after CT4 is due to an increased subgrade modulus for CT4.

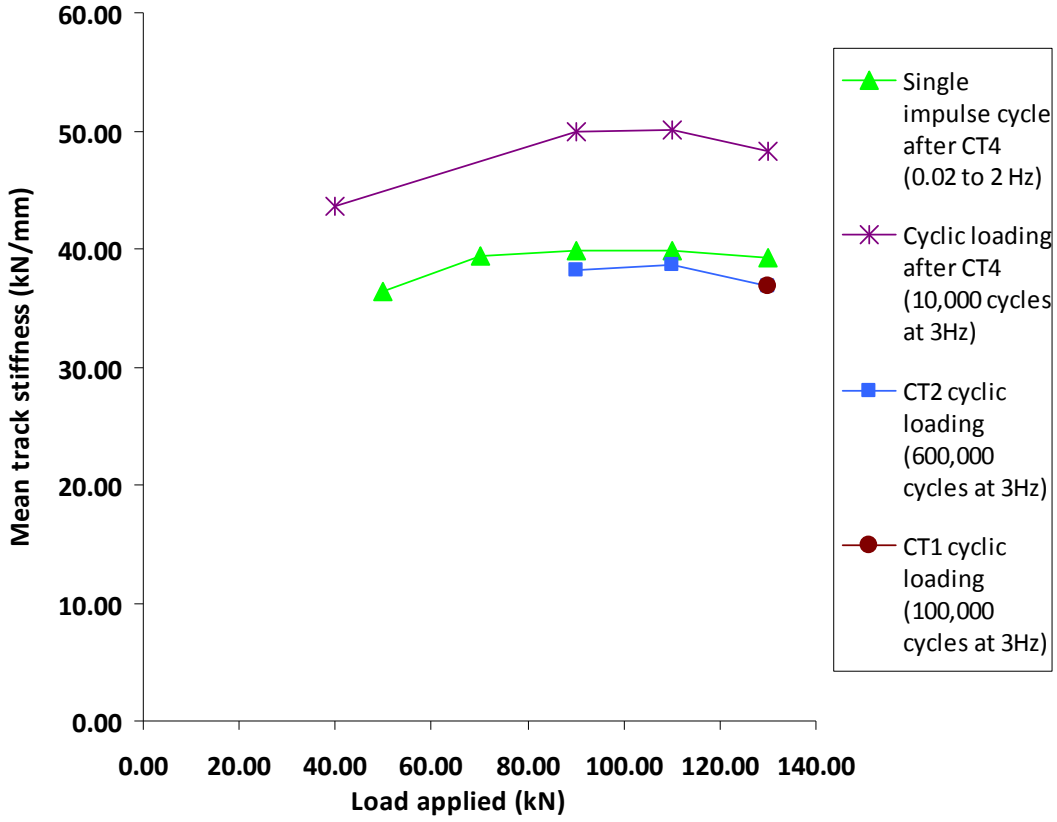

Figure 4.19. Influence of applied load level on track stiffness

Figure 4.20 to Figure 4.22 illustrate individual cycles from both cyclic loading and impulse loading after CT4 at different loading levels and different loading rates. Figure 4.20 shows that cyclic loading produces slightly less rail deflection for the same applied load compared with impulse loading. Figure 4.20 also shows that impulse loading at a higher rate produces less rail deflection than impulse loading at a lower rate.

If it is assumed that the track is in a resilient state after 500,000 applied cycles during CT4 then the non-linear trend shown in the data after CT4 in Figure 4.19 can be explained by considering the non-linear nature of the substructure response to loading. Resilient behaviour is represented by the resilient modulus, which is defined as the repeated deviator stress divided by the recoverable axial strain during unloading in the triaxial test (Selig and Waters, 1994). Extensive research in recent decades has shown nonlinearity in the resilient behaviour and the resilient modulus of soil (either coarse or fine-grained) is significantly affected by several parameters, such as stress/strain state, density and moisture content (Banimahd, 2008). Banimahd (2008) conducted an in depth review of nonlinearity in both granular ballast and clayey subgrade and found that in clayey subgrades, the resilient modulus depends mainly on shear stress while for granular soil, the resilient modulus depends on mean stress. Within granular soil subjected to cyclic loading, two contradictory phenomena may occur at the same time, namely an increase in the secant bulk modulus with bulk stress and a decrease in the secant modulus with deviatoric stress. Hence, the resilient behaviour of granular soils is governed by the interaction of both mechanisms and an increase in shear (deviatoric) stress or strain does not always result in a decrease in resilient stiffness. Brecciaroli and Kolisoja (2006) explained that at a low level of stress, the stiffness of the material increases as the stress increases; the particles are forced into new interlocked positions and the compacted material becomes more closely packed and harder to move. Strain softening is, however, observed as the stress level approaches the failure state. Whether strain hardening or softening mechanisms are dominant depends mainly on the level of shear strain/stress to which the granular soil is subjected. Banimahd (2008) also reported on several studies that found that the resilient modulus of clay decreases with deviatoric stress.

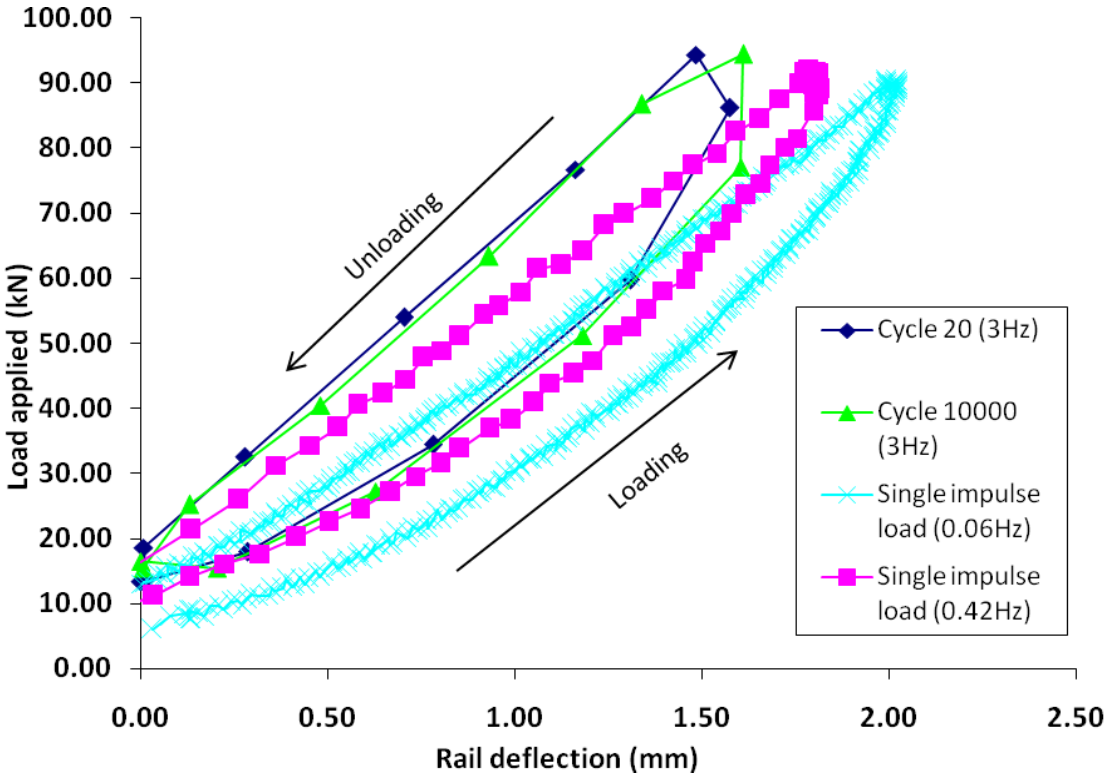

Figure 4.20. Vertical load-deflection curve after CT4 for different types of loading

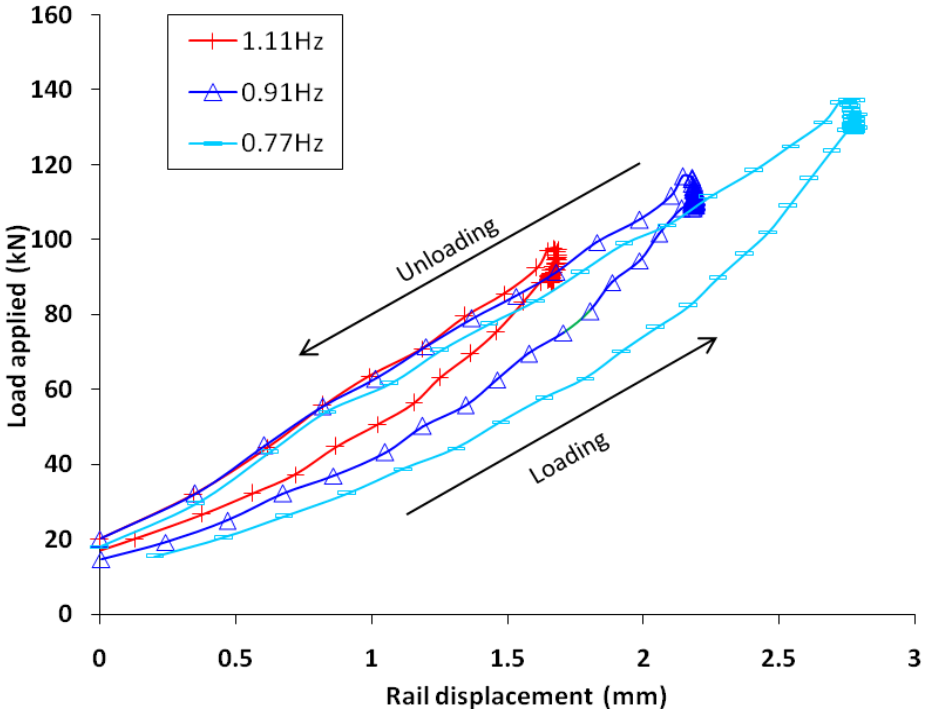

Figure 4.21. Load-deflection curves for various single impulse loads after CT4

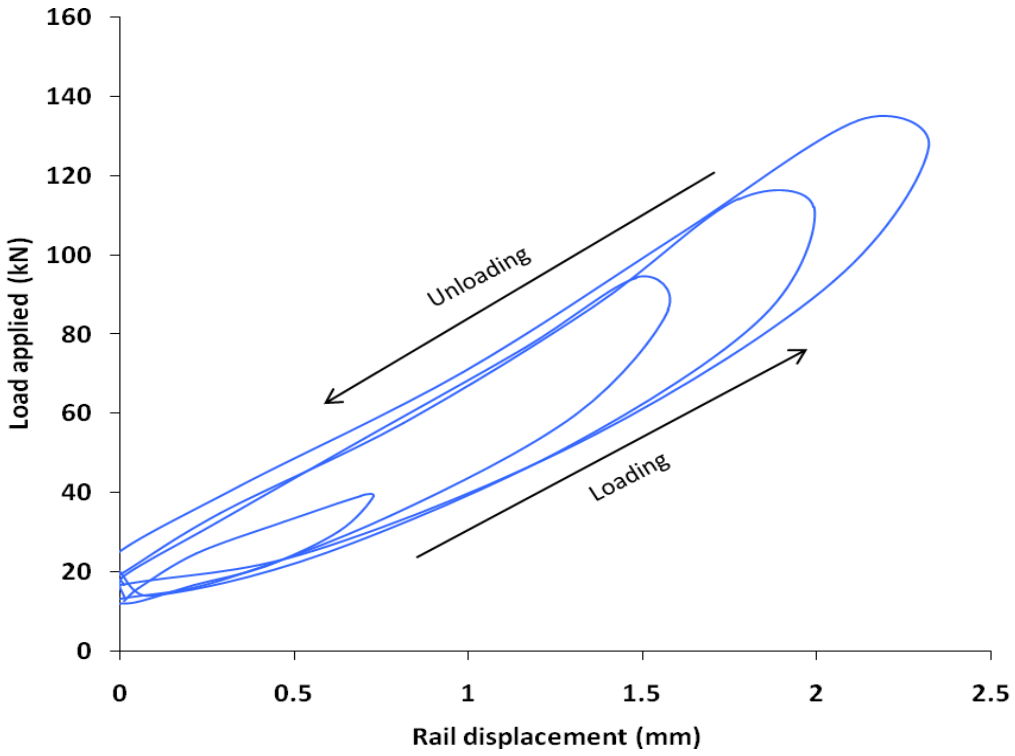

Figure 4.22. Load-deflection curves at cycle 20 for various cyclic loads after CT4

The effect on the subgrade modulus in GRAFT of varying the applied load is shown in Figure 4.23. It can be seen that the clay subgrade secant modulus decreases with an increase in applied load, as would have been expected. If higher load levels had been applied the subgrade modulus may have decreased to a low asymptotic value as found by Frost *et al*. (2004). This has direct implications when measuring the subgrade modulus of clay subgrade materials; the appropriate load should be applied to the subgrade from whatever in-situ testing technique is used, which is representative of the stress found on the subgrade when under repeated traffic loading. Further discussion of in-situ subgrade testing devices will be given in Chapter 6.

Therefore, assuming the confining pressure is constant within GRAFT, these short studies indicate that the non-linear resilient behaviour of both the clayey subgrade and ballast layers, with applied load, have been modelled accurately; i.e. an increase in applied load results in a reduction in clay stiffness and an increase in ballast stiffness for low load levels up to 110kN. Beyond an applied load of 110kN it is thought that the

ballast stiffness decreases and if the load applied to the ballasted tracks was increased further it is likely that the track stiffness would reduce considerably due to both ballast and subgrade stiffness degradation. These non-linear effects are highlighted again in Figure 4.24 where rail deflection has been plotted against applied load for the 10,000 loading cycles after CT4. The applied load values are slightly different from those stated in Table 3.8 and plotted in Figure 4.19 as these values are the values taken from the individual cycles, and as such the track stiffness for each applied load can be estimated directly from Figure 4.24. The non-linear effects can be seen by the changing gradient of the curve, representing a reduction in track stiffness as the applied load increases past 100kN. Hence, from Figure 4.19 and Figure 4.24 it is possible that the maximum achievable track stiffness in GRAFT (for the soil in its present condition) for CT4 is 50kN/mm/wheel within this relatively low range of frequency loading. To increase the stiffness further either ballast or subgrade reinforcement would be required if the ballast depth, sleeper spacing and track components were kept constant. Ballast reinforcement techniques will be covered in detail within the following chapter.

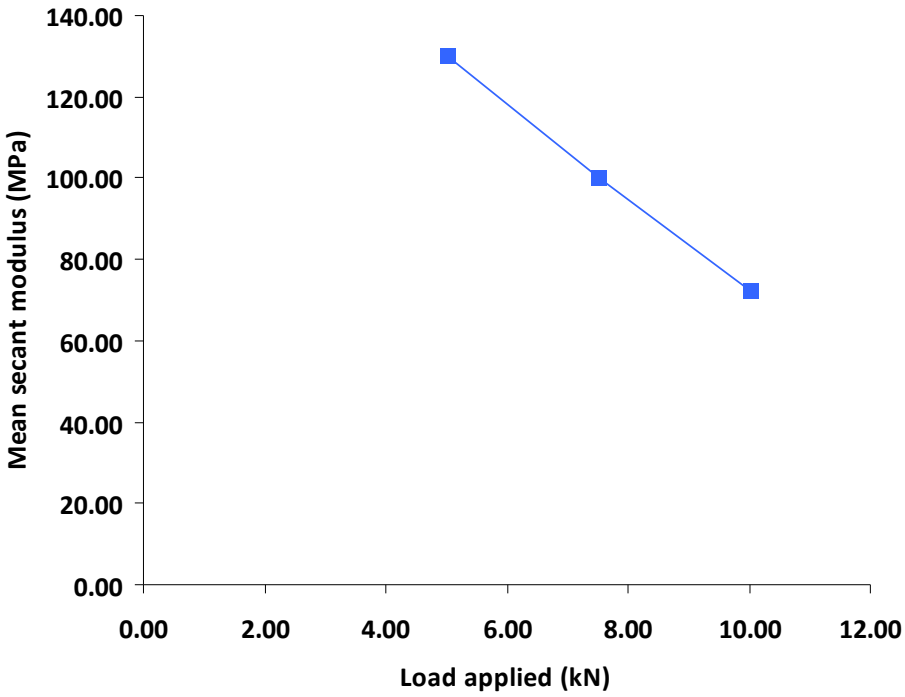

Figure 4.23. Clay subgrade secant modulus variation with applied load

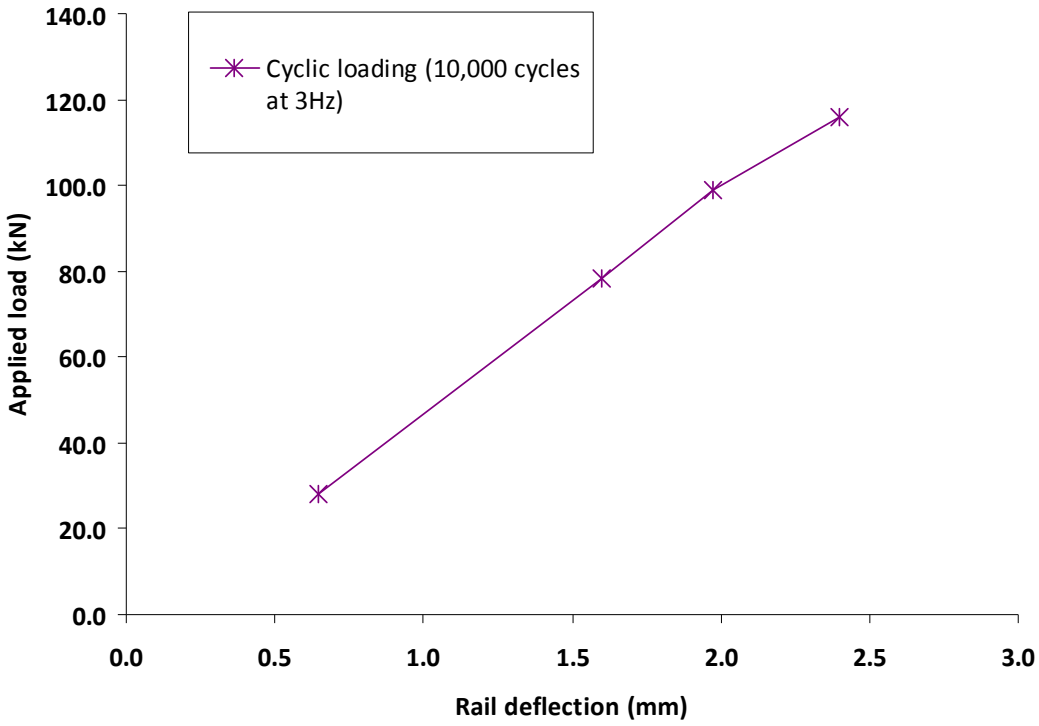

Figure 4.24. Effect of applied load on rail deflection

4.3.3 Influence of subgrade modulus

Recent research has suggested that the subgrade is the most significant factor governing track stiffness and hence the deterioration of vertical track geometry (Brough *et al*., 2006). This was also found by Hunt (2005) who stated that the subgrade properties are the primary determinant of the overall track stiffness. Using a static finite element model, Shahu *et al*. (1999) indicated that subgrade stiffness has the maximum influence on the track modulus when compared to the effects of ballast and subballast stiffness. The influence of the subgrade condition is further enhanced by the fact that the subgrade resilient modulus is the most variable quantity of the track; subject to change in soil type, environmental conditions and stress state. However, although subgrade stiffness is regarded by some researchers as the main contributing factor to track stiffness, limited research has been published to show the direct link. Hunt (2005) stated that this is an area that needs further research in order to better quantify the relationship.

Within this research Figure 4.15 has already highlighted that a direct relationship exists between subgrade and track stiffness and Figure 4.25 shows the load-deflection curves for the middle sleeper taken at cycle 100,000 for CT2 to CT4. Clearly as the subgrade modulus increases the track stiffness increases and Figure 4.26 shows the trends that can be drawn from the results. Figure 4.26 shows that logarithmic trend lines fit the data well with the tangent modulus correlation giving an R^2 value of 0.99, the reloading modulus correlation giving $R^2 = 0.95$ and the resilient modulus at breakpoint stress correlation giving an R^2 value of 0.98. The track stiffness value from CT1 has also been plotted in Figure 4.26 against the corresponding reloading modulus and it can be seen that by increasing the load from 90 to 130kN the track stiffness has reduced by around 7%, all other factors being equal. The tangent modulus correlation gives similar results although the resilient modulus correlation predicts a higher reduction in stiffness. This 7% reduction in track stiffness is greater than the 3% reduction shown in Figure 4.19 for the same load levels from the additional study undertaken after CT4. This is due to the track stiffness value for CT1 in Figure 4.26 being taken from the mean track stiffness over 100,000 applied cycles, while for the CT2-4 curves the mean track stiffness is based on 500,000 applied cycles. The mean track stiffness value would be higher for CT1 over 500,000 cycles and the reduction in track stiffness found from increasing the applied load from 90 to 130kN would be to closer to 3%, as found after CT4 for track assumed to be in a resilient state (Figure 4.19). Using Figure 4.26 the track stiffness in GRAFT at an applied load of 90kN at 3Hz can be predicted for any subgrade modulus for a track with the same ballast properties and track preparation procedures as in CT1 to CT4.

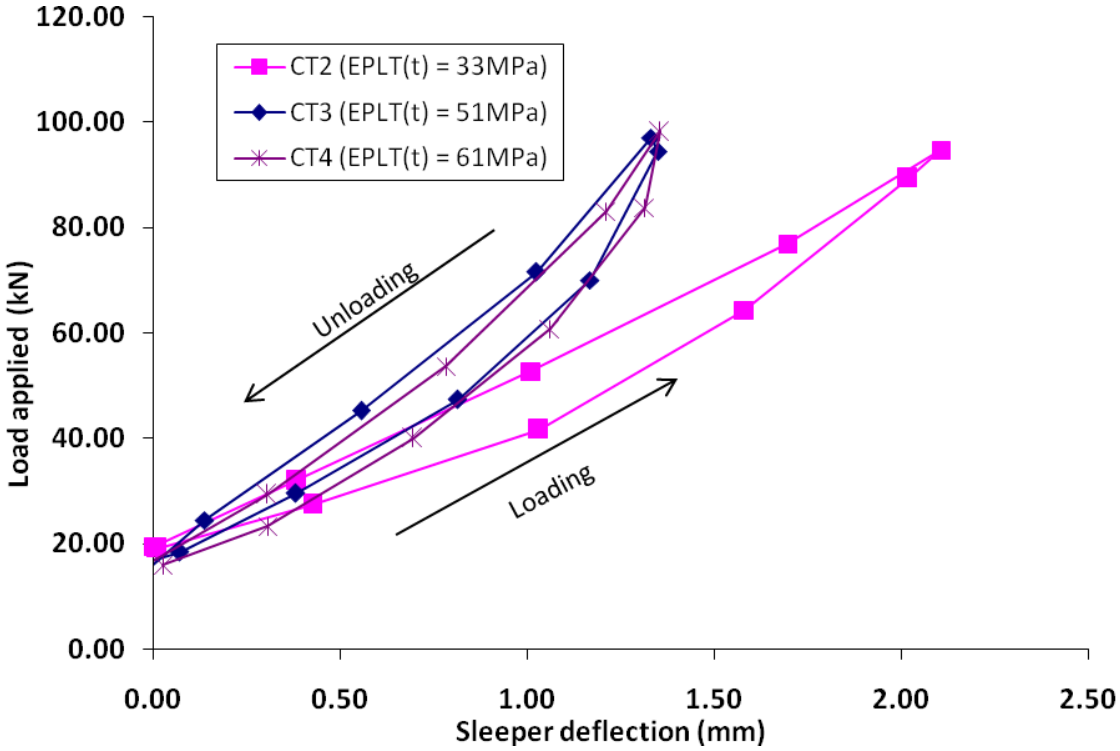

Figure 4.25. Vertical load-sleeper deflection curves taken at cycle 100,000

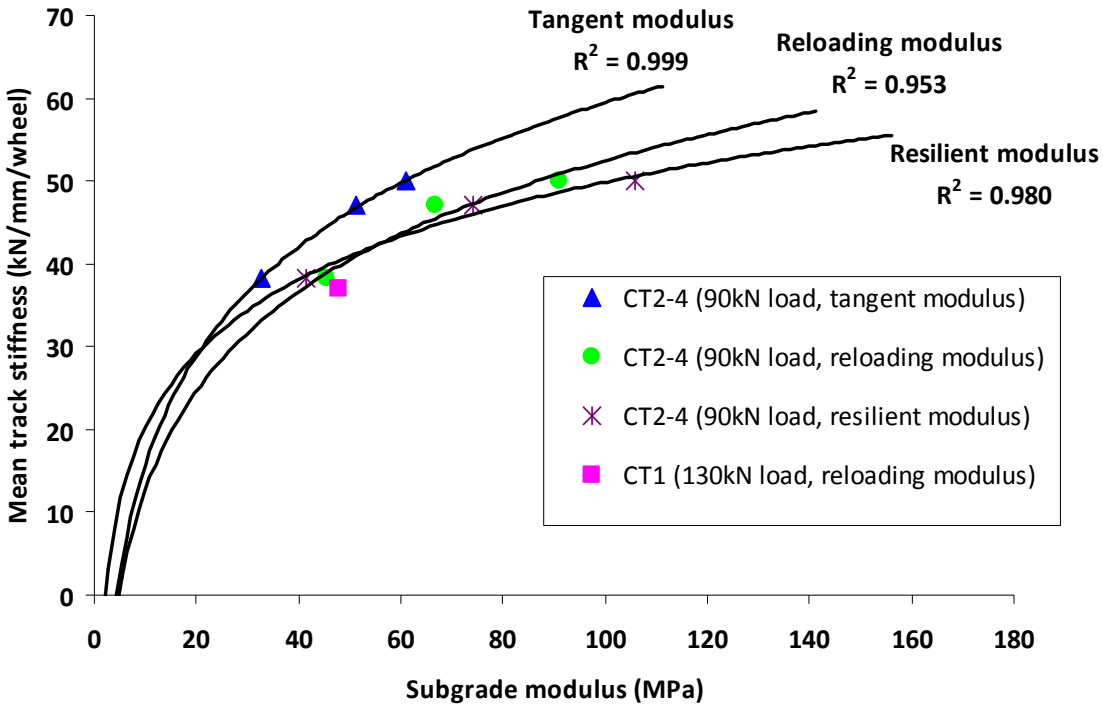

Figure 4.26. Influence of subgrade modulus on track stiffness

4.3.4 Relationship between track stiffness and settlement

As previously stated track stiffness is a useful factor to include in any track settlement model as it is one parameter that takes account of the whole track structure. Hunt (2005) stated that low track stiffness directly produces an increase in ballast settlement due to higher shear strains in the ballast. Furthermore, using a settlement model Dahlberg (2001) stated that a 10% increase in deflection yields a 27% increase in ballast settlement. In the development of a static track deterioration prediction model, based on a modified track settlement equation, Fröhling (1997) found that spatial variation of track stiffness contributes significantly to track deterioration, both in terms of differential track settlement and increased dynamic vehicle loading. The static model proposed by Fröhling (1997) is as follows:

$$\varepsilon_{Ni} = \left[\left[K_1 + K_2 \left(\frac{k_{2mi}}{K_3} \right) \right] \frac{P_{dyn}}{P_{ref}} \right]^{w} \log N \tag{4.23}$$

where ε_{Ni} is the track settlement in mm; K_1 and K_2 are material constants with values given for a particular site of 194kPa and -1.96x10^{-3} m^{-1} respectively; k_{2mi} is the track stiffness in kN/m at a particular sleeper; K_3 is a constant to convert between calculated and measured track stiffness values and a value of 1.34 is given by Fröhling (1997); P_{dyn} and P_{ref} are the dynamic and static reference wheel loads respectively; w is a settlement exponent to give a best fit to the measured track settlement and was given as 0.3 for a specific site; N is the number of applied cycles. Fröhling (1997) found that this equation could be used successfully for average track stiffness values between 60 and 132kN/mm; where deviatoric stress was found to vary linearly with track stiffness. The first part of the equation relates deviator stress to track stiffness linearly, with a decrease in deviator stress resulting in a linear increase in track stiffness. This is not what was found in GRAFT, however, different track stiffness ranges were encountered. Equation 4.23 also indicates that the change in deviator stress is approximately equal to the change in dynamic wheel load relative to static wheel load.

To develop a stiffness-settlement relationship from the GRAFT results, the applied load was divided by the mean track stiffness for all control tests and plotted against the K_1 constant found from the track settlement results (from equation 4.6). Figure 4.27 shows that a linear trend fits the data best for this range of applied loads with an R^2 value of 0.99. This trend line indicates that if track stiffness is increased K_1 reduces and hence initial settlement reduces, while if the applied load is increased the opposite occurs and track settlement increases. This is similar to the Fröhling (1997) equation above. Note, however, that this trend uses the mean track stiffness value found from all the applied cycles and thus ignores the initial increase in stiffness with cycles until the track reaches a resilient state. Furthermore, the K_1 constant is for short term non-linear track settlement that occurs after tamping or a ballast renewal and not for linear long term settlement that occurs once track is in a resilient state. Thus, the linear trend shown in Figure 4.27 is only appropriate for short term settlement before track reaches a resilient state.

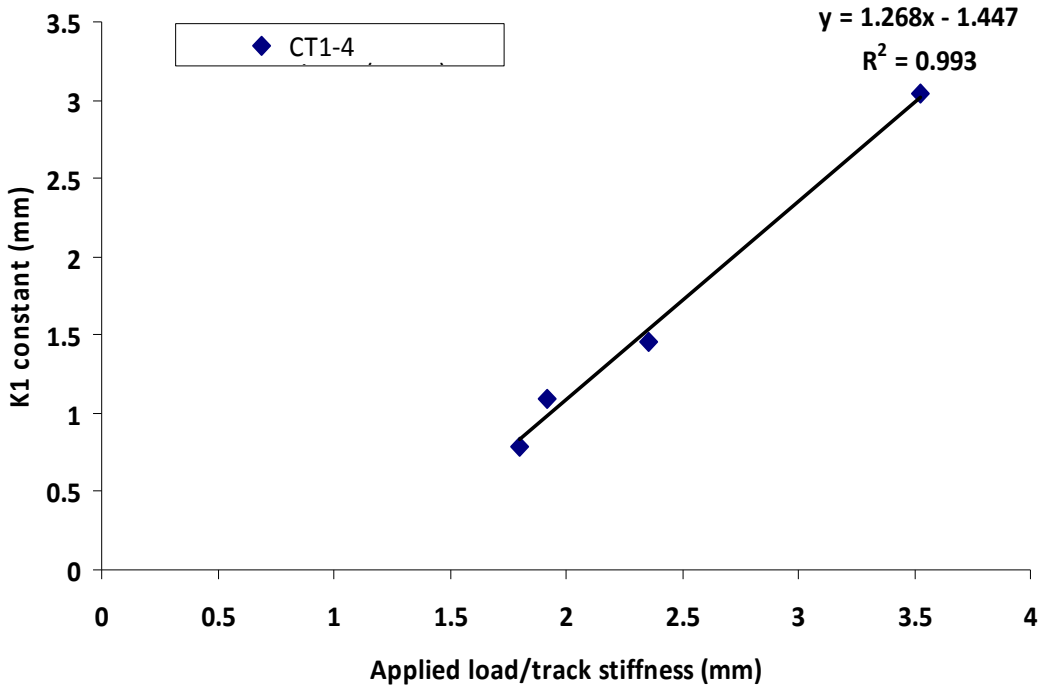

Figure 4.27. Variation of constant k_1 with applied load divided by track stiffness

Once the track becomes truly resilient the linear trend is unlikely to hold as the strain hardening or strain softening behaviour of railway ballast depends on the level of shear strain/stress. Figure 4.28 plots the track settlement against the applied load divided by the track stiffness for the additional study after CT4. Assuming that the track is in a resilient state, it is clear that there is a non-linear trend, which could be influenced by the resilient response of the ballast layer to loading. Further research is required to produce a full track settlement model based on track stiffness data for both initial and long term track settlement. This could be very useful in the field as a rough estimate of short term settlement after tamping or a track renewal could be given instantly based on the track stiffness measurement for the track. The issue then becomes requiring an accurate track stiffness measurement at the same applied load and frequency that the track experiences under repeated traffic loading. It should be noted here though that this estimate for the field is likely to underestimate track settlement due to the reduced depth of GRAFT. This will be discussed in Chapter 7

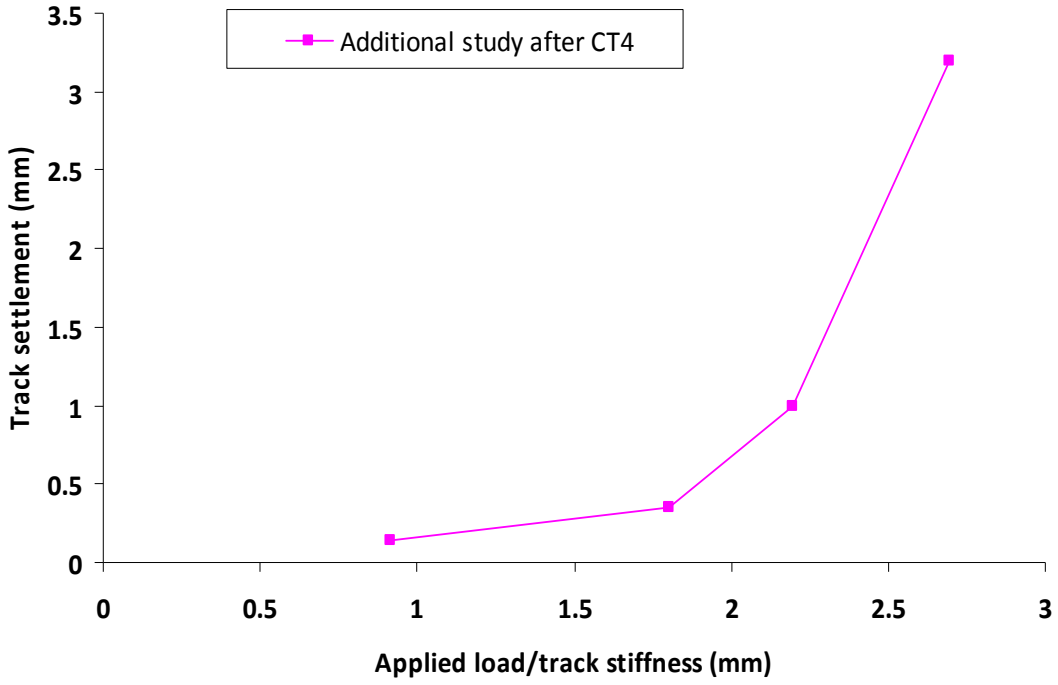

Figure 4.28. GRAFT track resilient response to loading after CT4

Using the limited linear trend found in Figure 4.27, the previous GRAFT subgrade modulus based settlement model (equations 4.9 and 4.10) can be modified to give a

track stiffness based settlement model for axle loads from 25 to 37 tonnes (with a minimum load to track stiffness ratio of 1.141mm):

$$y = (1.268(p/k) - 1.447)N^{0.23} \tag{4.24}$$

where y = settlement after N number of cycles in mm; p is the applied load in kN and k is the track stiffness in kN/mm/wheel. It should be noted here that the $\frac{p}{k}$ ratio equals the track deflection and as an alternative the track deflection could be used directly.

This model fits the settlement data from CT3 and CT4 well, but shows around a 15% error for both CT1 and CT2. This may be due to not having an LVDT on the rail for CT1 and CT2 and the track stiffness values having to be estimated from the LOS actuator. Figure 4.29 plots this track stiffness settlement model against CT4 settlement data and the original GRAFT subgrade modulus settlement model (equation 4.9).

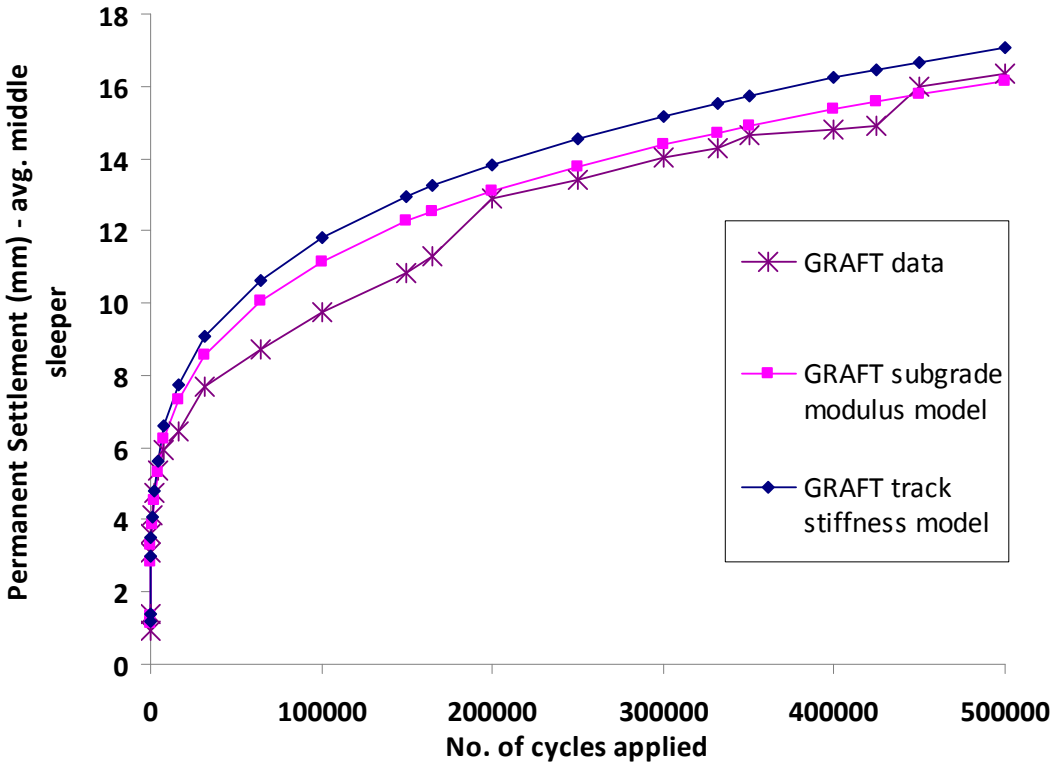

Figure 4.29. Comparison of settlement models with GRAFT data from CT4

Assuming the same track example as previously described for the GRAFT subgrade modulus settlement model this new stiffness model can be directly compared. Using Figure 4.26 we can assume that the track stiffness in GRAFT is 32kN/mm/wheel for a 25MPa tangent subgrade modulus with the same ballast conditions as in GRAFT. Therefore, adopting Equation 4.24 the calculation is as follows:

$$y = (1.268(89/32) - 1.447) \times 400{,}000^{0.23} = 40.4mm$$

This slightly underestimates the settlement when compared to the settlement predictions of 50mm and 45mm for the subgrade modulus GRAFT and Shenton (1985) models, respectively. For the improved subgrade case, the stiffness model above predicts a settlement of 15.9mm, which compares favourably with both the subgrade modulus GRAFT and Shenton (1985) models of 15.5mm and 16mm, respectively.

This example has shown how the GRAFT subgrade modulus settlement prediction equation can be used indicatively for real track and using the same assumptions made in this example, a design graph has been produced. Figure 4.30 shows the design graph for two different traffic levels and two different axle loads. The graph can be used to quickly estimate track settlement based on the track stiffness value and for a design track settlement value the required track stiffness to achieve this value (for given axle load and traffic) can be found. This graph is for the GRAFT track stiffness and settlement values however and these do not correlate directly to track values (discussed further in Chapter 7). Nonetheless, this graph could be used indicatively for real track.

However, out with the load range of 25 to 37 tonnes the linear stiffness model does not compare very well with the others. It is thought that a linear trend may not be appropriate for further data out with the data set in Figure 4.27. It may be that for a greater load to track stiffness ratio the trend becomes non-linear as settlement increases at a greater rate. Moreover, it is possible that the minimum load to track stiffness ratio of 1.141mm represents the optimum track stiffness for a specific applied load. Below this value the track stiffness may be too high for the applied load, which results in increased contact stresses in the track and thus increased degradation. For example, for

an applied axle load of 25 tonnes the minimum ratio yields a track stiffness of 78kN/mm/wheel. For any track stiffness value above 78kN/mm/wheel it is likely that the rate of track settlement will begin to increase. Further research is required here though to confirm this and as such the linear track stiffness model presented is currently limited to the load to track stiffness range of 1.141 to 3.523mm.

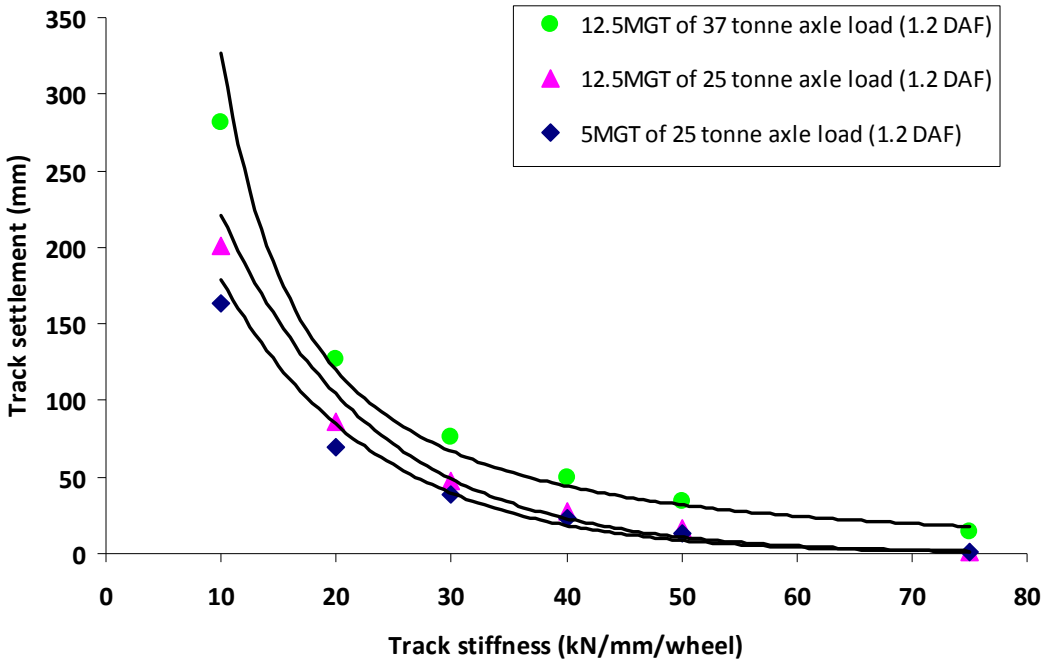

Figure 4.30. Track stiffness/settlement design chart

4.4 Conclusion

Railway track performance in terms of substructure deterioration was discussed within this chapter and the influence of subgrade Young's modulus and applied vertical load on track settlement and stiffness were investigated. Many other factors that can influence subgrade deterioration in terms of increased track settlement or reduced track stiffness have also been discussed, but it is widely considered that subgrade modulus and applied load are two of the most influential parameters. The influence of different parameters on track stiffness in GRAFT has shown that track stiffness varies with applied load, rate of loading, number of cycles, cyclic/monotonic loading and subgrade stiffness. Table 4.6

presents a summary of the estimated influence of each of these parameters on track stiffness for the current tests. It can be seen that for this range of values within GRAFT, subgrade stiffness was found to be the major contributor to track stiffness change. This matches what other railway researchers have suggested using FE modelling and also from the field observations (Selig and Waters, 1994, Hunt, 2005, Brough *et al*., 2006, Shahu *et al*., 1999, Sussmann *et al*., 2001), however, limited research has been published to show this direct link. The GRAFT results have also shown that the non-linear resilient behaviour of both the clayey subgrade and ballast layers with applied load have been simulated accurately within GRAFT while the non-linear load-deflection cycles have also been shown to be realistic. Hence, it is thought that the results from GRAFT realistically represent a typical track section under quasi-static loading at a typical frequency from low to medium speed train traffic, ignoring track irregularities (high frequency dynamic forces).

Parameter changed	Estimated influence on track stiffness from GRAFT results
Applied load (90 to 130kN)	4% reduction
Applied load (40 to 90kN)	14% increase
Cycles applied (0 to 500,000)	10 to 15% increase
Rate of loading applied (0.5 to 3Hz)	15 to 20% increase
Cyclic or impulse loading	5 to 15% increase with cyclic loading
Subgrade tangent stiffness (33 to 61 MPa)	31% increase

Table 4.6. Summary of estimated parameter influences on track stiffness found in these GRAFT tests

From the GRAFT results two track settlement prediction models have been presented that fit the GRAFT data. These can predict initial track settlement in GRAFT and could be used tentatively to estimate track settlement on track after tamping/ballast renewal. As previously stated though it is likely that these equations will underestimate track settlement in the field due to the restricted depth of GRAFT and therefore should only be used to give indicative values of settlement. The relationship between track stiffness

and track geometry deterioration has been shown through the second model and it is clear that a reduction in track stiffness substantially increases track settlement. Both models have been shown to be accurate and when their parameters have been correlated with other well known track settlement models they have compared favourably. Nevertheless, both models have limitations. The track stiffness based model is probably most applicable to industry, but needs further research out with the axle load range of 25 to 37 tonnes. The initial track settlement model can be used for any applied axle load; however, specific ballast and subgrade properties are required to be known and the ballast properties must match the properties in GRAFT for these tests. In addition, these models have only been considered for a typical ballast depth of 300mm with a typical track construction and components, and mixed loads are not included. Furthermore, Thom and Oakley (2006) stated that all models are approximate and only represent a best fit approximation to the data for a particular railway with particular subgrade and ballast. Further research is therefore required both experimentally and numerically before either of these models could be widely used

From the GRAFT results it is recommended that the track stiffness model be concentrated on for further research as once a basic model is developed that incorporates track stiffness then the factors that influence track stiffness can be investigated and then further factors, such as type of sleepers, sleeper spacing, rail type etc. can be incorporated to get a full track settlement model. When in place and once an effective and practical measuring device for track stiffness is used, this could be the key to predicting track settlement across the network and could form part of the maintenance decision making process for poor quality areas. Hunt (2005) stated that track stiffness is a very important parameter in determining life cycle performance of the track and for a new track construction, consideration of track stiffness and its optimisation seem to be justified. For existing tracks, sub-optimal track stiffness results in increased maintenance costs (track geometry due to differential settlement and rail issues) and reduced life of components. The main issue however for existing tracks seems to be the cost of remedial work versus the life cycle cost savings and associated benefits. As the subgrade is thought to be the most important factor dictating track stiffness and as subgrade stiffness modification is relatively expensive and time consuming it may be

practical to state an optimum track stiffness range for a given subgrade stiffness and given traffic conditions. Hence, as seen in GRAFT for the CT4 test the maximum achievable track stiffness for a tangent subgrade modulus of 61MPa was 50kN/mm/wheel for an equivalent axle loading range between 25 and 31 tonnes being applied at 3Hz with a ballast depth of 300mm (unknown ballast stiffness), old wooden sleeper sections and an equivalent BS113A rail section. Therefore, to improve the track stiffness in this test without modifying the subgrade layer the ballast stiffness could be increased by increased compaction or by reinforcement such as geosynthetics, the ballast depth could be increased, larger dimension concrete sleepers could be used & spaced closer together, and a stiffer rail section such as UIC60 could be incorporated. This is an area that Hunt (2005) highlighted as the top priority for future research activity. Several ballast reinforcement solutions will be examined in the next chapter and their performance in terms of improving track stiffness in GRAFT investigated with the other track parameters kept constant. The cost implications of these solutions have not been examined.

Chapter 5 - Track Performance: Influence of Geosynthetics

5.1 Introduction

Geosynthetics have been used in various ways in new rail tracks and track rehabilitations for almost three decades and when appropriately designed and installed they provide a cost-effective alternative to more traditional techniques (Indraratna *et al*., 2006). These geosynthetics have been developed to meet highly specific requirements on the track and ultimately they undertake various functions within the substructure to increase track resistance to deformation. These functions include:

- Separation – separate the ballast layer from the subgrade to prevent ballast contamination and subgrade attrition
- Reinforcement – reinforce the ballast layer to reduce ballast settlement and stress on the subgrade soil
- Filtration – prevent subgrade pumping and to dissipate high pore water pressures built up under cyclic train loading
- Drainage – to prevent excessive wetting of the subgrade

Fundamental and experimental studies by Indraratna *et al*. (2004) found that a reinforced geocomposite can increase the load bearing capacity of the ballast bed while minimising the lateral movement of ballast and reducing degradation. Furthermore, it was stated that the use of composite geosynthetics can reduce the occurrence of liquefied soil (slurry) and upward pumping that would foul the ballast. Enhancing the performance of rail tracks by geosynthetics is now widely undertaken by the rail industry due to the relatively low cost and proven performance in a number of railway applications. However, although several of these products are used in track around the world, and geogrid reinforcement is used within the Network Rail standard on formation treatments (NR/SP/TRK/9039), very little research has been done to compare

their performance on a like for like basis. In addition, in many instances geosynthetics have been used in conjunction with track renewals and as such the improvement in track performance purely due to the geosynthetic installation is often difficult to assess.

The purpose of this chapter is to compare the influence of four different geosynthetic products on the performance of the track and to relate them to the control tests without geosynthetics. Under normal GRAFT test conditions (same as control tests) two ballast reinforcement products have been tested; XiTRACK reinforcement and geocell reinforcement. A multi-functional reinforced geocomposite that is primarily used for separation and filtration purposes has also been tested under the same conditions to compare the functions of the three different geosynthetics. In addition, a geocomposite product designed to replace a traditional sand blanket has been tested in GRAFT under flooding conditions. Sand blankets are used on the tracks where severe subgrade erosion conditions prevail. XiTRACK reinforcement, geocell reinforcement and the sand blanket replacement geocomposite have all been used in the UK network at different problematic areas. However, to date XiTRACK reinforcement had never undergone such full-scale laboratory testing as in GRAFT, while only very limited laboratory testing has been under taken on the other geosynthetic products tested within this research.

5.2 XiTRACK reinforcement

XiTRACK is a 3D polymer track reinforcement technique that improves the load distributing properties of ballast by forming a flexible but very resilient geocomposite across the formation, significantly reducing long-term settlements at high loading locations (Woodward *et al*., 2007). The polymer used is a urethane-cross linked type (polyurethane) and it is applied to the surface of the ballast through mixing equipment that can apply the two component (isocyanate and polypol) rapidly-reacting polymer in a controlled distribution. As the polymer penetrates the ballast it forms a reinforcing cage that allows the track to move in the desired manner. In a typical application around 26% of the void structure is taken up by polymer, which still allows drainage within the

ballast to be maintained (Woodward *et al*., 2009c). The rheology of the polymer can be modified for each track treatment, allowing its engineering properties to be pre-defined for each track application and the catalyst level can be changed to define the penetration depth (Woodward *et al*., 2009c). Typically the polymer cures within 10 to 15 seconds, with around 90% of its stiffness formed within one hour. Moreover, XiTRACK is adaptable and it can be used to reinforce lower levels of ballast to provide formation protection, allowing maintenance to still take place, or a side beam could be reinforced to increase lateral resistance.

The improvement in track stiffness using XiTRACK reinforcement was shown by Woodward *et al*. (2009b) where FE analysis found that a 400mm XiTRACK layer overlain by 100mm of unreinforced ballast improved the track stiffness by 53% compared to an unreinforced 500mm ballast layer. In addition, XiTRACK has been applied to many different sites in the UK over the last 10 years, including bridge transitions, cross-overs, turnouts, clearance issues, tunnel formations, track over poor ground, concrete slab-track transitions, lateral stability issues etc. and it has been shown to significantly reduce maintenance by limiting the ballast densification process and formation bearing pressures (Woodward *et al*., 2009a). Full details of the application of XiTRACK reinforcement at various sites around the UK can be found in Woodward *et al*. (2004), Woodward *et al*. (2007), Woodward *et al*. (2009a) and Woodward *et al*. (2009b). Within GRAFT the full 300mm ballast depth was reinforced for formation protection and ballast settlement reduction, while some additional tests were undertaken out with GRAFT to look at the side beam application. These additional tests will briefly be described at the end of this section.

The substructure for the XiTRACK test within GRAFT was prepared as per the preparation procedures described in Chapter 3. The only difference to a standard GRAFT test was that tarpaulin had to be sealed round the inside of the tank to cover the neoprene rubber as XiTRACK would have bonded to the rubber. Plus, in order to remove the XiTRACK ballast slab from GRAFT at the end of the test two 2 tonne capacity slings were covered and placed at the bottom of ballast layer to allow for the whole ballast slab to be removed as a single unit from the overhead cranes. To apply

XiTRACK in GRAFT a trained engineer poured the polymer onto the ballast through a pump. The application of XiTRACK in GRAFT is shown in Figure 5.1. The application process is timed to distribute the polymer evenly and the application took around 30 minutes with XITRACK being cured after around 15 minutes. The final formed XiTRACK layer is shown in Figure 5.2. When placing the track panel onto the track, gravel was used directly under each sleeper to help the sleepers bed in to the track and to provide uniform support to the sleepers from the ballast (prevent sleepers from being supported from only a few ballast particles protruding from the surface as the track geometry is fixed). The LVDT positions for the XITRACK test were changed slightly from the standard GRAFT tests as the LVDT's could be placed directly on the ballast bed due to the XiTRACK geocomposite; two LVDT's were placed on the ballast bed adjacent to the middle sleeper and one LVDT was placed on one side of the middle sleeper. Track stiffness measurements were taken from the LOS actuator readings. The XiTRACK reinforced track under test within GRAFT is shown in Figure 5.3.

Figure 5.1. Application of the polymer to form XiTRACK within GRAFT

Figure 5.2. Formed XiTRACK layer within GRAFT

Figure 5.3. XiTRACK reinforcement under test in GRAFT

The development of permanent track settlement throughout the XiTRACK test is shown in Figure 5.4. It can be seen that the middle sleeper shows slightly more settlement than the ballast bed adjacent to the middle sleeper, which is thought to be due to some settlement occurring in the sleeper itself. To directly compare the XiTRACK test with other tests the middle sleeper settlement was used. It can be seen that the conventional settlement curve found for the control tests undertaken in GRAFT (Figure 4.1) is not observed here. This is due to the track rebounding when left unloaded overnight. It was not possible to continuously load overnight with the LOS due to University regulations. The magnitude of the rebound is significant in this XiTRACK test relative to the low level of plastic settlement accumulation. This overnight elastic rebound was not found to the same level in any of the control tests undertaken in GRAFT and it is thought that it is due to the resilient properties of the XiTRACK ballast layer. It is thought that the whole XiTRACK ballast layer is moving together under load due to the load distributing properties of XiTRACK reinforcement, and as such the whole slab is rebounding when left unloaded. In addition, some of the settlement shown is thought to be due to crushing of the gravel particles placed underneath the sleepers to bed in the track panel as crushed particles were found at the end of the test. Nonetheless, these effects are thought to be minimal.

The comparison of XiTRACK reinforcement to unreinforced ballast tests is shown in Figure 5.5 where it can be seen that the settlement of the XiTRACK reinforced track is considerably less than CT1 and CT2, even though both CT1 and CT2 were undertaken with an increased subgrade modulus and CT2 had a reduced applied load. Using equations 4.5, 4.6 and 4.7 developed within Chapter 4, the predicted GRAFT settlement for unreinforced ballast with the same subgrade modulus and applied load as the XiTRACK test has also been plotted in Figure 5.5. This predicted settlement curve highlights the significant reduction in track settlement (99% over 500,000 cycles or 18.5MGT) that can be achieved by using XiTRACK reinforcement on track that has heavy axle loads (44.4 tonnes including DAF) running over soft underlying subsoil (subgrade tangent modulus of 25MPa). For an unreinforced track to obtain the same level of settlement in GRAFT as shown in the XiTRACK test the subgrade modulus

required would be 814MPa, a 3156% increase. Essentially XiTRACK made the track performance elastic (giving slab-track performance).

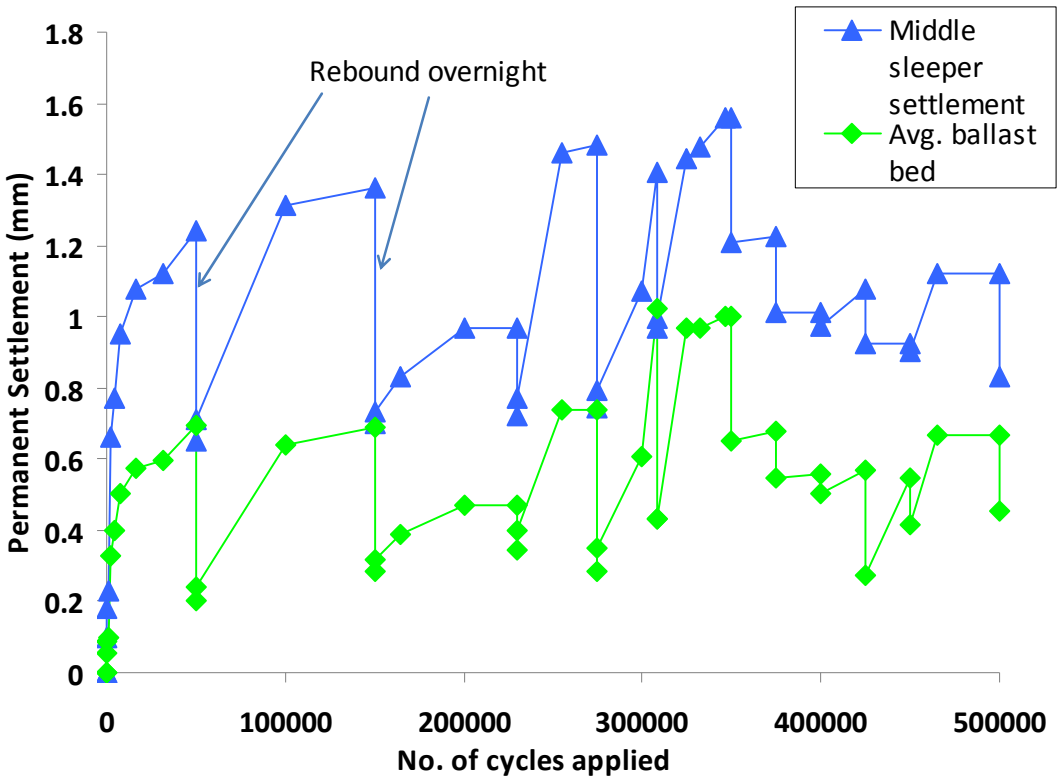

Figure 5.4. Permanent settlement throughout XiTRACK reinforcement test

The load-deflection curve found for the XiTRACK test after 10,000 cycles is illustrated in Figure 5.6. The mean GRAFT track stiffness found from the LOS actuator displacement readings for the XiTRACK test over the 500,000 applied cycles was 47.1kN/mm/wheel with a mean GRAFT track modulus value of 25.7MPa. Comparing this value to the GRAFT stiffness values found for the GRAFT unreinforced control tests as shown in Figure 4.26, it can be seen that XiTRACK improves the track stiffness by around 43% when compared to unreinforced track with the same subgrade modulus as the XiTRACK test. When taking into account the higher applied load in the XiTRACK test, the improvement increases to around 55%. Alternatively, using equation 4.24 an estimate of track stiffness for an unreinforced track in GRAFT, with the same subgrade modulus and applied load as in the XiTRACK test, could be made. The settlement value used in the equation was taken from the predicted GRAFT

settlement for unreinforced track after 500,000 cycles from Figure 5.5. The calculation is as follows:

$$y = (1.268(130/k) - 1.447) \times 500{,}000^{0.23} = 88.4mm$$

$$\therefore k = 28.6kN/mm/wheel$$

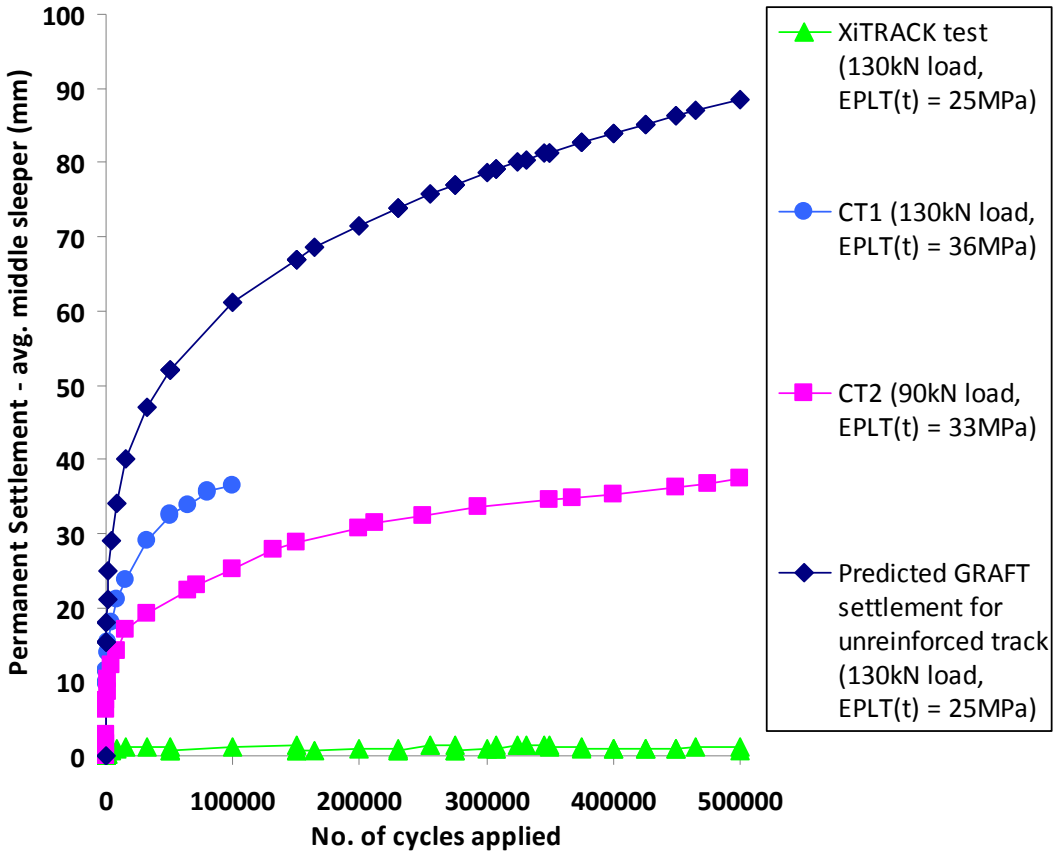

Figure 5.5. Comparison of XiTRACK reinforcement to unreinforced track

Using this value for unreinforced track in GRAFT one can see that XiTRACK reinforcement has improved the stiffness by around 65%. Therefore, it has been shown that XiTRACK reinforcement significantly increases track stiffness of unreinforced track by between 55 and 65% over 500,000 cycles, as well as reducing track settlement by around 99%. This stiffness improvement is similar to the improvement found by Woodward *et al*. (2009c) using FE analysis as discussed earlier.

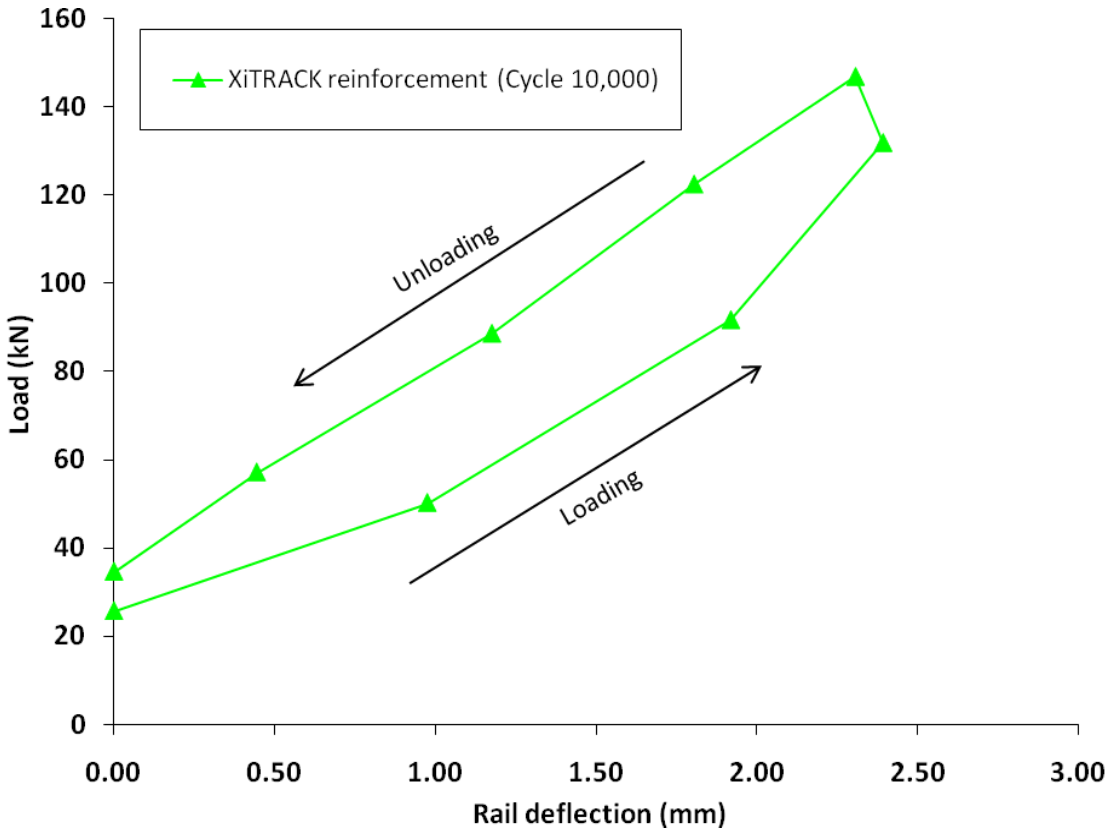

Figure 5.6. XiTRACK vertical load-deflection curve measured on rail

At the end of the XiTRACK test the XiTRACK reinforced sample was removed in one section, as shown in Figure 5.7, and the section did not show any signs of fatigue or breakage. However, on inspection of the formation after the removal it was found that the polymer had not fully penetrated down to some of the ballast at the bottom of the layer, due to the amount of fines present at these particular ballast sections. Although the fouling is minimal and has been kept consistent throughout the testing programme, it was enough to prevent full penetration of XiTRACK as the contamination had settled to one particular area in the ballast bags used; causing relatively heavy fouling at a few specific locations. On site, highly fouled ballast can prevent XiTRACK from operating successfully. After the XiTRACK sample was removed from GRAFT water was poured over it to check the drainage properties. As is shown in Figure 5.8 the XiTRACK sample remained fully free draining after the 500,000 applied load cycles.

Figure 5.7. XiTRACK removal after 500,000 load cycles

Figure 5.8. XiTRACK sample still free draining after 500,000 load Cycles

5.2.1 Additional XiTRACK tests

Two additional XiTRACK sections were poured at the same time as the XiTRACK sample was poured in GRAFT. These included a 1100-1150mm wide by 1200mm long by 250mm high slab section and a 290-300mm wide by 1200mm long by 290-310mm high beam section. The slab section represents a typical XiTRACK reinforced section for tunnel applications (slab-track), while the beam section represents a reinforced side channel to provide lateral tolerance to the ballast shoulders. Figure 5.9 shows these additional ballast sections prior to the application of XiTRACK. Wooden shutters were used as the formwork for these sections, which meant that the ballast could not achieve a high level of compaction due to bulging. Both sections were cement capped in the centre onto which plates were placed for load to be applied. The side beam section was also cement capped along its full length underneath the sample to allow a flat surface to which the load could be transferred to the LOS platform (the beam was rotated for testing).

Figure 5.9. Additional ballast slab and beam sections prior to the application of the XiTRACK polymer

5.2.1.1 Slab section

To load the slab section three stacked 250mm x 420mm x 130mm thick steel plates were used (Figure 5.10) and once the sample was set up for loading in the LOS machine 50 cycles were initially applied at a load of 200kN and a frequency of 0.5Hz. Then two monotonic load cycles were applied up to 1000kN at a rate of 0.02mm/s before the sample was tested to failure at a monotonic loading rate of 0.05mm/s. Figure 5.11 shows the load-displacement plot of the initial 50 cycles and Figure 5.12 shows the load-displacement graph for the three monotonic cycles. From Figure 5.11 it can be seen that ballast densification occurs on the initial application of load up to 100kN and the sample continues to compact as the number of applied cycles increase. This is thought to be due a combination of the poor level of ballast compaction achieved prior to the application of XiTRACK and the set-up effects (cement, steel plates etc.). These effects can also be seen in Figure 5.12 on the initial application of the load for each monotonic cycle before the curves become linear.

Figure 5.10. XiTRACK slab section under load

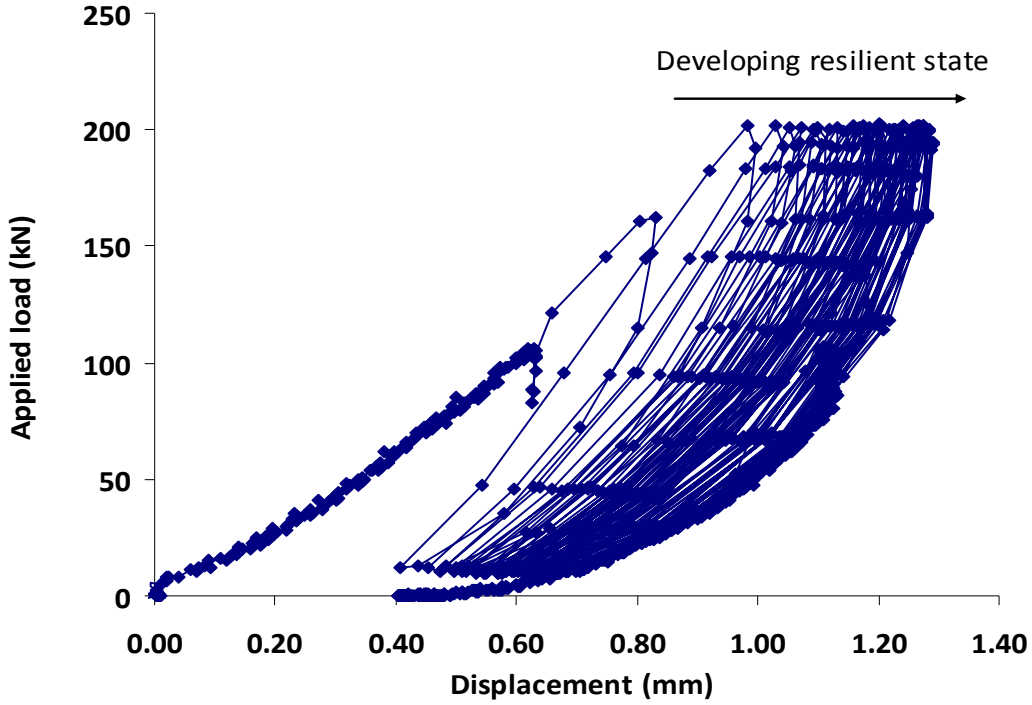

Figure 5.11. Load-displacement plot of 50 cycles applied to XiTRACK slab sample

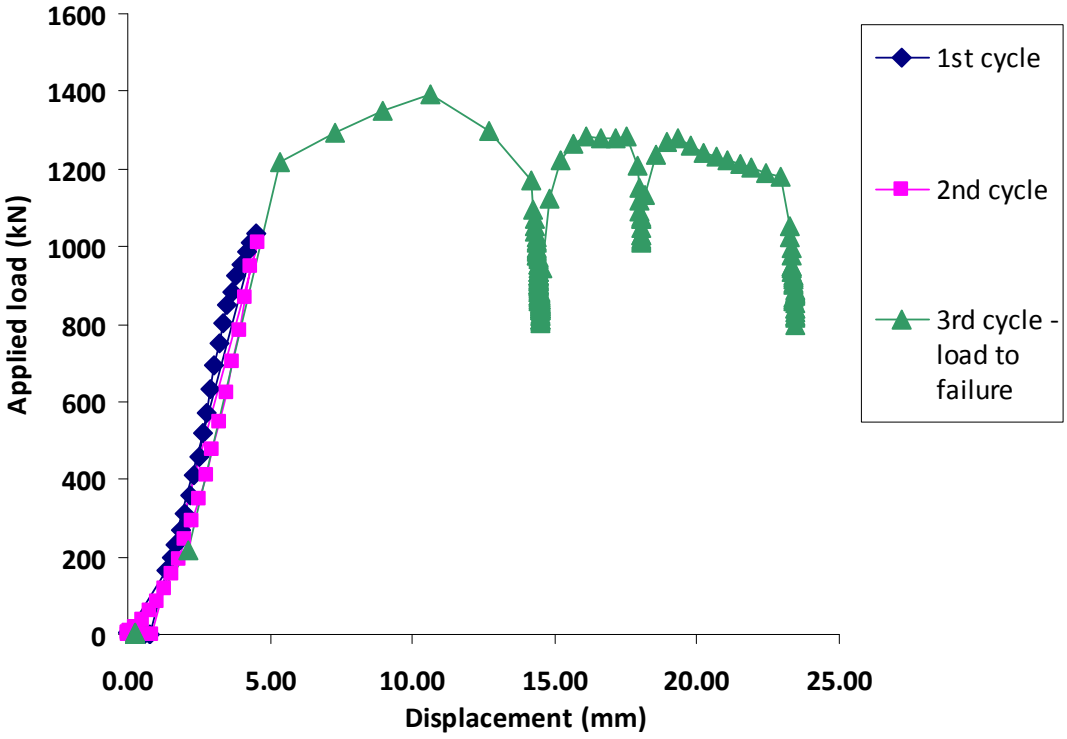

Figure 5.12. Load-displacement plot of monotonic cycles applied to XiTRACK slab sample

Figure 5.12 shows that the sample failed at an applied load of 1390kN, which correlates to an applied stress of 13.2MPa (shown in Figure 5.13). This stress level is over ten times higher than the highest typical stress level existing in tracks (1250kPa) for heavy freight trains (Lackenby *et al*., 2007) and is within the range of the tensile strength capacity of individual ballast particles (12.3 to 54.8MPa depending on particle size and ballast type) as found by single particle crushing tests undertaken by Lim (2004). It should be noted here that the stress level in the ballast depends on the ballast void ratio, which is a function of particle shape (Lim *et al*., 2005), and as the initial void ratio of the ballast used for the XiTRACK slab section test was high, due to a poor level of compaction, the stress level is unlikely to reach 13MPa within the cycles applied. The plastic vertical strain of the XiTRACK slab section at these high applied stress levels (2% at 1200kN and 4% at 1390kN) highlights the significant performance of XiTRACK reinforcement. Lackenby *et al*. (2007) stated that failure of large unreinforced ballast specimens under repeated loading during triaxial tests can be defined by an axial strain greater than 25%. Although this is an arbitrary limit, under this criterion the XiTRACK sample had not actually failed when the test was stopped (10% axial strain). This highlights the high ductility of XiTRACK reinforced ballast at high applied stresses, which illustrates the energy absorbing potential of the XiTRACK system, while still retaining track geometry (Woodward *et al*., 2007). The high level of applied stress was evident at the end of the test as it was observed that the cement had started to crush under the loading plates.

The axial stiffness of the slab sample can be estimated from both the monotonic and cyclic applied loads. From Figure 5.11 the axial stiffness from the last cycle is 516MPa at an applied stress similar to that experienced in the field from a heavy axle freight train. The last cycle was used to reduce the effects of the poorly compacted ballast and initial set up. From Figure 5.12 the tangent modulus calculated from the straight line portion of the stress-strain curve gives a value of 940MPa, ignoring the initial non-linear section thought to be due to poor compaction and set up effects. The resilient modulus of unreinforced ballast has been investigated by many other researchers through large scale triaxial testing and a range of values have been quoted from 40 to 500MPa. Banimahd (2008) adjusted well known ballast model parameters to represent a

reasonable change in ballast stiffness with induced stress level and found that 50 to 180MPa is a reasonable range for ballast stiffness. This range matches well with Shahu *et al*. (1999), and Aursudkij *et al*. (2009). Assuming an unreinforced ballast stiffness of 180MPa under heavy axle loading, using XiTRACK reinforcement has increased the ballast stiffness by approximately 187%, compared to the XiTRACK axial stiffness value from the last cycle in Figure 5.11.

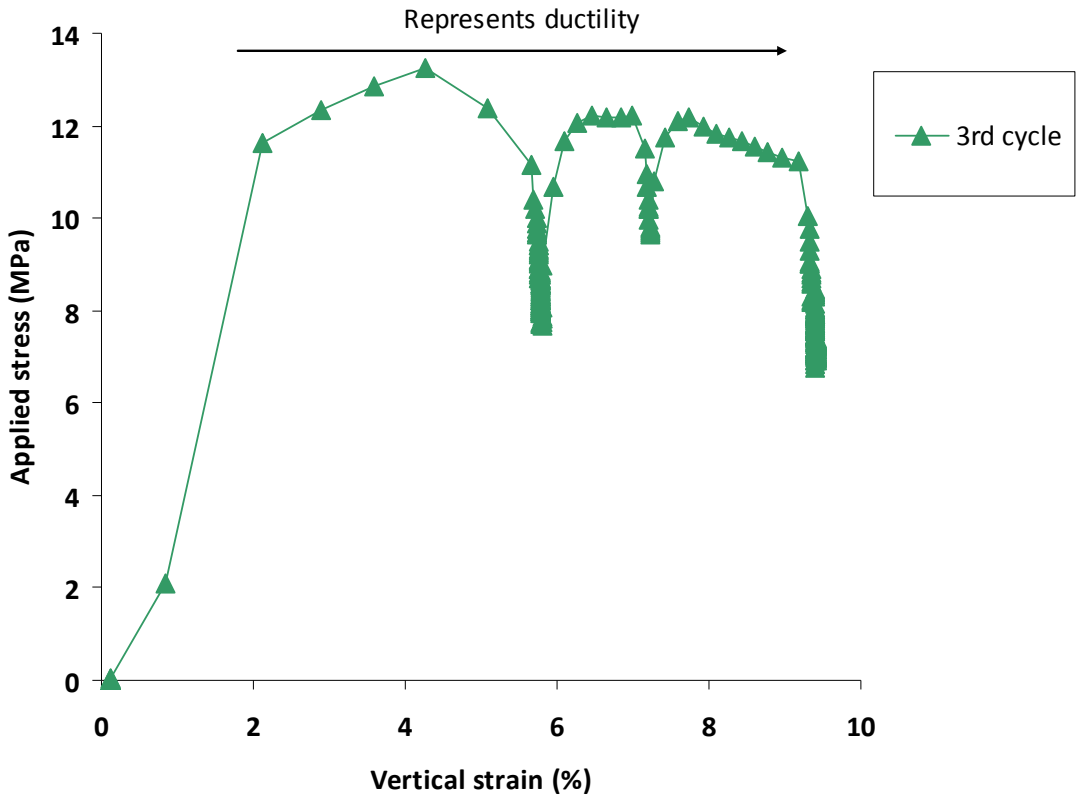

Figure 5.13. Stress-strain plot of 3rd monotonic cycle applied to XiTRACK slab sample

5.2.1.2 Beam section

The side beam section was loaded centrally from two stacked 250mm x 420mm x 130mm thick steel plates (Figure 5.14) to represent the lateral load from the end of a sleeper to a tunnel wall as a train passes. Ten cycles of 100kN were applied initially at 0.016Hz then 1000 cycles of 50kN were applied at 3Hz before a further 5000 cycles of 100kN at 3Hz and 5000 cycles of 200kN at 3Hz were applied. After the cyclic loading

two monotonic load cycles were applied up to 500kN; the first one at 0.05mm/s and the second one at 0.02mm/s. Finally, the sample was loaded to failure at a monotonic loading rate of 0.02mm/s. Figure 5.15 illustrates the load-displacement graph for the final monotonic cycle and Figure 5.16 shows the stress-strain response. It can be seen that the sample failed at an applied load of 730kN (applied stress of approx. 10MPa). Within these Figures the influence of the poorly compacted ballast and initial set up can be seen again at the initiation of the applied load. The vertical plastic strain of the XiTRACK beam section at these high applied stress levels (0.66% at 550kN and 1.67% at 730kN) again highlights the significant performance of XiTRACK reinforcement.

Figure 5.14. XiTRACK beam section under load

These additional XiTRACK tests have shown the resiliency and ductility of a XiTRACK reinforced ballast sample while also highlighting the versatility of using XiTRACK reinforcement for both vertical and lateral reinforcement.

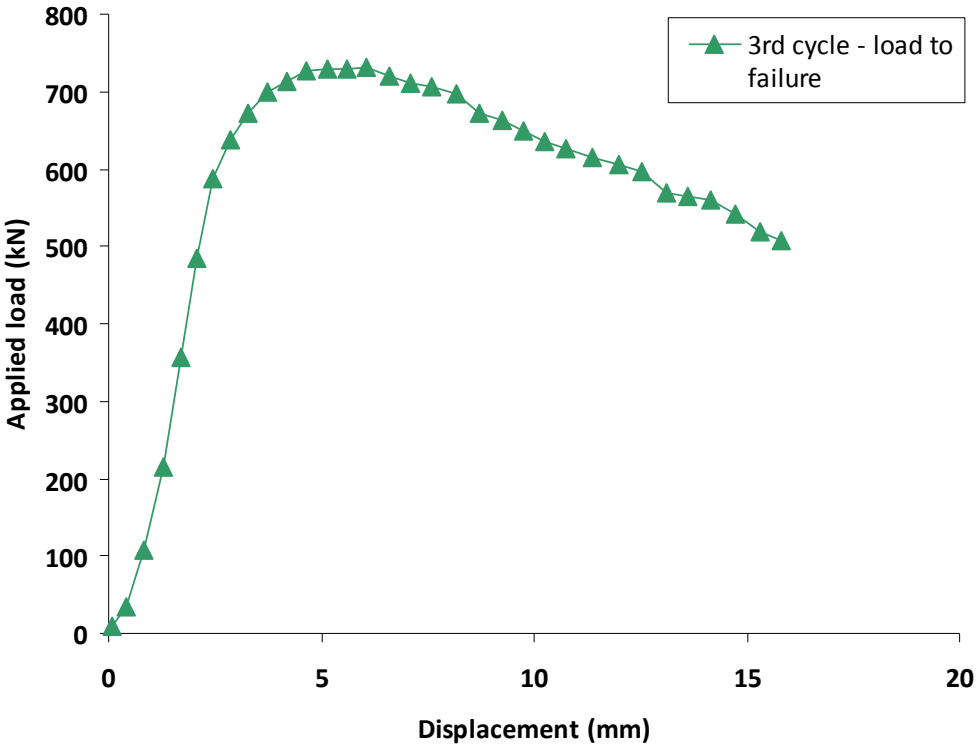

Figure 5.15. Load-displacement plot of final monotonic cycle applied to XiTRACK side beam sample

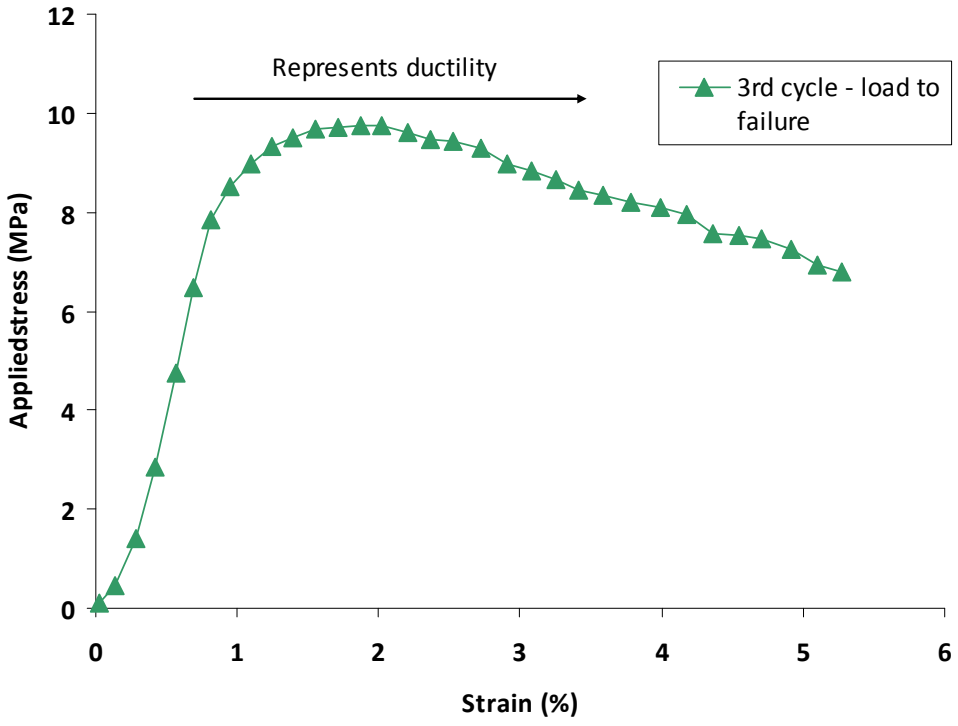

Figure 5.16. Stress-strain plot of final monotonic cycle applied to XiTRACK side beam sample

5.3 Geocell reinforcement

Geocell reinforcement consists of surfaced textured strips of polyethylene ultrasonically welded together to form a mattress of interconnected seamed cells into which granular materials are placed and compacted. Once filled each cell acts in conjunction with adjacent cells to form a stabilised composite mattress that assists in dispersing load and shear failure. The geocell cellular confinement mechanism is thought to improve the properties of granular material by restricting the lateral movement, allowing a soil matrix to be developed so that compacted granular fill can reach good compressive strength (Presto Geosystems, 2009). Research has shown that the pseudo-3D cellular confinement mechanism of geocell reinforcement retains desirable characteristics of 2D planar geogrid reinforcement and may offer an increased stability to the granular fill. The increase in maximum load carrying capacity of an interconnected cellular mattress has been found to range from 27% (Dash *et al*., 2003) to 187% (Sitharam *et al*., 2005) greater than that of planar reinforcement. Furthermore, reporting on static load tests in the laboratory and in situ field tests, Emersleben and Meyer (2008) found that the load carrying capacity of infill materials could be improved by between 1.1 and 1.7 times due to reinforcement with geocells. Emersleben and Meyer (2008) also found that a geocell reinforced road layer can reduce the vertical stresses on the subgrade by around 30% and increase the layer modulus by between 10 and 29% when compared to an unreinforced section. On the contrary, evaluating the static load-deformation behaviour of a single geocell filled with different coarse grained particles and compacted at various relative densities Kennedy *et al*. (2008) found that although single geocell systems can tolerate a high level of applied stress of up to 825kPa before failure; high levels of vertical strain were also found at around 20%. The tangent axial stiffness, calculated from the straight line portion of the stress-strain curve of a single geocell filled with coarse angular gravel particles at 60% relative density, indicated a value of around 6MPa.

For the geocell test in GRAFT the substructure was prepared as per the track preparation procedures. The geocell mattress was cut to fit GRAFT and the geocells used were made from high density polyethylene (HDPE) with the cell walls perforated

with 10mm diameter holes. The average certified cell seam strength of each cell is 2840N (Presto Geosystems, 2009). The final mattress included 15 cells longitudinally and 4 transversally. The geocell mattress was placed directly on the subgrade and steel bars were used to stretch and anchor the mattress into the underlying clay formation in both directions (Figure 5.17). Indraratna *et al*. (2004) stated that it is convenient to place geosynthetics at the bottom of the ballast layer to allow for maintenance requirements; to allow for tamping geosynthetics need to be placed at least 150mm below the sleeper. In the field a minimum of 50mm additional ballast cover would therefore be required, compared to GRAFT (using 200mm geocell depth). In GRAFT, for a direct comparison with other reinforcement geosynthetics and with unreinforced ballast, this additional required ballast has been ignored as no tamping was undertaken.

To fill the geocell mattress ballast was poured, directly filling each cell as shown in Figure 5.18. Each filled cell was found to have a depth of 200mm, length of approximately 230mm, and width of approximately 200mm. The total amount of ballast to be poured onto the geocell mattress to fill each cell was calculated as 950kg (assuming a bulk density after compaction of around 1.60Mg/m³ and taking account of any voids at the interface between the geocell mattress and the tank walls). The ballast was compacted in each cell individually with a Kango hammer for 10 seconds. Once the cells were compacted, one layer of ballast (100mm thick) was placed on top and compacted with vibrating plate as usual.

The development of permanent track settlement throughout the geocell test is shown in Figure 5.19. It is shown that the track settles uniformly with no tilting of the sleeper sections. The comparison of geocell reinforcement to unreinforced ballast tests and to XiTRACK reinforcement is shown in Figure 5.20. The settlement of the geocell reinforced track is 37% greater over the 10,000 applied cycles than both CT4, with a similar subgrade modulus, and the predicted track settlement of an unreinforced track in GRAFT with the same subgrade modulus. Suggestions for the explanation of this behaviour are given at the end of this section.

Figure 5.17. Geocell mattress placed within GRAFT

Figure 5.18. Geocell ballast layer prior to compaction and placement of top layer of ballast

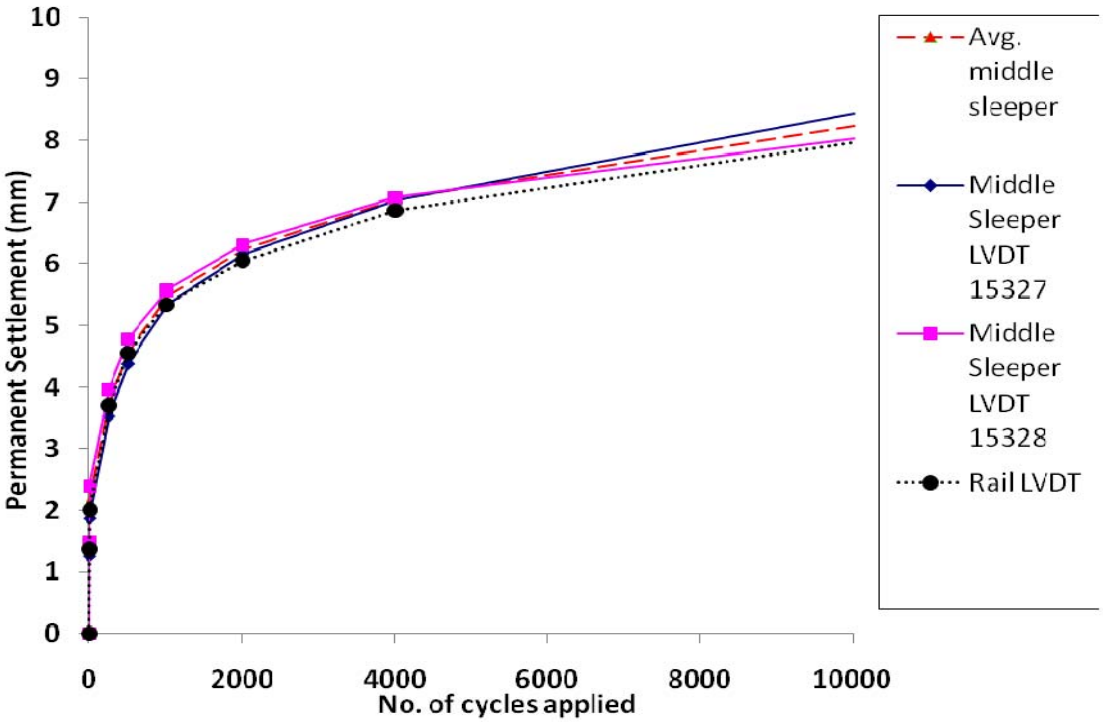

Figure 5.19. Permanent settlement development throughout geocell test

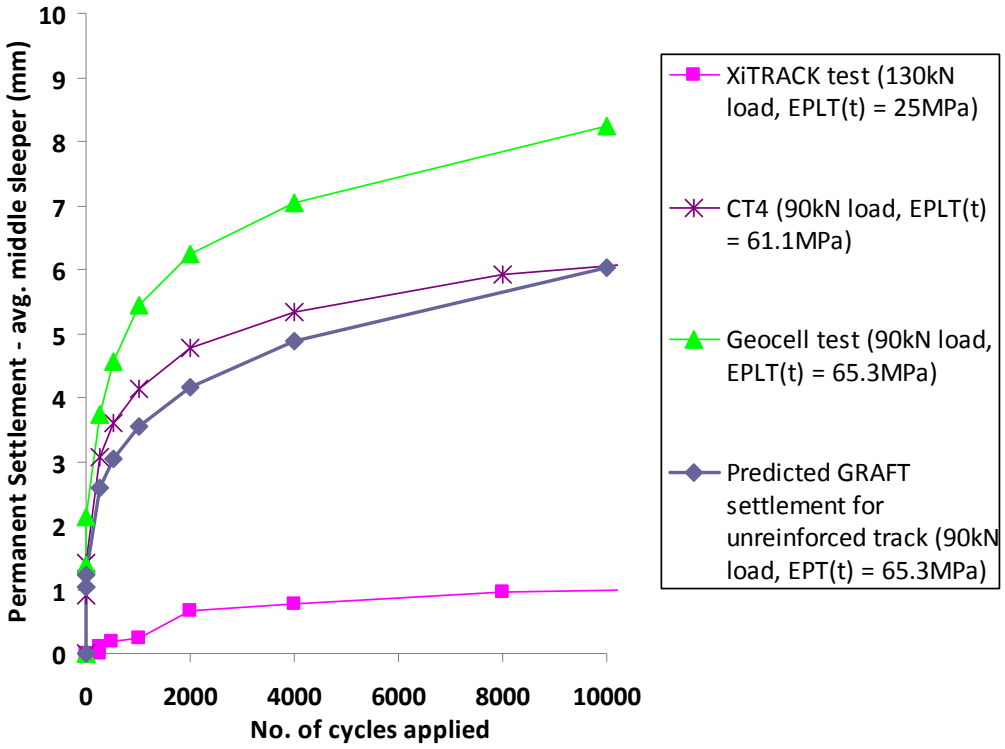

Figure 5.20. Comparison of 3D ballast reinforcement to unreinforced track in GRAFT

The load-deflection curve found for the geocell test after 10,000 cycles is illustrated in Figure 5.21. The mean GRAFT track stiffness found over the 10,000 applied cycles was 48.7kN/mm/wheel with a mean GRAFT track modulus value of 26.9MPa. Comparing this value to the stiffness values found for the GRAFT control tests shown in Figure 4.26 it can be seen that geocell reinforcement has reduced the track stiffness by around 5% compared to unreinforced track with the same subgrade modulus and applied load. Using equation 4.24 to predict the track stiffness for an unreinforced track in GRAFT with the same subgrade modulus and applied load as in the geocell test yields a 7% reduction (settlement value used in the equation taken from the predicted settlement for unreinforced track after 10,000 cycles from Figure 5.20).

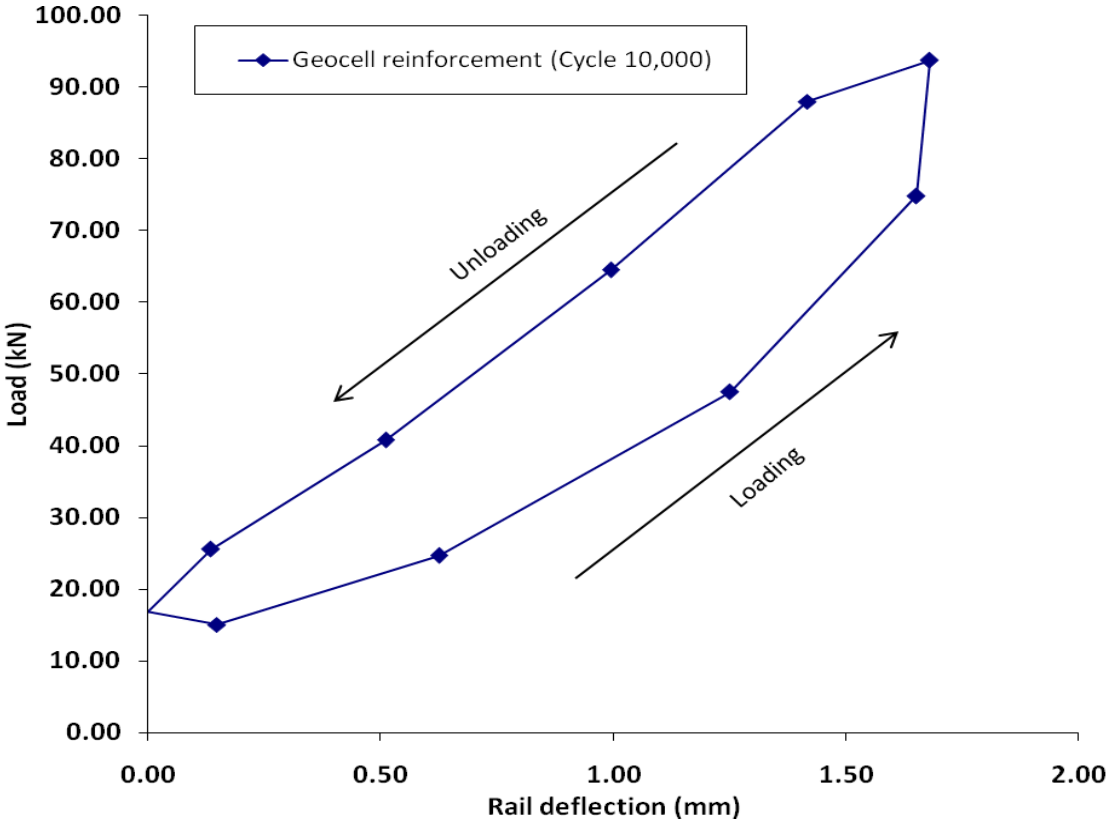

Figure 5.21. Geocell vertical load-deflection curve measured on rail

Overall, it has been shown in GRAFT that when comparing two 3D track ballast reinforcement techniques (XiTRACK & Geocell reinforcement) XiTRACK reinforcement performs considerably better than geocell reinforcement in terms of both

track settlement and track stiffness. In addition, it has also been shown that geocell reinforcement can actually reduce track performance when compared to an unreinforced track (37% increase in settlement, 5 to 7% reduction in stiffness) after 10,000 cycles (0.25MGT) of a 25 tonne axle load (with 1.2 DAF) on a stiff clay subgrade (subgrade tangent modulus of 65MPa). This is in contrast to what has been suggested by others and it is thought to be due in part to the difficulty in forming a compacted reinforced ballast layer with geocell reinforcement and non-interlocking of ballast across the walls of the geocells. This is thought to be the case even though individual cells were compacted with a Kango hammer in GRAFT. This has direct implications for using geocell reinforcement in track as it is not practical to individually compact cells and hence, even less compaction would take place than in this GRAFT test. It is therefore recommended that further research is undertaken on geocell reinforcement, possibly at different placement depths and with different compaction methods to investigate if the performance can be improved.

5.4 Reinforced geocomposite

In order to compare 3D ballast reinforcement products to 2D planar geocomposites used primarily for separation and filtration, the DuPont Typar HR 55/55 reinforced geocomposite was tested in GRAFT. The geocomposite is reinforced with high-tenacity polyester yarns that are permanently combined with a nonwoven base by weft insertion knitting to provide a strong multi-functional geosynthetic (DuPont, 2009). The full mechanical and hydraulic properties of Typar HR 55/55 can be found in reference DuPont (2009).

The GRAFT substructure was prepared as per the track preparation procedures for the reinforced geocomposite test with exception that the formation was not replaced. The reinforced geocomposite was cut to size to fit GRAFT and it was placed directly onto the underlying clay formation with the reinforced side face up to be in contact with the ballast. This is the typical placement position for 2D geocomposites to separate the underlying fine subgrade soil and coarse ballast material and to provide filtration

functions. Figure 5.22 shows the placement of the reinforced geocomposite in GRAFT without any anchoring. Ballast was poured directly onto the reinforced geocomposite (Figure 5.23) and compacted in three layers as per the standard GRAFT track construction procedures.

The development of permanent track settlement throughout the reinforced geocomposite test is shown in Figure 5.24. It can be seen that no tilting of the middle sleeper occurred and the track settled uniformly. The track settlement found in the 2D reinforced geocomposite test compared to the 3D XiTRACK reinforcement test, 3D geocell reinforcement test, and unreinforced CT4 is shown in Figure 5.25. The settlement of the reinforced geocomposite test is shown to be 25% less over the 10,000 applied cycles than both CT4 with a similar subgrade modulus and the predicted track settlement of an unreinforced track in GRAFT, with approximately the same subgrade modulus. Furthermore, the reinforced geocomposite shows a 45% reduction in track settlement when compared to geocell reinforcement with the same applied load and approximately same subgrade modulus.

Testing a geocomposite made from bonding a bi-oriented geogrid with a non-woven polypropylene geotextile in a large prismoidal triaxial rig Indraratna *et al*. (2004) found similar results to GRAFT; 35% improvement in track settlement over 10,000 cycles of a 25 tonnes axle load on a 50mm clay subgrade with a 100mm sand-gravel subballast layer. The influence of the interaction between the subballast layer and the geocomposite is unknown. Indraratna *et al*. (2004) also tested the performance of a bi-oriented geogrid (rectangular apertures of 27 x 40mm) and a high strength woven geotextile within their testing rig. It was found that they both performed well (21% settlement reduction with geogrid, 27% settlement reduction with geotextile over 10,000 cycles of 25 tonnes axle load), but not as good as the geocomposite. Indraratna *et al*. (2004) stated that the enhanced filtration and separation functions provided by the geocomposite with its non-woven geotextile component may have attributed to its higher effectiveness.

Figure 5.22. Reinforced geocomposite placed in GRAFT

Figure 5.23. Placement of ballast on top of reinforced geocomposite

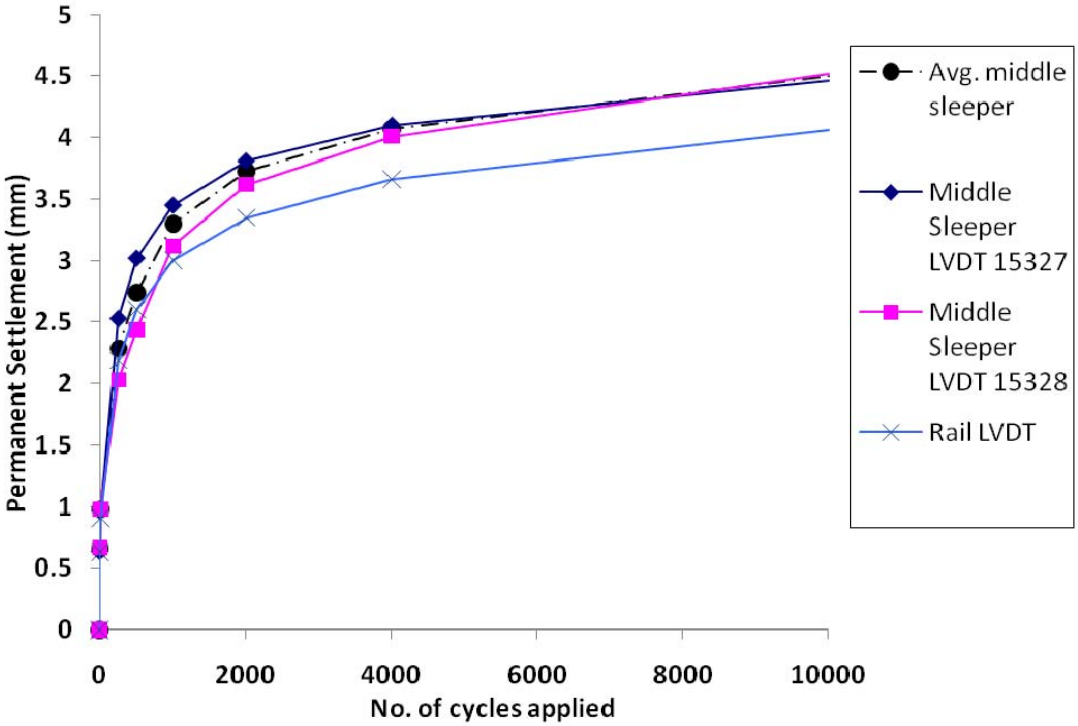

Figure 5.24. Settlement development throughout reinforced geocomposite test

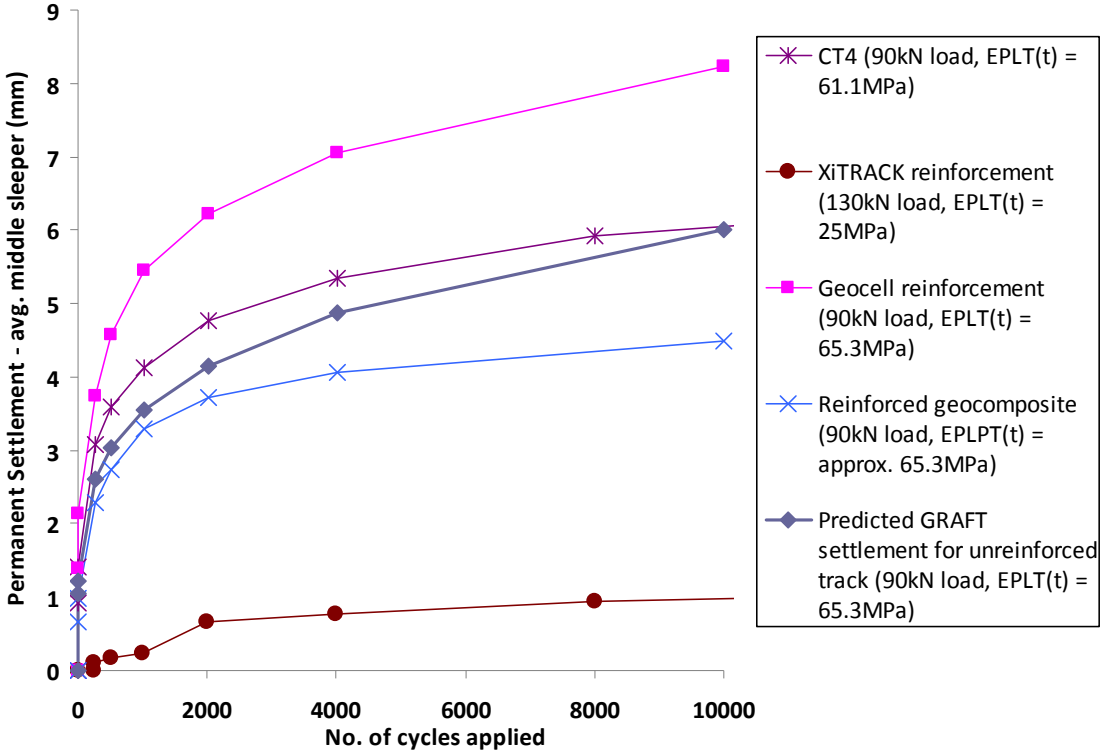

Figure 5.25. Comparison of ballast reinforcement products tested in GRAFT (note the difference in load & subgrade modulus)

The load-deflection curve found for the reinforced geocomposite test after 10,000 cycles is illustrated in Figure 5.26. The mean GRAFT track stiffness over the 10,000 applied cycles was 57.4kN/mm/wheel with a mean GRAFT track modulus value of 33.4MPa. Using Figure 4.26 it can be seen that the reinforced geocomposite increased the track stiffness by around 12% compared to an unreinforced track with the same subgrade modulus and applied load. Alternatively, using equation 4.24, with settlement taken from the predicted settlement for unreinforced track after 10,000 cycles from Figure 5.25, gives a 9% improvement. A comparison of all the estimated improvements in mean GRAFT track stiffness for the reinforced to unreinforced tracks with the same subgrade modulus and applied loads is shown in Table 5.1.

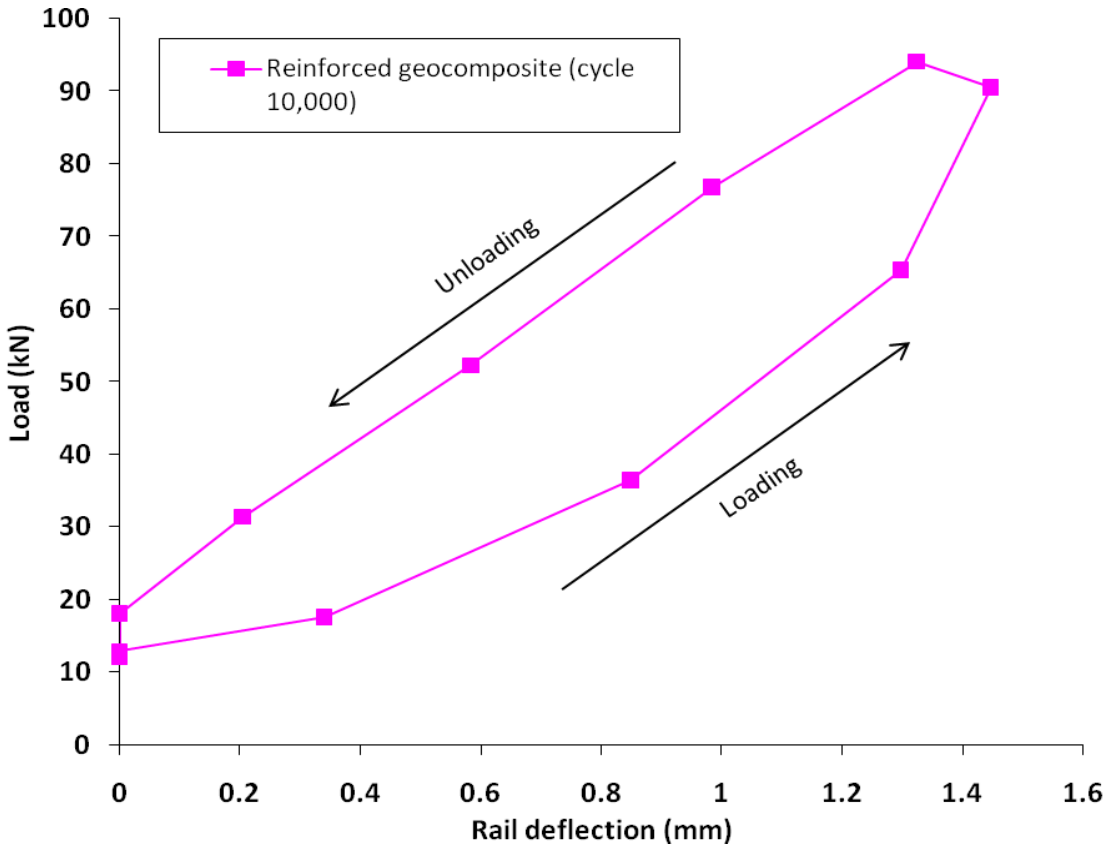

Figure 5.26. Reinforced geocomposite vertical load-deflection curve measured on rail

GRAFT reinforced test	Estimated improvement in mean GRAFT track stiffness of unreinforced track with same subgrade modulus and applied load as GRAFT reinforced test
XiTRACK reinforcement	55 to 65%
Geocell reinforcement	-7 to -5%
Reinforced geocomposite	9 to 12%

Table 5.1. Comparison of estimated improvement in track stiffness of reinforced to unreinforced tracks with the same subgrade modulus and applied loads

It should be noted here that the GRAFT subgrade modulus value for the reinforced geocomposite test is approximate as the formation was not replaced and hence the same formation was used for the geocell test as the reinforced geocomposite test. Although the subgrade is thought to be in a resilient state at this point and both PLT and in-situ testing results show little change in subgrade modulus before and after the final series of tests with the same formation (geocell test, reinforced geocomposite test, CT5), the 70mm formation layer may have slightly influenced track performance between the geocell test and reinforced geocomposite test due to an additional 10,000 cycles being applied to it. Unfortunately, the data for CT5, which was undertaken after the reinforced geocomposite test and was planned to investigate the influence of using the same 70mm formation, could not be used as a hydraulic error occurred with the LOS machine resulting in a high load being applied to track at the start of the test.

From these results it can be concluded that the reinforced geocomposite has performed well compared to unreinforced and 3D geocell reinforced track over 10,000 cycles (0.25MGT) of a 25 tonne axle load (with 1.2 DAF) on a stiff clay subgrade (subgrade tangent modulus of approx. 65MPa). This is thought to be due to the reinforced

geocomposite preventing angular corners of individual ballast particles penetrating into the underlying clay formation. However, some of this improvement may be due to using the same formation for the reinforced geocomposite test as the Geocell test. This influence is thought to be negligible as only 10,000 cycles were applied, but it is unknown. Hence, it is recommended that further research be undertaken on the reinforced geocomposite to confirm these results and in order to investigate the reason for the enhanced performance further tests should be undertaken on the individual components of the geocomposite (non-woven geotextile component and reinforcing component) with the stress level in the ballast and on the subgrade monitored. These tests would explain if the separation, filtration or reinforcement functions of the geocomposite provide the enhanced performance.

5.5 Track reinforcement settlement models

From Figure 5.25 it is interesting to note that after the initial rapid settlement (up to 2000 cycles) the settlement varies linearly with number of cycles for all the tests, irrespective of type of reinforcement. Indraratna *et al*. (2006) found the same relationship while testing ballast layered with geosynthetics in a large triaxial cell and concluded that the vertical strain of the ballast is related linearly to the number of load cycles, irrespective of the type of ballast or reinforcement. Fitting trend lines to the geosynthetic test curves in Figure 5.25 and assuming that the stress state (p), physical state (E_{PLT}) and soil type (b) parameters used in equation 4.11 remain the same in these geosynthetic tests as in the unreinforced control tests, simplified settlement equations for each of the geosynthetic products tested can be produced. From equation 4.11, the only parameters that have changed with the inclusion of the geosynthetics are parameters a and m, which are dependent on soil type and ballast properties. It is assumed that by including geosynthetics the ballast properties have changed, although this is a generalisation. To arrive at these new equations, equation 4.11 was used with p and E_{PLT} taken from the individual geosynthetic tests and b assumed to be constant at 0.23 as the soil type is constant throughout all GRAFT testing. The track settlement (y) was taken from the settlement after 10,000 cycles for both the geocell test and the

reinforced geocomposite test while y was taken at both 10,000 cycles and 500,000 cycles for the XiTRACK test. This left the unknown parameters a and m for each geosynthetic equation and to solve the equations one parameter was made constant at a time, which resulted in two equations being developed for each geosynthetic product tested. For example, the parameter a was initially made constant at 1281 (from control test equation 4.9 with tangent modulus values) which resulted in the parameter m being found for each geosynthetic equation with different y, p and E_{PLT} values. When calculating the parameter a for each geosynthetic equation, the parameter m was kept constant at -1.3342 (equation 4.9). The final calculated parameters for each geosynthetic equation are shown in Table 5.2. The parameters for the XiTRACK equation have been taken from the average of the values found for both 10,000 cycles and 500,000 cycles as they vary due to the overnight rebound that occurred after 50,000 cycles onwards. The average value has been taken to simulate irregular traffic patterns in the field.

GRAFT geosynthetic test	Geosynthetic model 1 parameter a (with parameter m = -1.3342)	Geosynthetic model 2 parameter m (with parameter a = 1281)
XiTRACK reinforcement	24.3	-2.298
Geocell reinforcement	1755	-1.2780
Reinforced geocomposite	959	-1.3838

Table 5.2. Geosynthetic equation parameters for different geosynthetics tested in GRAFT

From these estimated model parameters presented in Table 5.2 the track settlement in GRAFT using any of the three geosynthetics can be estimated for any number of cycles (up to 500,000) for any applied load and subgrade modulus. Figure 5.27 compares the geosynthetic settlement model 1 for each of the geosynthetics to the test data from

GRAFT. It can be seen that the geocell and reinforced geocomposite models give a reasonable match with the measured data in GRAFT, given that they are only based on the settlement after 10,000 cycles. The settlement estimation from the XiTRACK model over 500,000 cycles is shown in Figure 5.28. For each of the geosynthetics, the geosynthetic settlement model 2 has been omitted from these Figures as it gives very similar results to model 1.

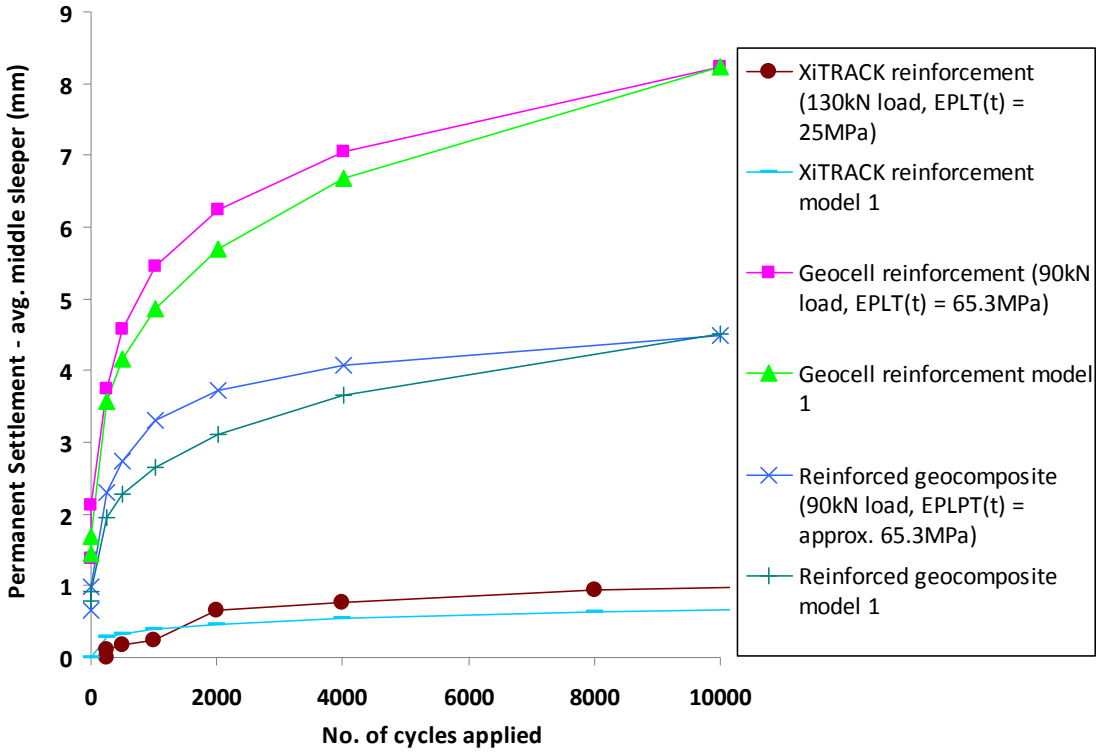

Figure 5.27. Comparison of GRAFT data to GRAFT geosynthetic models over 10,000 cycles (note the difference in load & subgrade modulus)

To give an example of how the XiTRACK settlement model could be used the same track example from section 4.2.3 has been adapted. If ballast reinforcement was considered in this example, after the initial settlement prediction of 50mm for the unreinforced track with a subgrade tangent modulus of 25MPa, the following model 1 equation could be used:

XiTRACK reinforcement (Table 5.2 & Equations 4.5 & 4.9): $y = 24.3 \times t^{-1.3342} \times N^{0.23}$

From the example given in section 4.2.3: $t = 105$ and $N = 400{,}000$

$\therefore y = 24.3 \times 105^{-1.3342} \times 400{,}000^{0.23} = 0.95mm$ (98% reduction)

Improving subgrade modulus to 60MPa (Example in section 4.2.3): $y = 15.5mm$ (69% reduction)

If the other geosynthetic models were extrapolated past the 10,000 cycles tested in GRAFT:

Geocell reinforcement (Table 5.2): $y = 1755 \times 105^{-1.3342} \times 400{,}000^{0.23} = 68.6mm$ (37% increase)

Reinforced geocomposite (Table 5.2): $y = 959 \times 105^{-1.3342} \times 400{,}000^{0.23} = 37.5mm$ (25% reduction)

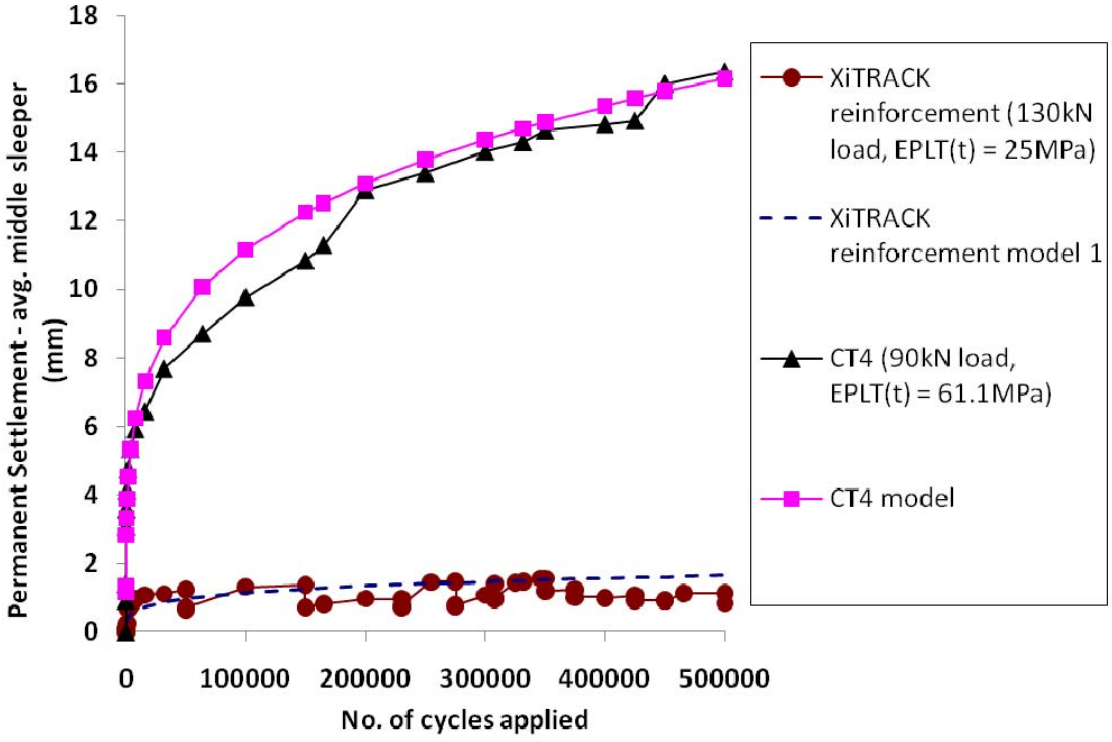

Figure 5.28. Comparison of GRAFT data to GRAFT models over 500,000 cycles (note the difference in load & subgrade modulus)

It should be noted these extrapolated estimations can only be regarded as approximate due to the limited number of cycles tested. Nonetheless, these calculations again show the vastly superior track settlement reduction possible with XiTRACK reinforcement compared to geocell reinforcement and the reinforced geocomposite. For example, to limit the track settlement to that estimated from the XiTRACK reinforcement settlement model, using the design graph shown in Figure 4.6 it can be seen that the track parameter (t) would have to be around 2000 (at 10MGT); giving either a subgrade tangent modulus of around 475MPa at an applied axle load of 25 tonnes with a 1.2 DAF, or an axle load of around 1.5 tonnes with a 1.2 DAF at a subgrade modulus of 25MPa. These measures are not practical and the only way to reduce the unreinforced track settlement down to 0.95mm after 10MGT of traffic would be to undertake both an increase in subgrade modulus and a decrease in axle load; an unreinforced track with a subgrade tangent modulus of around 150MPa and an axle load of around 8 tonnes with a 1.2 DAF would achieve 0.95mm settlement after 10MGT of traffic after a track renewal/tamping.

This example has shown how the GRAFT geosynthetic settlement models can be used for estimations on track and using the same assumptions made in this example a new design graph has been produced that incorporates XiTRACK reinforcement and the reinforced geocomposite and is shown in Figure 5.29. This graph is applicable for track settlement after 12.5MGT of traffic after a track renewal/tamping for track on a clay subgrade with a 300mm ballast depth with the same ballast properties, ballast stiffness and track construction and layout as in GRAFT (typical older track in UK that can suffer from maintenance issues). This graph has the potential to be extremely relevant to the railway industry as it could be used for preliminary cost-benefit analysis of different solutions to reduce the required maintenance on the track (geosynthetics, reduced load, improved subgrade) depending on the required settlement of the specific track after a certain amount of traffic (up to equivalent of 500,000 GRAFT cycles). For example, if a maximum of 5mm of settlement is specified after 12.5MGT of a 25 tonnes axle load with 1.2 DAF on a problematic site; from Figure 5.29 on an unreinforced track the subgrade modulus could be increased to 146MPa, or XiTRACK reinforcement could be used with a subgrade modulus of 7.5MPa, or the reinforced geocomposite could be used

with a subgrade modulus of 117MPa. The costs, practicalities and additional factors involved with each option could then be assessed accordingly. However, prior to this stage further tests need to be undertaken with XiTRACK reinforcement and the reinforced geocomposite to confirm the results found in GRAFT and refine their settlement equations. Currently the settlement models and subsequent design graph are only based on single GRAFT tests with a reduced subgrade depth over a limited number of cycles. Geocell reinforcement has not been included in Figure 5.29 as the results found in GRAFT showed a reduction in track performance.

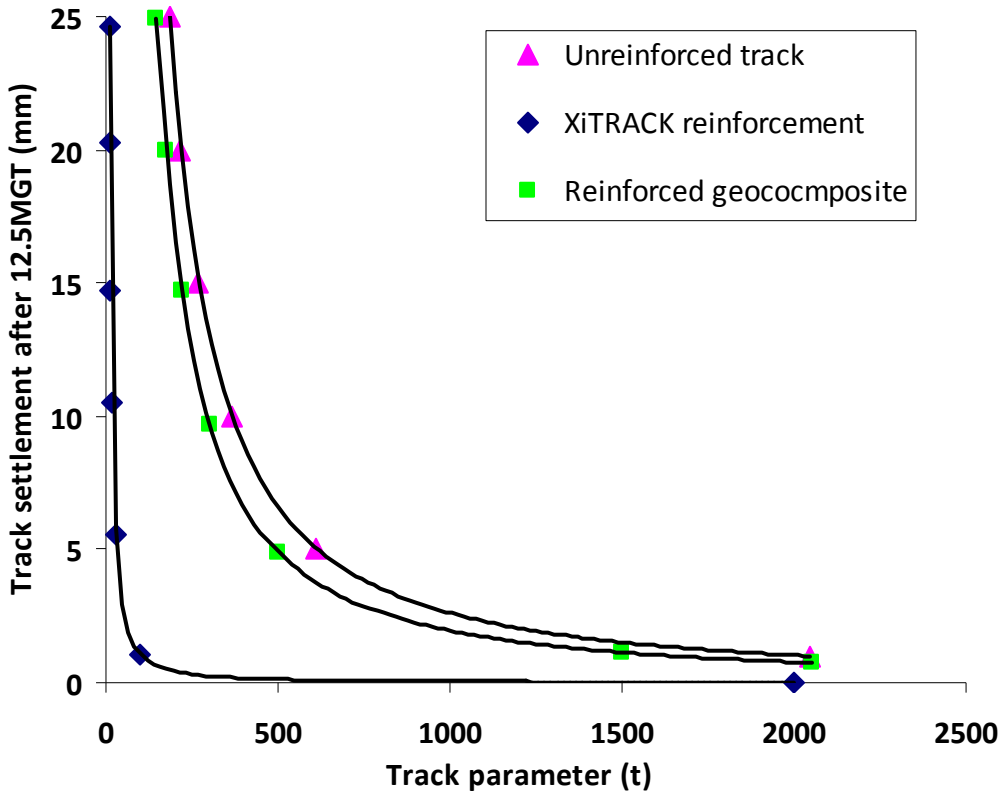

Figure 5.29. Initial track settlement design chart for track reinforcement (typical track with 300mm ballast depth on clay subgrade)

Although this design chart is limited due to the reduced depth of GRAFT and as it does not consider the influence of different ballast depths and properties, different track constructions and track components, mixed loads, different train speeds and high

cumulative tonnages (greater than around 15MGT) it can be used for a lot of typical track in the UK and with further research some of these factors could be included. In addition, further research could be undertaken on other track reinforcement options that could be added to this design graph to give a fully quantifiable track improvement design chart. To the authors knowledge no specific track improvement design charts currently exist that compare various options, although a range of different options are used on the railway tracks. A full review of comprehensive design models used around the world will be discussed in Chapter 7.

The track stiffness/settlement design graph shown in Figure 4.30 can be adapted to incorporate XiTRACK reinforcement and the new graph is shown in Figure 5.30. It can be seen that to achieve a desired track settlement after a specific amount of traffic (for an axle load range between 25 to 37 tonnes) on a typical UK track, after a track renewal/tamping, a lower required track stiffness can be specified if XiTRACK reinforcement is used. For example if 5mm track settlement is required after 12.5MGT of a 37 tonne axle load with a 1.2 DAF, then an unreinforced track stiffness of 181kN/mm/wheel would be required, but if XiTRACK reinforcement was used a track stiffness of around 45kN/mm/wheel could be used. Assuming that XiTRACK improves the stiffness of an unreinforced track by 60% (Table 5.1), an unreinforced track with a low track stiffness of 28kN/mm/wheel can be improved to an equivalent track stiffness of 181kN/mm/wheel, in terms of track settlement reduction. The reinforced geocomposite has not been shown in Figure 5.30 as only 10000 cycles were applied (0.25MGT).

Figure 5.30 also shows the lower required track stiffness that can be specified for use on UK railways, according to Network Rail standard NR/SP/TRK/9039, if geogrid reinforcement is used. Network rail state that for existing lines the minimum dynamic sleeper support stiffness (measured using FWD) can be reduced from 60 to 30kN/mm/sleeper end if geogrid reinforcement is used (for a maximum axle load of 25 tonnes). From Figure 5.30, this reduction assumes that geogrid reinforcement can reduce track settlement by around 90% compared to unreinforced track (after 12.5 MGT of a 25 tonne axle load with 1.2 DAF). However, to the authors understanding no

published research has shown this level of settlement reduction with geogrid reinforcement. Several researchers (Aursudkij, 2007, Brown *et al*., 2007a, Brown *et al*., 2007b, Hall, 2009, Shin *et al*., 2002, Sharpe *et al*., 2006, Raymond 2002) suggest that a reduction in track settlement with geogrid reinforcement of between 10 to 40% has been found in both the laboratory and in the field. Assuming an average value of 25% settlement reduction, the track settlement at a track stiffness of 30kN/mm/wheel has been plotted in Figure 5.30. Comparing this value to the unreinforced curve at the same applied load (assumed to be 25 tonne axle load with 1.2 DAF) shows that the track stiffness can be reduced from 34kN/mm/wheel for an unreinforced track to 30kN/mm/wheel for a track with geogrid reinforcement. This is significantly less than the 60 to 30kN/mm/sleeper end reduction used in Network Rail standard NR/SP/TRK/9039.

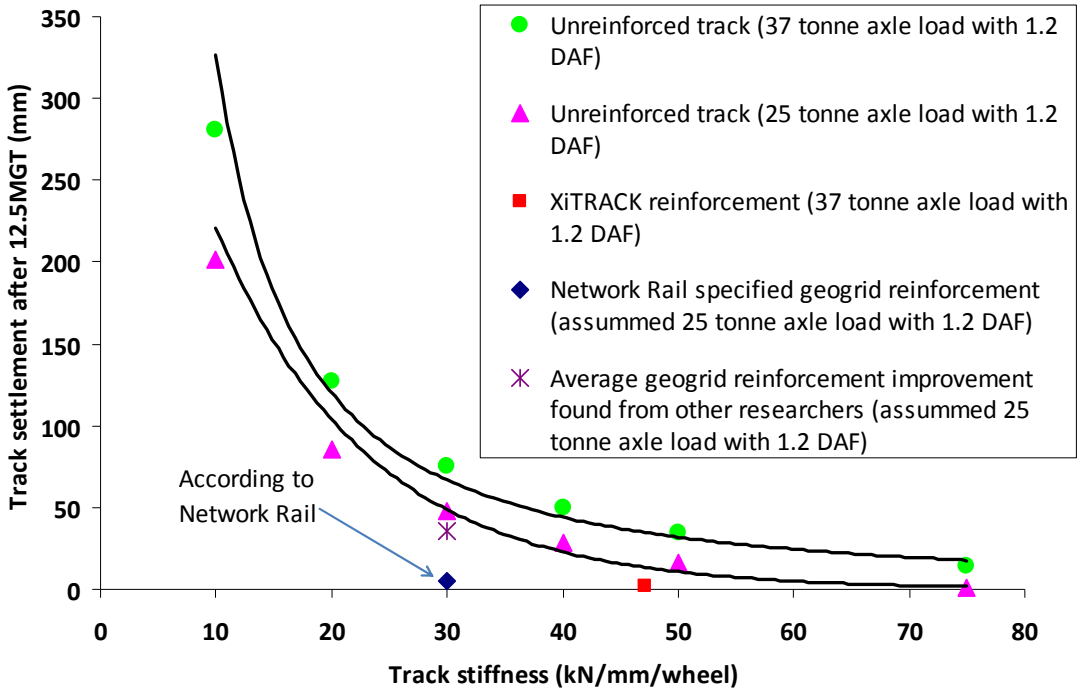

Figure 5.30. Track stiffness/settlement design chart for track reinforcement (typical track with 300mm ballast depth on clay subgrade)

It should be noted here that the geogrid reinforcement research that found reductions in track settlement with geogrid reinforcement showed large variations in their test

preparation procedures and most tests included a geotextile underlying the geogrid (effectively a geocomposite without the bonding). The performance therefore, cannot solely be considered to be due to the reinforcing action of the geogrids. Additionally, Brown *et al*. (2007a) found that geogrid reinforcement had no effect on subgrade stress level or on the resilient sleeper deflection and hence track stiffness. Moreover, Indraratna *et al*. (2004) showed that when comparing the settlement reduction of a geogrid, geotextile and geocomposite, the geogrid performed the worst. Further research is therefore required on geogrid reinforcement to fully quantify the performance improvement available compared to both XiTRACK reinforcement and the reinforced geocomposite tested in GRAFT. This is important as the reinforcement improvement may not be as high as suggested in NR/SP/TRK/9039, where geogrids can be specified to reduce the required ballast depth. It may be the case that a multi-functional geocomposite could provide the same performance or as shown here 3D XiTRACK reinforcement could considerably increase performance. This research would help to better specify the use of geosynthetics on track.

5.6 Sand blanket replacement geocomposite

Loading on railway tracks without adequate subgrade protection can result in subgrade attrition and in the presence of water this can result in the formation of a slurry at the ballast/subgrade interface (Selig and Waters, 1994). Under repeated train loading (cyclic loading) the slurry can be hydraulically pumped up through the voids into the overlying ballast. Local subgrade failures associated with pumping can lead to a loss of track alignment; due to lubrication of ballast particles resulting in a reduction in shear strength and stiffness, and local depressions of the subgrade resulting from a loss of material associated with the erosion of the subgrade. Areas on track where pumping can occur are generally known as wet spots and Ghataora *et al*. (2006) reported that in certain regions of the UK there are five wet spots per mile of railway track. Pumping failures can be prevented by providing adequate drainage on site to ensure that the surface of standing water is maintained below the level of the ballast/subgrade interface,

and by placing a layer of blanketing material between the ballast and the subgrade (after Selig and Waters, 1994) to:

- Prevent the formation of slurry by protecting the subgrade from attrition and penetration of the ballast.
- Prevent the upward migration of any slurry that forms at the ballast/subgrade interface, through the filtering properties of the blanketing material.

Geosynthetics (primarily geotextiles) can also be placed at the ballast/subgrade interface during track construction or renewal to try and reduce slurry pumping by providing separation and filtration functions. The separation function was initially thought to prevent fine-grained material entering the ballast layer from the subgrade under the action of repeated loading. The filtration function permits excess water in the subgrade, which may exist due to seepage or cyclic loading effects, to flow upwards into the ballast layer. Selig and Waters (1994) summarised the observations made by several researchers undertaking laboratory tests to evaluate the performance of geotextiles under repeated load:

- When the soil under the geotextile was clay, the repeated load caused the clay to pump through the geotextile, regardless of the geotextile; however, the rate of pumping varied with geotextile characteristics.
- The pumped slurry was formed at the contact points between the aggregate and clay through the geotextile with larger aggregates resulting in increased pumping.
- A sand layer in place of a geotextile was effective in preventing clay migration into the ballast; however, when used the geotextiles acted as an effective separator between the sand layer and ballast.

Indraratna *et al*. (2006) commented on similar results found under laboratory cyclic testing to evaluate the performance of a geotextile compared to that of a conventional sand blanket. It was found that generally, the use of geotextiles reduced the migration of fine-grained material into the upper ballast layer, but they could not prevent pumping of

soils consisting of only clay-size particles. It was concluded that geotextiles were mostly suitable when used to prevent pumping of fine soil that is broadly graded and contains significant amounts of sand-size particles. These findings were reiterated by Selig and Waters (1994) from field observations in both the UK and US where combinations of geotextiles, geomembranes and geogrids all proved insufficient in preventing pumping without a sand blanket. Further evidence of geotextiles in use on railway tracks have shown that after they have been in track for up to 48 months their permeability, tensile strength and transmisivity decreases significantly (Selig and Waters, 1994).

Undertaking full-scale laboratory testing in a railway testing facility on a range of geosynthetic products placed between the ballast and clay subgrade layer Sharpe and Caddick (2006) found that where there is a serious subgrade erosion problem no product can fulfil the function of a sand blanket. In general it was shown that without a 50mm sand blanket the settlements doubled for each of the geosynthetics tested after one million load cycles at 100kN. They did find however, that the inclusion of a geotextile separator above the sand blanket reduced the track settlement from 19.5mm (sand blanket only) to below 10mm on average. This is due to the prevention of the intermixing between sand and ballast. Sharpe and Caddick (2006) stated that although geosynthetic layers could not replace a sand blanket they could often enhance the performance of an existing trackbed, or reduce the required depth of construction to sufficiently warrant their use. A 25mm reduction in sand blanket thickness was reported by Sharpe and Caddick (2006) from site trials using a non woven geotextile separator between the sand and ballast. Raymond (2002) also found that a geotextile placed on top of a sand blanket could significantly reduce intermixing of the sand blanket and ballast.

It can be concluded from these findings that although a geotextile may reduce the rate of clay pumping it cannot prevent it alone and a sand blanket with a geotextile separator is a better system. This is now the adopted system in the UK and within Network Rail standard RT/CE/S/010, i.e. a non-woven geotextile separator is specified for use on track to separate a sand layer from ballast. A typical sand blanket construction requires a depth of 100mm and the grading specification for blanketing sand is given in Network

Rail standard RT/CE/S/033. Although geotextiles cannot replace sand blankets themselves Sharpe and Caddick (2006) stated there is further scope to investigate multi-functional geosynthetics (geocomposites) to try and reduce trackbed renewal costs and installation time incurred by laying sand blankets. They estimated that there are about 30 miles of sand blanket laid each year on UK railways. To fulfil the functions of a sand blanket a geosynthetic product must:

- Prevent upward migration of fines
- Resist abrasion under heavy dynamic loading
- Dry out any existing slurry
- Permit seepage of water from underlying subgrade
- Reduce stress on subgrade
- Prevent subgrade attrition by ballast
- Drain water from above and below

To this end a limited number of geocomposite products that fulfil these functions have been developed to try and replace the traditional sand blanket. Some of these products have been tested in the laboratory using both small and large scale apparatus (Ghataora *et al*., 2004, Burns *et al*., 2006, Ghataora *et al*., 2006, Li *et al*., 2007, Ghataora and Burrow, 2009). Ghataora and Burrow (2009) demonstrated that a highly permeable geocomposite could be used to reduce the thickness of the sand blanket by 60% without any migration of fines into the ballast layer. Burns *et al*. (2006) found that a prototype bonded sand geocomposite matched favourably with the performance of a sand blanket in terms of settlement and migration of fines, but not so favourably in terms of stiffness and subgrade strength reduction. Li *et al*. (2007) tested a similar 15mm thick bonded sand geosynthetic structure and found that the migration of fines through the geocomposite were mitigated up to 1 million load cycles, although it was noted that there may still be potential for fines migration in the long term (suggested by discoloured sand within the geocomposite). Li *et al*. (2007) also found that the geocomposite dried out the subgrade and slurried layers to a certain extent, with subsequent increases in surface shear strength. It was concluded by Li *et al*. (2007) that this geocomposite has the potential to perform typical blanketing sand functions on

marginal subgrade failure sites. Field performance audits in the UK of the same bonded sand geocomposite were described by Barker and Sharley (2009) from 18 track renewal sites, the majority of which were on low speed track (<50mph) with less than 15 equivalent million gross tonnes per annum (EMGTPA). They found that the track quality at the majority of the sites had improved since the renewal, although this is to be expected with a renewal, regardless of using a geocomposite. The data was inconclusive as only a limited number of track quality measurements had been taken to date.

To further investigate whether a geocomposite could replace a sand blanket a geocomposite designed to prevent the pumping of fines into the ballast layer and replicate the functions of a sand blanket was tested within GRAFT at a load of 90kN. The product was a 12mm thick geocomposite comprising bonded sand sandwiched between two permeable geotextile layers. The sand was bonded with a latex binding agent and had a geogrid embedded within it. To test it within GRAFT a typical wet spot was created by initially flooding and pre-loading GRAFT to achieve a weak slurried formation (Part 1) onto which the geocomposite was then placed and tested (Part 2). The unconfined compression strength and the moisture content of the formation layer, as well as the track settlement and stiffness, were all used to assess the performance of the geocomposite. In addition, at the end of the test the geocomposite sample was recovered with visual observations recorded and permeability tests undertaken. Table 3.7 shows the initial subgrade and formation properties found at the start of Parts 1 and 2 of the geocomposite test. Part 1 of this test was undertaken on the same track as CT1 after 100,000 applied cycles. It should be noted here that the formation unconfined compression strength value given for Part 2 of the geocomposite test is assuming that the formation is fully saturated.

The loading procedure undertaken for the geocomposite test was as follows:

- Part 1 – 0 to 5000 cycles without flooding to bed track in
- Part 1 – 5000 to 400,000 cycles with flooding to produce slurried formation
- Part 2 – 0 to 401,458 cycles with flooding to test the performance of the geocomposite

To flood the tank water was pumped into GRAFT from a dirty water submersible pump with automatic float that was located at the bottom of a container filled with water. The water was pumped across the full area of ballast through a perforated plastic pipe and it was drained out of the tank back into the container through a 3m long removable drainage pipe situated 50mm above the top of the formation layer. Flooding water was continually circulated through the tank during loading and hence the formation was continually under at least a 50mm head of water (this is consistent with tests undertaken on a similar geocomposite at Nottingham University by Li et al. (2007)). Figure 5.31 shows the water circulating system in GRAFT.

At the end of Part 1 the ballast layer was removed and clay slurry was clearly visible with severe ballast penetration into the formation layer. Figure 5.32 shows the formation layer after Part 1 of the test. It was considered that the formation was in a condition that replicates the poor conditions found on sites where wet spots are present on track.

Figure 5.31. Water draining out the side of GRAFT 50mm above the top of the formation layer

Figure 5.32. Formation after Part 1 of geocomposite test

The thin 12mm thick geocomposite sample was placed directly on top of the slurried formation created in Part 1 of the test (Figure 5.33) and sand was hand compacted around the edges to fill gaps between the tank walls and the geocomposite. The sand was used to prevent any slurry pumping round the edges of geocomposite and migrating into the ballast layer. The needle punched geotextile was placed directly onto the clay slurry formation while the reinforced geotextile was in contact with the bottom of the ballast layer. Figure 5.34 shows the full geocomposite layer placed on the formation. Ballast was placed and compacted in three layers directly on top of the geocomposite layer. The same ballast was used as in Part 1 of the test; it was washed with a power washer to remove any clay slurry contamination prior to replacement for Part 2 of test. The inside walls of tank were also washed.

The unconfined compression strength (q) of the formation layer was measured before and after Parts 1 and 2 of the testing programme. Three samples were taken from across the formation layer before Part 1 of the test started while two samples were taken each after Parts 1 and 2 of test (one from underneath centre sleeper and one from underneath adjacent sleeper). The average degree of saturation of the samples taken was found to be 95% for the samples taken after Part 1 of the test and 96% for the samples taken after

Part 2 and thus the formation was assumed to be fully saturated. The degree of saturation had increased from approximately 77% prior to the start of Part 1

Figure 5.33. Placement of geocomposite on slurried formation

Figure 5.34. Full geocomposite layer on formation

Figure 5.35 plots the average formation strength found from these samples after each stage. It should be noted here that this figure assumes that the formation before Part 1 of

the test is unsaturated and hence no correction is made to take into account the effect of barrelling of the samples during compression. From Figure 5.35 it can be seen that the average formation q reduced from 186kPa before Part 1 of the test to 112kPa after Part 1 of the test to 102kPa after Part 2 of the test. These values give average undrained shear strength values of 56kPa (Cu = q/2) after Part 1 and 51kPa after Part 2. These values indicate that after application of the geocomposite the formation strength continued to decrease. Note that some parts of the samples taken may have been slightly disturbed during coring and extrusion of sample from mould, and hence these values can only be regarded as indicative.

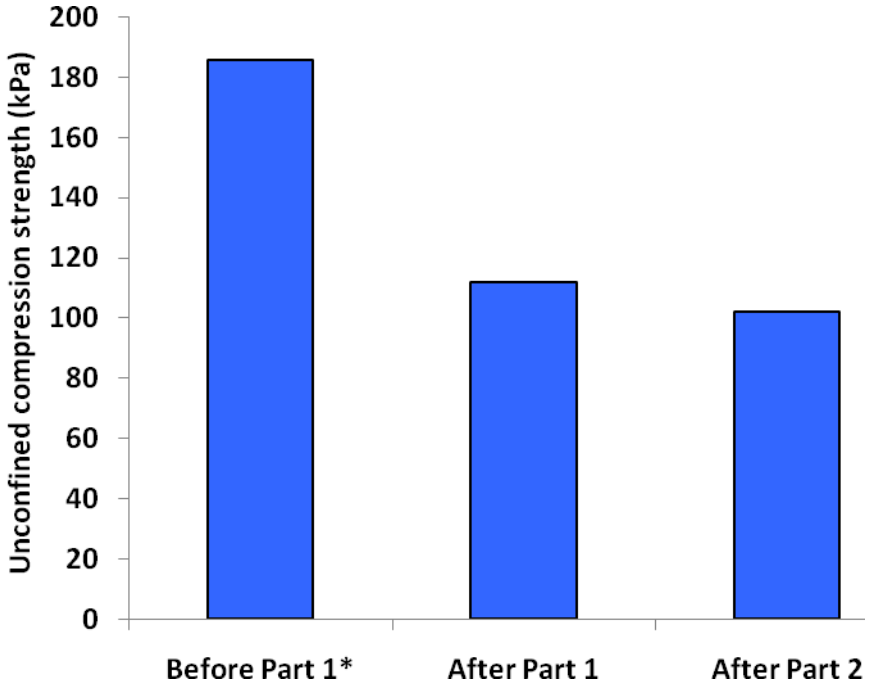

Figure 5.35. Average formation unconfined compression strength assuming fully saturated formation after Parts 1 and 2 of geocomposite test (*not at full saturation)

The moisture contents from a number of representative samples taken across the different formation layers show that the average formation moisture content before Part 1 of the test was 24.2% which increased to 31.4% after Part 1 and then increased slightly to 31.5% after Part 2. These increases coincide with the decreases in strength shown in Figure 5.35. Okada and Ghataora (2002) found a relationship between a

threshold moisture content (moisture content/optimum moisture content) and subgrade sample penetration. They stated that a wet subgrade exceeding its threshold moisture content could easily cause subgrade failure problems and that the plastic deformation of a soil occurs especially when the soil is nearly saturated. It was considered that a soil with a threshold moisture content of 1.4 was almost saturated. Using this relationship the formation in GRAFT after Part 2 of the test has a threshold moisture content of 1.33.

The development of permanent track settlement throughout Part 1 and Part 2 of the geocomposite test is shown in Figure 5.36 & Figure 5.37 respectively. In both these Figures titling of the middle sleeper is shown and it is evident that the tilting increases throughout each test. This is due to the continual clay formation erosion of the track during loading under flooding conditions. During Part 2 of the test (with the geocomposite under test) the tilting became unsustainable and the test had to be stopped after 273,000 cycles with the ballast tamped with a Kango hammer to bring the track back up to level. The track settlement pattern shown in Part 1 of the test is understood to be due to initial ballast densification followed by ballast penetration into the softened formation surface. It is thought that the longer the test was continued and the longer the formation layer was submerged under water the higher the rate of settlement would be. The settlement development during Part 1 of the test is different from the traditional settlement development of unreinforced railway track without continual flooding. The rate of track settlement does not decrease with the number of applied cycles and does not become linear after a certain stage. This highlights the severe track deterioration conditions that exist in wet spots. Selig and Waters (1994) stated that at times of heavy rainfall and flooding the strength of the subgrade soil can quickly diminish, which can lead to massive shear failure. There is therefore a need for improvement of track at these sites. Unfortunately the addition of the geocomposite tested in Part 2 of this test did not seem to have much effect and the track settlement was found to actually increase significantly after around 200,000 applied cycles.

To compare Parts 1 and 2 of the geocomposite test Figure 5.38 considers the test as a continuous number of cycles to highlight the difference in the gradient between the two independent parts. The rate of increase in settlement for Part 2 of the test after initial

ballast densification is visibly greater than Part 1 of test. It is thought that this may be due to the build up of pore water pressure beneath the geocomposite under the action of loading. This pore water pressure is thought to have resulted in water and clay piercing through the sand boundary between the tank walls and the geocomposite and infiltrating the ballast layer rather than the water pressure relieving through the geocomposite. This process would erode the clay formation layer and cause large settlements due to bearing failure. Further evidence of this failure mode was found when excavating the geocomposite and will be discussed later. Chrismer and Richardson (1986) reported on a similar failure where the accumulation of water and excess pore pressure under a low permittivity geotextile led to the subgrade failure of a railway test section. This failure mode has not been witnessed in smaller scale tests undertaken elsewhere on similar sand blanket replacement geocomposites (Li *et al*., 2007, Burns *et al*., 2006); this may be because the drainage path is smaller and hence pore water pressure can be dissipated quicker. In GRAFT, water has to travel 0.5m to the end of tank. It should be noted here that in the field the drainage path is even longer.

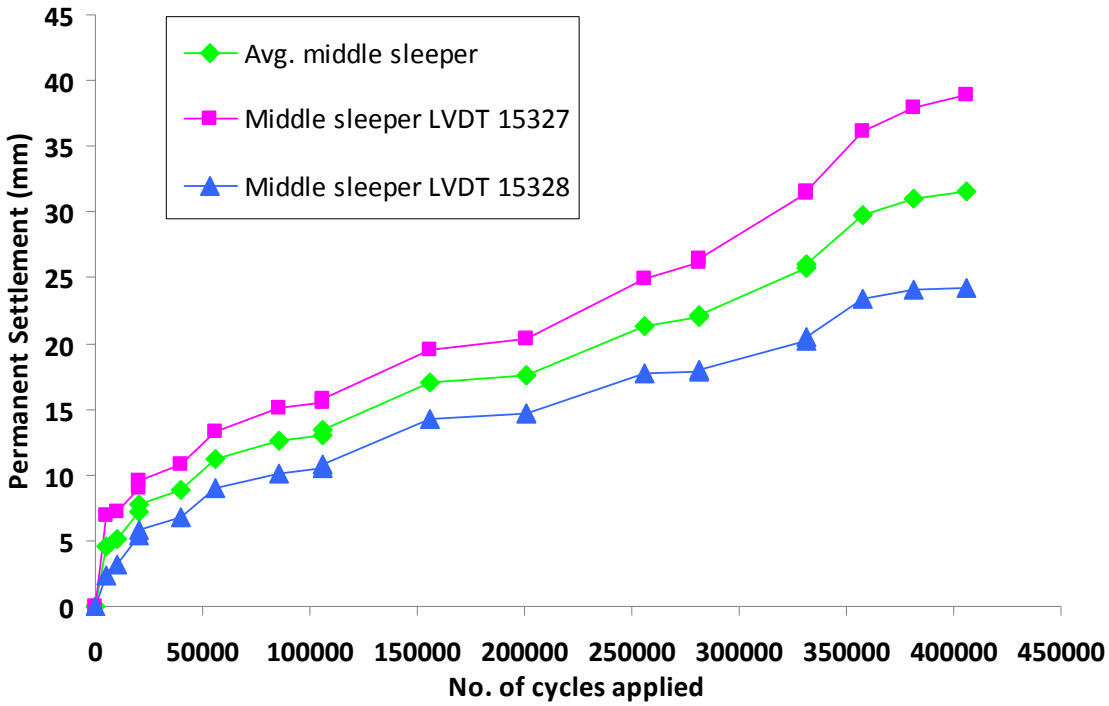

Figure 5.36. Permanent settlement development throughout Part 1 of the geocomposite test

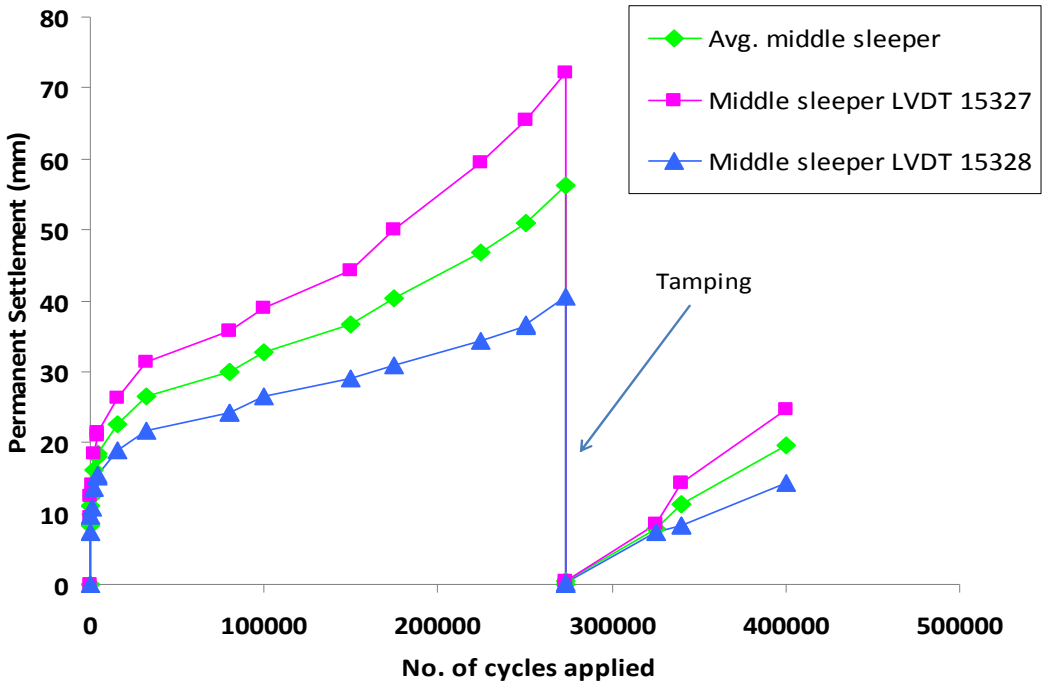

Figure 5.37. Permanent settlement development throughout Part 2 of the geocomposite test

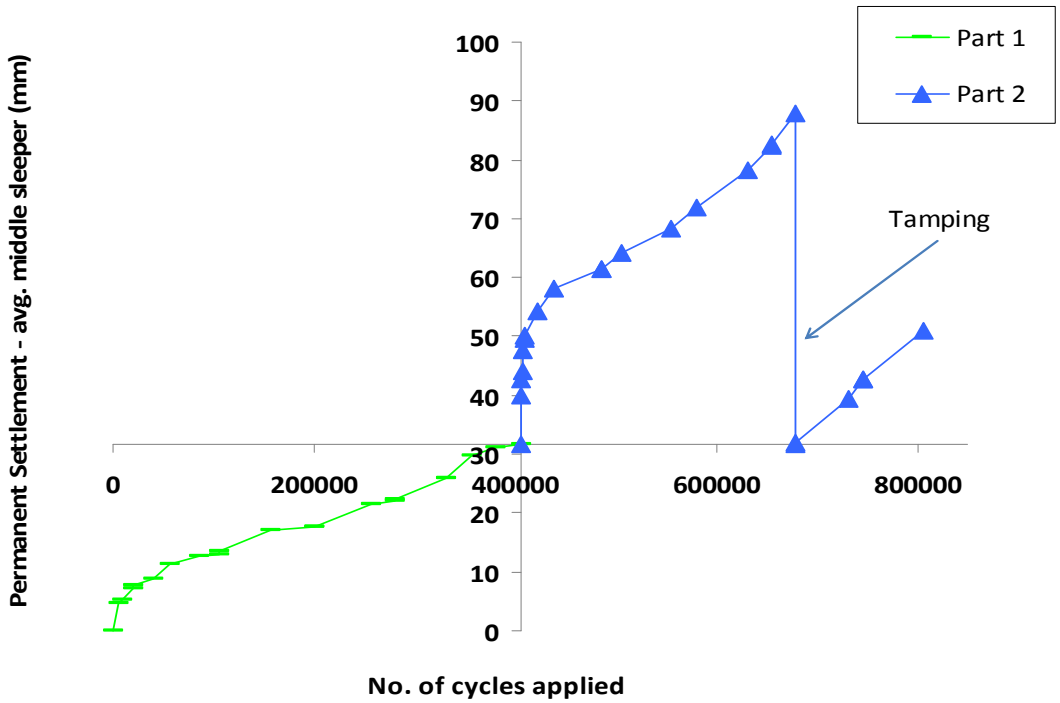

Figure 5.38. Permanent settlement of middle sleeper throughout Parts 1 and 2 of the geocomposite test

The increasing rate of permanent settlement throughout Parts 1 and 2 of this test was matched by decreasing track stiffness. The average central sleeper transient deflections plotted against the number of applied cycles for Part 1 and 2 of the geocomposite test are shown in Figure 5.39. The general trend shows that the deflection increases throughout both Parts 1 and 2 of the test, regardless of the geocomposite. The large spike during Part 2 of the test is due to the ballast tamping temporary increasing the stiffness.

Upon excavating the ballast layer at the end of Part 2 of the test it was found that the ballast was considerably contaminated with clay slurry. Also, three deep depressions were clearly visible on the formation layer below the geocomposite, two on either side of where the central sleeper was positioned (between sleeper end and tank walls) and one on the side of where an adjacent sleeper was positioned. After stripping back the geocomposite it was clear that bearing failure had occurred with the whole 70mm formation layer depth having been eroded on one side of GRAFT where the central sleeper was positioned (Figure 5.40). This explains the large settlements, increasing track deflections and tilting of the middle sleeper observed during the test.

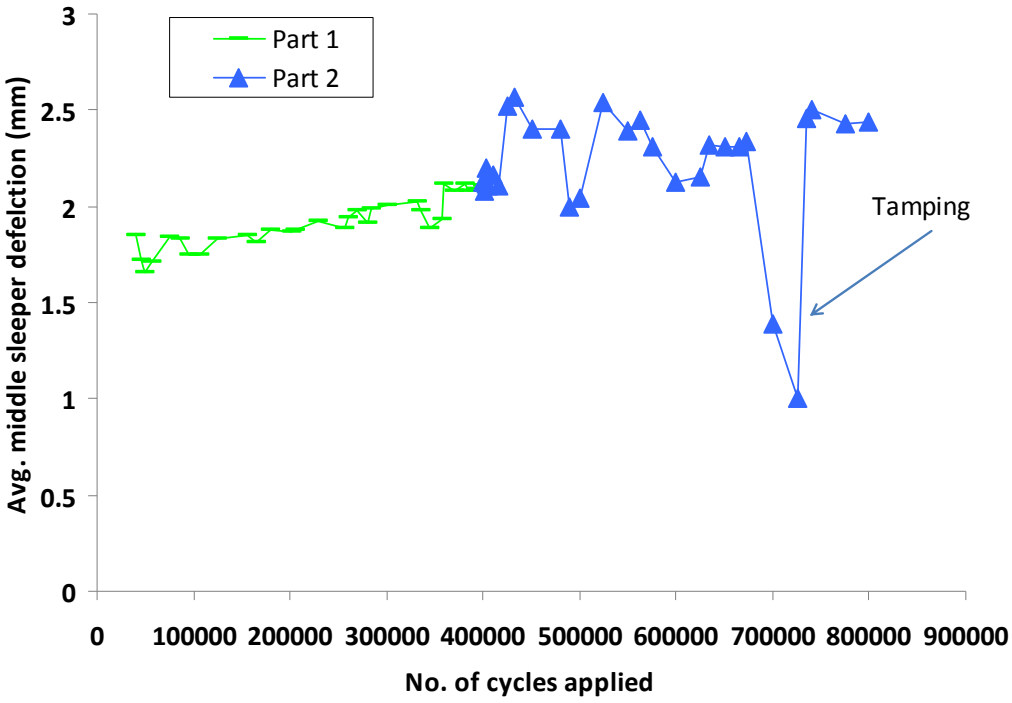

Figure 5.39. Centre sleeper deflection throughout Parts 1 and 2 of the geocomposite test

It is thought that pore water pressure developed underneath the geocomposite layer where the loads were applied and as the permeability of the geocomposite is less than sand the rapidly generated pore water pressure can only 'quickly' dissipate through the boundary sand at the interface of the geocomposite and the wall. Consequently, considerable water pressure may have built up underneath the geocomposite under loading where progressive formation erosion was occurring. This may have led to the water pressure removing the sand boundary and infiltrating the ballast layer with clay and water. It is thought that this process has been continual throughout the test. On removal of the geocomposite it was dissected to analyse the amount of fines that had migrated into it. Some discoloration was noticeable towards both sides of the geocomposite, but none in the middle and no significant clogging was found. The slurry on top of the geocomposite is, therefore, thought to be due to the clay migrating up through the sand boundary (under water pressure) as explained, and hence, not due to pumping of fines through the geocomposite.

Figure 5.40. Erosion of formation under centre sleeper

To assess any change in permeability of the geocomposite as a result of it becoming clogged with fines the permeability of a sample of the virgin geocomposite was

compared against that of a recovered sample taken after Part 2 of the test. The recovered sample was taken from directly underneath the middle sleeper adjacent to the deep depression caused by formation erosion and the needle punched geotextile was removed from the samples prior to the tests (samples could not be tested practically with geotextile). It is thought that the removal of the geotextile slightly increases the permeability of the samples, however this has not been measured. The tests were undertaken following BS 1377-5:1990 with a constant head filtration apparatus being used. The permeator cell had a 75mm diameter and was 260mm long with a distance of 100mm between manometer connection points. Note that using a constant head filtration apparatus can only give an estimation of the permeability as a special cell is required to accurately measure the permeability of geosynthetics (BS EN 14150:2007).

The permeability of the virgin geocomposite was found to be 5.99E-05m/s while after the test it had decreased to 2.42E-05m/s. In this range the permeability is typically less than sand (1.00E-04m/s) but greater than that of a clayey formation (1.00E-07m/s). In the authors opinion it is thought that this permeability was not high enough to prevent the build up of pore water pressure beneath the geocomposite under the action of repeated cyclic loading and it should be noted that although the permeability has not significantly decreased during the test, with time the permeability could decrease further due to deeper clay penetration into the geocomposite.

Overall, strength, settlement, stiffness and permeability measurements were taken along with visual observations made during testing in order to assess the performance of the geocomposite under a realistic track environment where subgrade erosion is present. Large settlements, increasing track deflections with cycles and visual observations have shown that significant formation erosion and subsequent track failure occurred in localised areas where the cyclic load was applied. Unconfined compression samples could not be taken from these areas and hence, although the average strength across the formation layer had not changed much with the addition of the geocomposite, the strength in these localised spots was likely to have decreased considerably. Pocket penetrometer and proving ring penetrometer measurements taken close to these areas indicate a decrease in undrained shear strength from the average values found across

whole layer of 13kPa and 14kPa respectively. In the authors opinion formation erosion is thought to have occurred during the test as a result of the development of excess pore water pressure beneath the geocomposite under cyclic loading.

5.7 Conclusion

Enhancing the performance of railway tracks by geosynthetics is now widely undertaken by the rail industry due to the relatively low cost and proven performance in a number of railway applications. However, although several of these products are used in track around the world very little research has been done to compare their performance on a like for like basis. Furthermore, in many instances geosynthetics have been used in conjunction with track renewals and as such the improvement in track performance purely due to the geosynthetics is often difficult to assess.

This chapter compared the influence of four different geosynthetic products on the performance of the track against the control tests without any geosynthetics. Under normal GRAFT test conditions (same as control tests) two ballast reinforcement products were tested; XiTRACK reinforcement and geocell reinforcement. These products intend to stabilise the ballast to avoid the generation of excessive plasticity and to reduce the induced stress level on the subgrade soil to prevent subgrade deterioration. They were compared to a reinforced geocomposite used primarily for separation at the ballast/subgrade interface and filtration of the underlying water from the subgrade. In addition, a geocomposite product designed to replace a traditional sand blanket, used on the tracks where severe subgrade erosion conditions prevail, has been tested in GRAFT under flooding conditions.

The results have shown that XiTRACK reinforcement (significantly) provides the best track performance, when compared to unreinforced track with the same track conditions, in terms of increased track stiffness and reduced track settlement. Additional tests on XiTRACK samples have also shown the resiliency, ductility and versatility of XiTRACK reinforced ballast. Geocell reinforcement did not perform well in GRAFT and it is recommended that further research be undertaken over a greater number of

applied cycles prior to further use on track. An improvement in performance was found with the reinforced geocomposite, which is thought to be due to it preventing angular corners of individual ballast particles penetrating into the underlying clay formation. This needs to be confirmed with further research however over a greater number of cycles. While testing the sand blanket replacement geocomposite it was found that formation erosion and subsequent track failure occurred in localised areas where the load was applied. It is thought that although the geocomposite prevented slurry pumping through it, and provided adequate separation between the subgrade and ballast layer, the permeability is too low to allow excess pore water pressures to quickly dissipate under cyclic loading. Currently, it is understood by the author that although some sand blanket replacement products are being used in the UK network, none can match the performance of a traditional sand blanket with a geotextile separator and as such much further research is required in this field.

From all the data recorded settlement models have been proposed for each of the three geosynthetics compared for reinforcement purposes and it was found that the models give a reasonable match with the GRAFT test data. These models formed the basis for design graphs that incorporate XiTRACK reinforcement and the reinforced geocomposite. These design graphs are applicable for track settlement after a track renewal/tamping for track on a clay subgrade with a 300mm ballast depth with the same ballast properties, ballast stiffness and track construction and layout as in GRAFT (typical track in UK that can have maintenance issues). As previously stated though it is likely that these equations will underestimate track settlement in the field due to the restricted depth of GRAFT and therefore should only be used to give indicative values of settlement. Currently in the UK, no such design graph is used for different track improvement options and geogrid reinforcement is the only form of track reinforcement in the Network Rail standard on formation treatments (NR/SP/TRK/9039). This standard states that for existing lines the minimum dynamic sleeper support stiffness can be reduced from 60 to 30kN/mm/sleeper end if geogrid reinforcement is used (for maximum axle load of 25 tonnes). However, based on the research by others on geogrid reinforcement, this may be an overestimation of the performance of geogrid reinforcement, as shown in this chapter. Further research in GRAFT is therefore

recommended on planar geogrid reinforcement to investigate the ballast reinforcement mechanism and stress level reduction under high loads, and ultimately the level of track settlement improvement available. In addition, it is also recommended that research be undertaken in GRAFT on geotextiles to investigate the direct role of the separation, filtration and reinforcement functions of geosynthetics on track performance. This would aid railway engineers when specifying the use of geosynthetics on track and it may be the case that a multi-functional geocomposite could provide the same performance as geogrid reinforcement, in terms of track stiffness and settlement, due to having similar levels of stress reduction in the ballast and on the subgrade.

With further research and the addition of other track improvement options these design graphs could form part of an initial cost-benefit analysis of different solutions to reduce the required ballast maintenance on the track depending on the required settlement of the specific track after a certain amount of traffic. Chapter 7 uses FE modelling of GRAFT to consider the influence on track stiffness on some simple alternative track improvement methods and compares the result to what other researchers have found. Prior to this though, in order to use the initial track settlement design graph (Figure 5.29) in the field and to have a subgrade modulus value for the FE model, a reliable measure of subgrade modulus needs to be made on track. Plate load tests, although known to be accurate, can be time consuming and costly and as such are not practical for frequent use on site. As a result several in-situ measuring devices can be used. Fleming *et al*. (2000) mentioned that although the static PLT is widely adopted, it is increasingly being replaced by portable and quicker in-situ dynamic plate tests. Chapter 6 investigates the accuracy of different in-situ devices tested in GRAFT.

Chapter 6 - Subgrade In-situ Testing Devices

6.1 Introduction

The importance of subgrade stiffness and strength on railway track performance has been described in detail within Chapters 4 and 5. Nonetheless, Brough *et al*. (2003) reported that the subgrade is rarely considered in the design and implementation of work proposals even though correlations between maintenance, track deterioration and subgrade condition have been identified. Brough *et al*. (2003) further stated that many examples have been found of expensive remedial work being carried out without eliminating the cause of the problem, which is often subgrade related. The trackbed investigation that was undertaken at such sites involved shallow pit excavation at 100m intervals with the aim of providing a subjective assessment of contaminated ballast and suspected subgrade problems. Indeed, the Network Rail standard on formation treatments (NR/SP/TRK/9039) states that 'while good stiffness characteristics are important to ensure good trackbed performance, it is not necessary to make direct stiffness measurements'. It further describes that where there has been difficulty in achieving the required track geometry in the past the 'Trackbed Index' (TI) can be used as an indicator of whether the trackbed depth is adequate. TI is equal to the undrained shear strength in kPa (indicative values accepted) times the depth of the trackbed in metres. A TI value of 40 is considered to be a minimum for main lines and if TI is consistently low then more detailed stiffness information is obtained. Clearly, in order to diagnose the cause of track geometry deterioration, predict the future track performance and to schedule future maintenance required on site a more detailed investigation of the trackbed is required.

For trackbed investigation to become a routine procedure the optimum test devices need to be identified so that regular monitoring can take place in an accurate, consistent and safe manner within the physical and time restrictions of working on the railway track (Brough *et al*., 2003). Simple, inexpensive and quick measuring devices would therefore be very beneficial to the railway industry.

This chapter investigates the accuracy of some typical in-situ testing devices, in measuring subgrade stiffness and strength, in order to enhance railway site investigation techniques. Soil stiffness and strength properties for track subgrade evaluation can be obtained from either; laboratory tests undertaken on good quality field samples or in-situ tests. Common laboratory tests used include the repeated load triaxial test, CBR test and the unconfined compression test. Disadvantages of laboratory tests are that they expensive, time consuming and many are needed to represent soil variability with depth and with position along the track. Moreover, the results may not be accurate due to sample disturbance and inadequate representation of in-situ physical state and stress conditions, which vary over time (Selig and Waters, 1994). In-situ tests on the other hand have the ability to provide estimates of soil properties rapidly and relatively inexpensively for larger areas of soil in its natural state of stress. The main disadvantage with most in-situ tests is that instead of measuring real soil properties they only measure some intermediate parameter which is a measured response of the soil behaviour. This measurement is then used to find a desired soil property through an empirical, semi-empirical or theoretical transformation. These transformations are usually associated with simplifying assumptions, and hence the accuracy of individual test results may be directly related to these assumptions (Selig and Waters, 1994).

Many in-situ measuring devices are available for obtaining parameters for predicting subgrade performance and in recent years an increasing number have been developed. Details of some of these devices can be found in Selig and Waters (1994). With the exception of identifying changes in the stratigraphy, which can affect the overall performance of the track system, the subgrade strength (for load bearing capacity) and subgrade stiffness (for deformation analysis) are essentially the only two track parameters that need to be evaluated when predicting track subgrade performance (Selig and Waters, 1994). The applicability of some in-situ devices in determining the strength and modulus for a typical clay subgrade soil can be found in Table 6.1, which has been modified from Selig and Waters (1994). It should be noted here though that depending on the strength of the clay the suitability of using each of these devices varies. Also, as soil properties are dependent on test conditions such as strain rate, stress path to failure, boundary conditions, and influence zones etc., different tests will provide different

values of the same parameter. Selig and Waters (1994) noted that it is important to assess within what accuracy each test may be used to predict the soil properties measured, which in many cases is limited to the quality of the assumptions made.

Test	Subgrade strength	Subgrade modulus
PLT – Plate load test	√	√
FWD – Falling Weight Deflectometer		√
LFWD – Light Falling Weight Deflectometer		√
DCP – Dynamic Cone Penetrometer	√	√
PMT – Pressuremeter Test		√
DMT – Dilatometer Test	√	√
GG – Geoguage		√
CSWS – Continuous Surface Wave System		√
CPTU – Piezocone	√	
CPT – Cone Penetration Test	√	
SPT – Standard Penetration Test	√	
FVT – Field Vane Test	√	
PP – Pocket Penetrometer (indicative test)	√	
PRP – Proving Ring Penetrometer (indicative test)	√	

Table 6.1. Application of different in-situ tests on a clay subgrade (modified from Selig and Waters, 1994).

Brough *et al*. (2003) investigated 21 different in-situ test devices traditionally used in the highways industry for suitability of use in the railway environment for assessing the subgrade condition. The causes of subgrade problems, railway loading conditions, and working restrictions applicable in the UK were all considered in their studies and used to assess the devices along with other variables such as repeatability, test procedure, economics, speed of implementation and ability to assess the performance of ground

improvement techniques. It was found that for short track possession times (1 hour) where large track lengths need to be assessed for identification of poor subgrade sites the DCP and CSWS devices were deemed suitable. For longer overnight possession times where the causes of track geometry deterioration at identified poor subgrade sites need to be evaluated the CPT and FWD were deemed suitable. Other devices such as the automatic ballast sampler, ground penetrating radar and profile probe were also found to be suitable for railway track investigations but have not been included in Table 6.1 as they do not give quantitative values of subgrade strength or stiffness. Within Network Rail standard NR/SP/TRK/9039 the FWD on sleepers, FWD on subgrade, PLT, FVT and PP are the in-situ methods recommended to determine the subgrade parameters. The laboratory tests recommended include the CBR and triaxial tests. The quality of each test measurement within NR/SP/TRK/9039 is stated as 'high' with the exception of the CBR, PP and FVT which are stated as indicative.

Within this research both laboratory (unconfined compression) and in-situ (PLT, LFWD, DCP, PP, PRP) tests have been undertaken to evaluate the subgrade and formation strength and stiffness throughout the testing programme from different sources. Unconfined compression, PP and PRP were used primarily for strength measurements while the PLT, DCP and LFWD were used for stiffness measurements. The DCP and LFWD are traditionally devices developed for use on roads, although their use on railway tracks is becoming more popular. Based on experience of using the different devices and as only limited time was available with the DCP and LFWD it was decided that the subgrade and formation strength would be taken from the laboratory unconfined compression strength tests throughout the GRAFT testing programme while the subgrade stiffness would be taken from the PLT. These tests were assumed to be accurate and were undertaken in the same way each time, as detailed in Chapter 3. This allowed the results from these tests to act as references for which the other in-situ devices used could be compared. It should be noted here though that high variability is likely with the unconfined compression test results due to sample disturbance during coring and extrusion from the mould. Mohammadi *et al*. (2008) reported that the coefficient of variance (c_v), which is the ratio between the standard deviation and the mean, for unconfined compression strength tests is between 6 and 100% with a

recommended average at 40%. Hence, although the unconfined compression strength values have been used as a reference for which the PP and PRP have been measured against, they only represent indicative strength values.

Twenty one PP readings and five PRP readings were taken across the full formation and subgrade layer for each GRAFT test while only a limited number of DCP and LFWD measurements were undertaken due to the availability of the devices. Table 6.2 shows when and where these measurements were taken throughout the GRAFT testing programme. To minimise the effects from the tank walls on the tests a minimum distance of 250mm from the DCP cone to the any neoprene covered wall was used for the DCP while a minimum distance of 300mm was used for the distance between the edge of the LFWD loading plate and the tank walls. The PLT minimum distance between the edge of the bottom loading plate and the tank walls was also taken as 300mm. These values were suggested from the results of similar studies undertaken by Mohammadi *et al*. (2008) and Alshibli *et al*. (2005). Mohammadi *et al*. (2008) investigated the influence of the side walls of laboratory circular moulds on the results of the DCP by testing in moulds with different diameters. It was found that all effects are completely negligible for moulds with a diameter equal to 500mm, meaning that a distance of 250mm between the DCP cone and the edge of the test mould is sufficient. Alshibli *et al*. (2005) undertook a preliminary study on the effects of laboratory box boundary conditions on the results from the LFWD and found that a minimum distance of 150mm between the edge of the LFWD loading plate and the side of the box is required. When possible the test sequence was undertaken so that the non-destructive PLT and LFWD were tested first prior to the minimally invasive DCP, which created a small hole throughout the depth of the subgrade. The effects of any overlap of the DCP tested areas or the influence of any further compaction or disturbance being induced in the formation or subgrade layers due to the PLT and LFWD have not been considered and are assumed negligible.

GRAFT test and layer	In-situ stiffness test at one end of GRAFT	In-situ stiffness test in middle of GRAFT	In-situ stiffness test at opposite end of GRAFT
CT3 subgrade	DCP, LFWD	DCP, LFWD, PLT	-
CT3 formation	LFWD	LFWD	LFWD
CT4 formation	LFWD	LFWD	LFWD
Geocell test subgrade	DCP, LFWD, PLT	DCP, LFWD, PLT	LFWD
After CT5 formation	DCP, LFWD	DCP, LFWD	LFWD
After CT5 subgrade	DCP	DCP, LFWD, PLT	LFWD

Table 6.2. In-situ stiffness measurements undertaken in GRAFT (limited due to availability of equipment)

6.2 Dynamic Cone Penetrometer (DCP)

The DCP is a simple, lightweight, fast and economical test that can provide continuous measurements of the in-situ strength/stiffness of pavement layers and subgrades (Alshibli *et al*., 2005). The DCP consists of an 8kg sliding cylindrical mass that drops through a height of 575mm to drive a cone tip with a 60 degree apex angle and a 20mm diameter into the underlying soil (Figure 6.1). The penetration of the cone tip from each drop is recorded and the sequence is repeated until the desired depth is reached up to a maximum depth of approximately 1m. The data is plotted as cumulative number of blows against depth and a change in slope of the plotted data represents a change in strength/stiffness of the material. Figure 6.2 shows a typical DCP test being undertaken in GRAFT. One problem with the test in cohesive soils is that frictional resistance can accumulate along the drill rods, reducing the ability to distinguish between distinct soil layers (Selig and Waters, 1994). To minimize the effect of skin friction the lower steel rod has a smaller diameter (16mm) than the cone (Mohammadi *et al*., 2008). At the end of the test the average penetration rate (PR) can be calculated (mm/blow) for each change of slope found. In the field the thickness of different strength layers are usually

confirmed by inspection (DMRB:Vol. 7, Section 3, Part 2, 2008). In GRAFT, as the clay subgrade is consistent throughout its 750mm depth the average PR found across the entire DCP penetration has been used here.

The DCP test results are shown in Figure 6.3 for all the DCP tests undertaken in GRAFT. The results show an increase in penetration resistance (strength/stiffness) as the testing programme advanced, similar to the results found from the PLT's and the unconfined compression tests. The slight change in gradient of the plotted slopes, after a depth of around 550mm, indicates that the 150mm depth of clay at the bottom of the tank is not as stiff as the overlying 550mm. This may be due to the nature of the load distribution throughout the clay subgrade layer.

Correlations exist between the strength and stiffness of the soil and its resistance to penetration. Alshibli *et al*. (2005) stated that the PR has been correlated to the California bearing ratio (CBR), subgrade elastic modulus and subgrade resilient modulus, by different researchers over the last decade. Many DCP-PR to CBR relationships have been found by various researchers based on both field and laboratory studies of different soils, reviews of which can be found in Abu-Farsakh *et al*. (2004) and Livneh (2007). The highways design code DMRB:Vol. 7, Section 3, Part 2 (2008) recommends using the following relationship developed by the Transport Research Laboratory:

$$\text{CBR} = 10^{(2.48-1.057\,LogPR)} \tag{6.1}$$

This is the relationship adopted in this thesis; however it is noted in DMRB:Vol. 7, Section 3, Part 2 (2008) that the accuracy of this relationship reduces for CBR values below 10%.

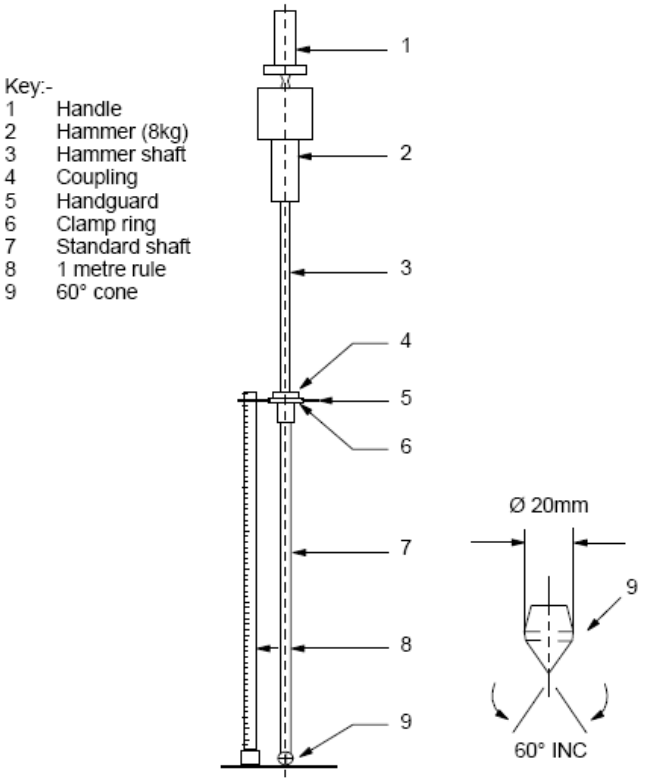

Figure 6.1. Dynamic cone penetrometer (DMRB:Vol. 7, Section 3, Part 2, 2008)

Figure 6.2. DCP test in GRAFT

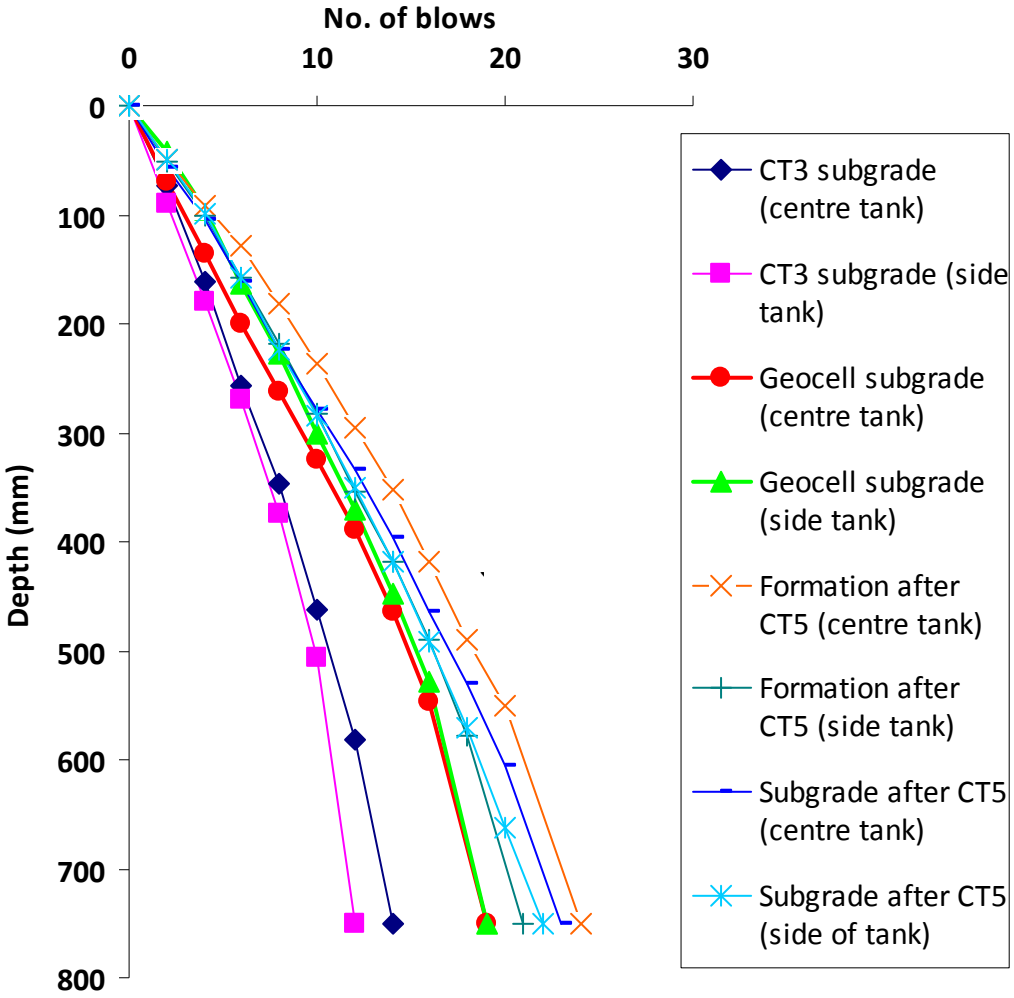

Figure 6.3. DCP results from GRAFT tests

This relationship is similar to the equation used by the US Army Corps of Engineers and Minnesota Department of Transport for a wide range of granular and cohesive materials (Abu-Farsakh *et al*., 2004):

$$CBR = 10^{(2.465 - 1.12 Log(PR))} \tag{6.2}$$

The DCP to subgrade modulus relationships found by various researchers can predict the subgrade modulus directly from the DCP-PR results or indirectly from the CBR. Again, reviews of the different correlations can be found in Abu-Farsakh *et al*. (2004)

and Livneh (2007). The following subgrade modulus-CBR relationship was developed by the Transport Research Laboratory:

$$M_r = 17.58 \times CBR^{0.64} \tag{6.3}$$

where M_r is the resilient modulus in MPa and CBR is in %. Abu-Farsakh *et al*. (2004) commented that other researchers had found that the resilient modulus calculated from the DCP-PR using equations 6.2 and 6.3 was comparable with the back calculated resilient modulus found from an FWD undertaken on the pavement surface. Livneh (2007) however, demonstrated the uncertainty associated with the use of pre-defined correlative expressions for converting in-situ DCP-PR results into CBR values. Livneh (2007) also found that comparing various CBR to resilient modulus correlations a difference of up to 300% existed in the estimated M_r values. Based on reviewing the technical literature it is the Author's opinion that such CBR correlations should only be used with caution.

Direct relationships comparing the DCP-PR with the subgrade elastic modulus include:

$$\mathrm{E} = 10^{(3.652 - 1.17 Log(PR))} \tag{6.4}$$

based on Pen (1990) where E is the subgrade elastic modulus in MPa;

$$\mathrm{E} = 10^{(2.44 - 0.4 Log(PR))} \tag{6.5}$$

based on Chau and Lytton (1981) who developed the relationship from a theoretical one-dimensional model.

Undertaking research at the Louisiana Transportation Research Centre laboratory Alshibli *et al*. (2005) undertook a series of DCP, LFWD, Geoguage and PLT measurements on a range of soils inside a large steel tank. The average PR values over the top 305mm depth were used to correlate with the PLT results. The 305mm depth for the DCP was chosen to correspond to the influence depth of the PLT. It should be noted

here though that it is widely recognised by others that the PLT has a deeper influence depth. Ping *et al*. (2002) stated that according to the theory the major portion of the total deformation occurs within a depth of two times the plate diameter and Abu-Farsakh *et al*. (2004) also reported that the influence depth of the PLT is about two times the diameter of the plate. The following relationships were found by Alshibli *et al*. (2005) between DCP-PR values and PLT initial tangent ($E_{PLT(t)}$) and reloading modulus values ($E_{PLT(r)}$), calculated similarly to the PLT values calculated in GRAFT:

$$E_{PLT(t)} = \frac{7000}{6.1 + PR^{1.5}} \tag{6.6}$$

$$E_{PLT(r)} = 2460PR^{-1.285} \tag{6.7}$$

These correlations have been taken from the laboratory tests on all soils and are not solely concentrated on clay as in GRAFT. Direct relationships comparing the DCP-PR with the subgrade resilient modulus include:

$$M_{r(FWD)} = 338(PR)^{-0.39} \quad \text{(for 10mm/blow < PR < 60mm/blow)} \tag{6.8}$$

based on the results of regression analysis conducted by Chen *et al*. (1995) between the FWD back-calculated resilient modulus ($M_{r(FWD)}$ in MPa) and the DCP-PR.

The American Association of State Highway and Transportation Officials (AASHTO) estimate that for clay soils the FWD back-calculated resilient modulus is approximately two to three times higher than the laboratory determined modulus (Ping *et al*., 2002). In contrast, however, Chen and Bilyeu (1999) found that subgrade laboratory triaxial resilient modulus values were two times higher than FWD-determined modulus. In reviewing research undertaken on the correlation between back-calculated M_r and laboratory measured M_r Livneh (2007) reported that ratios ranging from 0.2 to 1.2 had been documented, and that no unique relationship existed, just as no unique relationship existed between back-calculated M_r and CBR. Furthermore, Livneh (2007) reported

that similar scattered results were found when comparing the M_r calculated from FWD tests undertaken directly on the subgrade surface to laboratory measured M_r. In general it was found that direct FWD testing on the subgrade results in lower values of M_r than those obtained from the back-calculated M_r values found from FWD tests on the pavement surface. Moreover, Williams and Nazarian (2007) reported that research results from 700 pavement sections could not find a reasonable relationship between the FWD and laboratory measured M_r. They reported that the difficulties stem from uncertainties in the back-calculation methods and inherent problems with resilient modulus testing standards.

The relationships between the subgrade modulus obtained from the PLT's in GRAFT ($E_{PLT(t)}$ and $E_{PLT(r)}$) and the average DCP-PR (mm/blow) from the entire subgrade depth are presented in Figures 6.4 & 6.5. The following correlations were found:

$$E_{PLT(t)} = 229PR^{-0.369} \qquad (R^2=0.89) \tag{6.9}$$

$$E_{PLT(r)} = 839PR^{-0.6355} \qquad (R^2=0.83) \tag{6.10}$$

Comparisons between the correlations found in GRAFT and various other researchers are also shown in these Figures. It can be seen that most correlations match well with the results found in GRAFT, although the only direct comparison between PLT correlations (Alshibli *et al*., 2005 correlations) do not match very well. This may be due to the Alshibli *et al*. (2005) correlation corresponding to only the top 305mm depth, while here the full 750mm subgrade depth has been used. If the top 305mm depth was taken for the PR then the Alshibli *et al*. (2005) correlations would be closer to the other correlations due to the clay subgrade being stiffer at the surface; as shown in Figure 6.3. Note that for silty/clay road subgrade types the Minnesota Department of Transport recommends a limiting PR value of 25 mm/blow (Abu-Farsakh *et al*., 2004). Using the DCP-PR GRAFT correlations presented in equations 6.9 and 6.10, this corresponds to a $E_{PLT(t)}$ limiting value of 71MPa and a $E_{PLT(r)}$ limiting value of 109MPa.

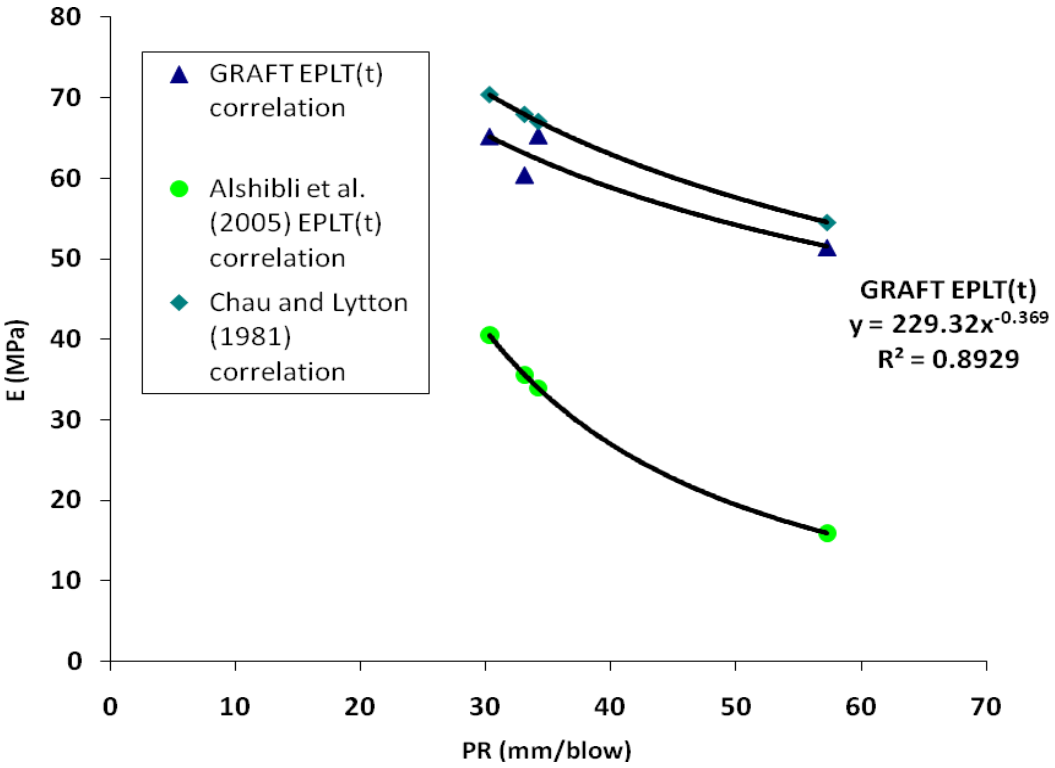

6.4. Correlation between DCP-PR and Young's modulus ($E_{PLT(t)}$)

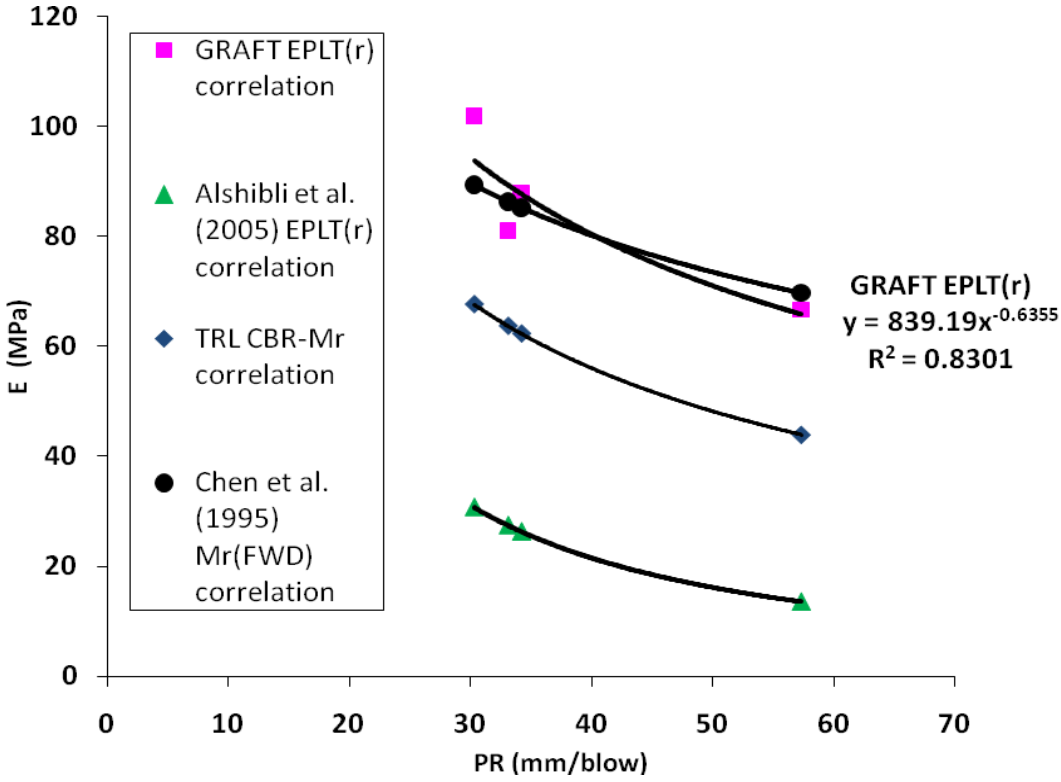

Figure 6.5. Correlation between DCP-PR and Young's modulus ($E_{PLT(r)}$)

Other correlations not plotted in Figures 6.4 & 6.5 include the Pen (1990) correlation presented by equation 6.5, which gives a reasonably good match to the GRAFT data, and several other local correlations discussed by Abu-Farsakh *et al*. (2004), Mohammadi *et al*. (2008) and Livneh (2007). These additional correlations have not been included in this thesis as they give wide ranging values. This may be due to different standards being used to undertake the different tests and due to the influence of different soil properties. Livneh (2007) noted that although some good correlations have been obtained in various cases, all the investigations have found that the results are material dependant. Moreover, based on field and laboratory test results Mohammad *et al*. (2007) found that DCP test results are influenced by the moisture content, dry unit weight and soil type.

Livneh (2007) further stated that the developed equations should only be used with a full understanding of the material properties of both the soil being tested, and of the soils on which the correlative expressions were developed. From the literature it is clear that the results are also test specific with different correlations for DCP-PR with PLT's, direct FWD tests on the subgrade, back calculated FWD tests on the pavement, indirect CBR determined M_r, and triaxial determined M_r. This is obviously a major issue in using such in-situ devices for obtaining track design parameters. For example, assuming the DCP-PR for a particular track subgrade was found to be 40mm/blow, using the GRAFT DCP correlation presented in equation 6.9 gives a tangent modulus of 59MPa, whereas using Alshibli *et al*. (2005) correlation given in equation 6.6 gives a tangent modulus of 27MPa. Using these values for track settlement estimation using the GRAFT subgrade modulus settlement equations 4.5, 4.6 and 4.7, assuming the same track properties as given in the example shown in section 4.2.3, gives track settlement values of 27mm for the GRAFT DCP correlation and 45mm for the Alshibli *et al*. (2005) correlation (after 10MGT). Some other correlations that have not been presented in this thesis give even larger variations. Therefore, much further investigation is required on the reasons behind these large variations and what can be done to reduce them.

6.3 Light Falling Weight Deflectometer (LFWD)

The LFWD is a portable and easy to handle version of the FWD that was developed as an alternative in-situ testing device to the PLT for foundation and formation testing (Abu-Farsakh *et al*., 2004). Generally, the LFWD consists of a loading device that produces a defined load pulse, a loading plate, and one geophone sensor to measure the centre surface deflection. Abu-Farsakh *et al*. (2004) reported that three main types of LFWD had been used in previous research; the German Dynamic Plate (GDP), the TRL Foundation Tester (TFT), and the Prima 100 LFWD. All three have similar mechanics of operation although some differences in design leads to variations in measured results. Fleming *et al*. (2000) stated that some of the differences may be attributed to different loading pulse shapes, or the function of the measurement transducers, or the way in which the measurements are converted into displacement. The Prima 100 LFWD (Figure 6.5) has been used in this research and within this thesis will simply be referred to as the LFWD. This equipment is also used on UK railway tracks to measure track stiffness.

The LFWD consists of a 10kg falling mass that drops on the loading plate via four rubber buffers to produce a load pulse of 15-20 milliseconds. It has a load range of 1-15kN and it can measure both force and deflection through a load cell and seismic sensor that are connected to a portable computer. The diameter of the loading plate is 300mm. Laboratory parametric studies by Abu-Farsakh *et al*. (2004) found that the influence depth of the LFWD ranged between 267 and 280mm (roughly one plate diameter), depending on the stiffness of the tested material. Mooney and Miller (2009), however, found that influence depths ranging from 1 to 2 plate diameters had been reported in the literature. Figure 6.6 shows an LFWD test in GRAFT. While testing, the centre deflection of the loading plate is measured after the application of the falling weight and the LFWD elastic modulus (E_{LFWD}) is then estimated and shown directly through a hand-held computer. Six measurements were taken for each LFWD test in GRAFT with the mass falling from different heights. The device software integrates the geophone signal to determine the maximum deflection value. The expression used to calculate the E_{LFWD} is as follows:

$$E_{LFWD} = \frac{A(1-\nu^2)\sigma R}{\delta_c} \tag{6.11}$$

where A is the plate rigidity factor (A = 2 for a flexible plate and $\pi/2$ for a rigid plate); ν is Poison's ratio; σ is the applied stress; R is the radius of the plate; and δ_c is the centre deflection of the plate. The results from the LFWD testing in GRAFT are shown in Table 6.3 and it can be seen that the values vary from different GRAFT tests and from different test locations within GRAFT. Generally the E_{LFWD} in the middle of GRAFT is greater than that at the sides, although large variations can be seen in some tests.

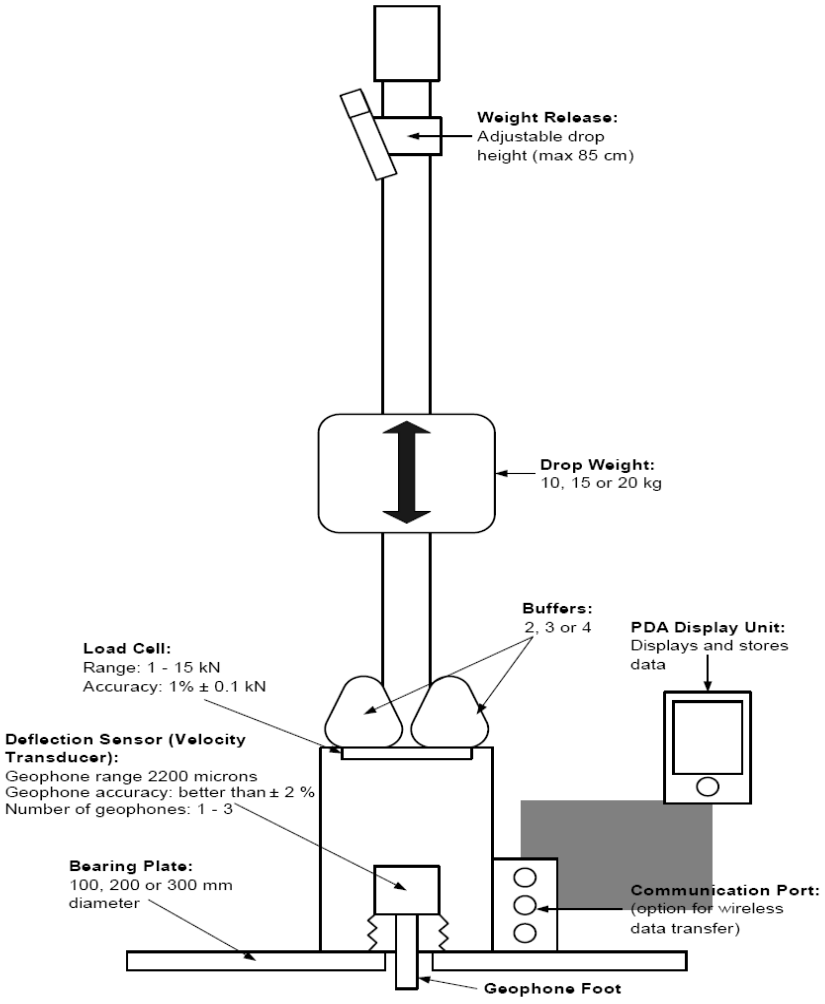

Figure 6.5. Light Falling Weight Deflectometer (Fleming *et al*., 2007)

Comparing the results of LFWD and PLT laboratory tests undertaken in the Louisiana Transportation Research Centre Alshibli *et al*. (2005) found that the following relationships between E_{LFWD} and PLT initial tangent ($E_{PLT(t)}$) and reloading modulus values ($E_{PLT(r)}$):

$$E_{PLT(t)} = 0.907E_{LFWD} - 1.812 \tag{6.12}$$

$$E_{PLT(r)} = 25.25e^{0.006E_{LFWD}} \tag{6.13}$$

Alshibli *et al*. (2005) noted however that although good statistical correlations were found between E_{LFWD} and the moduli obtained from the PLT, the LFWD showed a wide scatter and poor repeatability of measurements, especially when testing weak subgrade layers. In addition, Fleming *et al*. (2007) reported that the range of Coefficient of Variance (C_v) was 25-60% for LFWD measurements in fine grained subgrade soils.

Figure 6.6. LFWD test in GRAFT

GRAFT test and layer	E_{LFWD} at one side of GRAFT (MPa)	E_{LFWD} in centre of GRAFT (MPa)	E_{LFWD} at opposite side of GRAFT (MPa)
CT3 subgrade	142	108	-
CT3 formation	65	123	44
CT4 formation	54	108	46
Geocell subgrade	90	201	98
After CT5 formation	176	418	107
After CT5 subgrade	-	82	207

Table 6.3. LFWD results from GRAFT testing

Comparing LFWD field tests to PLT results and FWD back calculated modulus results Abu-Farsakh *et al*. (2004) found three alternative correlations:

$$E_{PLT(t)} = 22 + 0.7E_{LFWD} \tag{6.14}$$

$$E_{PLT(r)} = 20.9 + 0.69E_{LFWD} \tag{6.15}$$

$$M_{r(FWD)} = 0.97E_{LFWD} \tag{6.16}$$

Undertaking site and laboratory trials using the LFWD Fleming *et al*. (2007) concluded that such device correlations noted above were likely to be site, material and device specific, similar to what Livneh (2007) found for the DCP aforementioned correlations. Fleming *et al*. (2007) undertook a laboratory study to investigate the influence of several LFWD variables on the stiffness measurement and observed that the plate surface contact can have a major effect of the reported stiffness. For example, the same site was reported to have a stiffness of 75MPa for an area with poor surface contact while a reading of 145MPa was given for an area with good surface contact. Fleming *et*

al. (2007) noted that further research should be undertaken to examine the data signal generated at the time of test, and possibly the development of a routine within the software to identify poor quality impact data. It was also noted by Fleming *et al*. (2007) that for weaker materials the contact between the geophone and the material surface was seen to raise concerns over punching failure under the foot. To alleviate this problem, it was recommended that the spring stiffness could be reduced or a larger foot could be used.

The relationships found in GRAFT between the subgrade modulus obtained from the PLT's ($E_{PLT(t)}$ and $E_{PLT(r)}$) and the LFWD are presented in Figure 6.7 & 6.8. It can be seen that from the GRAFT data no correlations were found as the data was scattered and did not show consistency. Comparisons with correlations found by other researchers are also shown in these Figures. The reason for the scattered data may be due to the plate-surface contact in GRAFT. Each LFWD test in GRAFT appeared to be in reasonable contact with the subgrade surface and bedding in loads were applied to try and provide good contact, however, as the subgrade surface in GRAFT was not perfectly flat some errors may have occurred. Fleming *et al*. (2007) stated that this is an area that can cause problems when using the LFWD on site as the judgement of poor contact is subjective, and on-site assessment of impact quality is difficult. Therefore, the acceptance or rejection of individual test data based on the user perception of impact quality could be contractually difficult. High scatter with the LFWD in the laboratory was also found by Alshibli *et al*. (2005) who concluded that further research using the LFWD is required before it can be recommended for use in quality control procedures. Several variables require further research including the influence of the soil properties on the LFWD and the LFWD specific device variables; plate-surface contact, rate of loading, diameter of plate used, drop height, drop weight, contact between geophone foot and material surface. Research by Kavussi *et al*. (2010) found that the LFWD moduli increases with increasing drop weight, but did not change with drop height. They also found that the moduli determined using a 100mm plate was 1.85 times greater than that of a 300mm plate.

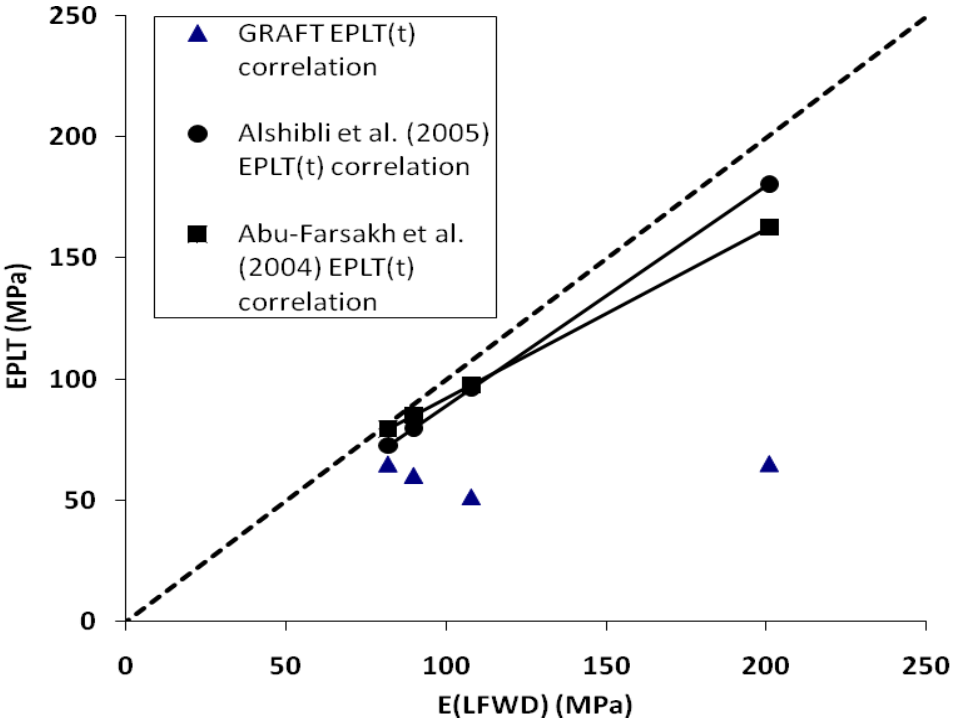

Figure 6.7. Correlation between LFWD and Young's modulus found from PLT ($E_{PLT(t)}$)

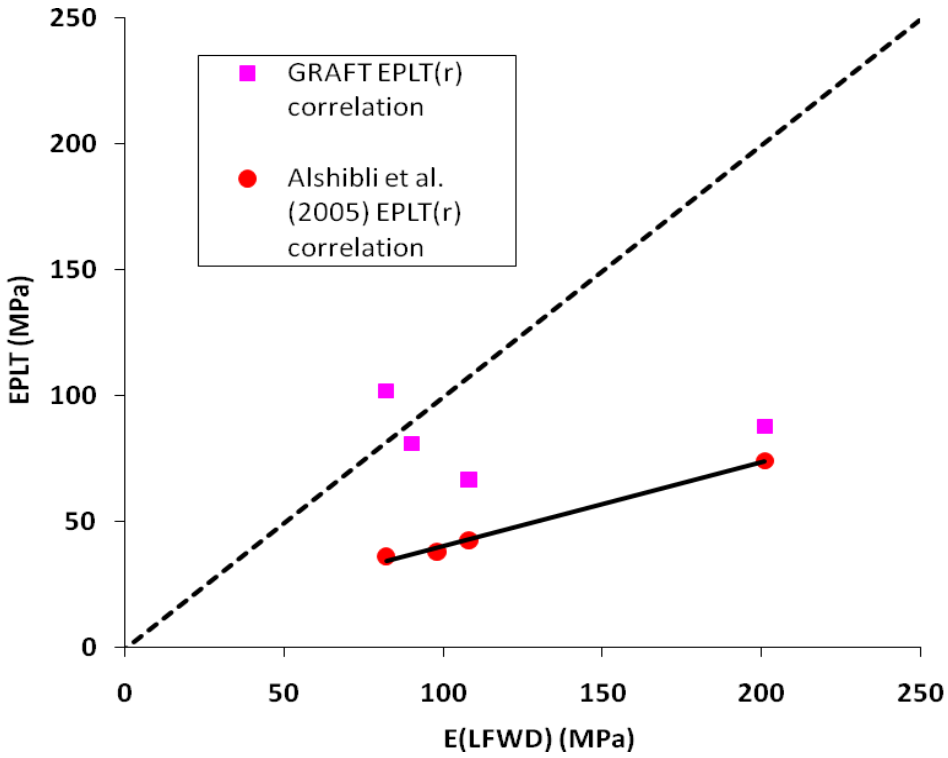

Figure 6.8. Correlation between LFWD and Young's modulus found from PLT ($E_{PLT(r)}$)

The advantages of using portable and economical in-situ devices in the railway industry to measure subgrade stiffness, such as the LFWD and the DCP investigated within this thesis are potentially wide ranging and these devices merit research. From the laboratory research in GRAFT the DCP showed consistent results and good correlations were found between the DCP-PR and the PLT initial tangent modulus (R^2=0.90) and reloading modulus (R^2=0.83). However, a wide range of different correlations was found in the literature with reference to PLT and FWD devices, and laboratory measured M_r and indirect CBR determined M_r. This is thought to be due to different soil conditions and the use of different test standards as well as the inherent variability and error associated with each individual test. Selig and Waters (1994) explained that the variability of the measured soil property is a combination of both soil and test variability. For example, the Coefficient of Variance (C_v) of the CBR test has a recommended value of 25% (Mohammadi *et al*., 2008) and the C_v of laboratory M_r testing has a recommended value of 15% (Williams and Nazarian, 2007). Mohammadi *et al*. (2008) calculated the C_v of the DCP for a laboratory study and found that it varied between 0 and 28.3%. They concluded that the results of the DCP could be considered repeatable compared with the recommended C_v values of other soil engineering tests (CBR, SPT, unconfined compression etc.).

The LFWD did not show consistency when used in GRAFT and it is thought that much further research on the device as well as on the influence of the tested soil properties is required. The reported range of C_v is 25-60% for LFWD measurements in fine grained subgrade soils (Fleming *et al*., 2007). Fleming *et al*. (2007) mentioned that the focus in the UK so far has been on demonstrating the usefulness and reliability of the LFWD through field trials and little work has been done on the assessment of the influence of the test device variables on the measurements. It appears that this is an area where further research is required before the LFWD can confidently be taken forward in the railway industry.

Overall, it appears at present that the existing correlations between the DCP and LFWD in-situ testing devices are influenced by the soil properties and by what the devices are

referenced to. It is to be expected that different devices will give slightly different results due to different stresses, rates of loading, boundary conditions, influence zones etc. applied to the soil and this is likely to be the reason why different correlations were found for the same devices on different soils. This means that correlations for different devices need to incorporate soil properties while eliminating device specific variables by following a unified test to a unified standard with a specific device. Prior to this stage much further research is required on each in-situ device used in each correlation to investigate the influence of different variables, e.g. plate-surface contact in LFWD. A research review should also be undertaken to determine exactly why the published correlations between the same devices vary so much, be it soil, device or test procedure related. It may be found that certain devices are not reliable enough to be used for subgrade modulus determination. Until that point however, it is recommended that the DCP only be used as an indicative measure of subgrade stiffness and a site specific correlation should be made instead of using existing correlations. If the LFWD is used the results should be interpreted with caution and with the Coefficient of Variance quoted.

6.4 Pocket and Proving Ring Penetrometers

The pocket penetrometer is a simple and compact spring loaded device that is used to give an approximate value of the unconfined compression strength of soils. The penetrometer reading is taken by pushing the foot of the penetrometer by hand into the soil to a depth of 6.35mm (indicated by a grove on the penetrometer). A pocket penetrometer measurement in GRAFT is shown in Figure 6.9. The maximum reading shown on the penetrometer scale is taken as the unconfined compression strength of the soil. The effective spring compression is correlated to the unconfined compression strength determined through other methods. As a precautionary note the manufacturers of pocket penetrometers state that due to the small testing area of the pocket penetrometer it cannot replace laboratory testing of unconfined samples (ELE International, 2009).

The proving ring penetrometer is a cone type penetrometer which can serve as a rapid means of determining the penetration resistance of soil at shallow depths. It consists of a T handle, 457mm penetration rod, 1kN proving ring with dial indicator, removable 30 degree cone and an attachable extension rod. The penetrometer reading is taken by pushing the cone point into the soil at a uniform rate until the top of the cone goes just below the surface (Figure 6.10), at which point the dial indicator reading is recorded. The penetration resistance is obtained by dividing the penetration load by the cone base area (645.16mm^2).

The correlations found in GRAFT between the unconfined compression test results and the pocket penetrometer and proving ring penetrometer are shown in Figure 6.11 and Figure 6.12 respectively. The average values have been taken from all the measurements taken across each layer for each GRAFT test. From Figure 6.11 it can be seen that the pocket penetrometer measurements in GRAFT showed a high degree of scatter and for the majority of the readings the pocket penetrometer unconfined compression strength readings were approximately 1.5 to 3.5 times greater than the unconfined compression strength tests. The scale of the pocket penetrometer actually reached its maximum value on many occasions, as shown in Figure 6.11. The measurements do show however, that at lower strength values (100kPa) the pocket penetrometer matched well with the unconfined compression strength test, albeit only two measurements were taken at these levels. These measurements were recorded on the formation directly after parts 1 and 2 of the sand blanket replacement geocomposite test where GRAFT was flooded and the formation was assumed fully saturated. Therefore, from the measurements in GRAFT it appears that the pocket penetrometer may be more accurate on softer saturated soils rather than stiffer unsaturated soils where the limit of the pocket penetrometer may be reached (i.e. the PP spring stiffness correlation with soil strength may only be accurate at lower values of strength). Nonetheless, the PP is a useful indicative device to use on site that can give an additional quick measurement of soil strength, although as recommended by the manufacturer it should not be used in place of traditional laboratory testing.

Figure 6.9. Pocket penetrometer measurement in GRAFT

Figure 6.10. Proving ring penetrometer measurement in GRAFT

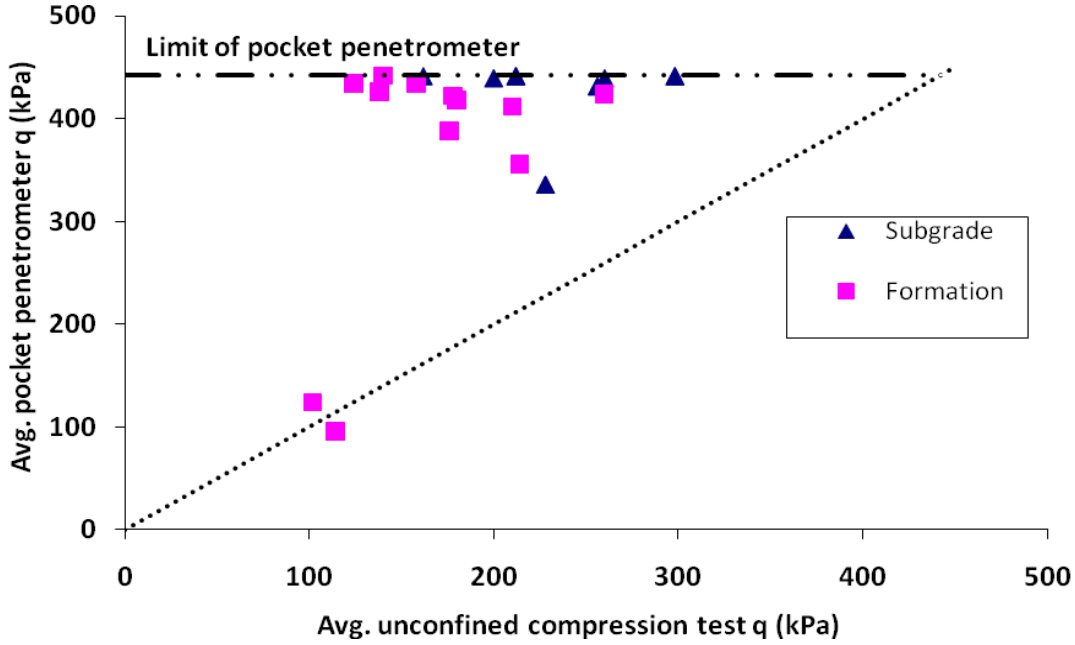

Figure 6.11. Correlation between unconfined compression strength found from pocket penetrometer and from unconfined compression test

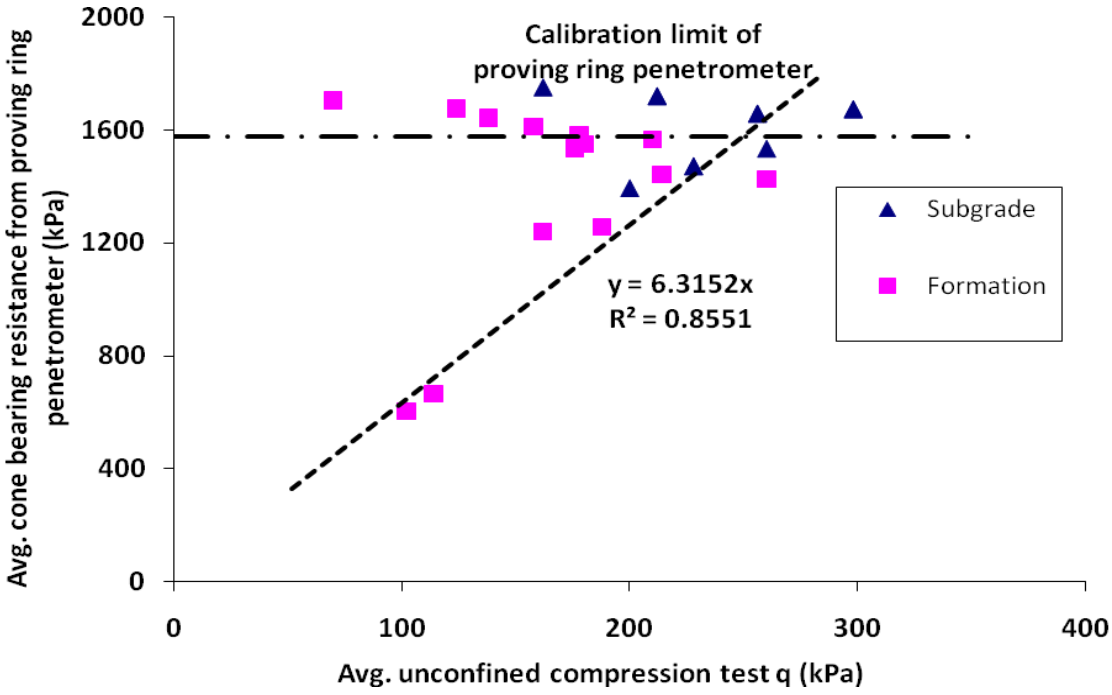

Figure 6.12. Correlation found between cone bearing resistance from proving ring penetrometer and unconfined compression strength from unconfined compression test

Figure 6.12 shows that a similar high scatter of results were found with the proving ring penetrometer and the calibration limit on the proving ring was also reached several times throughout testing. Ignoring the readings that exceed the calibration limit however, a linear trend line can be plotted through the remaining data points. Regression analysis produces the following equation from the trend line:

$$q_c = 6.3q \qquad (R^2 = 0.85) \tag{6.17}$$

where q_c is the cone bearing resistance (kPa) and q is the unconfined compression strength (kPa). This relationship is similar to the relationship between undrained shear strength (C_u) and the cone tip resistance suggested by Bowles (1992) and De Ruiter and Beringen (1979):

$$C_u(tip) = \frac{q_c(tip)}{N_k} \tag{6.18}$$

where N_k is a cone factor ranging from 10 to 30, with values between 15 and 20 commonly used. Bowles (1992) suggested an approximate correlation between the Plasticity Index and N_k that can be used; for a plasticity index of 23 as found for the Kaolin clay in GRAFT, N_k is between 13.5 and 17.5. The lower bound value is close to what was found in GRAFT if it is assumed that the clay is fully saturated (12.6 if one uses $C_u = q/2$). Therefore, within the limits of the calibrated proving ring the proving ring penetrometer may give an accurate indication of the cone bearing resistance of clay and with correlations, such as the one suggested by Bowles (1992), a reasonable indication of the strength of the soil may be given.

6.5 Conclusion

Currently in the UK the level of subgrade investigation is poor considering the importance of the subgrade in determining the overall performance of the track. It is

thought that if easy to use, inexpensive and quick measuring devices could be used to investigate the subgrade parameters then subgrade investigation could be incorporated into a strategy for monitoring track performance, and planning maintenance and remedial action. This chapter has investigated the accuracy of the DCP, LFWD, PP and PRP devices in measuring subgrade stiffness and strength in order to investigate whether they could be used as part of this strategy. Out of the devices considered only the Pocket Penetrometer is mentioned within Network Rail standard NR/SP/TRK/9039 ('indicative shear strength measuring tool for fine-grained subgrade soils').

The results of this chapter have shown that when measuring subgrade stiffness the DCP is more consistent when compared to the LFWD, which gave scattered data. A good correlation was found between the DCP penetration rate and the PLT modulus in GRAFT (R^2=0.89 for initial tangent modulus and R^2=0.83 for reloading modulus). These correlations were consistent with some other correlations found by various researchers. Abu-Farsakh *et al*. (2004) found similar results and noted that compared with the LFWD, the DCP has a longer history and is more credible. This is consistent with the Coefficient of Variability (C_v) values recorded for the DCP and LFWD by different researchers; Mohammadi *et al*. (2008) found the C_v for the DCP ranged between 0 and 28.3% while Fleming *et al*. (2007) reported a C_v range of 25-60% for the LFWD in fine grained subgrade soils.

In the literature however, a wide range of correlations was found for the DCP with reference to PLT, FWD, triaxial, and CBR tests. Due to different applied stresses, rates of loading, boundary conditions, influence zones etc. it is expected that different devices will give different results, although varying correlations have been found for the same devices. This is thought to be due to a combination of soil conditions, test procedures, and inherent soil testing variability. It is recommended therefore that future correlations need to incorporate soil properties while eliminating device specific variables by following a unified standard for each specific device. Selig and Waters (1994) noted that although nothing can be done to eliminate soil variability apart from recording separate soil strata, test variability can be reduced by using standardised equipment and procedures. A review of published research is also recommended in order to determine

exactly why the existing correlations between the same devices vary so much. From the results found in GRAFT it is believed that this recommended further research is merited on the DCP to get to a stage where it could be incorporated into a subgrade investigation strategy. This is similar to the findings of Brough *et al*. (2003) who conducted a study on 21 different in-situ test devices traditionally used in the highways industry and found that the DCP was one of the devices deemed suitable for assessing the subgrade strength and stiffness properties in the railway environment.

The other devices found to be suitable included CSWS, CPT and FWD devices, depending on length and purpose of track possession. It was not possible to test these other devices in GRAFT, however as found in this Chapter and in Chapter 4, the typical wide scatter of results with the FWD is a cause for concern. It is thought that if tested in GRAFT the FWD data would be similar to that found with the LWFD (a wide range of scatter). It is also thought that the CPT would give reliable data if tested in GRAFT as much experience of using the CPT and interpreting the data has been built up over the years. The CPT is widely used in the geotechnical community to provide detailed information on soil type and stratigraphy, allowing on-site assessment of various engineering parameters. Brough *et al*. (2003) stated that a CPT test can be undertaken in about the same time as it takes to excavate and log a traditional trial pit in a railway crib.

The PP and PRP devices used for subgrade strength measurements in GRAFT have shown that the PP may be more accurate on softer saturated soils rather than stiffer unsaturated soils where the limit of the Pocket Penetrometer may be reached. It is not recommended to use the PP for anything else other than quick indicative measures of cohesive formation or subgrade strength, for which it is currently used in NR/SP/TRK/9039. Similarly, the PRP measurements indicate that within the limit of the calibrated proving ring the PRP may give an accurate indication of the cone bearing resistance of cohesive soils, which can be equated to shear strength based on soil parameters such as Plasticity Index. The PRP however is also only recommended to give a quick indicative measure of cohesive formation or subgrade strength and should not be used to replace laboratory strength testing.

In order to get to a stage where a strategy for monitoring track performance and planning maintenance and remedial action could be implemented the accuracy of site data is essential, as shown in the developed subgrade modulus unreinforced and reinforced track settlement models developed in Chapters 4 and 5. For example, using the design chart shown in Figure 5.29, a modest 15% underestimation in subgrade modulus for an unreinforced track can yield a 25% overestimation in track settlement. This design chart, however, has been developed based on the subgrade modulus measured in a specific way using the PLT, as detailed in Chapter 3, and is thus based on rules and standards. This is of particular importance when comparing the PLT against other in-situ elastic modulus measuring devices (Adam *et al*., 2009). The variables involved in the PLT include the size and shape of the plate, magnitude of force applied, number of load cycles and time of loading (Ping *et al*., 2002).

This research is important and industry relevant as Brough *et al*. (2003) reported that several researchers have begun to approach trackbed investigation with the view that site investigation data should not only be used to diagnose the causes of track failure, but also predict perceived track performance and schedule necessary work proposals. Apart from the FWD currently only the Trackbed Index exists within NR/SP/TRK/9039 as an indicative subgrade monitoring procedure that is undertaken to assess whether the trackbed depth is adequate on sites that have had difficulty in achieving the required track geometry. The Trackbed Index is based on indicative measurements of the subgrade undrained shear strength, which according to NR/SP/TRK/9039 can presumably be found using devices such as the Pocket Penetrometer. From the PP results found in GRAFT for firm unsaturated soil the majority of the measurements made with the PP were 1.5 to 3.5 times greater than the unconfined compression strength tests and hence, if used, the PP may vastly overestimate the Trackbed Index. This could lead to an insufficient ballast depth and subsequent track geometry problems. The next chapter considers more robust track design strategies that could be implemented to estimate track performance based on different track parameters measured using the test devices discussed within this thesis.

Chapter 7 - Application of a 3D Finite Element Railway Model (SART3D)

7.1 Introduction

A three dimensional finite element (FE) computer program termed SART3D (Static Analysis of Railway Track 3D) has been used to validate the results found in GRAFT and the analysis will be presented in this chapter. Several railway track models have been developed in recent decades to study the performance of track under loading and comprehensive reviews of such models can be found in Banimahd (2008), Selig and Waters (1994), and Shahu *et al*. (1999). Selig and Waters (1994) state that such models provide the basis for predicting track performance, and can therefore be used tentatively for track design and maintenance planning. They do however note that accurate analysis is limited by complex track properties that change with traffic, maintenance and environmental conditions.

SART3D is specifically designed to simulate and predict the static behaviour of railway tracks using three dimensional finite elements; the 20-noded isoparametric brick element for example (Woodward *et al*., 2005) is used for the substructure. Each component of the track structure can be modelled in the program, from the superstructure components to the substructure ballast and subgrade layers. The program uses an elastic-perfectly plastic Mohr-Coulomb failure criterion implemented with a visco-plastic algorithm (Woodward *et al*., 2009b). Typically static loading is applied to the track in 60 increments and the stresses and strains are calculated in the x, y and z planes for each gauss point within each element (8 points per element). SART3D can be used for linear elastic or linear elasto-plastic analysis. Elastic analysis can be used to represent track that is in a fully resilient state (i.e. it has had significant cyclic axle loads applied to it and excessive plasticity in the ballast and subgrade is not generated per load cycle). Plastic analysis is generally used to represent track that is not at a resilient state (i.e. full plasticity can be developed in the ballast and subgrade). Details of the constitutive models and relationships used in the SART3D program can be found in

Woodward *et al*. (2005). It should be noted that SART3D does not give the long term plastic settlement with load cycles; other finite element programs have been developed to do this. A typical mesh from SART3D is shown in Figure 7.1 and a typical magnified displaced mesh for an axle load of 250kN is shown in Figure 7.2.

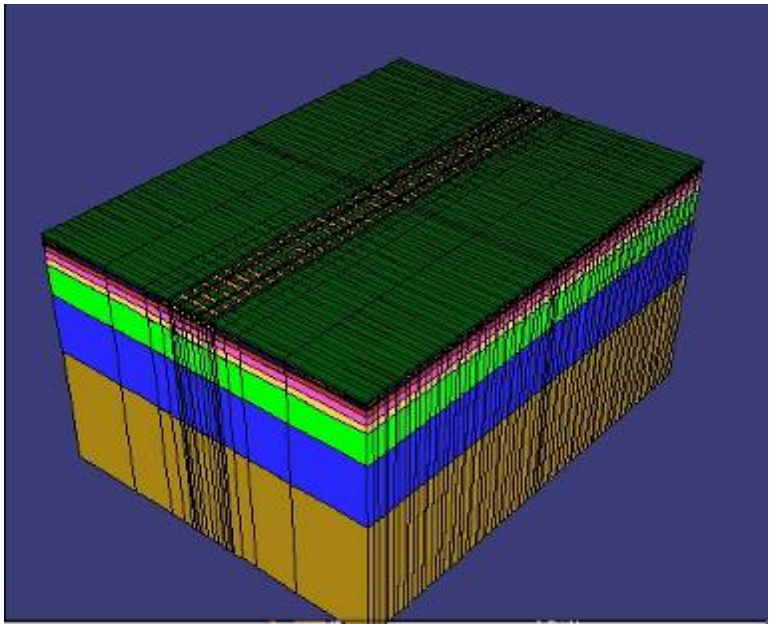

Figure 7.1. Typical SART3D mesh of railway track (Woodward *et al*., 2009b)

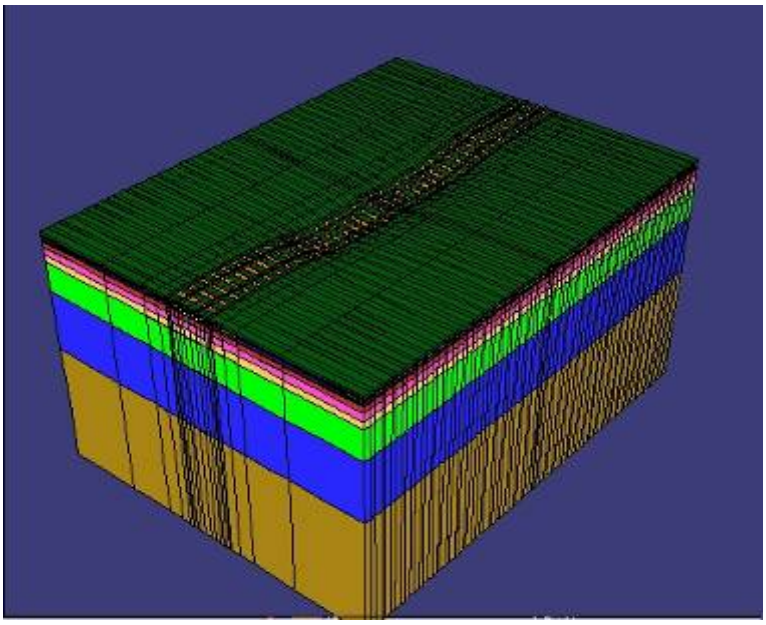

Figure 7.2. Typical SART3D displaced mesh of railway track (displacement at magnification x50) (Woodward *et al*., 2009b)

The recommended approach for using such railway track models is to first calibrate the program to actual track behaviour prior to using the model for predictive purposes (Woodward *et al*., 2005). To calibrate SART3D to GRAFT the mesh was modified for the dimensions in GRAFT and the GRAFT track properties were input into the model. 12 elements were used in the X direction (1.06m internal width of GRAFT), 15 elements in the Y direction (2.96m internal length of GRAFT) and 9 elements in the Z direction (1.15m depth of GRAFT), representing the sleepers, ballast, formation, subgrade and neoprene lining layers. The rail was connected directly to the sleepers with the rail pads ignored, as in GRAFT. The GRAFT mesh is shown in Figure 7.3.

The sleeper, rail and neoprene properties used in the SART3D model are shown in Table 7.1. The sleeper dimensions and spacing's were input directly as they are in GRAFT (245mm x 125mm x 600mm sleepers at 650mm spacing), as were the ballast and subgrade properties and depths, and applied actuator load for each GRAFT test modelled. The formation, subgrade and ballast properties used in the GRAFT SART3D model are shown in Table 7.2. The reloading modulus values were used for the stiffness and the undrained shear strength was assumed to be half the measured unconfined compression strength values. The formation stiffness was assumed equal to the subgrade stiffness and the formation undrained shear strength was assumed constant for all the tests at 93kPa (unconfined compression strength = 186kPa). The ballast dilatancy angle was input as 0° as the load applied in GRAFT was considerasbly less than the load required to induce failure in the ballast. These properties were found to provide a good match between the SART3D results and the GRAFT control tests, which will be presented in the next section. A limited sensitivity analysis was performed, but the above values gave a good representation of the GRAFT response for the actual measured properties input.

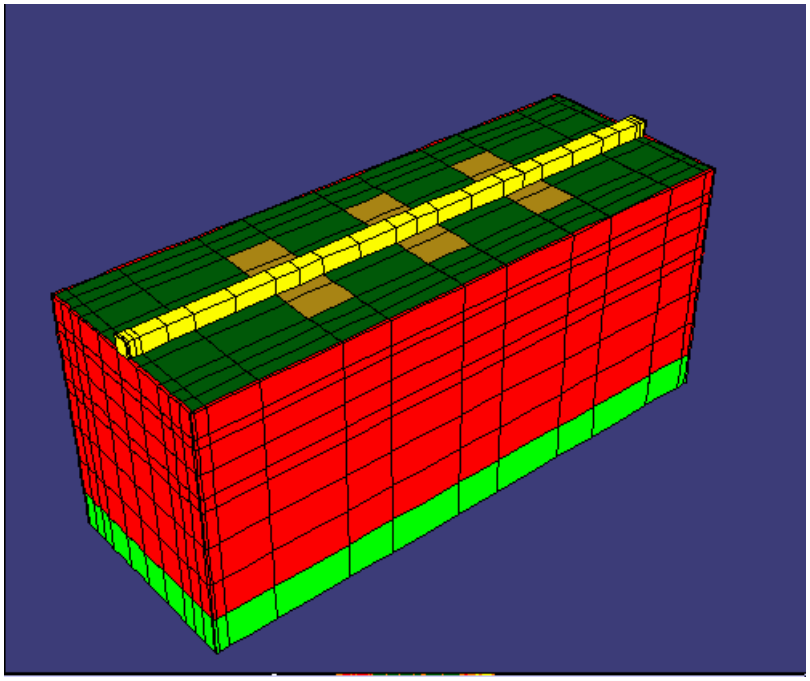

Figure 7.3. GRAFT SART3D mesh

SART3D Input	Rail	Sleeper	Neoprene
E (Young's Modulus, GPa)	200	10	2.500×10^{-4}
Poisson's ratio	0.29	0.25	0.49
Bulk density (kg/m³)	7500	2100	200
Bending stiffness around x (m^4)	2.210×10^{-5}	-	-
Bending stiffness around z (m^4)	7.060×10^{-6}	-	-
Torsional stiffness around y (m^4)	2.920×10^{-5}	-	-
Area (m^2)	4.710×10^{-3}	-	-

Table 7.1. Rail, sleeper and neoprene properties used in GRAFT SART3D model

SART3D Input	Formation	Subgrade	Ballast
Layer depth (mm)	70	750	300
Poisson's ratio	0.49	0.49	0.42
Bulk density (kg/m³)	1800	1800	1600
CT1 Undrained shear strength (kPa)	93	143	-
CT2 Undrained shear strength (kPa)	93	136	-
CT3 Undrained shear strength (kPa)	93	151	-
CT4 Undrained shear strength (kPa)	93	172	-
CT1 E (Young's Modulus, MPa)	47.9	47.9	135
CT2 E (Young's Modulus, MPa)	45.6	45.6	135
CT3 E (Young's Modulus, MPa)	66.7	66.7	135
CT4 E (Young's Modulus, MPa)	91.1	91.1	135
Friction angle (°)	-	-	58
Dilatancy angle (°)	-	-	0

Table 7.2. Subgrade, formation and ballast properties used in GRAFT SART3D model

7.2 Calibration of SART3D to GRAFT

SART3D simulations were run with the GRAFT model for CT1 to CT4 properties to calibrate the SART3D model to GRAFT and validate the results found in GRAFT. The only changes required for each test run were the subgrade strength and stiffness, formation stiffness, and the applied load for CT1 (130kN). The track load-deflection results from the SART3D runs are shown in Figures 7.4 and 7.5 with both the elastic and plastic results illustrated. The non-linear effects of the plastic analyses for all the test runs can be seen with the changing gradients of the curves, representing a reduction in track stiffness with applied load. The track stiffness for each test can be taken directly from Figures 7.4 and 7.5 by dividing the applied load by the rail deflection. For example, for CT4 the track stiffness at peak load is 46.8kN/mm/wheel for the plastic analysis run and 66.4kN/mm/wheel for the elastic analysis run. The mean track stiffness

found in GRAFT over 500,000 applied cycles for CT4 was 50kN/mm/wheel (from Table 4.4). This matches favourably with the plastic analysis value and could indicate that the GRAFT track in CT4 is still undergoing some plasticity and has not reached a full a resilient state yet. This has been shown with the continued track settlement development shown for all control tests in GRAFT up to 500,000 applied cycles (Figure 4.1). It should be noted here that these track stiffness values are for GRAFT only and are not field values (i.e. a correction needs to be applied to convert from the GRAFT deflection to the deflection in the field).

Some single GRAFT cycles from CT4 have been compared directly to the SART3D load-deflection results for the CT4 run in Figure 7.6. It can be seen that as the GRAFT cycles accumulative the track slowly moves from plastic towards elastic for the FE parameters considered. This is not reflected in the mean track stiffness values quoted for the GRAFT tests as the change is not significant over the 500,000 applied cycles. If a much greater number of cycles were applied then it would be appropriate to quote both elastic and plastic track stiffness values. The non-linear increase in track stiffness with applied load that is shown for the GRAFT cycles is not directly modelled in the SART3D program. Also, the rate of loading is not directly accounted for in the SART3D model, which was found to influence the deflection as presented in Chapter 4. The non-linearity witnessed in the GRAFT tests is thought to be due to ballast particle re-arrangement during densification and is similar to what others have found on track and in the laboratory (Hunt, 2005, Hosseingholian *et al*., 2009, Crawford *et al*., 2001). A program that can analyse this phenomenon is ALTICA (Woodward and Molenkamp, 1999).

For a reasonable representation of the non-linear behaviour it is common practise to plot the secant stiffness to the design axle loading (Hunt, 2005). The secant stiffness has been plotted in Figure 7.6 as a best fit for the three GRAFT cycles shown. Using the secant track stiffness definition given in equation 4.18, with point a being taken as the minimum applied load and resulting deflection and point b the maximum, the secant stiffness line gives a stiffness value of around 49kN/mm/wheel for CT4. It is interesting to note here though that if a linear regression line between 30% and 90% of the

difference between the maximum and minimum applied forces is taken for the GRAFT cycles, as used by Hosseingholian *et al*. (2009) to define track stiffness, the track stiffness matches exactly with the SART3D plastic analysis. This is shown in Figure 7.7 for GRAFT cycle 270,000. The secant track stiffness calculated from this regression line equals 46.8kN/mm/wheel.

Similar matches were found between all the GRAFT control tests and SART3D simulations. The track stiffness values from all the GRAFT model SART3D runs are compared against the measured GRAFT mean track stiffness values in Table 7.3. It can be seen that the SART3D values increase as the subgrade stiffness and strength increase, exactly as found in the measured values. The reason that the measured mean track stiffness values for CT1 and CT2 are slightly less than the lower bound (plastic) SART3D values may be because the rail deflections from these tests were taken from the LOS actuator instead of the rail LVDT and may not be as accurate. Overall, the SART3D GRAFT model has been shown to accurately match the load-deflection behaviour found in GRAFT with the estimated ballast properties used (stiffness, strength and Poisson's ratio) and thus the SART3D GRAFT model has therefore been accurately calibrated. In turn, SART3D has proven that GRAFT produces the correct level of track deflection for the applied load and track properties. This means that the SART3D model can be used to accurately simulate the track response in GRAFT for a range of different tests. This allows the effects on track stiffness of changing different parameters to be investigated in a much shorter time than undertaking a full GRAFT test. Therefore, SART3D can act as a preliminary tool to investigate the effect on track stiffness of changing certain parameters before it is decided whether or not a full scale test is required. A short parametric study has been undertaken using SART3D and will be presented later in this chapter.

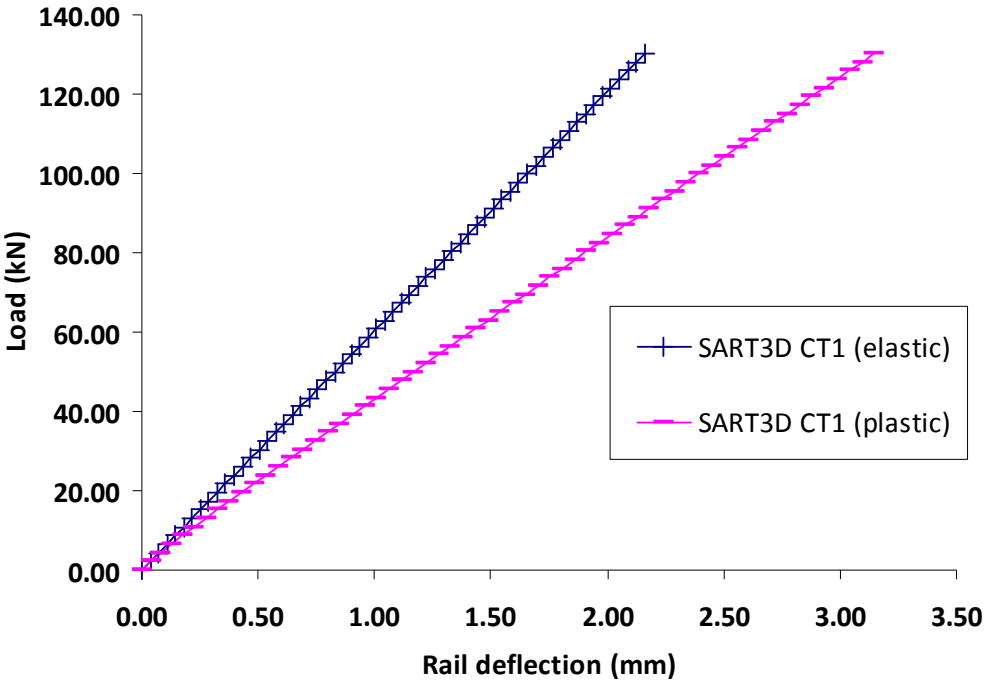

Figure 7.4. SART3D load-deflection results from CT1 run

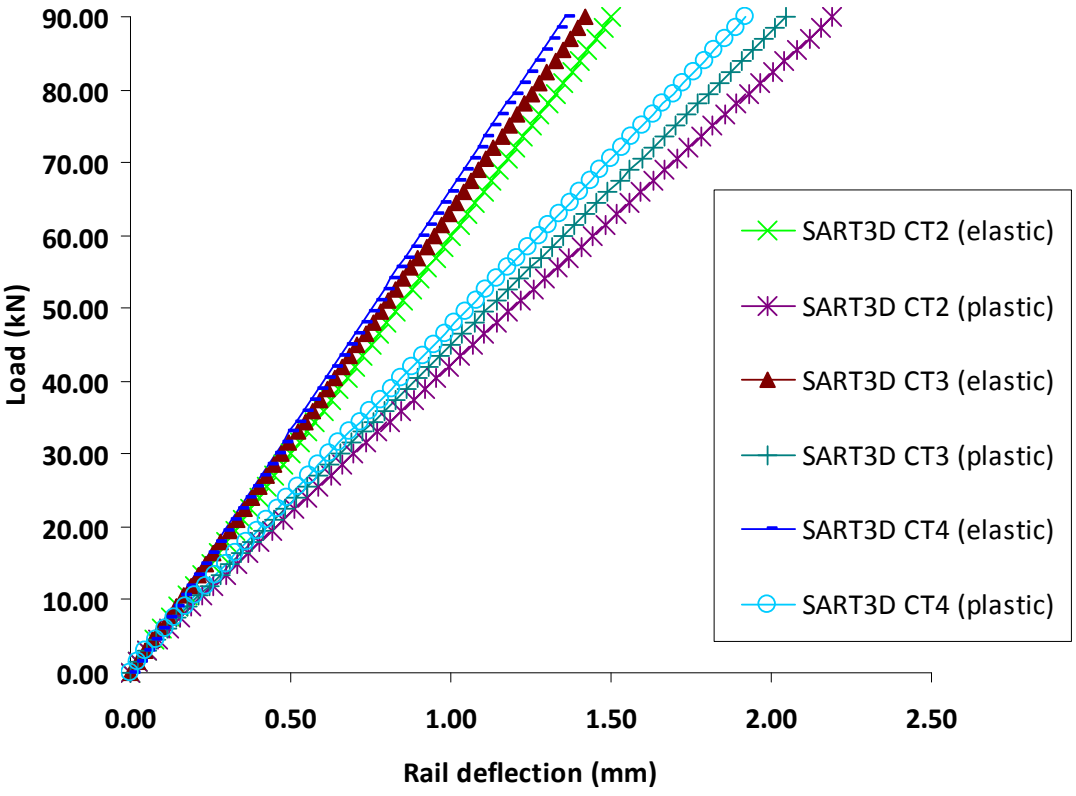

Figure 7.5. SART3D load-deflection results from CT2 to CT4 runs

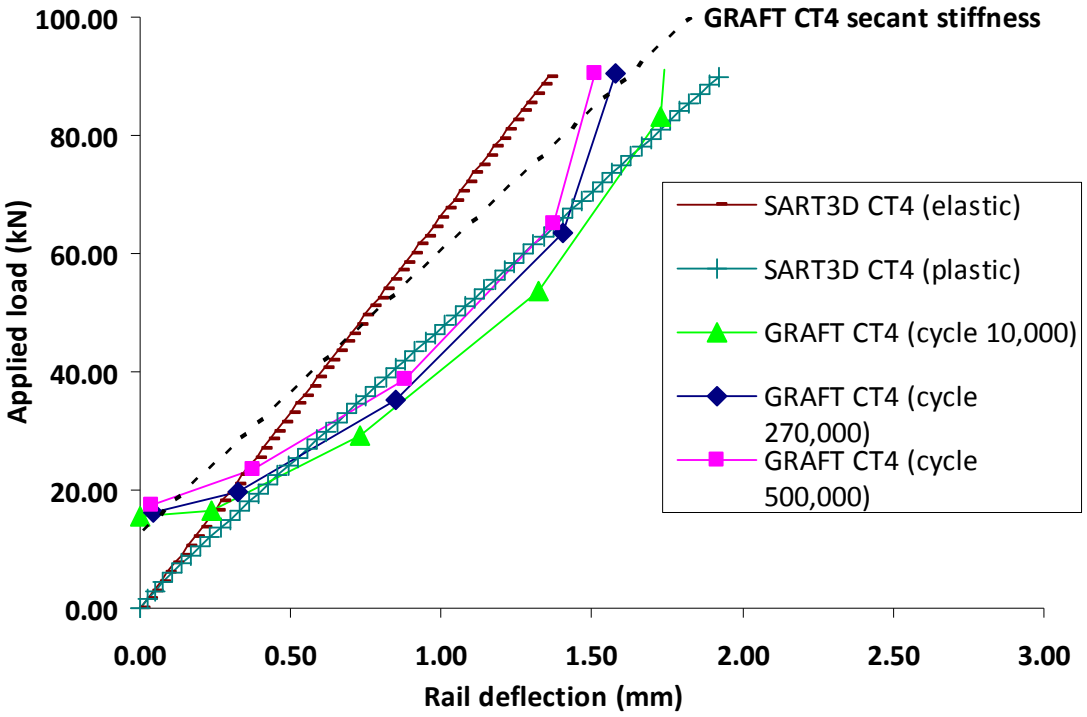

Figure 7.6. Comparison between SART3D and GRAFT load-deflection results for CT4

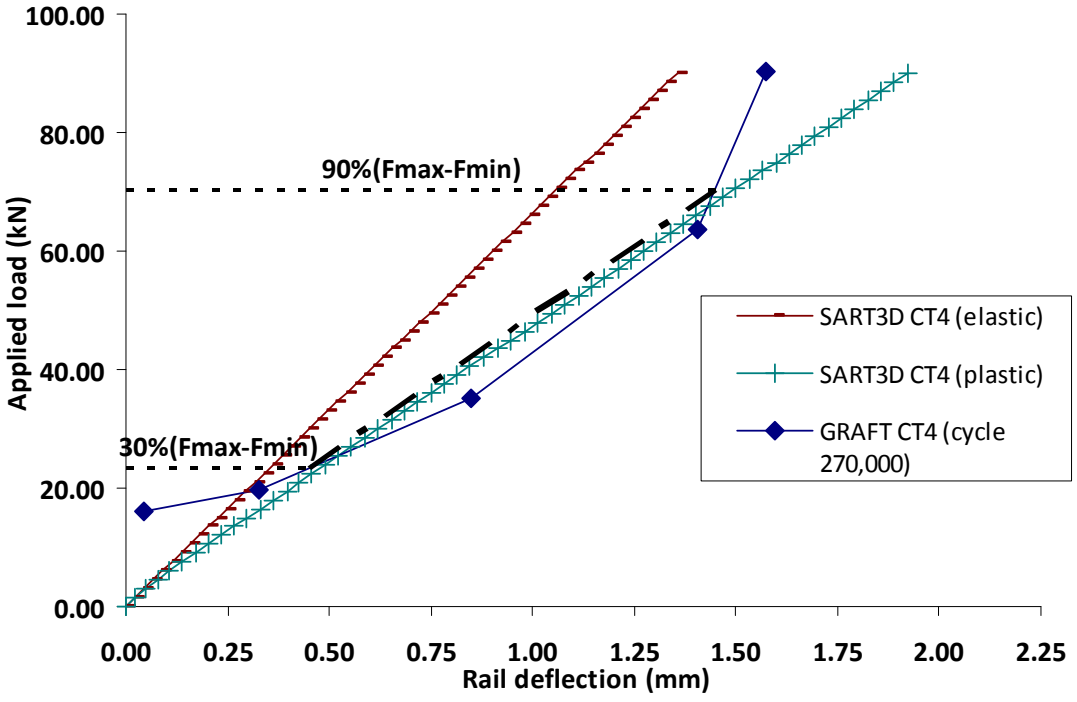

Figure 7.7. Comparison between SART3D and GRAFT load-deflection results for CT4 using linear regression between 90% and 30% of the cyclic load

GRAFT test	SART3D plastic track stiffness (kN/mm/wheel)	SART3D elastic track stiffness (kN/mm/wheel)	GRAFT mean track stiffness (kN/mm/wheel)
CT1	41.1	59.9	36.9
CT2	41.4	60.3	38.2
CT3	43.9	63.4	47.0
CT4	46.8	66.4	50.0

Table 7.3. Comparison between measured and simulated GRAFT track stiffness values

Although long term track settlement cannot be directly estimated from SART3D, using equation 4.24 the track settlement after N number of cycles can be estimated from the track stiffness value. In addition, using equations 4.9 and 4.10 an estimation of track settlement can be given from the subgrade modulus values. These equations have not been calibrated for different track constructions and ballast properties (these are out with the scope of this thesis). However they can be used to provide indicative track settlement values for the field. This strategy can form part of a preliminary empirical-numerical based design method for predicting the future performance of track based on the track properties and the applied load. This strategy will be discussed at the end of this chapter and will be compared against other track design methods.

Prior to this stage it is important to check that the applied load in GRAFT accurately represents the induced stresses in the field for an equivalent axle load. This will be discussed in the next section. As the GRAFT SART3D model has been calibrated the stresses output from the model for specific tests are assumed to be reasonably accurate. The vertical track displacement contours, induced formation deviatoric shear stress contours and the induced formation vertical stress contours at both the formation layer and the top ballast layer for CT2 (plastic analysis) are shown in Figures 7.8 to 7.13. The induced formation deviatoric shear stress ratio (mobilised formation deviatoric shear stress divided by the maximum available formation deviatoric shear stress) directly under the railhead was found to be 0.309 (plastic analysis) at gauss point 1 (lower half of element). This relatively low deviatoric stress ratio illustrates that the stress

concentrations in the formation are not significant to cause high plastic strains. It should be noted here that these values vary between elements and between the gauss points within each element. For convenience, in this thesis, only gauss point 1 has been analysed for the two elements directly below the centre of the middle sleeper at the formation layer (one element directly under railhead and other element is adjacent). This gauss point was found to give a reasonable approximation to the values computed.

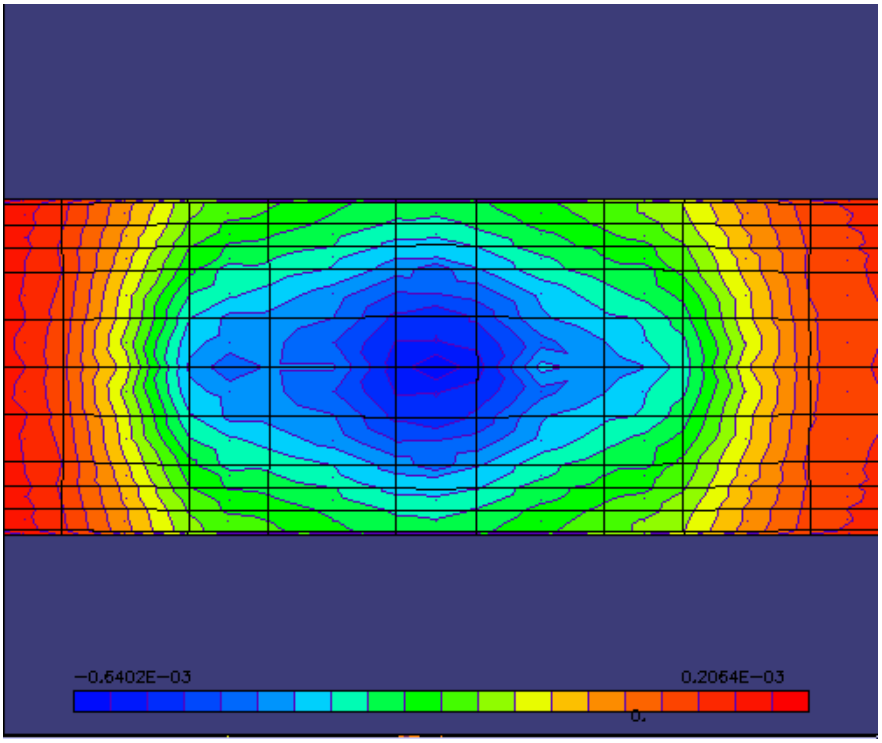

Figure 7.8. Vertical displacement contours at formation level for CT2 plastic analysis (m)

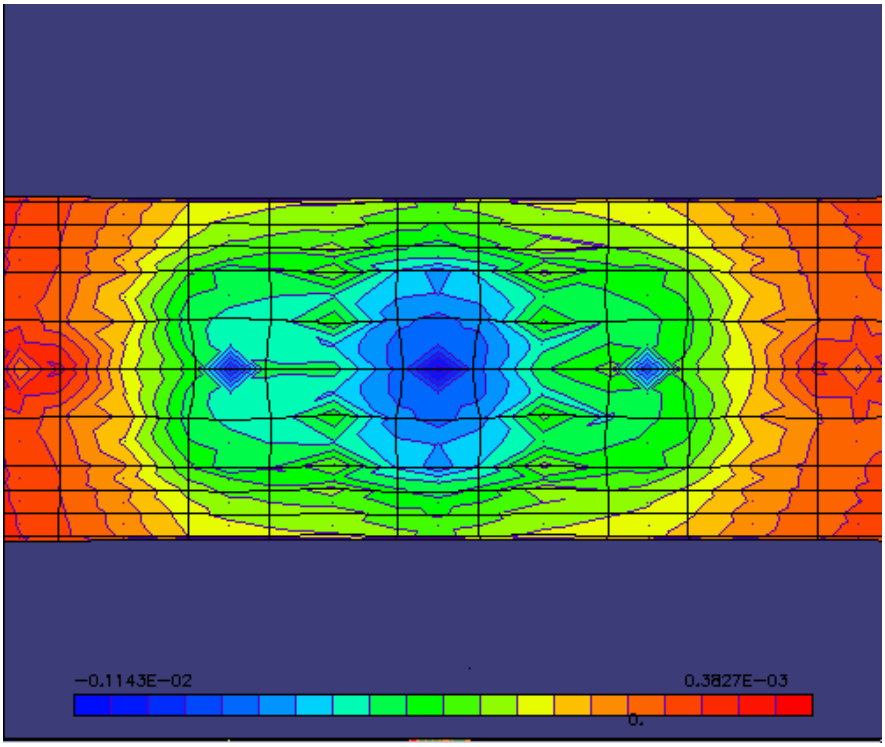

Figure 7.9. Vertical displacement contours at ballast level for CT2 plastic analysis (m)

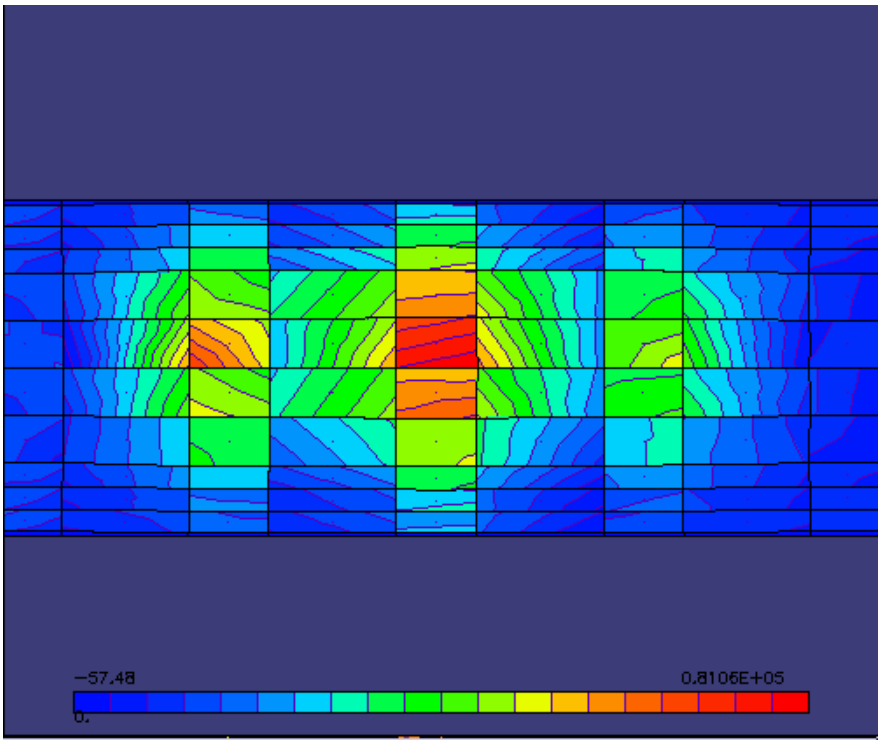

Figure 7.10. Induced deviatoric shear stress at formation level for CT2 plastic analysis (Pa)

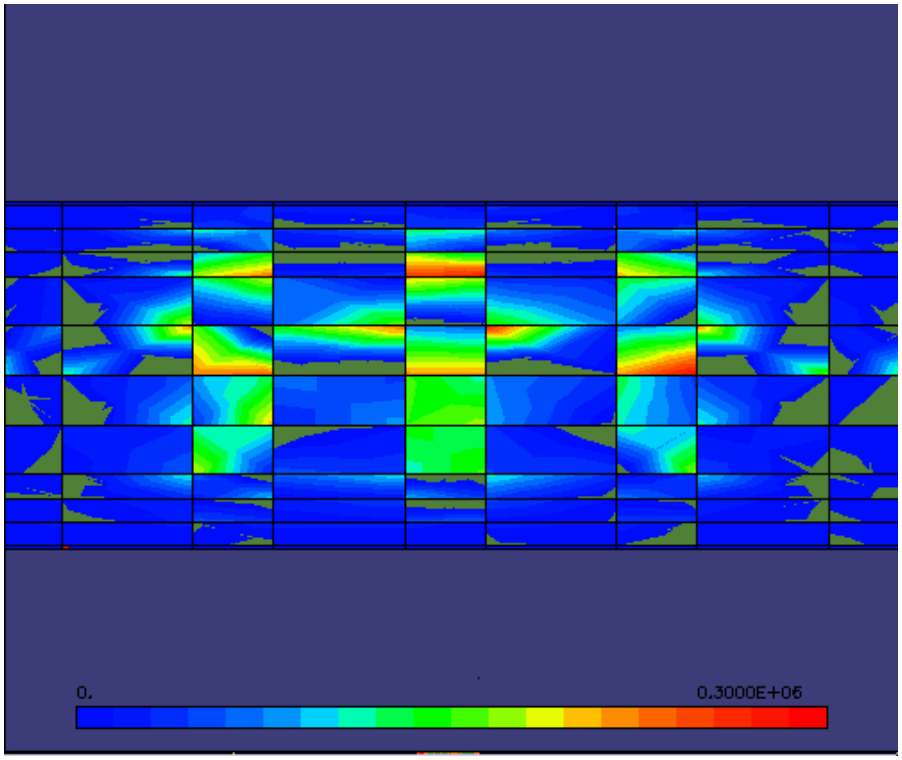

Figure 7.11. Induced deviatoric shear stress at ballast level for CT2 plastic analysis (Pa)

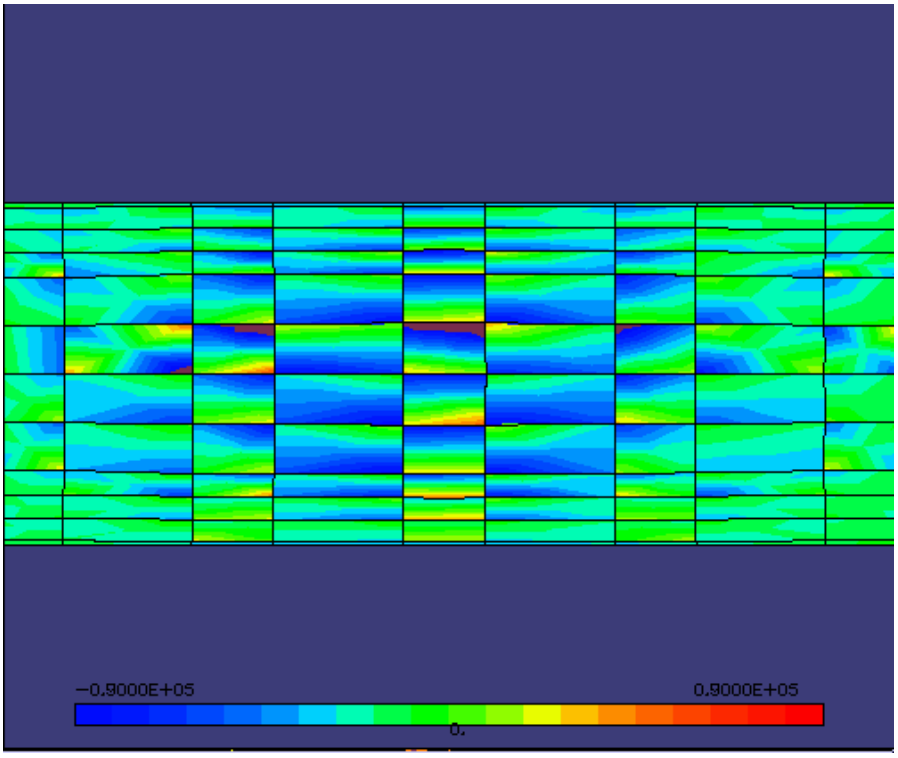

Figure 7.12. Induced vertical stress at formation level for CT2 plastic analysis (Pa)

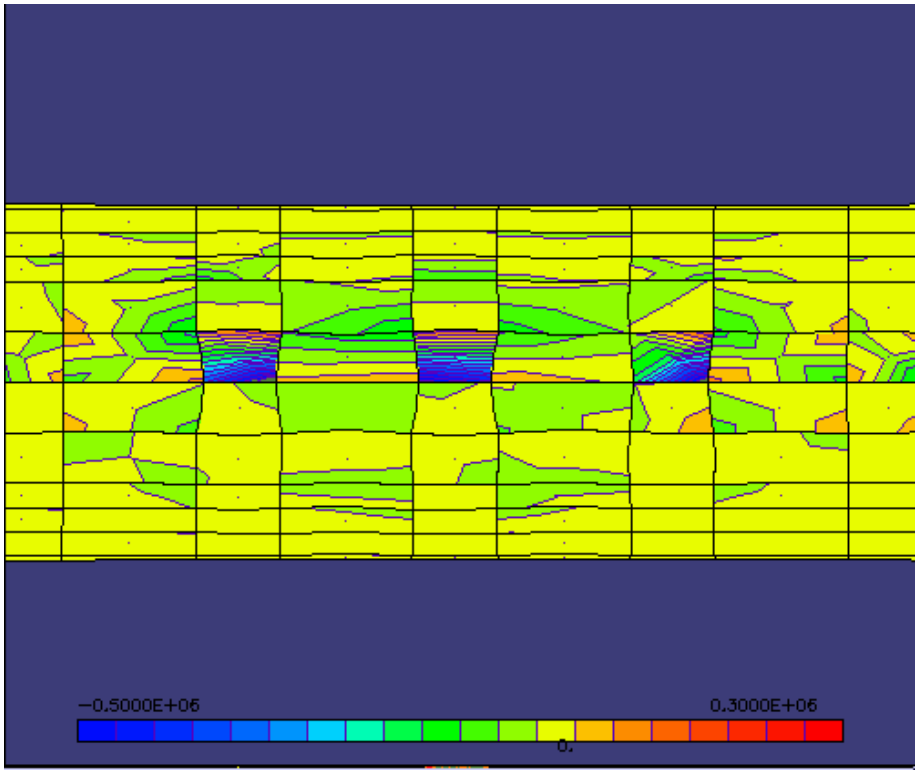

Figure 7.13. Induced vertical stress at ballast level for CT2 (plastic analysis)

As an example the deviatoric shear stress for CT2 directly below the railhead has been plotted with depth in Figure 7.14 and along the sleeper section in Figure 7.15 for the plastic analyses. Figure 7.14 indicates a marked reduction in deviatoric shear stress at the ballast-formation interface, which is attributable to the stiffer ballast layer overlying the softer formation and subgrade layers. Figure 7.15 illustrates that along the sleeper the induced stresses are highest beneath the railhead on both the formation and ballast surfaces. At the formation surface the stresses are more uniform along the sleeper than at the ballast surface. These findings are in agreement with FE modelling studies by Selig and Waters (1994) and Shahu *et al*. (1999).

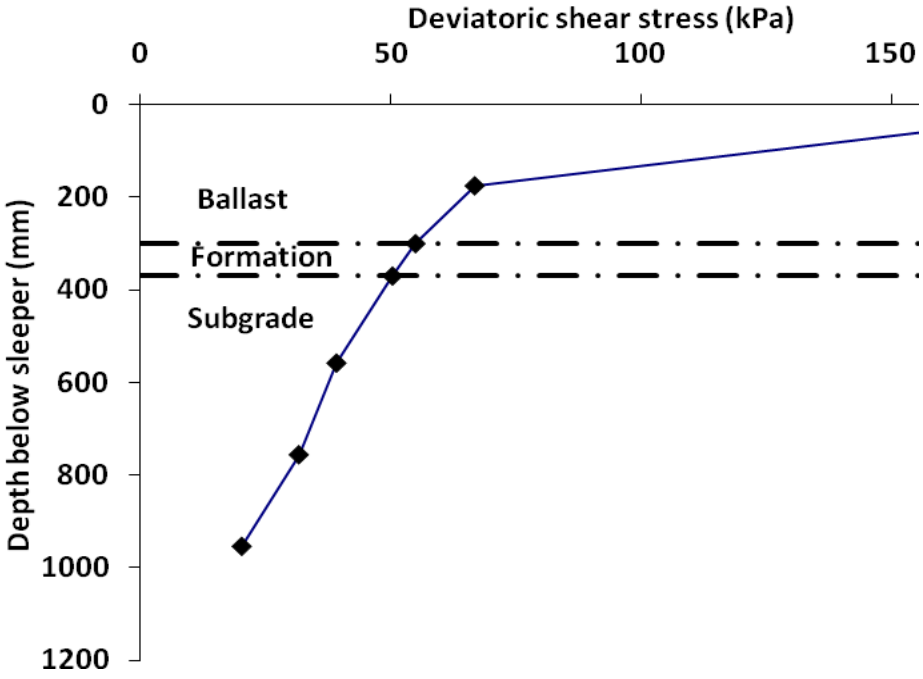

Figure 7.14. Deviatoric shear stress under railhead with depth (plastic analysis)

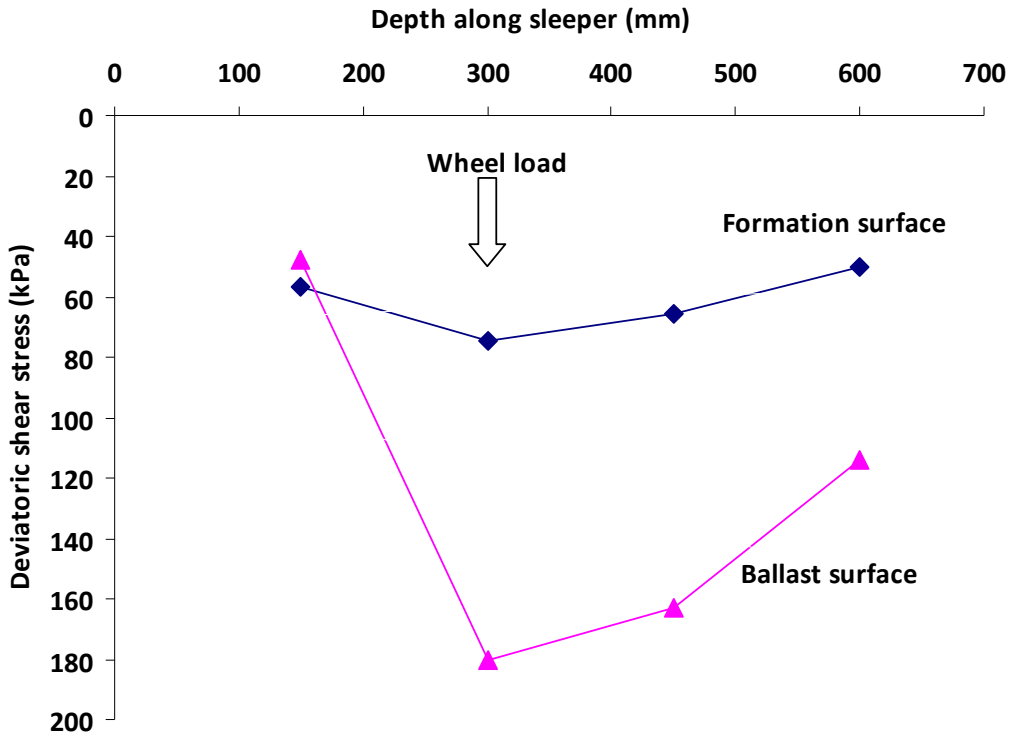

Figure 7.15. Deviatoric shear stress along sleeper section

Table 7.4 shows the induced stress values found for all the GRAFT model SART3D plastic analysis test runs. The average values have been shown for the two central elements below the railhead. The vertical stress values are within the range of 71 to 196kPa quoted by Brough *et al*. (2003) for stresses at a depth of 300mm below the underside of the sleepers and they match closely with the vertical subgrade surface stress values recorded by Selig and Waters (1994) and Shahu *et al*. (1999) using FE modelling. Table 7. shows that as the track stiffness increases from CT2 to CT4 the stress concentrations in the track increase. This is because the ballast-sleeper contact stresses increase with increasing track stiffness (Selig and Waters, 1994). Shahu *et al*. (1999) found similar results and noted that an increase in subgrade stiffness from 10 to 50MPa increased the subgrade surface deviatoric stress by around 44%. Therefore, as stated in Chapter 4, an optimum track stiffness for a specific applied load is likely to exist for railway tracks. Below the optimum track stiffness the track deflections will be high and the track stresses low, while as the track stiffness approaches optimum the track stresses increase and the deflections decrease. It is likely that when the track stiffness is greater than the optimum the induced track stresses result in an increased rate of track degradation.

After the calibration of SART3D to GRAFT the influence of the neoprene lining was investigated by running GRAFT simulations with and without the neoprene for a typical GRAFT test (CT2 was used). The results are shown in Table 7. where it can be seen that the vertical track deflection and induced stresses are less for the GRAFT track without the neoprene. This illustrates that the neoprene lining in GRAFT acts to increase the sleeper deflection, which leads to increased plastic strains developing and hence permanent settlement. This is a result of the neoprene lining reducing the confinement effects from the tank walls. The elastic analysis gave similar results, although the differences between the track, with and without the neoprene, are less due to no plasticity being developed.

Table 7. also shows the results from a load distribution study that was undertaken to investigate the effect of reducing from 5 to 3 sleepers in GRAFT. It can be seen that changing from 3 to 5 sleepers reduces the induced formation deviatoric shear stress ratio

by around 15% and thus, it can be assumed that the two end sleepers account for around 7.5% each. This analysis confirmed that the GRAFT sleeper load factor of 85% used in equation 3.1 to convert from 5 sleepers to 3 sleepers is appropriate. Figure 3.5 shows the assumed load distribution along successive sleepers used in GRAFT.

GRAFT test	Vertical track deflection at peak load increment (mm)	SART3D avg. induced formation deviatoric shear stress (kPa)	SART3D avg. induced formation deviatoric shear stress ratio	SART3D avg. induced formation vertical stress (kPa)
CT1 (130kN load)	3.15	96	0.527	78
CT2	2.19	70	0.386	60
CT3	2.05	83	0.462	72
CT4	1.92	91	0.543	81
CT2 (without neoprene)	1.95	62	0.343	55
CT2 (5 sleepers)	1.66	59	0.328	52

Table 7.4. Stress comparison between SART3D test runs (avg. plastic analysis results from two elements directly below railhead)

7.3 GRAFT applied load validation

To check the applied load in GRAFT represents the induced stresses in the field accurately for an equivalent axle load the stresses from the GRAFT SART3D model were compared with those from a full SART3D track model with the same track properties. Due to symmetry along the centreline of the railway track only half the track

is required to be modelled. The full track model therefore consisted of 10 elements in the X direction (1.3m length sleeper section and 10m outside track and embankment width), 39 elements in the Y direction (12.5m track length with 19 sleepers), and 10 elements in the Z direction (16m track depth). The sleeper, ballast, formation and subgrade dimensions, spacing's and properties input into the model were the same as in the CT2 GRAFT model. The rail properties were that of a 113lb rail section used in industry and rail pads were ignored. The load applied was taken as the equivalent track axle load from the 90kN load applied in GRAFT using equation 3.1. The applied load was 302.5kN over 60 increments of 5.04kN each, which represented approximately a 25 tonne axle load with 1.2 DAF (actual load = 25.7 tonne axle load).

Table 7.5 compares these induced stress and displacement values to the values found for the GRAFT model for the CT2 run. It can be seen that the formation stress concentrations match well and hence the applied load in GRAFT, to simulate a 25 tonne axle load with 1.2 DAF, is accurate in terms of the induced stresses on the formation. The track deflection in GRAFT is around 23% less compared to the field model due to the reduced depth of clay in GRAFT. This is unavoidable and means that when comparing GRAFT to the field a conversion factor has to be applied to the resulting transient deflection values in GRAFT:

$$\delta_{field} = 1.3 \times \delta_{GRAFT} \tag{7.1}$$

It can be seen in Figure 7.14 that some induced vertical stress still exists at the base of GRAFT which accounts for the 23% less track deflection. Therefore, the track stiffness values in GRAFT with the equivalent axle load for the field overestimate the track stiffness found in the field for the same track conditions. The next logical step would be to compare the track settlement values found in GRAFT to track settlement values found in the field for similar conditions as in GRAFT; however this is out with the scope of this thesis.

SART3D test run	Vertical track deflection at peak load increment (mm)	SART3D avg. induced formation deviatoric shear stress (kPa)	SART3D avg. induced formation deviatoric shear stress ratio	SART3D avg. induced formation vertical stress (kPa)
GRAFT model CT2 test run	2.19	70	0.386	60
Full track model CT2 test run	2.86	68	0.377	63

Table 7.5. SART3D output comparison between GRAFT and full track models (avg. plastic analysis results from two elements directly below railhead)

7.4 SART3D parametric study

In order to investigate the influence of some track parameters that were not changed in GRAFT a short parametric study was undertaken with the GRAFT SART3D model. The variables considered include ballast depth, ballast stiffness, rail type, sleeper type and sleeper spacing and the fixed parameters were the same as in the CT2 test run. In addition to these variables the influence of change in subgrade stiffness and strength, and applied load has also been studied through the changes in test runs CT1 to CT4. Table 7.6 gives the track properties that were used in the parametric study and Table 7.7 gives the specific rail and sleeper properties. The subgrade strength has not been included in Table 7.6 as the influence of subgrade strength has been coupled together with the influence of subgrade stiffness. For the applied load variable between test run CT1 and CT2 it is assumed that the subgrade stiffness and strength are the same (stiffness difference = 48 to 46MPa and strength difference = 142 to 136kPa). All test runs undertaken are typical of different railway tracks used worldwide and as such it is

interesting to note the wide variation that can be encountered on track. The track responses investigated were vertical track deflection, vertical track stiffness, formation vertical stress, formation deviatoric shear stress, and formation deviatoric shear stress ratio. The predicted track responses found for the eight different track variations from CT2 are presented in Figures 7.16 to 7.20. The average values from the two central elements below the railhead have been used in these Figures from the plastic analysis runs.

The track deflection (Figure 7.16) was influenced most by the applied load and sleeper type while subgrade and ballast stiffness had a smaller influence. The rest of the parameters had less of an affect. An increase in applied load from 90 to 130kN increased the track deflection by around 45% and changing from wooden to concrete sleepers decreased the track deflection by around 32%. As expected the track stiffness response (Figure 7.17) is exactly the same as the track deflection response with the exception of the applied load parameter. These findings indicate that to improve the track stiffness on a railway track the parameters that should be considered are the sleeper type, subgrade stiffness and ballast stiffness. A cost-benefit analysis of these different solutions could then be undertaken. If concrete sleepers are already in use then the subgrade and ballast stiffness should be evaluated for improvement.

Varied parameter	CT2 value	Values used keeping all other parameters fixed at CT2 value
Ballast depth (mm)	300	500
Ballast stiffness (MPa)	135	180
Rail type	BS113A equivalent	UIC60
Sleeper type	Wooden	Concrete
Sleeper spacing (mm)	650	800
Subgrade stiffness (MPa)	46	66, 91
Applied load (kN)	90	130

Table 7.6. Varied track properties used in parametric study

	Rail		Sleeper	
Varied parameter	BS113A equivalent	UIC60	Wood	Concrete
E (Young's Modulus, GPa)	200	200	10	21
Poisson's ratio	0.29	0.29	0.25	0.20
Bulk density (kg/m³)	7500	7500	2100	2400
Bending stiffness around x (m^4)	2.210×10^{-5}	2.791×10^{-5}	-	-
Bending stiffness around z (m^4)	7.060×10^{-6}	5.019×10^{-6}	-	-
Torsional stiffness around y (m^4)	2.920×10^{-5}	3.293×10^{-5}	-	-
Area (m^2)	4.710×10^{-3}	7.321×10^{-3}	-	-

Table 7.7. Rail and sleeper properties used in parametric study

Subgrade stiffness improvements are often not practical and ballast stiffness improvements, such as XiTRACK reinforcement, can be effective. As shown in Chapter 5 from the GRAFT test results XiTRACK reinforcement can increase track stiffness by around 55 to 65% over 500,000 applied cycles. It is interesting to note here that increasing the ballast depth from 300 to 500mm had an insignificant influence on the track stiffness response. Woodward *et al*. (2009b) noted that this is due to the inability of the unreinforced ballast to form an effective geopavement as it cannot support tensile forces.

The formation vertical stress response (Figure 7.18) was influenced the most by subgrade stiffness, sleeper spacing and applied load. Ballast depth and rail type had less of an influence for the values considered. As previously discussed, an increase in subgrade stiffness from 46 to 91MPa increased the formation vertical stress by 35%. An increase in sleeper spacing from 650 to 800mm increased the formation vertical stress by around 32% while increasing the applied load from 90 to 130kN increased it by 30%.

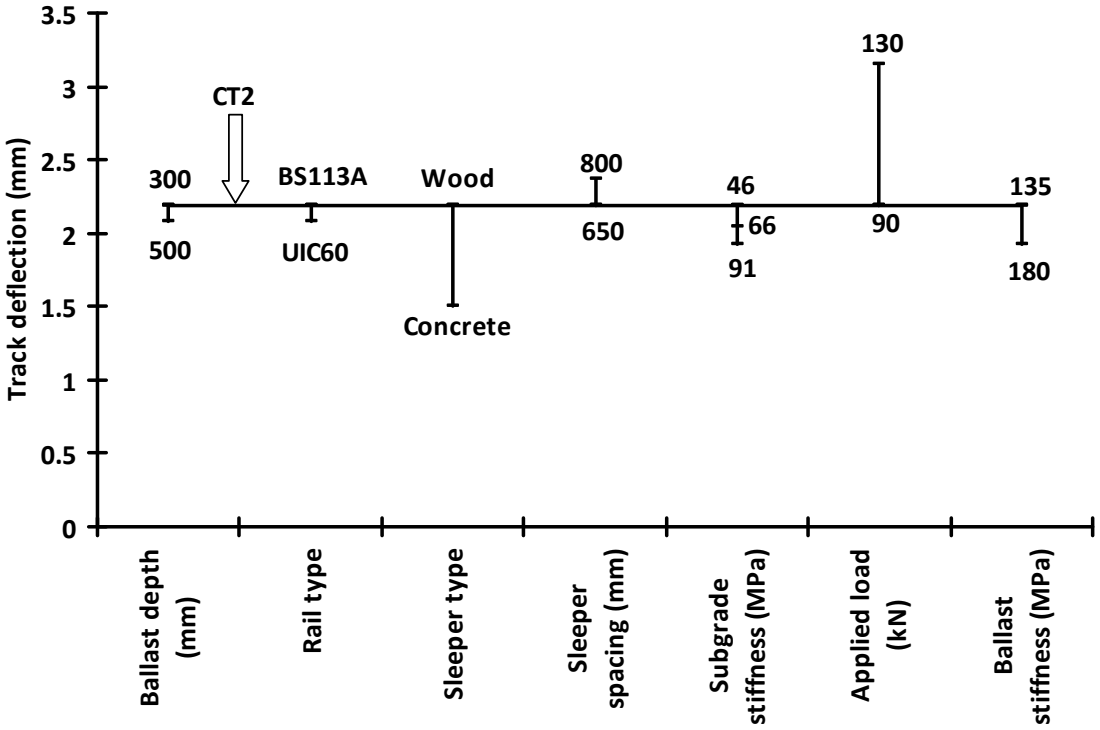

Figure 7.16. SART3D track deflection response to parametric study (plastic analysis)

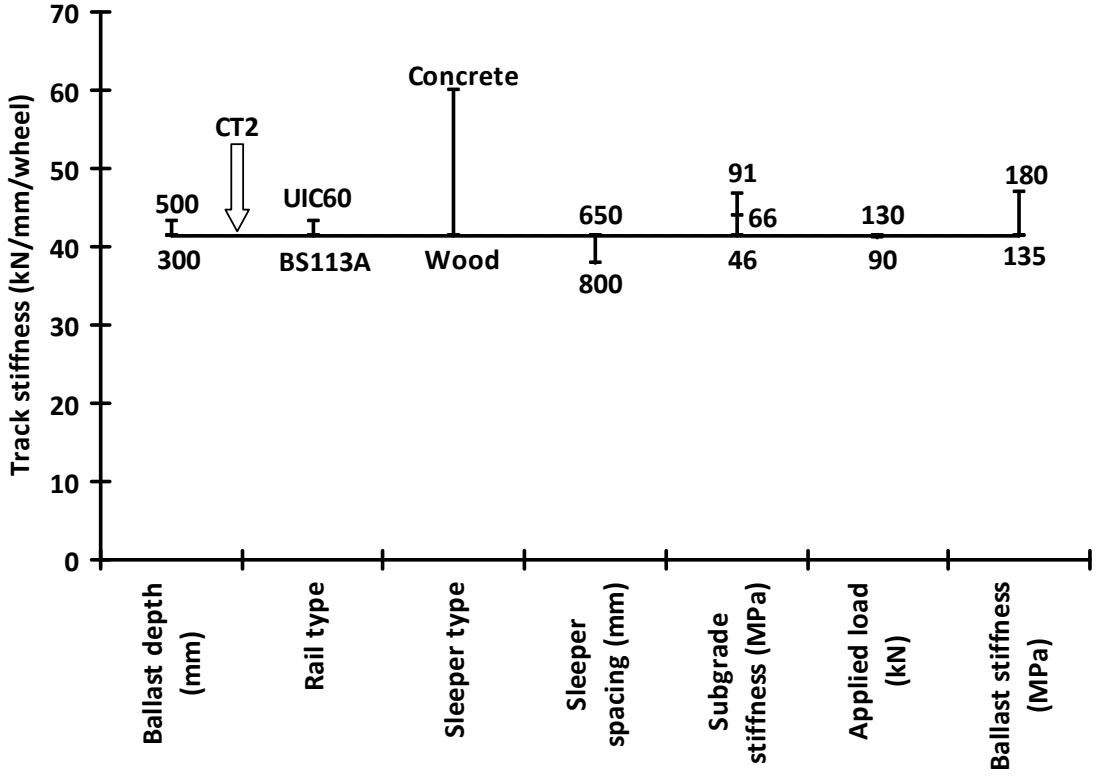

Figure 7.17. SART3D track stiffness response to parametric study (plastic analysis)

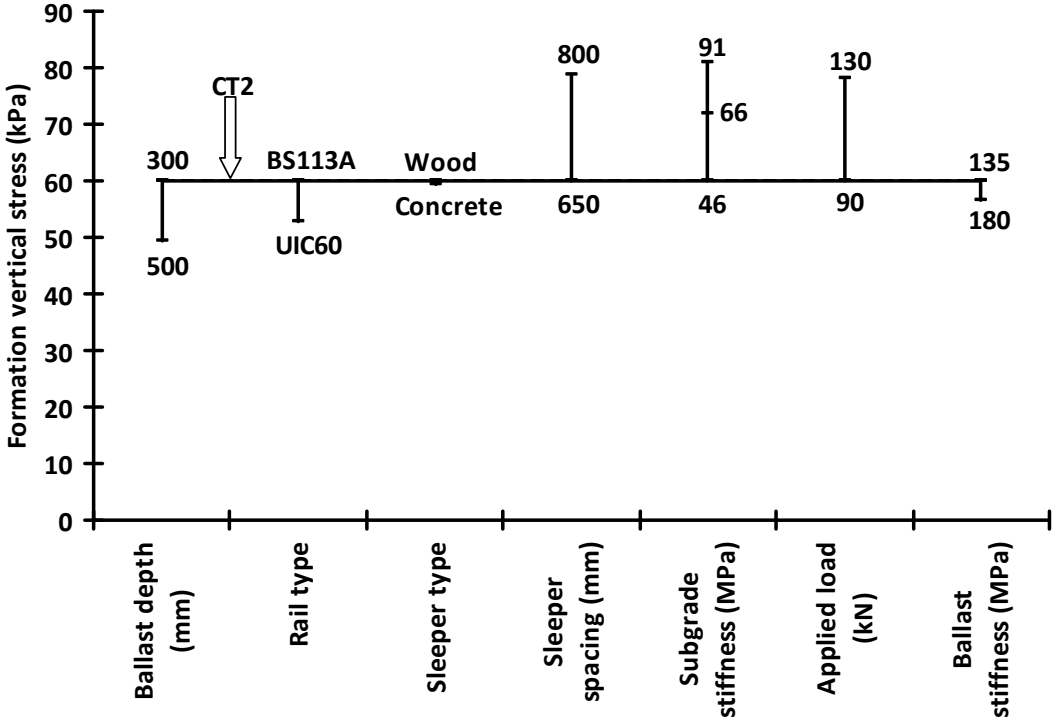

Figure 7.18. SART3D formation vertical stress response to parametric study (plastic analysis)

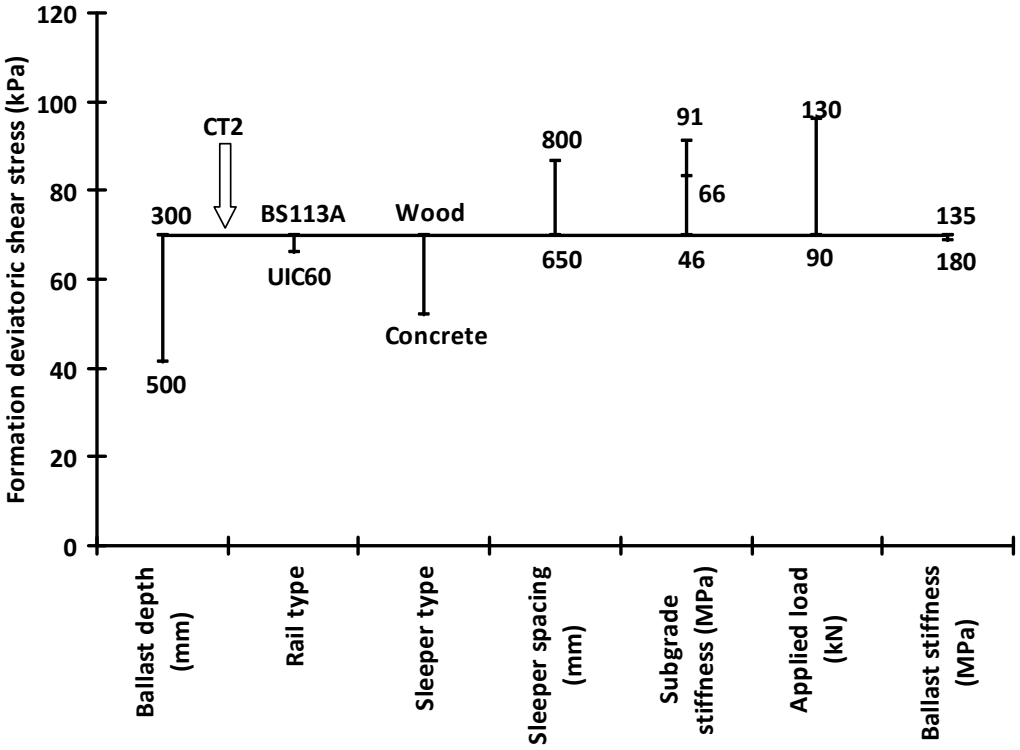

Figure 7.19. SART3D formation deviatoric shear stress response to parametric study (plastic analysis)

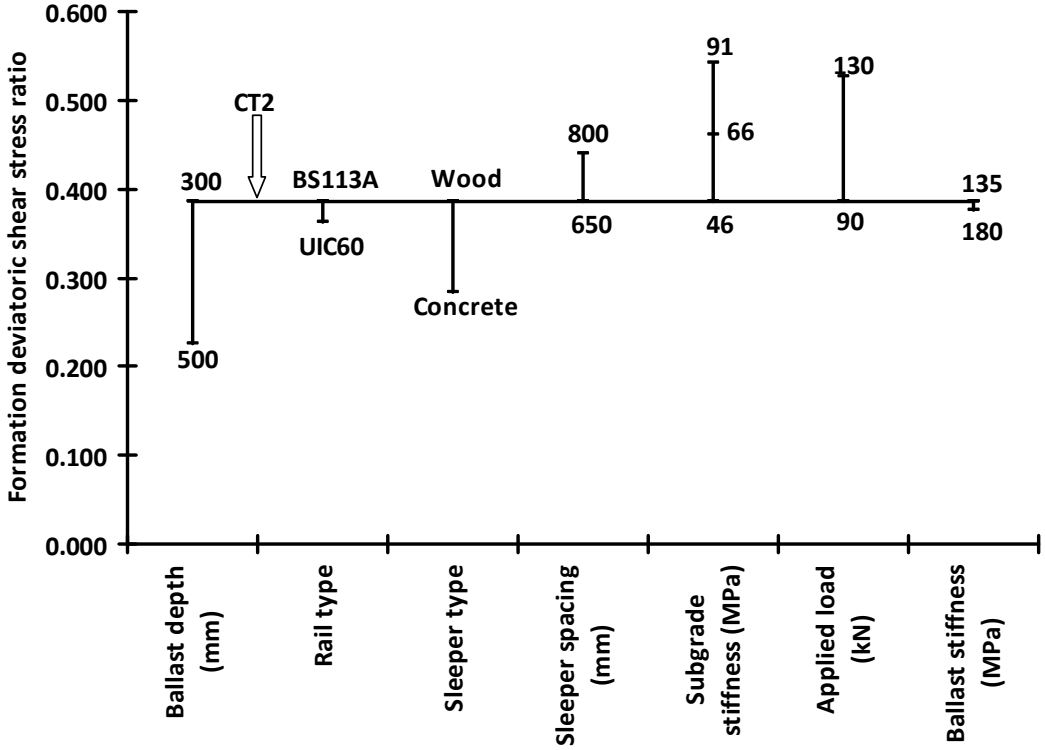

Figure 7.20. SART3D formation deviatoric shear stress ratio response to parametric study (plastic analysis)

The formation deviatoric shear stress (Figure 7.19) and formation deviatoric shear stress ratio (Figure 7.20) responses were influenced the most by ballast depth, applied load, subgrade stiffness, sleeper spacing and sleeper type. Increasing the ballast depth from 300 to 500mm reduced the formation deviatoric shear stress and the formation deviatoric shear stress ratio by around 41%. Therefore, although increasing the ballast depth may not significantly increase track stiffness it can considerably reduce the induced deviatoric stresses in the formation and subgrade layers. Li and Selig (1998a) and Shahu *et al*. (2000) stated that to control cumulative plastic strain at the subgrade surface either the subgrade strength can be improved or deviator stress transmitted to the subgrade can be reduced. This study has shown that to reduce the stresses transmitted to the subgrade effectively (and practically) the ballast depth could be increased, the applied load reduced, or concrete sleepers could replace existing wooden sleepers. Again, a cost-benefit analysis could be undertaken to determine the most appropriate solution.

The results of this parametric study have shown that subgrade stiffness and applied load are probably the two parameters that influence the overall railway track behaviour the most in terms of both track deflections and induced formation/subgrade stresses. These two parameters have been investigated in considerable depth within this thesis and their influence on both track settlement and track stiffness reported. Other significant parameters include sleeper type and sleeper spacing. Ballast stiffness has a direct influence on track stiffness while ballast depth has a considerable influence on the induced stresses on the formation layer. The rail type has a less significant influence on the track responses considered in this study; although it is likely to have more of an influence on ballast induced stresses and ballast strain. These findings are similar to research by Selig and Waters (1994) and Shahu (1999) who also undertook an FE modelling parametric study (although not as advanced as the SART3D analysis). These findings are important for track design and maintenance planning, as the correct parameter can be changed depending on the desired effect required. Shahu (1999) noted that for practising engineers such a study is very useful for economic design and maintenance of tracks. For example, if the load bearing capacity of the track (with fixed spaced concrete sleepers) is a cause for concern the ballast depth could be increased, or applied load reduced or subgrade strength increased. Whereas if track deformation was the primary cause for concern the applied load could be reduced, or the subgrade or ballast stiffness could be increased (increased compaction or XiTRACK reinforcement). A proposed design method will be discussed in the next section along with a review of existing design methods.

7.5 Track design implications

Different railway track design methods are used around the world with the main objective being to protect the subgrade from deterioration (Burrow *et al*., 2007a). The main modes of subgrade deterioration were explained in Chapter 2. Of these modes, foundation track design methods are based on preventing excessive plastic deformation and progressive shear failure in the subgrade (Burrow *et al*., 2007a). Burrow *et al*. (2007a) state that several approaches can be adopted to help prevent these failure modes

developing including using non-ballasted track forms, increasing the flexural rigidity of the rail and using soil stabilisation. They also mention however, that the use of appropriate thicknesses of the trackbed layers is likely to be effective and economical. Therefore, the majority of track design methods concentrate on designing the trackbed thickness. A detailed review of different track design methods can be found in Burrow *et al*. (2007a). A brief summary is presented here.

The International Union of Railways (UIC 719 R, 1994) gives a set of recommendations for the design and maintenance of railway tracks. A single combined thickness of the trackbed layers (ballast and subballast) is specified based on the descriptive quality of the subgrade soil, the traffic characteristics, the track configuration and quality, and the thickness of the prepared subgrade (treated layer below subballast included if subgrade requires improvement). British Rail (Heath *et al*., 1972) developed a method to prevent excessive plastic deformation of the subgrade by limiting the stress level in the subgrade to a threshold value. The threshold value is based on soil laboratory cyclic triaxial testing while the induced stresses are calculated from a single layer homogeneous linear elastic model of the track system. Design charts were produced to relate the threshold stress to the required trackbed layer thickness for a given axle load.

The West Japan Railway Company (WJRC, 2000a and b) construction and maintenance standards give minimum required trackbed depths based on annual tonnage and speed. For high-speed lines the minimum required depth is 300mm whereas for commuter lines the minimum depth is 200mm for a track carrying less than 10MGT and 250mm for a track carrying greater than 10MGT. These limits are assuming that the substructure has a bearing capacity of at least 288kPa. If it is less than this then ground improvement is required. Network Rail code of practise, NR/SP/TRK/9039 relates the required thickness of the trackbed layers to undrained subgrade modulus for three different values of dynamic sleeper support stiffness measured from the FWD (30, 60 and 100kN/mm/sleeper end). The values relate to minimum requirements for existing main lines with and without geogrid reinforcement and new track, respectively. No technical details of how the chart was derived are given and within this thesis uncertainties about elements of the design chart have been presented (sections 4.3 and 6.2 raise concerns

about the accuracy of the FWD, section 5.5 raises concerns about the level of track improvement achievable from geogrid reinforcement, and section 6.5 raises concerns about how the undrained subgrade modulus used in the design chart is measured for firm unsaturated soils).

Li and Selig (1998a and 1998b) proposed a method to limit the stresses in the subgrade such that plastic strain is at an acceptable level. Subgrade stresses are determined from a static multi-layered elastic analytical model of the track system (GEOTRACK) while the allowable stresses are determined from an empirical equation that relates subgrade plastic strain to the number of loading cycles (shown in equations 4.1 and 4.2). For design purposes, Li and Selig (1996) suggest that subgrade plastic strain and deformation should be limited to 2% and 25mm, respectively. Separate design charts were presented by Li and Selig (1996) to give the minimum required thickness of the trackbed layers to prevent progressive shear failure and to prevent excessive subgrade plastic deformation.

A summary of the factors accounted for in these design methods was presented by Burrow *et al*. (2007a) and has been reproduced here in Table 7.8. Burrow *et al*. (2007a) compared all five design methods by determining the combined thickness of the trackbed layers specified by each method under different conditions relating to subgrade, axle load, speed, and cumulative tonnage. It was found that there is a large variation in the specified thickness of the trackbed layers among the procedures and that the design thickness specified by each method is a function of at least one of the four variables considered. Only the method presented by Li and Selig (1998a and 1998b) gave a variation in required thickness with all of the variables and it was suggested that this procedure follows most closely that of an analytical methodology.

Factors	Li and Selig (1998a & 1998b)	UIC 719 R	British Rail	NWR code 039	WJRC
Static axle load	Via GEOTRACK	Yes	Via elastic model	No – but 25 tonne axle load limit on UK network	No
Sleeper type, length and spacing	Via GEOTRACK	Yes	No	No	No
Rail section	Via GEOTRACK	No	No	No	No
Train speed	Using DAF	Yes	No	Via min. requirement for the dynamic sleeper support stiffness	Crude variation – high-speed has greater depth than commuter lines
Annual tonnage	Yes	Yes	No	No	Commuter lines only
Cumulative tonnage	From annual tonnage multiplied by design life	No	No	No	No
Subgrade condition	Charts provided for different subgrade types in terms of resilient modulus and soil strength	Yes	Using threshold stress for material in question	Undrained subgrade modulus or undrained shear strength	Bearing capacity of subgrade assumed to be 288kPa otherwise ground improvement required

Table 7.8. Summary of factors accounted for in different track design methods (modified from Burrow *et al*., 2007a)

These design methods are generally satisfactory for light axle loads and low to medium train speeds; however for heavy axle loads and faster trains these methods can lead to extensive track maintenance (Shahu *et al*., 2000). In addition, these methods do not consider excessive plastic deformation in the ballast layer that leads to ballast maintenance. As described in Chapter 4, the majority of track settlement is caused by ballast deformation and not subgrade deformation, unless the subgrade is very weak. Therefore, designing track with the objective of limiting subgrade deterioration will not prevent the generation of overall track plastic deformation. Ballast deformation needs to be considered separately as increasing the ballast depth may not necessarily reduce ballast deformation. This was found in the parametric study in the previous section, which showed that while an increased ballast depth can reduce the induced stress level on the underlying formation/subgrade, track stiffness may not be increased by much.

Banimahd (2008) found that if the subgrade is very weak increasing the ballast depth will not solve the problem and the subgrade will need to be improved. This is due to the ballast undergoing large reversing shear strains that generate ballast settlement as a result of large track deflections (Woodward *et al*., 2009b). Therefore, these current track design methods could be improved to include ballast deformation as well as subgrade deterioration. Also, consideration should be given in the design process to methods that can reduce ballast deformation. This thesis has shown that an increased subgrade stiffness can reduce ballast deformation as well as ballast reinforcement techniques such as XiTRACK reinforcement. The parametric study has also shown that implementing concrete sleepers can also have a significant effect.

Banimahd (2008) proposed an alternative track design procedure to include ballast deformation based on a 3D dynamic multi-layered FE model. The main objectives of the procedure were to protect the subgrade from deterioration and to decrease the level of ballast maintenance. The subgrade is protected from deterioration by limiting the deviatoric shear stress in the subgrade to a threshold value that is proportional to the failure stress, or limiting the plastic strain or deformation as suggested by Li and Selig (1998a and 1998b). This should prevent excessive plastic deformation and progressive shear failure in the subgrade. The level of ballast maintenance is reduced by limiting the

stress level in the ballast layer to a threshold to avoid excessive plasticity. The threshold can be based on the deviatoric stress in the ballast or the ballast deviatoric shear stress ratio (Banimahd, 2008). An alternative approach can be based on limiting the ballast layer deformation or strain, both of which are calculated using empirical relationships (Banimahd, 2008).

The design procedure proposed by Banimahd (2008) involves initially estimating the Rayleigh wave velocity for the track configuration considered. If the train speed is greater than 70% of the Rayleigh wave velocity or the subgrade is too weak, the subgrade will probably need to be improved. This fits in with Network Rail code NR/SP/TRK/9039 which states that a significant improvement in critical velocity can only be made by deep ground improvement. The weakness of the subgrade can be based on the stress of deformation level under the static train load or low speed. If the subgrade stiffness is considered sufficient then improvement of the ballast layer is designed to limit the stress levels in the ballast and subgrade to an acceptable level.

From the findings of this thesis additions to the Banimahd (2008) design procedure can be made for tracks where the train speed is less than 70% of the Rayleigh wave velocity. For example, for a specific track configuration and given axle load the weakness of the subgrade can be assessed for how much the track will settle (new track or existing track after track renewal/tamping) after a certain amount of traffic by using the empirical design graph presented in Figure 4.6. It should be noted that this graph may give an underestimation of track settlement due to reduced depth of GRAFT. The subgrade deterioration can quickly be evaluated by using the SART3D program to estimate the subgrade deviatoric shear stress ratio. If subgrade deterioration is not considered a problem, although track settlement is high, then ballast reinforcement could be considered and the reduction in track settlement can be estimated from Figure 5.29. The level of track settlement reduction from the ballast reinforcement estimated in Figure 5.29 can be compared against the level of settlement reduction for increasing the subgrade stiffness from the same graph (example shown in section 5.5). This would allow a cost-benefit analysis of the subgrade or ballast reinforcement solutions that could achieve the desired reduction in track settlement to be undertaken. In addition,

from the parametric study undertaken in the previous section it was found that changing from wooden to concrete sleepers could also have a significant effect on track stiffness, which in turn could considerably reduce track settlement. If changing the sleepers was considered a feasible option then the track stiffness output from the SART3D program could be used to estimate track settlement using Figure 4.30. It should be noted here though that this graph has only been calibrated for wooden sleepers. A downside of using concrete sleepers is that they tend to damage the ballast more (i.e. attrition).

If the subgrade deviatoric stress ratio was perceived to be too high then different track configurations may be considered if practical for the specific site. For example, as shown in the parametric study undertaken above to reduce the subgrade deviatoric shear stress ratio for a given axle load the ballast depth could be increased, concrete sleepers could be used or the sleepers could be spaced closer together. In addition, a subballast layer could be used to provide an additional load distributing layer (Shahu *et al*., 2000). Also, using FE analysis Woodward *et al*. (2009c) found that XiTRACK reinforcement can reduce the induced formation deviatoric shear stress by distributing the load across the formation layer. Alternatively, the subgrade stiffness could be increased. Shahu *et al*. (2000) recommended that this could be achieved by lowering the ground water table, stabilising the subgrade soil, or using a geosynthetic. The influence on the subgrade deviatoric shear stress ratio of changing these parameters could quickly be assessed using the SART3D program and a shortlist of acceptable methods could be collated that could be taken forward for further analysis. The influence of these parameters on track settlement could then be tentatively estimated using Figure 5.30, based on the track stiffness output from the specific SART3D test run. The predicted track settlement from this method can only be regarded as indicative as the empirical equations used to form these design graphs are based on a typical track configuration in GRAFT (reduced clay depth) with 300mm ballast depth and have not been calibrated for any alternatives. In addition, mixed loads, different train speeds and high cumulative tonnages (greater than around 15MGT) have not been considered. Nonetheless, this design procedure is quick and simple and could form the initial part of a complete track design procedure for new track or track after a track renewal/tamping; where the preliminary cost-benefit analysis

of different solutions to reduce the required track maintenance (subgrade and ballast related) could be assessed.

The full design procedure can be outlined as follows:

1. Trackbed investigation undertaken to determine the track parameters that are used in SART3D model and empirical design equations developed in this thesis (subgrade measuring devices were discussed in Chapter 6).
2. Estimate the Rayleigh wave velocity and if the train speed is higher than 70% the subgrade probably needs to be improved. If this is the case undertake dynamic design procedure following Banimahd (2008).
3. If train speed is less than 70% of the Rayleigh wave velocity assess the track for subgrade deterioration and track settlement (initially using a conventional ballast depth of 300mm) using SART3D and the empirical design equations. Calibrate the SART3D program to the specific track.
4. If the induced subgrade deviatoric shear stress ratio or the track settlement is too high undertake practical modifications to the track design as described above and repeat the analysis until acceptable.
5. Undertake preliminary cost-benefit analysis of each acceptable solution identified.
6. Undertake dynamic analysis using 3D model developed by Banimahd (2008) to check the chosen design.
7. Once the track has been constructed track stiffness measurements should be undertaken to check the design and then track geometry monitoring should be undertaken periodically to validate the design procedure and plan any future maintenance required (track stiffness measuring devices were discussed in Chapter 4).

This design procedure offers an optimised design and maintenance strategy in terms of life-long performance and cost of track and is more robust than the current Network Rail track design method (Table 7.8). With further research in GRAFT the track settlement empirical equations and design charts used in this procedure could be calibrated for full depth track and refined to include a range of different track forms,

mixed loads, high cumulative tonnages etc. as well as other ballast reinforcement solutions and conventional ballast maintenance operations such as tamping.

An example of the design procedure is presented here. Assume a track with the same parameters as in the GRAFT test CT2 and assume that the train speed is less than 70% of the Rayleigh wave velocity. The SART3D plastic analysis found an average formation deviatoric shear stress ratio of 0.386 for the two elements directly below the railhead. This is relatively low and subgrade deterioration can be considered not a serious concern. Using Figure 4.6 with an applied axle load of 25 tonnes and subgrade tangent modulus of 32.7MPa the track settlement after 12.5MGT can be estimated to be about 37mm. Clearly this is a high level of settlement and as such using Figure 5.29 it can be found that using XiTRACK reinforcement would reduce the settlement to around 0.70mm. To achieve the same level of track settlement by increasing the subgrade stiffness the subgrade modulus would need to be increased to around 732MPa. Alternatively, if concrete sleepers were used instead of wood then using SART3D the track stiffness would increase to around 60kN/mm/wheel and using Figure 4.30 the track settlement would potentially reduce to approximately 9mm after 12.5MGT. Depending on the required settlement and the practical considerations at the site the most appropriate solution could be chosen. A similar methodology is undertaken when the subgrade deviatoric stress ratio is perceived to be too high for a specific track.

7.6 Conclusion

This chapter has used a 3D FE program called SART3D to show that GRAFT is accurate in terms of the stresses applied on the formation for an equivalent 25 tonne axle load with 1.2 DAF applied on track. Therefore the load applied in GRAFT accurately represents the field loading and the findings of this thesis are valid. SART3D was calibrated to GRAFT and the SART3D GRAFT model accurately matched the load-deflection behaviour found in GRAFT with the estimated ballast properties used. Thus, for the track properties and the load applied in GRAFT the deflections are correct and GRAFT can accurately simulate the response of track for a range of tests. However, due to the restricted depth of clay in GRAFT the deflections in GRAFT underestimate the

deflections in the field for the same track properties and equivalent applied load by a factor of 1.3. This means that the track stiffness and track settlement values found in GRAFT do not directly give the final field values and as such need to be converted. Nonetheless, the GRAFT models developed within this thesis can still be used in conjunction with SART3D for preliminary track design and optioneering. A review of design procedures used in the railway industry was provided in this chapter and a new design procedure to reduce the required track maintenance was presented. The new procedure combines the numerical design method presented by Banimahd (2008) with the empirical results of this thesis to offer an optimised design and maintenance strategy. An example of the method was presented and with further research the design procedure could become more robust. In addition, a parametric study with the GRAFT SART3D model was performed in this chapter and it showed that subgrade stiffness and applied load are probably the two parameters that influence the overall railway track behaviour the most in terms of both track deflections and induced formation/subgrade stresses. Using SART3D to undertake such studies in the future could allow the affects on track stiffness, of changing different parameters, to be investigated in a much shorter time than undertaking a full GRAFT test. Therefore, SART3D can act as a preliminary tool to investigate the affect on track stiffness of changing certain parameters or implementing different track reinforcements before it is decided whether or not a full scale test is required.

Chapter 8 - Conclusions and Recommendations

8.1 Conclusions

Within this thesis a full-scale laboratory Geopavement & Railway Accelerated Fatigue Testing (GRAFT) facility has been developed to enable accelerated testing of full-scale railway tracks and new innovative railway products under realistic railway loading conditions. The new GRAFT facility consists of a track constructed within a steel tank 1.072m wide x 3.0m long x 1.15m high. The track includes three 600mm length hardwood sleeper sections overlain by a 3m long I-section steel beam which has similar stiffness properties to a BS 113 A rail section. Cyclic loading is applied to the track at a frequency of 3 Hz from a hydraulic testing machine with the centre sleeper directly under the loading actuator. The loading mechanism replicates a repeated quasi static single wheel load on the central sleeper of one half of a 3m long section of railway track and the effects of principal stress rotation are not considered. The performance of the track is therefore based on the middle sleeper only. Initial analytical analysis and further finite element modelling of GRAFT found that an applied actuator load in GRAFT of 90kN represents an axle load of 25 tonnes with a 1.2 dynamic amplification factor (DAF) while an applied load of 130 kN in GRAFT represents an axle load of 37 tonnes with a 1.2 DAF. To limit the lateral support to the substructure, provided from the rigid walls of the steel tank and to provide lateral support similar to the horizontal residual support experienced in the field, the tank sides were lined with 12 mm thick neoprene rubber. The track subgrade and overlying formation layer was constructed from Kaolin clay, the properties of which can be found in Table 3.5. For the four full-scale tests undertaken within this study the clay subgrade depth was 750 mm with a formation depth of 70 mm and ballast depth of 300mm.

Using the GRAFT facility a series of unreinforced GRAFT control tests were initially undertaken to investigate the factors that influence the unreinforced substructure performance. The influence of subgrade Young's modulus, applied vertical load and number of applied cycles on track settlement and stiffness were studied in detail while

other factors such as the rate of loading, mixed loading and ballast depth were also considered. Empirical relationships were developed between unreinforced track performance in terms of track settlement and stiffness and the track parameters subgrade modulus, applied load and number of applied cycles. These relationships fit the GRAFT data presented in this thesis well and it is thought that they could be used (tentatively) to estimate track settlement on track after tamping/ballast renewal. These models were shown to be consistent when their parameters were correlated with other track settlement models.

GRAFT was then utilised to undertake tests on track implemented with different geosynthetics to quantify the improvement in track performance available with each product under various track conditions. The performance of each modified track was compared to the performance of the control tests without any geosynthetics. Under normal GRAFT test conditions (same as control tests) two ballast reinforcement products were tested; XiTRACK reinforcement and geocell reinforcement. These were compared to a reinforced geocomposite used primarily for separation at the ballast/subgrade interface and filtration of the underlying water from the subgrade. In addition, a geocomposite product designed to replace a traditional sand blanket, used on the tracks where severe subgrade erosion conditions prevail, has been tested in GRAFT under flooding conditions. From all the data recorded empirical settlement models have been proposed for each of the three geosynthetics compared for reinforcement purposes. These models formed the basis for design graphs that incorporate XiTRACK reinforcement and the reinforced geocomposite. These design graphs are applicable for track settlement after a track renewal/tamping for track on a clay subgrade with a 300mm ballast depth with the same ballast properties, ballast stiffness and track construction and layout as in GRAFT (typical track in UK that can have maintenance issues). It has been proposed that these design charts could form part of an initial cost-benefit analysis of different track reinforcement techniques considered for improving track performance and reducing maintenance depending on the required settlement of the specific track after a certain amount of traffic. In order to use these track settlement design graphs developed within this thesis (in the field) a reliable measure of subgrade modulus needs to be made on track. Several in-situ measuring devices that could

potentially be used to measure subgrade stiffness and strength in the field were tested within GRAFT. The devices studied included Dynamic Cone Penetrometer (DCP), Light Falling Weight Deflectometer (LFWD), Pocket Penetrometer and Proving Ring Penetrometer. The accuracy of these devices was compared to Plate Load Tests (PLT) and unconfined compression strength tests.

The GRAFT facility and the results found in GRAFT were validated using a basic static 3D FE computer model termed SART3D (Static Analysis of Railway Track 3D). The program was calibrated to GRAFT by modifying the FE mesh for the dimensions of GRAFT and inputting the GRAFT track properties. The program was then run to validate that the applied load in GRAFT produces the same level of stresses within the track substructure for a 25 tonne axle load with 1.2 DAF applied on track. A short parametric study was presented to look at the influence of changing some of the track properties that could not practically be studied within the GRAFT experimental program. A review of design procedures used in the railway industry was provided and a new design procedure to reduce the required track maintenance was produced. The new procedure combines the numerical design method presented by Banimahd (2008) with the empirical results of this thesis to offer an optimised design and maintenance strategy.

The findings from this research are as follows:

- The GRAFT facility using simple hydraulics (repeated quasi-static single wheel loading at a typical track loading frequency) can give the same results as more complicated rolling wheel testing facilities and can be used to simulate the complicated loading mechanism of railway tracks. The initial limitations of testing in GRAFT were overcome by; lining the tank with neoprene rubber to reduce the confinement effects from the walls of the tank; incorporating 600mm length sleeper sections (similar to twin block sections) to allow 230mm between the end of the sleeper sections and the tank walls (to reduce confinement affects and allow some tensile force development for reinforced geosynthetics in the transverse direction); and by focussing on the performance of the middle sleeper

only and ignoring rolling wheel affects and the complex loading frequencies on track (1 GRAFT cycle = 1 wheel load).

- Using 5 sleeper sections in GRAFT the track develops additional support from the end sleepers as the test proceeds and settlement occurs underneath the middle sleeper. This was found during the initial GRAFT test after around 70,000 cycles where a void was visible between the underside of the I-section section and the middle sleeper when the load was at a minimum of each cycle. Three sleeper sections should be used in GRAFT to prevent this.

- The load distribution over three sleepers found in GRAFT showed that on average the central sleeper beneath the applied load carries 40% of the load while the adjacent sleepers carry 30% each. This matches well with several other researchers and it is generally accepted that the sleeper under load takes 40-50% of the load. Using the SART3D FE code found that reducing from five to three sleepers increases the induced stress on the formation layer by around 15%.

- GRAFT can realistically represent different railway track conditions such as wet spots and is ideal for studying the performance of various innovative railway products used to solve various track problems. To this end, GRAFT can be used as part of a formal assessment procedure for track products prior to field trials.

- Throughout the testing program in GRAFT it was found that the subgrade stiffness increased. Replacing the 70mm thick formation layer was insufficient to prevent this increase. The reason that the subgrade modulus and strength properties increased throughout the testing programme until the subgrade reached a resilient state is thought to be due to cumulative subgrade compaction, consolidation and changes in the moisture content with an increasing number of cycles applied.

- The ballast D50 particle size and internal friction angle found from samples of the re-used ballast after each GRAFT test indicated that no significant changes

occurred throughout the testing programme. It is thought that new ballast can sustain a high level of loading (at least 80MGT) prior to significant ballast particle breakage and reduction in strength.

- It was found from the GRAFT test results that subgrade stiffness (Young's modulus) and applied vertical load contribute significantly to track settlement on a typical track. These parameters both showed non-linear trends when plotted against settlement and a threshold value seems to exist on both factors beyond which track settlement increases significantly. Similar threshold values have been found for increases in deviator stress for both fine-grained materials (Frost *et al*., 2004), granular materials (discussed in Banimahd (2008)) and track behaviour (Dahlberg, 2001).

- The two stages of track settlement development of ballasted track after tamping/new ballast, as identified by Dahlberg (2001), were observed in the GRAFT control tests. An initial non-linear stage (initial ballast densification) was followed by a progressively more linear stage. It is thought that the non-linear influence of both the applied cyclic load and subgrade modulus may impact the initial non-linear stage of track settlement development with time and load (cycles in GRAFT case). To account for this a GRAFT track parameter (t) was defined in this thesis based on the subgrade modulus and applied cyclic load in GRAFT. The length and magnitude of the initial non-linear stage of track settlement is dictated by (t) for each GRAFT test.

- Using the GRAFT track parameter (t) a particular GRAFT subgrade modulus track settlement model was presented in Chapter 4. This model can predict initial non-linear stage track settlement in GRAFT after a number of cycles (up to 500,000) for any applied load and clay subgrade modulus. For the ballast properties considered the model fits the measured data in GRAFT well and is similar to field measurements found by other researchers. The model is similar to the fine-grained subgrade model proposed by Li and Selig (1996) in that settlement is dependent on stress state and soil physical state and structure. The

limitations of this particular model have been discussed thoroughly within this thesis. At this stage this model can only be used indicatively to predict track settlement in the field due to the restricted depth of GRAFT. To use this model to predict track settlement in the field specific ballast and subgrade properties are required to be known and the ballast properties must match the properties in GRAFT for the tests in this thesis.

- From additional GRAFT tests it has been suggested that longer term settlement, that is linear with applied cycles, is less dependent on subgrade modulus.

- Increasing the applied load in GRAFT from 90 to 110kN at the end of CT2 significantly increased the rate of settlement. Similar results were reported by Selig and Waters (1994) from triaxial tests. A procedure was set out to incorporate this increased load into the GRAFT subgrade modulus settlement prediction model. This model for the increased load section slightly underestimates the observed settlement over the additional 100,000 applied cycles and it seems as if this underestimation is increasing with cycles.

- Reducing the ballast depth from 300 to 250mm as part of the additional study after CT4 found that the settlement increased by 350% over 10,000 cycles for the same applied load level (40kN). This is thought to be due to an increase in the induced formation deviatoric shear stress.

- The GRAFT tests demonstrated that track stiffness varies with applied load, rate of loading, number of cycles, cyclic/monotonic loading and subgrade stiffness. For this range of values within GRAFT, subgrade stiffness was found to be the major contributor to track stiffness change. The additional GRAFT tests after CT4 showed that an increase in applied load results in a reduction in clay stiffness and an increase in ballast stiffness for low load levels up to 110kN (assuming constant confining pressure within GRAFT). Beyond an applied load of 110kN it is thought that the ballast stiffness decreases and if the load applied to the ballasted tracks was increased further it is likely that the track stiffness

would reduce considerably due to both ballast and subgrade stiffness degradation.

- The results from the GRAFT tests directly correlate track stiffness with track settlement and it has been shown that track settlement increases non-linearly with an increase in track deflection. A particular GRAFT track stiffness based settlement prediction model was presented in Chapter 4 to show this relationship and this model is probably more applicable to industry as no measurement of subgrade modulus is required. This model can be used within the axle load range of 25 to 37 tonnes. To use this model indicatively for real tracks the track deflection within this load range needs to be measured. However, the track settlement prediction may underestimate track settlement in the field due to the restricted depth of GRAFT.

- Reinforced GRAFT tests demonstrated that XiTRACK reinforcement improved the stiffness of unreinforced track with the same subgrade modulus and applied load by between 55 and 65% as well as reducing track settlement by around 99% after 500,000 cycles of a 44.4 tonne axle load (including DAF) on soft underlying subsoil (subgrade tangent modulus of 25MPa). The XiTRACK sample remained fully free draining at end of the test and showed no signs of fatigue.

- XiTRACK slab and beam tests undertaken within the LOS illustrated the resiliency and ductility of a XiTRACK reinforced ballast sample while also highlighting the versatility of using XiTRACK reinforcement for both vertical and lateral reinforcement. The plastic vertical strain of the XiTRACK slab section was 2% at 1200kN and 4% at 1390kN. The vertical plastic strain of the XiTRACK beam section was 0.66% at 550kN and 1.67% at 730kN.

- Geocell reinforcement did not perform well in GRAFT. When compared to unreinforced track with the same subgrade modulus and applied load it was found that geocell reinforcement increased track settlement by 37% and reduced

track stiffness by 5 to 7% after 10,000 cycles of a 25 tonne axle load (with 1.2 DAF) on a stiff clay subgrade (subgrade tangent modulus of 65MPa).

- The reinforced geocomposite showed a 25% improvement in settlement and a 9 to 12% improvement in track stiffness when compared to unreinforced track with the same subgrade modulus and applied load after 10,000 cycles of a 25 tonne axle load (with 1.2 DAF) on a stiff clay subgrade (subgrade tangent modulus of 65MPa). This improvement is thought to be due to the geocomposite preventing angular corners of individual ballast particles penetrating into the underlying clay formation.

- From all the reinforced track test data recorded track settlement models have been proposed for each of the three geosynthetics compared for reinforcement purposes and it was found that the models give a reasonable match with the GRAFT test data. These models formed the basis for design graphs that incorporate XiTRACK reinforcement and the reinforced geocomposite. These design graphs are applicable for track settlement after a track renewal/tamping for track on a clay subgrade with a 300mm ballast depth with the same ballast properties, ballast stiffness and track construction and layout as in GRAFT (typical track in UK that can have maintenance issues). As previously stated though these equations may underestimate track settlement in the field due to the restricted depth of GRAFT and therefore should only be used to give indicative values of settlement.

- Based on the research by others on geogrid reinforcement the Network Rail standard on formation treatments (NR/SP/TRK/9039) may overestimate the performance of geogrid reinforcement. This thesis has found that Network Rail assume that geogrid reinforcement can reduce track settlement by around 90% compared to unreinforced track (after 12.5 MGT of a 25 tonne axle load with 1.2 DAF). However, within the literature the level of track settlement reduction found varies between 10 to 40%.

- While testing the sand blanket replacement geocomposite in GRAFT it was found that formation erosion and subsequent track failure occurred in localised areas where the load was applied. It is thought that although the geocomposite prevented slurry pumping through it, and provided adequate separation between the subgrade and ballast layer, the permeability is too low to allow excess pore water pressures to quickly dissipate under cyclic loading. Currently, it is understood by the author that although some sand blanket replacement products are being used in the UK network, none can match the performance of a traditional sand blanket with a geotextile separator.

- When measuring subgrade stiffness in GRAFT using in-situ devices the DCP gave more consistent results when compared to the LFWD, which gave scattered data. These findings are consistent with other researchers. A good correlation was found between the DCP penetration rate and the PLT modulus in GRAFT (R^2=0.89 for initial tangent modulus and R^2=0.83 for reloading modulus).

- The PP and PRP in-situ devices used for subgrade strength measurements in GRAFT showed that the PP may be more accurate on softer saturated soils rather than stiffer unsaturated soils where the limit of the Pocket Penetrometer may be reached. It is not recommended to use the PP for anything else other than quick indicative measures of cohesive formation or subgrade strength, for which it is currently used in NR/SP/TRK/9039. The PRP measurements indicated that within the limit of the calibrated proving ring the PRP may give an accurate indication of the cone bearing resistance of cohesive soils, which can be equated to shear strength based on soil parameters such as Plasticity Index. The PRP is also only recommended to give a quick indicative measure of cohesive formation or subgrade strength and should not be used to replace laboratory strength testing.

- Using SART3D it was found that for the track properties and the load applied in GRAFT the deflections are correct. Due to the restricted depth of clay in GRAFT however the deflections in GRAFT underestimate the deflections in the

field for the same track properties and equivalent applied load by a factor of 1.3. This means that the track stiffness values found in GRAFT need to be modified to give the field values. Nonetheless, the GRAFT models developed within this thesis can still be used in conjunction with SART3D for preliminary track design and optioneering.

- The results of the SART3D parametric study confirmed that subgrade stiffness and applied load are probably the two parameters that influence the overall railway track behaviour the most in terms of both track deflections and induced formation/subgrade stresses. These two parameters have been investigated in considerable depth within this thesis and their influence on both track settlement and track stiffness reported. Other significant parameters include sleeper type and sleeper spacing. Ballast stiffness has a direct influence on track stiffness while ballast depth has a considerable influence on the induced stresses on the formation layer. The rail type has a less significant influence on the track responses considered in this study; although it is likely to have more of an influence on ballast induced stresses and ballast strain. These findings are similar to research by Selig and Waters (1994) and Shahu (1999) who also undertook an FE modelling parametric study.

- It was discussed that traditional design procedures are generally satisfactory for light axle loads and low to medium train speeds, but for heavy axle loads and faster trains these methods can lead to extensive track maintenance. These methods are based on reducing the stress or plastic settlement level in the subgrade, but do not consider excessive plastic deformation in the ballast layer. As described in this thesis the majority of track settlement is caused by ballast deformation and not subgrade deformation, unless the subgrade is very weak. A new design procedure to reduce the required track maintenance was proposed. The new procedure combines the numerical design method presented by Banimahd (2008) with the empirical results of this thesis to offer an optimised design and maintenance strategy.

8.2 Recommendations for future research

The following areas are recommended for future research:

- To develop the testing facilities further the following could be considered:

    1. In the existing GRAFT facility thin pressure cells could be placed at the interface between the formation and the ballast to measure the stress level in GRAFT under different tests. This could be checked against SART3D to validate that the stresses predicted from SART3D are accurate for GRAFT.
    2. Half a single full length sleeper could be placed longitudinally in GRAFT and loaded at 60kN to represent a 25 tonne axle load with 1.2 DAF (250kN x 40% (Sleeper load factor) x 50% (Load area stress factor) x120% (Dynamic load factor)). The track settlement and stiffness results from this test could be checked against a traditional GRAFT test with the same track properties to validate the method. In addition SART3D could be adapted to model this set up and check the results. This alternative testing method adds versatility to GRAFT and would allow a more focussed study on innovative track superstructure components, e.g. ballast mats, new baseplates, fixings etc.
    3. A second GRAFT test box could be constructed to allow one box to be prepared for test while one box was under test. This would dramatically reduce the turn over time for each test from around 3 to 4 weeks (500,000 cycle test) to 2 weeks, barring any problems with the LOS machine. The second box could include a detachable reinforced clear Perspex panel at one side of the tank that would allow the substructure deformation mechanisms to be viewed under load and also easier reconstruction of the track after each test.
    4. A new rolling wheel testing facility could be developed at Heriot-Watt University with multi loading actuators. A large scale concrete slab testing facility that is no longer in use could be adapted for this purpose.

This would allow the simulation of the complicated loading mechanism of railway tracks. The results could be checked against GRAFT and SART3D to monitor for any differences due to the loading mechanism. Having two facilities would allow more flexibility as the LOS machine is prone to faults.

5. Collaboration with the railway industry could be undertaken to get access to field measurements of track. These field conditions could then be simulated in GRAFT and the limitation found in this thesis due to the restricted clay depth of GRAFT confirmed. The results from such a study could be used to engage the railway industry in fully accepting the results from full-scale testing facilities.

- To continue on from the unreinforced and reinforced track research undertaken within this thesis the following interesting studies could be made within GRAFT:

    1. The empirical models developed within this thesis could be expanded by testing other variables in detail such as different ballast depths, fouled ballast, mixed loads, different track constructions (sleeper spacing etc.), track superstructure components, and high tonnages (long term linear track settlement). The relationship between track stiffness and settlement could be investigated out with the range of 25 to 37 tonnes.
    2. Areas of track that cause problems on site could be simulated in GRAFT, such as track irregularities (transition zones, joints, rail defects etc.).
    3. Slab track could be tested in GRAFT and the performance added to the reinforced design graph presented in this thesis.
    4. As XiTRACK showed the best results in terms of reinforcing the track a more detailed study could be undertaken on XiTRACK reinforcement looking at different ballast depths, subgrade properties, applied loads, polymer weightings, types of application (e.g. under sleepers only). The results from these studies could be added to the track reinforcement design graph for cost-benefit analysis comparisons to be undertaken.

5. To investigate the direct role of the separation, filtration and reinforcement functions of geosynthetics on track performance a series of tests could be undertaken in GRAFT on different geosynthetic products. This would aid railway engineers when specifying the use of geosynthetics on track and it may be the case that a multi-functional geocomposite could provide the same performance as the currently used geogrid reinforcement, in terms of track stiffness and settlement, due to having similar levels of stress reduction in the ballast and on the subgrade.
6. Geogrid reinforcement could be tested in GRAFT to confirm the results of others and to confirm that the Network Rail standard on formation treatments (NR/SP/TRK/9039) vastly overestimates the performance of geogrid reinforcement on track.
7. Regarding in-situ track measuring devices further research is required on the DCP and LWFD prior to their full use on track. A review of published research is recommended in order to determine exactly why the existing correlations between the same devices vary so much. In the Authors opinion this variation is thought to be due to a combination of soil conditions, test procedures, and inherent soil testing variability. Research is also required on the FWD, which is specified in NR/SP/TRK/9039, to compare the dynamic FWD sleeper support stiffness to both quasi-static and dynamic stiffness measurements from standstill TLV and rolling wheel devices.
8. The reinforced and unreinforced results of this thesis should be modelled numerically using an advanced 3D finite element program, such as ALTICA (Woodward and Molenkamp, 1999), to confirm the settlement trends found. This could validate the empirical models fundamentally and could lead to a more comprehensive design approach than currently exists for track deterioration.

References

Abu-Farsakh, M., Alshibli, K. A., Nazzal, M. and Seyman, E. (2004). Assessment of in-situ technology for construction control of base courses and embankments. Louisiana Transportation Research Centre Technical Report, Report No. FHWA/LA.04/389.

Adam, C., Adam, D., Kopf, F. and Paulmichl, I. (2009). Computational validation of static and dynamic plate load testing. Acta Geotechnica, 4: 35-55.

Alshibli, K. A., Abu-Farsakh, M. and Seyman. E. (2005). Laboratory evaluation of the geogauge and light falling weight deflectometer as construction control tools. Journal of Materials in Civil Engineering, 17(5): 560-569.

American Association of State Highway and Transportation Officials (AASHTO) (1986). Guide for design of pavement structures, Volume 1 Joint task force on pavements, Highway subcommittee on design.

American Railway Engineering Association (AREA) (1984). Manual for railway engineering.

Aursudkij, B. (2007). A laboratory study of railway ballast behaviour under traffic loading and tamping maintenance. PhD thesis, University of Nottingham, UK.

Banimahd, M. (2008). Advanced finite element modelling of coupled train-track systems: a geotechnical perspective. PhD thesis, Heriot-Watt University, UK.

Barker, E. and Sharley, P. (2009). Early performance audits of Geosand in the operational environment. 10th International Railway Engineering Conference, University of Westminster, London.

Berggren, E. (2009). Railway track stiffness. Dynamic measurements and evaluation for efficient maintenance, PhD thesis, KTH Royal Institute of Technology, Stockholm, Sweden.

Bowles, J. E. (1992). Engineering properties of soils and their measurements. 4th ed. McGraw –Hill.

Bowness, D., Lock, A. C., Powrie, W., Priest, J. A. and Richards, D. J. (2007). Monitoring the dynamic displacement of railway track. Proceedings of the Institution of Mechanical Engineers, Part F: Journal of Rail and Rapid Transit, 221: 13-22.

Brecciaroli., F. and Kolisoja, P. (2006). Deformation behaviour of railway embankment materials under repeated loading. Finnish Railway Administration, Helsinki, Finland.

British Standard (1990). BS 812-102:1990 Testing aggregates. Methods for sampling.

British Standard (1990). BS 1377-2:1990 Methods of test for soils of civil engineering purposes. Classification tests.

British Standard (1990). BS 1377-4:1990 Methods of test for soils of civil engineering purposes. Compaction related tests.

British Standard (1990) BS 1377-5:1990 Methods of test for soils of civil engineering purposes. Compressibility, permeability and durability tests.

British Standard (1990). BS 1377-7:1990 Methods of test for soils of civil engineering purposes. Shear strength tests (total stress).

British Standard (2007). BS EN14150:2007. Geosynthetic barriers. Determination of permeability to liquids.

British Standard (2007). BS EN1997-2:2007. Eurocode 7. Geotechnical design. General rules.

Brough, M. J., Ghataora, G. S., Stirling, A. B., Madelin, K. B., Rogers, C. D. F. and Chapman, D. N. (2003). Investigation of railway track subgrade. Part 1: In-situ assessment. Proceedings of the Institute of Civil Engineers, Transport, 156(3): 145-154.

Brough, M. J., Ghataora, G. S., Stirling, A. B., Madelin, K. B., Rogers, C. D. F. and Chapman, D. N. (2006). Investigation of railway track subgrade. Part 2: Case study. Proceedings of the Institute of Civil Engineers, Transport, 159(2): 83-92.

Brown, S. F., Lashine, A. K. F., and Hyde, A. F. L. (1975). Repeated load triaxial testing of silty clay. Geotechnique, 25(1): 95-114.

Brown, S. F. (2004). Design considerations for pavement and rail track foundations. Proceedings on the International Seminar on Geotechnics in Pavement and Railway Design and Construction, Athens, Greece, 61-74.

Brown, S. F., Brodrick, B. V., Thom, N. H. and McDowell, G. R. (2007a). The Nottingham railway test facility, UK, Proceedings of the Institute of Civil Engineers, Transport, 160(2): 59-65.

Brown, S. F., Kwan, J. and Thom, N. H. (2007b). Identifying the key parameters that influence geogrid reinforcement of railway track. Geotextiles and Geomembranes 25: 326-335.

Burns, B., Ghataora, G. S. and Sharley, P. (2006). Development and testing of Geosand composite layers using a pumping index test. Proceedings of Railway foundations conference: Railfound 06, University of Birmingham, UK, 385-393, ISBN 9780704426009.

Burrow, M. P. N., Bowness, D. and Ghataora, G. S. (2007a). A comparison of railway track design methods. Proceedings of the Institution of Mechanical Engineers, Part F: Journal of Rail and Rapid Transit, 221: 1-12.

Burrow, M. N. P., Chan, A. H. C. and Shein, A. (2007b). Deflectometer-based analysis of ballasted railway tracks. Proceedings of the Institute of Civil Engineers, Geotechnical Engineering, 160(3): 169-177.

Chen, J., Hossain, M. and LaTorella, T. (1995). Use of Falling Weight Deflectometer and Dynamic Cone Penetrometer in pavement evaluation. Transportation Research Record, 1655: 145-151.

Chen, D. and Bilyeu, J. (1999). Comparison of resilient modulus between field and laboratory testing: a case study. Transportation Research Board Annual Meeting.

Chua, K. M. and Lytton, R. L. (1981). Dynamic analysis using the portable dynamic cone penetrometer. Transportation Research Record, 1192: 702-708.

Chrismer, S. M. and Richardson, G. N. (1986). In track performance of geotextiles at Caldwell, Texas. Transportation Research Record, 1071: 72-80.

Clarke, C. W. (1957). Track loading fundamentals – parts 1-7. Railway Gazette, 106.

Cloburn Quarry Company Ltd. (2008). [Online] available from: <http://www.cloburn.co.uk/railtrack.html>. Accessed November 2009.

Crawford, S., Murray, M. and Powell, J. (2001). Development of a mechanistic model for the determination of track modulus. Proceedings of the 7th International Heavy Haul Conference, Brisbane, Australia.

Dahlberg, T. (2001). Some Railroad settlement models – a critical review. Proceedings of the Institution of Mechanical Engineers, Part F: Journal of Rail and Rapid Transit, 215: 289-300.

Dash, S. K., Sireesh, S. and Sitharam, T. G. (2003). Model studies on circular footing supported on geocell reinforced sand underlain by soft clay. Geotextiles and Geomembranes, 21:197 – 219.

Design Manual for Roads and Bridges (2008). Volume 7 Pavement design and Maintenance, Section 3 Pavement maintenance assessment, Part 2 Data for Pavement assessment, Chapter 5:1- 11.

De Ruiter, J. and Beringen, F. L. (1979). Pile foundations for large North Sea structures. Marine Geotechnology, 3(3): 267-314.

Du Pont (2009). [Online] available from: <http://www2.dupont.com/typar>. Accessed June 2009.

ELE International (2009). [Online] available from: <http://www.ele.com/euro/pdfs/65-66.pdf>.

Emersleben, A. and Meyer, N. (2008). The use of geocells in road construction over soft soil: vertical stress and falling weight deflectometer measurements. Proceedings of 4th European Geosynthetics Conference, Edinburgh, UK (2008).

Esveld, C. (2001). Modern Railway Track. MRT Productions, ISBN 9789080032439.

Fair, P. (2003). The geotechnical behaviour of ballast materials for railway track maintenance. PhD thesis, The University of Sheffield, UK.

Fleming, P. R., Frost, M. W. and Lambert, J. P. (2007). A review of the Lightweight Deflectometer (LWD) for routine in-situ assessment of pavement material stiffness. Transportation Research Board Annual Meeting.

Fleming, P. R., Frost, M. W. and Rogers, C. D. F. (2000). A comparison of devices for measuring stiffness in-situ. Dawson, A.R. (ed.), Proceedings of the 5th International symposium on unbound aggregates, UNBAR 5, Nottingham, UK, 193-200.

Frost, M. W., Fleming, P. R., and Rogers, D. F. C. (2004). Cyclic triaxial tests on clay subgrades for analytical pavement design. Journal of Transportation Engineering, 130(3): 373-386.

Fröhling, R. D. (1997). Deterioration of railway track due to dynamic vehicle loading and spatially varying track stiffness. PhD thesis, University of Pretoria, South Africa.

GC/RT5023, issue 01 (1995). Track standards Manual – Section 1: Basic Track Category Matrix. Railtrack PLC, London.

Ghataora, G. and Burrow, M. (2009). Assessing the suitability of composites at the ballast/subgrade interface in railway track foundations. 10th International Railway Engineering Conference, University of Westminster, London.

Ghataora, G., Burrow, M. and Matson, N. (2004). A laboratory investigation into the effectiveness of a geocomposite as sand blanket replacement. Geotechnics in pavement and railway design and construction, Millpress, Rotterdam, The Netherlands, 201-208.

Ghataora, G., Burns, B., Burrow, M. P. N. and Evdorides, H. T. (2006). Development of an index test for assessing anti-pumping materials in railway track foundations. Proceedings of Railway foundations conference: Railfound 06, University of Birmingham, UK.

Hall, C. D. (2009). A new generation of geogrid for railway ballast stabilisation to reduce trackbed maintenance costs. GeoAfrica 2009, 1st African Regional Conference on Geosynthetics, Cape Town, South Africa.

Head, K. H. (1982). Manual of soil laboratory testing. Vol. 2. London: Pentech Press Limited.

Heath, D. L., Shenton, M. J., Sparrow, R. W. And Waters, J. M. (1972). Design of conventional rail track foundations. Proceedings of the Institute of Civil Engineers, 51: 251-267.

Hosseingholian, M., Froumentin, M. and Levacher, D. (2009). Continuous method to measure track stiffness. A new tool for inspection of rail infrastructure. World Applied Sciences Journal, 6(5): 579-589.

Hunt, G. (2005). Review of the effect of track stiffness on track performance, Rail Safety and Standards Board (RSSB), Research Project T372.

Ionescu, D. (2004). Evaluation of the engineering behaviour of railway ballast. PhD thesis, University of Wollongong, New South Wales, Australia.

Indraratna, B., Khabbaz, H. and Salim, W. (2004). A laboratory study on improvement of railway ballast using geosynthetics. Geo-Trans 2004: Geotechnical engineering for transportation projects, Los Angeles, CA, USA, 617-626.

Indraratna, B., Khabbaz, H., Salim, W. and Christie, D. (2006). Geotechnical properties of ballast and the role of geosynthetics in rail track stabilisation. Ground Improvement, 10(3): 91 – 101.

International Union of Railways (1994). Earthworks and track-bed layers for railway lines. UIC Code 719 R, Paris, France.

Iwnicki, S., Grassie, S. and Kik, W. (1999). Track settlement prediction using computer simulation tools. Vehicle System Dynamics, 33(Suppl.): 37-46.

Jeffs, T. and Marich, S. (1987). Ballast characteristics in the laboratory. Conference on Railway Engineering, Perth, Australia.

Kavussi, A., Rafiei, K. and Yasrobi, S. (2010). Evaluation of PFWD as potential quality control tool of pavement layers. Journal of Civil Engineering and Management, 16(1): 123-129.

Karstunen, M., Krenn, H., Wheeler, S. J., Koshinen, M. and Zentar, R. (2005). Effect of anisotropy and destruction on the behaviour of Murro test embankment. International Journal of Geomechanics, 5(2): 87-95.

Karstunen, M. and Koshinen, M. (2008). Plastic anisotropy of soft reconstituted clays. Canadian Geotechnical Journal, 45: 314-328.

Kennedy, J. H., Woodward, P. K., Banimahd, M. and Medero, G. M. (2008). Application of geocell reinforcement in stabilising railway track substructures, Proceedings of 4th European Geosynthetics Conference, Edinburgh, UK.

Kennedy, J. H., Woodward, P., Medero, G. and McKinney, J. (2009a). Full-scale cyclic Geopavement & Railway Accelerated Fatigue Testing. 10th International Railway Engineering Conference, University of Westminster, London.

Kennedy, J. H., Woodward, P. and Medero, G. (2009b). Validation of the new full scale geopavement & railway testing facility at Heriot-Watt University, UK. Proceedings of GIGSA GeoAfrica Conference, Cape Town, South Africa.

Kerr, A. D. (2000). On the determination of the rail support modulus k. International Journal of Solids and Structures, 37: 4335:4351.

Lackenby, J., Indraratna, B., McDowell, G. and Christie, D. (2007). Effect of confining pressure on ballast degradation and deformation under cyclic triaxial loading. Geotechnique, 57(6): 527-536.

Li, D. and Selig, E. T. (1994). Resilient modulus for fine-grained subgrade soils. Journal of Geotechnical Engineering, 120(6): 939-957.

Li, D. and Selig, E. T. (1996). Cumulative plastic deformation for fine-grained subgrade soils. Journal of Geotechnical Engineering, 122(12): 1006-1013.

Li, D. and Selig, E. T. (1998a). Method for railroad track foundation design. Part 1: development. Journal of Geotechnical and Geoenvironmental Engineering, 124(4): 316-322.

Li, D. and Selig, E. T. (1998b). Method for railroad track foundation design. Part 2: applications. Journal of Geotechnical and Geoenvironmental Engineering, 124(4): 323-332.

Li, K. H., Brough, M., Sharley, P., Thomas, B., Sharpe, P. and Thom, N. (2007). Alternative to sand blanket: anti-pumping geocomposite in maintenance & track renewal. 9th International Conference, Railway Engineering, University of Westminster, London.

Lim, W. L. (2004). Mechanics of railway ballast behaviour. PhD thesis. University of Nottingham, Nottingham, UK.

Lim, W. L., McDowell, G. R. and Collop, A. C. (2005). Quantifying the relative strengths of railway ballasts. Proceedings of the Institute of Civil Engineers, Geotechnical Engineering, 158(2): 107-111.

Lin, H. and Penumadu, D. (2005). Experimental Investigation on Principal Stress Rotation in Kaolin Clay. Journal of Geotechnical and Geoenvironmental Engineering, 131: 633-642.

Livneh, M. (2007). Uncertainty associated with pre-defined correlative expressions of various in-situ test outputs. FAA Worldwide Airport Technology Transfer Conference, New Jersey, USA, 123-133.

Lundqvist, A. and Dahlberg, T. (2005). Load impact on railway track due to unsupported sleepers. Proceedings of the Institution of Mechanical Engineers, Part F: Journal of Rail and Rapid Transit, 219: 67-77.

Mohammad, L. N., Herath, A., Abu-Farsakh, M. Y., Gaspard, K. and Gudishala, R. (2007). Prediction of resilient modulus of cohesive subgrade soils from dynamic cone penetrometer test parameters. Journal of Materials in Civil Engineering, 19(11): 986-992.

Mohammadi, S. D., Nikoudel, M. R., Rahimi, H. and Khamehchiyan, M. (2008). Application of the Dynamic Cone Penetrometer (DCP) for determination of the engineering parameters of sandy soils. Engineering Geology, 101: 195-203.

Monismith, C. L., Ogawa, N. and Freeme, C. R. (1975). Permanent deformation characteristics of subgrade soils due to repeated loading. Transportation Research Record, 537: 1-17.

Mooney, M. A. and Miller, P. K. (2009). Analysis of Lightweight Deflectometer test based on in-situ stress and strain response. Journal of Geotechnical and Geoenvironmental Engineering, 135(2): 199-208.

Narayanan, R. M., Jakub, J. W., Li, D. and Elias, S. E. G. (2004). NDT&E International, 37: 141-151.

NR/SP/TRK/9039, issue 01, (2005). Formation treatments, Network Rail, London.

Okada , K. and Ghataora, G. S. (2002). Use of cyclic penetration test to estimate the stiffness of railway subgrade. NDT&E International, 35: 65-74.

Pen, C. K. (1990). An assessment of the available methods of analysis for estimating the elastic moduli of road pavements. Proceedings of the 3rd International Conference on Bearing Capacity of Roads and Airfields, Trondheim, Norway, 56-63.

Ping, V. W., Yang, Z. and Gao. Z. (2002). Field and laboratory determination of granular subgrade moduli. Journal of Performance of Constructed Facilities, 16(4): 149-159.

Pita, A. L., Teixeira, P. F. and Robuste, F. (2004). High speed and track deterioration: The role of vertical stiffness of the track. Proceedings of the Institution of Mechanical Engineers, Part F: Journal of Rail and Rapid Transit, 218: 31-40.

Presto Geosystems (2009). [online] available from: <http://beta.alcoa.com/alcoa-geo/en/home.asp>. Accesed January 2009.

Priest, J. A. and Powrie, W. (2009). Determination of dynamic track modulus from measurement of track velocity during train passage. Journal of Geotechnical and Geoenvironmental Engineering, 135(11): 1732-1740.

Priest, J. A., Powrie, W., Yang. L., Grabe. P. J. and Clayton, C. R. I. (2010). Measurements of transient ground movements below a ballasted railway line. Geotechnique, DOI: 10.1680/geot.7.00172.

Profillidis, V. A. (2006). Railway management and engineering, Ashgate Publishing Ltd., Hampshire, UK. ISBN 9780754648543.

Radampola, S. S. (2006). Evaluation and modelling performance of capping layer in rail track substructure. PhD thesis, Queensland University, Australia.

Rammah K. I., Val D. V., Puzrin A. M. (2004). Effects of ageing on small-strain stiffness of overconsolidated clays. Géotechnique, 54: 319-322.

RT/CE/S/006, issue 03, (2000). Track ballast and stoneblower aggregate, Network Rail, London.

RT/CE/S/010, issue 02, (1996). Geotextiles, Network Rail, London.

RT/CE/S/033, issue 02, (1998). Track blanketing sand, Network Rail, London.

Raymond, G. P. (2002). Reinforced ballast behaviour subjected to repeated load. Geotextiles and Geomembranes, 20: 39-61.

Sachan A. and Penumadu D. (2007). Effect of Microfabric on Shear Behaviour of Kaolin Clay. Journal of Geotechnical and Geoenvironmental Engineering, 133: 306-318.

Sadeghi, J. and Askarinejad, H. (2007). Influences of track structure, geometry and traffic parameters on railway deterioration. International Journal of Engineering, Transactions B: Applications, 20(3): 292-300.

Sato, Y. (1995). Japanese studies on deterioration of ballasted track. Vehicle System Dynamics, 24 (Suppl.): 197-208.

Seed, H. B., Chan, C. K. and Monismith, C. L. (1955). Effects of repeated loading on the strength and deformation of compacted clay. Proceedings of Highway Research Record, 34: 541-558.

Selig, E. T. and Waters, J. M. (1994). Track geotechnology and substructure management, Thomas Telford Publications, London, UK.

Shahu, J. T., Kameswara Rao, N. S. V. and Yudhbir (1999). Parametric study of resilient response of tracks with a subballast layer. Canadian Geotechnical Journal. 36(6): 1137-1150.

Shahu, J. T., Yudhbir and Kameswara Rao, N. S. V. (2000). A rational method for design of railroad track foundations. Soils and Foundations, Japanese Geotechnical Society, 40(6): 1-10.

Sharpe, P., Brough, M. J. and Dixon, J. (2006). Geogrid trials at Coppull Moor on the West Coast main line. Proceedings of Railway foundations conference: Railfound 06, University of Birmingham, UK, 367-375.

Sharpe, P. and Caddick, V. R. (2006). Accelerated testing of geosynthetics in trackbed using Europe's largest full scale rail rig. GEOfabrics Ltd. UK.

Shenton, M. J. (1974). Deformation of railway ballast under repeated loading conditions. Rapport RP5, British Railways Research and Development Division, Pergamon, Oxford.

Shenton, M. J. (1985). Ballast deformation and track deterioration. Proceedings of the Conference on Track Technology, University of Nottingham, UK, 253-265.

Shin, E. C., Kim, D. H. and Das, B. M. (2002). Geogrid reinforced railroad bed settlement due to cyclic load. Geotechnical and Geological Engineering, 20: 261-271.

Sirinivasan, M. (1969). Modern permanent way. Somaiga Publications, Bombay, India.

Sitharam, T. G., Sireesh, S. and Dash, S. K. (2005). Model studies of a circular footing supported on geocell-reinforced clay. Canadian Geotechnical Journal, 42: 693 – 703.

Stanton Bonna (2009). [Online] available from: <http://www.stanton-bonna.co.uk/pdfs/sleepers.pdf>

Stewart, H. E. and O'Rourke, T. D. (1988). Load factor method for dynamic track loading. Journal of Transportation Engineering, 114(1): 21-39.

Suiker, A. S. J., Selig, E. T. and Frenkel, R. (2005). Static and cyclic triaxial testing of ballast and subballast. Journal of Geotechnical and Geoenvironmental Engineering, 131(6): 771-782.

Sussmann, T. R., Ebersöhn, W. and Selig, E. T. (2001). Fundamental non-linear track load-deflection behaviour for condition evaluation. Transportation Research Board, 1742: 61-67.

Talbot, A. N. (1918). Stresses in railroad tracks. Report of the Special Committee on Stresses in Railroad Track, American Railway Engineering Association (AREA).

Thom, N. and Oakley, J. (2006). Predicting differential settlement in a railway trackbed. Proceedings of Railway foundations conference: Railfound 06, University of Birmingham, UK, 190-200.

Thom, N. (2007). Factors affecting trackbed maintenance requirements: a theoretical study. 9th International Conference, Railway Engineering Conference, University of Westminster, London.

Thomson, M. R. and Robnett, Q. L. (1979). Resilient properties of subgrade soils. Transportation Engineering Journal, 105(1): 71-87.

Thu T. M., Rahardjo H., Leong E. C. (2006). Shear Strength and Pore-Water Pressure Characteristics during Constant Water Content Triaxial Tests. Journal of Geotechnical and Geoenvironmental Engineering, 132: 411-419.

West Japan Railway Company (WJRC) (2002a). Construction and maintenance standards for commuter and local railway track. West Japan Railway Company, Osaka, Japan.

West Japan Railway Company (WJRC) (2002b). Construction and maintenance standards for Shinkansen track. West Japan Railway Company, Osaka, Japan.

Williams, R. R. and Nazarian, S. (2007). Correlation of Resilient and seismic modulus test results. Journal of Materials in Civil Engineering, 19(12): 1026-1032.

Woodward, P. K., Kennedy, J. H. and Medero, G. M. (2009a). XiTRACK reinforcement of high speed railway track over peat formations. 10th International Railway Engineering Conference, University of Westminster, London.

Woodward, P. K., Kennedy, J. H. and Medero, G. M. (2009b). Reinforcing railway tracks using insitu polymer geocomposites. Proceedings of GIGSA GeoAfrica Conference, Cape Town, South Africa.

Woodward, P. K., Kennedy, J. H. and Medero, G. M. (2009c). Three dimensional track reinforcement using polymer geocomposites. Proceedings of the American Railway Engineering and Maintenance of Way Association (AREMA), Chicago, USA.

Woodward, P. K. and Molenkamp, F. (1999). Application of an advanced multi-surface kinematic constitutive soil model. International Journal for Numerical and Analytical methods in Geomechanics. 23: 1995-2043.

Woodward, P. K., Nicholl, G. and Zettor, B. (2004). Applications of XiTRACK Geocomposite technology to Bletchley Points on the West Coast main line. 7th International Railway Engineering Conference, University of Westminster, London.

Woodward, P. K., Thompson, D. and Banimahd, M. (2007). Geocomposite technology: reducing railway maintenance. Proceedings of the Institute of Civil Engineers, Transport, 160(3): 109-115.

Woodward, P. K., Zettor, B., Kaddouri, A. and Banimahd, M. (2005). Advanced non-linear dynamic finite element modelling of railway track behaviour. 8th International Railway Engineering Conference, University of Westminster, London.

XiTRACK Ltd. (2010). [Online] available from: <http://www.xitrack.com/>. Accessed March 2010.